CANADIAN THESES ON MICROFICHE

THÈSES CANADIENNES SUR MICROFICHE

National Library of Canada
Collections Development Branch

Canadian Theses on
Microfiche Service

Ottawa, Canada
K1A 0N4

Bibliothèque nationale du Canada
Direction du développement des collections

Service des thèses canadiennes
sur microfiche

NOTICE

The quality of this microfiche is heavily dependent upon the quality of the original thesis submitted for microfilming. Every effort has been made to ensure the highest quality of reproduction possible.

If pages are missing, contact the university which granted the degree.

Some pages may have indistinct print especially if the original pages were typed with a poor typewriter ribbon or if the university sent us an inferior photocopy.

Previously copyrighted materials (journal articles, published tests, etc.) are not filmed.

Reproduction in full or in part of this film is governed by the Canadian Copyright Act, R.S.C. 1970, c. C-30. Please read the authorization forms which accompany this thesis.

AVIS

La qualité de cette microfiche dépend grandement de la qualité de la thèse soumise au microfilmage. Nous avons tout fait pour assurer une qualité supérieure de reproduction.

S'il manque des pages, veuillez communiquer avec l'université qui a conféré le grade.

La qualité d'impression de certaines pages peut laisser à désirer, surtout si les pages originales ont été dactylographiées à l'aide d'un ruban usé ou si l'université nous a fait parvenir une photocopie de qualité inférieure.

Les documents qui font déjà l'objet d'un droit d'auteur (articles de revue, examens publiés, etc.) ne sont pas microfilmés.

La reproduction, même partielle, de ce microfilm est soumise à la Loi canadienne sur le droit d'auteur, SRC 1970, c. C-30. Veuillez prendre connaissance des formules d'autorisation qui accompagnent cette thèse.

THIS DISSERTATION
HAS BEEN MICROFILMED
EXACTLY AS RECEIVED

LA THÈSE A ÉTÉ
MICROFILMÉE TELLE QUE
NOUS L'AVONS REÇUE

Canada

NL 339 (r. 86/09)

National Library of Canada | Bibliothèque nationale du Canada

Ottawa, Canada
K1A 0N4

37

TC –

ISBN 0-315-21232-2

CANADIAN THESES ON MICROFICHE SERVICE – SERVICE DES THÈSES CANADIENNES SUR MICROFICHE

PERMISION TO MICROFILM – AUTORISATION DE MICROFILMER

• Please print or type – Écrire en lettres moulées ou dactylographier

AUTHOR – AUTEUR

Full Name of Author – Nom complet de l'auteur

KENNETH G. STEELE

Date of Birth – Date de naissance	Canadian Citizen – Citoyen canadien
OCT 14, 1957	☒ Yes / Oui ☐ No / Non
Country of Birth – Lieu de naissance	**Permanent Address – Résidence fixe**
CANADA	#804 9927 114 ST EDMONTON ALBERTA T5K 1P8

THESIS – THÈSE

Title of Thesis – Titre de la thèse

UTILIZING GLACIAL GEOLOGY IN URANIUM EXPLORATION, DISMAL LAKES, N.W.T.

Degree for which thesis was presented Grade pour lequel cette thèse fut présentée	Year this degree conferred Année d'obtention de ce grade
MSc	1985
University – Université	**Name of Supervisor – Nom du directeur de thèse**
UNIVERSITY OF ALBERTA	N.W. RUTTER

AUTHORIZATION – AUTORISATION

Permission is hereby granted to the NATIONAL LIBRARY OF CANADA to **microfilm** this thesis and to **lend** or **sell copies of the film.**

The author reserves other publication rights, and neither the thesis nor extensive extracts from it may be printed or otherwise reproduced without the author's written permission.

L'autorisation est, par la présente, accordée à la BIBLIOTHÈQUE NATIONALE DU CANADA de **microfilmer** cette thèse et de **prêter** ou de **vendre des exemplaires du film.**

L'auteur se réserve les autres droits de publication; ni la thèse ni de longs extraits de celle-ci ne doivent être imprimés ou autrement reproduits sans l'autorisation écrite de l'auteur.

ATTACH FORM TO THESIS – VEUILLEZ JOINDRE CE FORMULAIRE À LA THÈSE

Signature	Date
Kenneth Steele	FEB 7 1985

NL-91 (r. 84/03)

Canada

THE UNIVERSITY OF ALBERTA

"UTILIZING GLACIAL GEOLOGY IN URANIUM EXPLORATION, DISMAL LAKES, NORTHWEST TERRITORIES"

by

KENNETH GEORGE STEELE

A THESIS

SUBMITTED TO THE FACULTY OF GRADUATE STUDIES AND RESEARCH

IN PARTIAL FULFILMENT OF THE REQUIREMENTS FOR THE DEGREE

OF MASTER OF SCIENCE

DEPARTMENT OF GEOLOGY

EDMONTON, ALBERTA

SPRING, 1985

THE UNIVERSITY OF ALBERTA

RELEASE FORM

NAME OF AUTHOR KENNETH GEORGE STEELE

TITLE OF THESIS "UTILIZING GLACIAL GEOLOGY IN URANIUM EXPLORATION, DISMAL LAKES, NORTHWEST TERRITORIES"

DEGREE FOR WHICH THESIS WAS PRESENTED MASTER OF SCIENCE

YEAR THIS DEGREE GRANTED SPRING, 1985

Permission is hereby granted to THE UNIVERSITY OF ALBERTA LIBRARY to reproduce single copies of this thesis and to lend or sell such copies for private, scholarly or scientific research purposes only.

The author reserves other publication rights, and neither the thesis nor extensive extracts from it may be printed or otherwise reproduced without the author's written permission.

(SIGNED) Kenneth Steele

PERMANENT ADDRESS:

#804 9927 114 St.

Edmonton, Alberta

T5K 1P8

DATED December 31 19 84

THE UNIVERSITY OF ALBERTA

FACULTY OF GRADUATE STUDIES AND RESEARCH

The undersigned certify that they have read, and recommend to the Faculty of Graduate Studies and Research, for acceptance, a thesis entitled "UTILIZING GLACIAL GEOLOGY IN URANIUM EXPLORATION, DISMAL LAKES, NORTHWEST TERRITORIES" submitted by KENNETH GEORGE STEELE in partial fulfilment of the requirements for the degree of MASTER OF SCIENCE.

.....

Supervisor

.....

.....

.....

.....

Date ..... Dec 21, 1984 .....

Abstract

The study was undertaken to delimit the bedrock source of a field of uraniferous sandstone boulders. The detailed study area is a broad drift covered valley extending west from Dismal Lakes. The valley is bounded on the north and south by bedrock outcrops. The study was divided into three main components: investigations of (1) glacial geology, (2) the uraniferous sandstone boulder field, and (3) till geochemistry.

The boulders were eroded and transported by the last glacial ice in the area. Striae at high elevations indicate the regional flow of the last ice was westward, although local ice flow was modified by bedrock topography. Ice flowed northwest along the Dismal Lakes valley before being diverted to an azimuth of 260 ° in the vicinity of the boulder field.

Erosion of the uraniferous sandstone occurred at the warm base of a thick ice sheet. Pressure and stress gradients created by ice flow over an irregular bedrock surface likely caused fracture of the uraniferous sandstone. The fractured sandstone was plucked by the plastic flow of ice into the lee side of bedrock protuberances and / or by regelation in a region of warm basal freezing. An area of increased sandstone erosion and plucking was mapped 5 to 7 km east from the main concentration of boulders. The boulders were transported above the ice sheet base. The boulders were sheared upwards from the ice sheet base in close proximity to the zone of plucking. The boulders may have been deposited during subglacial melt-out of ice block(s) stagnating below the active ice sheet. Stagnation would have been in response to ice flowing into a widened and deepened valley and over an irregular bedrock surface, causing a change in ice flow dynamics.

The distribution of the boulders forms a crude fan, with the orientation of two possible fan axes less than 10 ° different from the last ice flow direction. The fan apex is 4.7 km east of the main concentration of boulders. The fan shape indicates dispersion from a point source. The sharp decline in boulders at right angles away from either axis indicates the fan results from only one glacial advance. The high density of boulders at the fan centre suggests the boulders travelled a short distance. Maximum and minimum

transport distances of 9 km and 2.5 km , respectively, are proposed. The distribution of boulders within the fan indicates a transport distance approximately midway between these extremes.

Till samples along a line eastward from the main boulder concentration, parallel to the last ice flow direction, contain elevated uranium values. The largest area of anomalous uranium values occurs 6.2 km east of the main boulder concentration. In general, uranium values decrease westward from this anomalous area. No correlation between boulder concentration and concentration of uranium in till exists at west Dismal Lakes. A correlation between uranium content and copper content of till may exist. There is no correlation of uranium content with any of the other elements analyzed.

The likely bedrock source of the boulders is 6 to 6.6 km east-northeast of the main concentration of boulders. A 1.5 km gap exists between the proposed source and the nearest uraniferous boulder. The proposed source area closely agrees with anomalous uranium areas in the till, an area of increased fracturing and plucking of sandstone, the last ice flow direction, and boulder transport distance indicators.

Acknowledgements

The author gratefully acknowledges the advice and assistance provided by Dr. N. W. Rutter throughout this study. Discussions in the field and office with Dr. C. M. Trigg, D. J. Pawliuk and Dr. R. A. Olson, all with Trigg, Woollett, Olson Consulting Ltd., were extremely beneficial. Dr. Trigg originally suggested the topic for the study. Discussions with and suggestions made by Dr. M. M. Fenton, Alberta Reseach Council, greatly improved this study.

The assistance of Dr. W. W. Shilts, Geological Survey of Canada, in providing grain size separations for the geochemical till samples and in funding some of the trace element analyses, is greatly appreciated. Dr. D. A. St-Onge, Geological Survey of Canada, kindly provided a working manuscript of a paper concerning the deglaciation pattern in the Dismal Lakes region. I thank John Duke, University of Alberta SLOWPOKE facility, for donating his time, knowledge and assistance with the DNC and INAA analyses. Dr. F. J. Longstaffe, Department of Geology, University of Alberta, kindly provided x-ray diffraction facilities. Fellow graduate students in the geology department, particularly those of the "Quaternary Research Group", provided much advice, assistance and friendship. Although I cannot name everyone, the friendship of Bob St. Louis, Dave Proudfoot, Norm Catto, Vic Levson, Peter Bobrowsky, John Kulig and others, will always be a special part of this study and my days at the University of Alberta. To all of the above, many thanks, I could not have done it without you.

Esso Minerals Canada financially supported the field work. Trigg, Woollett, Olson Consulting Ltd. provided logistic support in the field and office. The assistance of these two organizations is gratefully acknowledged. The Department of Geology, University of Alberta, provided financial support to the author by means of teaching assistanceships and computer funds.

Special recognition is extended to my wife Cindy. I thank her for help with computing, drafting and proof reading. But even more I thank her for her constant encouragement, patience and financial support throughout this project. Her constant aggressiveness for results, never allowing me to stagnate in pot-holes of indecision, will

always be a part of this study. I thank her for this and even more.

Table of Contents

Chapter		Page
I.	INTRODUCTION	1
	A. DRIFT PROSPECTING	1
	B. OBJECTIVES OF STUDY	1
	C. LOCATION	2
	D. PREVIOUS INVESTIGATIONS	2
	E. ENVIRONMENT	4
	F. REGIONAL GLACIAL GEOLOGY	5
	G. BEDROCK GEOLOGY	7
	DISMAL LAKES AREA GEOLOGY	7
	WEST DISMAL LAKES GEOLOGY	8
	H. ECONOMIC GEOLOGY	10
	I. EXPLORATION HISTORY OF WEST DISMAL LAKES AREA	11
II.	PURPOSE AND METHODOLOGY	13
	A. GLACIAL GEOLOGY	13
	B. BOULDER FIELD	14
	C. TILL GEOCHEMISTRY	15
	D. NUMERICAL ANALYSIS TECHNIQUES	18
III.	RESULTS AND DISCUSSION	20
	A. GLACIAL GEOLOGY	20
	ICE FLOW DIRECTION	20
	SURFICIAL SEDIMENTS	29
	DRIFT THICKNESS	37
	B. URANIFEROUS BOULDER FIELDS	38
	WEST DISMAL LAKES BOULDER FIELD	38
	PEC BOULDER FIELDS	53
	C. TILL GEOCHEMISTRY	58
	WEST DISMAL LAKES GEOCHEMICAL SAMPLES	58
	X-RAY DIFFRACTION	80
	MUDBOIL VERSUS TILL SAMPLES	81

PEC GEOCHEMICAL SAMPLES 81

IV. THEORETICAL DISCUSSIONS OF GLACIAL ICE CONDITIONS AND POST GLACIAL PROCESSES 87

A. GLACIAL ICE CONDITIONS 87

B. POST GLACIAL PROCESSES 109

C. A MODEL FOR THE EROSION, TRANSPORT AND DEPOSITION OF WEST DISMAL LAKES URANIFEROUS SANDSTONE BOULDERS 111

V. CONCLUSIONS AND RECOMMENDATIONS 115

A. GLACIAL GEOLOGY 115

B. BOULDER FIELD 118

C. TILL GEOCHEMISTRY 119

D. BOULDER SOURCE AREA 119

E. METHODS EVALUATION 121

F. RECOMMENDATIONS FOR FUTURE WORK 122

VI. REFERENCES 124

VII. APPENDICES 133

A. APPENDIX A 133

B. APPENDIX B 135

C. APPENDIX C 136

D. APPENDIX D 137

E. APPENDIX E 138

F. APPENDIX F 142

G. APPENDIX G 149

H. APPENDIX H 157

I. APPENDIX I 164

Tables

Table 1: Surficial geology units - west Dismal Lakes 30

Table 2: Comparison of west Dismal Lakes and Uke Lake boulder fields 57

Table 3: West Dismal Lakes geochemical results - Descriptive measures 60

Table 4: Reanalyzed fluorometry U results 62

Table 5: INAA results 66

Table 6: Comparison of U by fluorometry and DNC 68

Table 7: Correlation matrix of geochemistry results 75

Table 8: Comparison of uranium values between mudboils and undisturbed till samples .. 82

Table 9: PEC geochemistry results - Descriptive measures 85

Table 10: Factors controlling areas of increased abrasion, fracturing and plucking 101

Table 11: Till types and typicial characteristics 107

Figures

Figure 1: Location of the study area 3

Figure 2: Bedrock geology - west Dismal Lakes 9

Figure 3: Glacial striae - Dismal Lakes area 21

Figure 4: Glacial striae - west Dismal Lakes 22

Figure 5: Landforms indicating the last ice flow direction - Dismal Lakes area 24

Figure 6: Combined till pebble fabric - west Dismal Lakes 26

Figure 7: Surficial geology - west Dismal Lakes 31

Figure 8: Till matrix envelope - west Dismal Lakes 33

Figure 9: Pebbles oriented by gelifluction 36

Figure 10: West Dismal Lakes boulder field 40

Figure 11: Prospecting grids - west Dismal Lakes 41

Figure 12: Contoured plot of boulder distribution 42

Figure 13: Contoured plot of boulder volume 43

Figure 14: Contoured plot of boulder radioactivity 45

Figure 15: Plot of boulder angularity versus distance west of 67E 46

Figure 16: Boulder distribution away from 67E and 11N 49

Figure 17: Glacial dispersion curves 50

Figure 18: Uke Lake boulder train 54

Figure 19: Plot of boulder angularity versus transport distance - PEC 56

Figure 20: West Dismal Lakes geochemical sample sites 59

Figure 21: Contoured uranium by fluorometry results 63

Figure 22: Contoured uranium by DNC results 65

Figure 23: Plot of uranium DNC and fluorometry values 69

Figure 24: Contoured copper results 71

Figure 25: Copper trend surface, third degree 72

Figure 26: Contoured zinc and lead results 73

Figure 27: Uranium, manganese and zinc values at PEC 84

Figure 28: The Wisconsinan Glacier Complex 90

Figure 29: Zones of increased erosion and plucking 102

Figure 30: Model of boulder transport and deposition 113

Figure 31: Boulder source area 120

Map pocket: West Dismal Lakes compilation map ..... Map pocket

Symbols and Abbreviations used

asl	above sea level
cps	counts per second
RPM	revolutions per minute
PPM	parts per million
DNC	Delayed Neutron Counting
AAS	Atomic Absorption Spectrometry
INAA	Instrument Neutron Activation Analysis
N.W.T.	Northwest Territories
B.P.	before present
IP	induced polarization
EM	electromagnetic
%	per cent
ha	hectare
km	kilometre
m	metre
cm	centimetre
mm	millimetre
µm	micron
l	litre
ml	millilitre
g	gram
µg	microgram
°	degrees
'	minutes
°C	degrees Celsius
s	seconds
n	neutrons
cts	counts

N	number of samples
D	distance
S	angularity (Bayrock, 1980)
K	constant, dependent upon lithology (Bayrock, 1980)
d	interplanar spacing within mineral crystal
θ	angle of incidence
CoK_{α}	cobalt K_{α} x-rays
>	greater than
<	less than
U	uranium
Th	thorium
Cu	copper
Pb	lead
Zn	zinc
Ni	nickel
Cr	chromium
Co	cobalt
Mo	molybdenum
Fe	iron
Mn	manganese
Al	aluminum
Pt	platinum
HNO_3	nitric acid
NaF	sodium fluoride
HCl	hydrogen chloride
BF_3	boron fluoride
U_3O_8	uranium oxide
$CaCl_2.2H_2O$	calcium chloride dihydrate
KCl	potassium chloride

I. INTRODUCTION

A. DRIFT PROSPECTING

Conventional geological prospecting for mineral deposits in areas of glaciated terrain can be difficult where glacial sediments mask extensive areas of bedrock. Drift prospecting has aided the exploration for mineral deposits in many areas of Scandinavia and Canada. Drift prospecting rests on the principle that till deposited directly from ice that has overridden and eroded an ore body will be enriched in mineralized debris, and that the debris will form a dispersion fan away from the ore body. Tracing of mineralized boulders was the first use of glacial material as an exploration tool. More recently exploration programs have utilized trace element geochemistry of the finest size fractions of till.

In the summer of 1978, Trigg, Woollett, Olson Consulting Ltd. (formerly Trigg, Woollett Consulting Ltd. and Trigg Woollett & Associates Ltd.) working for Esso Minerals Canada (a subsidiary of Imperial Oil Ltd.) discovered three uraniferous sandstone boulders in a broad valley with thick glacial drift west of Dismal Lakes, N.W.T.. Subsequent systematic radiometric prospecting in 1979 through 1981 resulted in the discovery of more than 500 uraniferous boulders in an area 2.0 km by 5.5 km. The boulders produce radioactivity ranging from 130 counts per second (cps) to greater than 15,000 cps; most boulders produce radioactivity between 1,000 and 5,000 cps (Grant and Woollett, 1979). The west Dismal Lakes area is 40 km northwest of the PEC uranium deposit. The PEC deposit, which straddles the PEC and YUK claim blocks, is contained within rock of similar lithology to the west Dismal Lakes boulders. Boulder trains extend west and northwest from the PEC deposit.

B. OBJECTIVES OF STUDY

The primary objective of this study was to delimit the possible bedrock source(s) of the uraniferous sandstone boulders by utilizing glacial geology and geomorphology. Secondary objectives were:

(1) to reconstruct the last glacial and post glacial geologic history, with respect to the uraniferous sandstone boulders and west Dismal Lakes valley sediments, and

(2) to evaluate boulder tracing and till geochemistry methods of drift prospecting for uranium exploration in the Dismal Lakes area.

C. LOCATION

Dismal Lakes N.W.T. are located 550 km north-northwest of Yellowknife and 90 km southwest of the village of Coppermine (Figure 1). Detailed work was undertaken at west Dismal Lakes (Figure 1). This area is covered by National Topographic Series sheets 86N/12 (southern quarter) and 86N/5 (northern quarter), and is approximately outlined by latitude 67°28' to 67°33' north and longitude 117°30' to 117°50' west, hence the detailed study area comprises 120 km². Reconnaissance work was done in the Dismal Lakes area (Figure 1). This area extends from 12 km west of Dismal Lakes along the south shore of Dismal Lakes to Teshierpi Mountain.

D. PREVIOUS INVESTIGATIONS

Various approaches have been taken in utilizing glacial geology in mineral exploration. Boulder tracing methods in Canada and Scandinavia are reviewed by Dreimanis (1958) and Hyvarinem *et al*. (1973), respectively. Drift prospecting using different grain-size fractions of till is described by Shilts (1976, 1977) and Bjorklund (1976a). Shilts (1972) studied the effectiveness of mudboil sampling for exploration geochemistry. Reconnaissance and regional exploration for uranium in the Northwest Territories using the geochemistry of the -2 μm fraction of till are outlined by Klassen and Shilts (1977b) and DiLabio (1979). An evaluation of geochemical methods in an area of continuous permafrost in the Coppermine River area is presented by Allan and Hornbrook (1971). Ridler and Shilts (1973), Cameron (1977), and Miller (1979) studied geochemical dispersion in permafrost areas of Canada.

The first geological investigations in the Coppermine River country were by Samuel Hearne of the Hudson's Bay Company in 1771 (Kindle, 1972). Between 1911 and 1912, George M. Douglas, Lionel Douglas, and Dr. August Sandberg visited and geologically mapped the Coppermine River and Great Bear Lake area (Douglas, 1913). Regional bedrock mapping in the Dismal Lakes area was done by geologists with the Geological Survey of Canada (Fraser *et al*., 1960; Baragar and Donaldson, 1973). Detailed bedrock

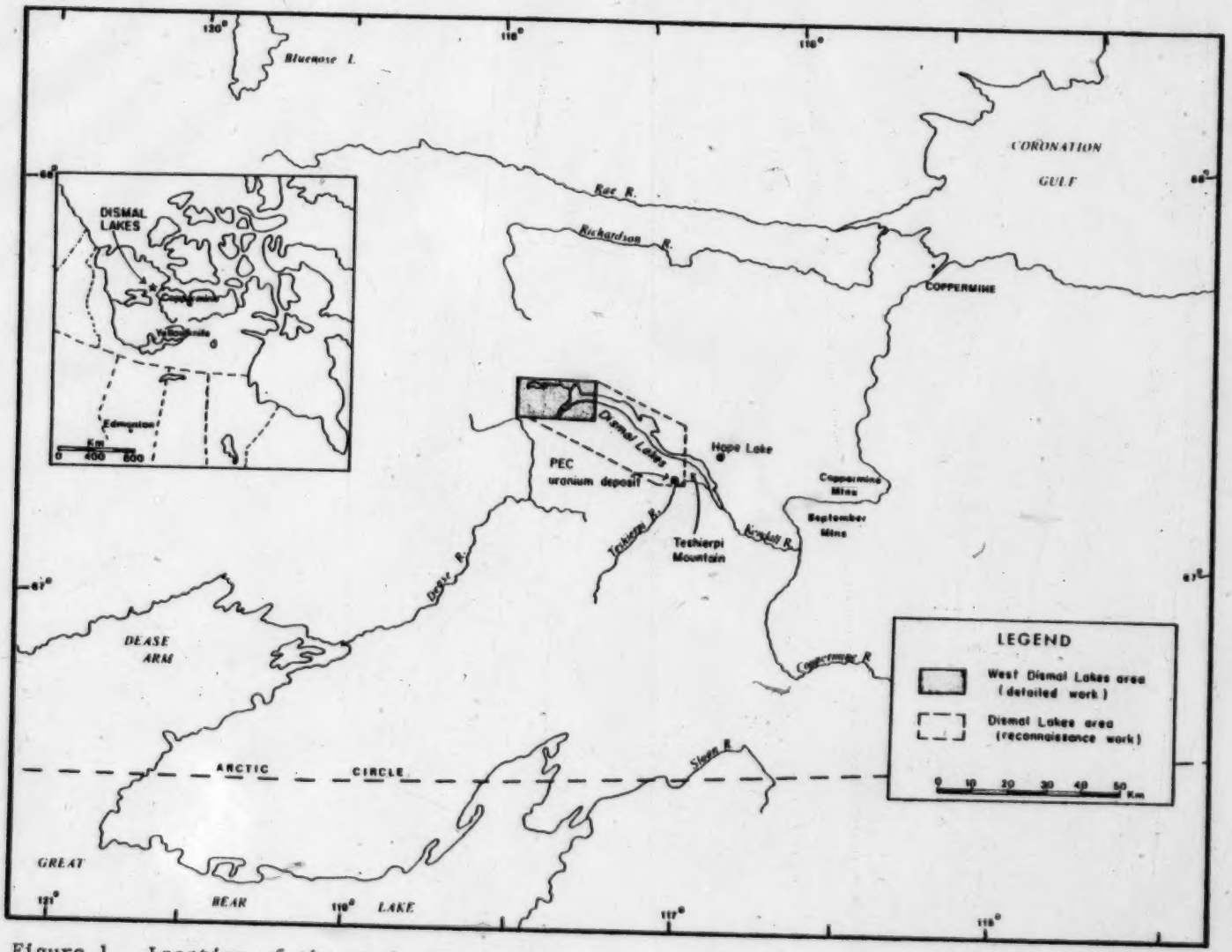

Figure 1. Location of the study area

geology of the PEC deposit area is reviewed in Abercrombie and Trigg (1980). Bedrock geology of the west Dismal Lakes area is given in Grant (1980).

The first surficial geology report covering the Dismal Lakes area was prepared by Craig (1960) on the north-central District of Mackenzie. St-Onge (1980, 1983) and St-Onge *et al.* (1981) have recently reported on glacial and post glacial sediments of the Coppermine River valley. Uranium exploration in the Dismal Lakes area in the 1970's included a surficial geology report by Vagners (1977) on the YUK claim block. Reports by Grant and Woollett (1979), Vagners (1979), Grant (1980) and Pawliuk and Trigg (1981) include information on surficial geology and boulder tracing in the west Dismal Lakes area.

E. ENVIRONMENT

The Dismal Lakes area lies within the barren grounds north of the Arctic Circle. The area is part of the Coronation Hills physiographic region of the Canadian Shield. It consists of tundra with grasses, lichen, low shrubs, mosses, and numerous arctic flowering plants. The area is treeless except for small trees along the southwest arm of Dismal Lakes and in the Kendall River valley. Cryosolic soils are dominant in the area.

The Dismal Lakes area is classified as cold desert within the zone of continuous permafrost. The area has an active layer of about 1 m in thickness. Climatic data for the village of Coppermine, the nearest recording station, indicate a mean daily January temperature of -29 °C and a mean daily July temperature of 9 °C. The lakes are generally ice-free by mid-July. Rainfall is approximately 10 cm, and snowfall is about 75 cm annually.

Dismal Lakes are 255 m above mean sea level (asl). Dismal Lakes drain to the southeast through the Kendall River and thence northward via the Coppermine River to the Arctic Ocean (Figure 1). Major topographic features in the region include: a granitic upland south of the western end of Dismal Lakes with a maximum elevation of 683 m asl, Teshierpi Mountain located between the Teshierpi River and Dismal Lakes, and dolomite and basalt cliffs north of Dismal Lakes that produce a terraced topography. Numerous bedrock outcrops have a local topographic relief of up to 150 m. The remaining area consists of gently rolling valleys and flat lowlands.

West of Dismal Lakes the area is dominated by a broad, flat, drift covered valley that extends greater than 20 km, widening from 3 km at Dismal Lakes to over 8 km at its western end. The valley is bounded on the north by dolomite cliffs and on the south by large outcrops of sandstone.

The Dismal Lakes area exhibits many periglacial features including: mudboils, block fields, ice-wedge polygons, non-sorted stripes, string bogs, beaded drainage, active layer slope failures (French, 1976), sorted steps and gelifluction benches (Washburn, 1973). Of these, mudboils, block fields, gelifluction benches, sorted steps and non-sorted stripes are present in the west Dismal Lakes area.

F. REGIONAL GLACIAL GEOLOGY

Based on cross cutting striae, Craig (1960) believed that the Dismal Lakes region has been overridden by at least two Quaternary glaciations. However, only Late Wisconsinan Laurentide ice sheet deposits have been identifed in the field (St-Onge, 1980; St-Onge *et al.*, 1981; Vagners, 1977).

Regional ice flow patterns have been determined from the orientation of striae, drumlins and major eskers. These features indicate a west-northwest flow of Laurentide ice in the Dismal Lakes region (Craig, 1960; St-Onge *et al.*, 1981). North of Dismal Lakes, ice was directed west along the valley of the Richardson River and then deflected to the southwest by the highlands south of Bluenose Lake (Craig, 1960). Drumlinoid ridges forming a broad arc between Dismal Lakes and the Richardson River provide the evidence for the shift in ice flow direction. Associated with each ice advance was the erosion, transport and deposition of older drift, if it existed, and bedrock fragments. Till of variable thickness covers large areas of the Dismal Lakes region.

The deglaciation pattern has been inferred from the mapping of successive ice front positions. Successive ice front positions have been located by mapping moraines (Craig, 1960; St-Onge, 1983) and deposits of a glacial lake which occupied the Coppermine River valley (St-Onge, 1983). Ice front positions mapped in the Dismal Lakes region indicate ice retreated to the northeast. St-Onge (1983) speculated that a moraine ridge north of Dease Arm, Great Bear Lake, represents an early frontal position of the last ice lobe in the Dismal Lakes region. Further east, St-Onge (1983) proposed four ice front

positions in the immediate Dismal Lakes area. His interpretation of the deglaciation sequence is presented below.

The earliest ice front position extended south from the west end of Dismal Lakes and connected with the Forcier Lake Moraine. The moraine was constructed by ice flowing west. The ice front rested against the southwest side of the Dismal Lakes valley channelling meltwaters through the Lac Rouviere basin. St-Onge speculated that west of Dismal Lakes, the ice front rested against the southern boundary of the west Dismal Lakes valley. The sand plain between Dismal Lakes and the Dease River was deposited by meltwater flowing from the earliest ice front.

The second ice front position resulted in Glacial Lake Coppermine occupying the Coppermine River valley south of the Kendall River. The lake drained west through the Sloan River, and the Lac Rouviere drainage route was abandoned. The ice front lay on the south side of the Kendall River valley and prevented the drainage of the lake through Dismal Lakes. The ice front crossed the Dismal Lakes immediately northwest of Teshierpi Mountain where St-Onge mapped a moraine. Meltwater flowing from the west end of the Dismal Lakes valley moved through the southwest arm of Dismal Lakes.

In the Dismal Lakes valley the third ice front position was 1 to 5 km northeast of the previous one. The retreat allowed Glacial Lake Coppermine to spill into the Dismal Lakes valley and to abandon the Sloan River outlet. St-Onge speculated that drainage of the lake may have been through the channel at the southwest arm of Dismal Lakes or, if the ice front had retreated far enough, across the plateau north of Dismal Lakes.

At the fourth position, the ice front was at the mouth of the Rae River and abutted the September Mountains. When the ice front was at this position, Glacial Lake Coppermine had drained into the Coronation Gulf and the Dismal Lakes region had adopted the present drainage pattern. Carbon 14 dates suggest that glacier ice had retreated from the Coronation Gulf lowlands as early as 10,200 years B.P., and therefore ice retreat from the Dismal Lakes valley was about 10,500 years B.P..

G. BEDROCK GEOLOGY

DISMAL LAKES AREA GEOLOGY

The following summary of Dismal Lakes area geology is condensed from Abercrombie and Trigg (1980). Their work modified the mapping of Baragar and Donaldson (1973). Unit designations used in this study are consistant with those used in the above works. A table of bedrock units in the west Dismal Lakes area is given in the legend of Figure 2.

The Dismal Lakes area is underlain by rocks of the Bear Structural Province of the Canadian Shield. The Bear Structural Province consists of the Aphebian Wopmay Orogen and the Helikian / Hadrynian Amundsen Basin. All the rocks of the Dismal Lakes area are Proterozoic in age.

The youngest tectonic unit of the Wopmay Orogen is the Great Bear Batholith. The Great Bear Batholith consists of subvolcanic and volcanic rocks (Unit 7) of the MacTavish Supergroup intruded by granitic plutons (Unit A). Rocks of the Wopmay Orogen were faulted, uplifted and eroded prior to deposition of Helikian strata.

The oldest tectonic unit of the Amundsen Basin is the Coppermine Homocline. In the Dismal Lakes area the Coppermine Homocline consists of three rock stratigraphic units: Paleohelikian Hornby Bay Group, Neohelikian Dismal Lakes Group and Neohelikian Coppermine River Group.

Hornby Bay Group rocks (Units 8, 9 and 10) form a conformable sedimentary sequence. Unit 8 consists of a basal conglomerate grading upwards to a medium grained sandstone. Unit 9 is a partly silicified, locally stromatolitic dolostone. Unit 10 consists of red siltstone, shale and sandstone. Hornby Bay Group rocks were faulted, intruded by diabase, uplifted and eroded prior to deposition of Neohelikian rocks.

The Dismal Lakes Group, a conformable sequence of sedimentary rocks (Units 11 through 16), were deposited unconformably on the older rock units. The Dismal Lakes Group, from base to top, consists of: Unit 11, a basal conglomerate overlain by quartzose sandstone; Unit 12, interbedded black shale, quartzose sandstone and siltstone; Unit 13, tan weathered dolomite and calcareous mudstone; Units 14, 15 and 16, stromatolitic dolomite. Dismal Lakes sedimentation was terminated by regional uplift during which there

was little or no erosion. Diabase dikes intruded into Dismal Lakes Group and older rocks. North trending faults, commonly intruded by diabase, occur locally. The intrusions may have been contemporaneous with the extrusion of the Coppermine River Group basalts which unconformably overlie the Dismal Lakes Group .

The Coppermine River Group is comprised of the Copper Creek Formation (Unit 17) and the Husky Creek Formation (Unit 18). The Copper Creek Formation consists of over three thousand metres of flood basalts, conformably overlain by sandstones, siltstones and intercalated basalt flows of the Husky Creek Formation.

Faulting, uplift and erosion in the Dismal Lakes area occurred during the Late Paleozoic and Mesozoic. Further uplift, erosion and glaciation modified the landscape during the Cenozoic.

WEST DISMAL LAKES GEOLOGY

The bedrock geology of the west Dismal Lakes area is based on detailed mapping by Grant (1980) and is presented as Figure 2.

Granitic rocks (Unit A) of the Aphebian Wopmay Orogen are the oldest rocks in the west Dismal Lakes area. The granitic rocks consist of medium to coarse grained, equigranular, hematite stained granodiorite to quartz monzonite, normally containing 5-10% hornblende (King *et al*., 1979). Massive outcrops of granitic rocks occur on both sides of the southwestern arm of Dismal Lakes.

Unit 8, representing Neohelikian Hornby Bay Group strata, outcrops north of the granitic rocks. Unit 8 consists of reddish sandstone with kaolin or sericite cement. The contact zone between Unit 8 and the granitic rocks is marked by extensive quartz veining and quartz breccia stockwork. Although outcrops of Hornby Bay Group dolomite (Unit 9) do not exist in the west Dismal Lakes area, dolomite boulders are common in areas of Unit 8 and Unit 10 outcrops, and Unit 9 probably exists beneath glacial drift (Grant, 1980). Unit 10 red siltstone, shale and sandstone exist north of Unit 8.

Two large outcrops, numerous small outcrops, and extensive areas of block fields of Dismal Lakes Group Unit 11 sandstone occur at the western end of Dismal Lakes. Unit 11 consists of quartzose sandstone with quartz cement. All uraniferous boulders located

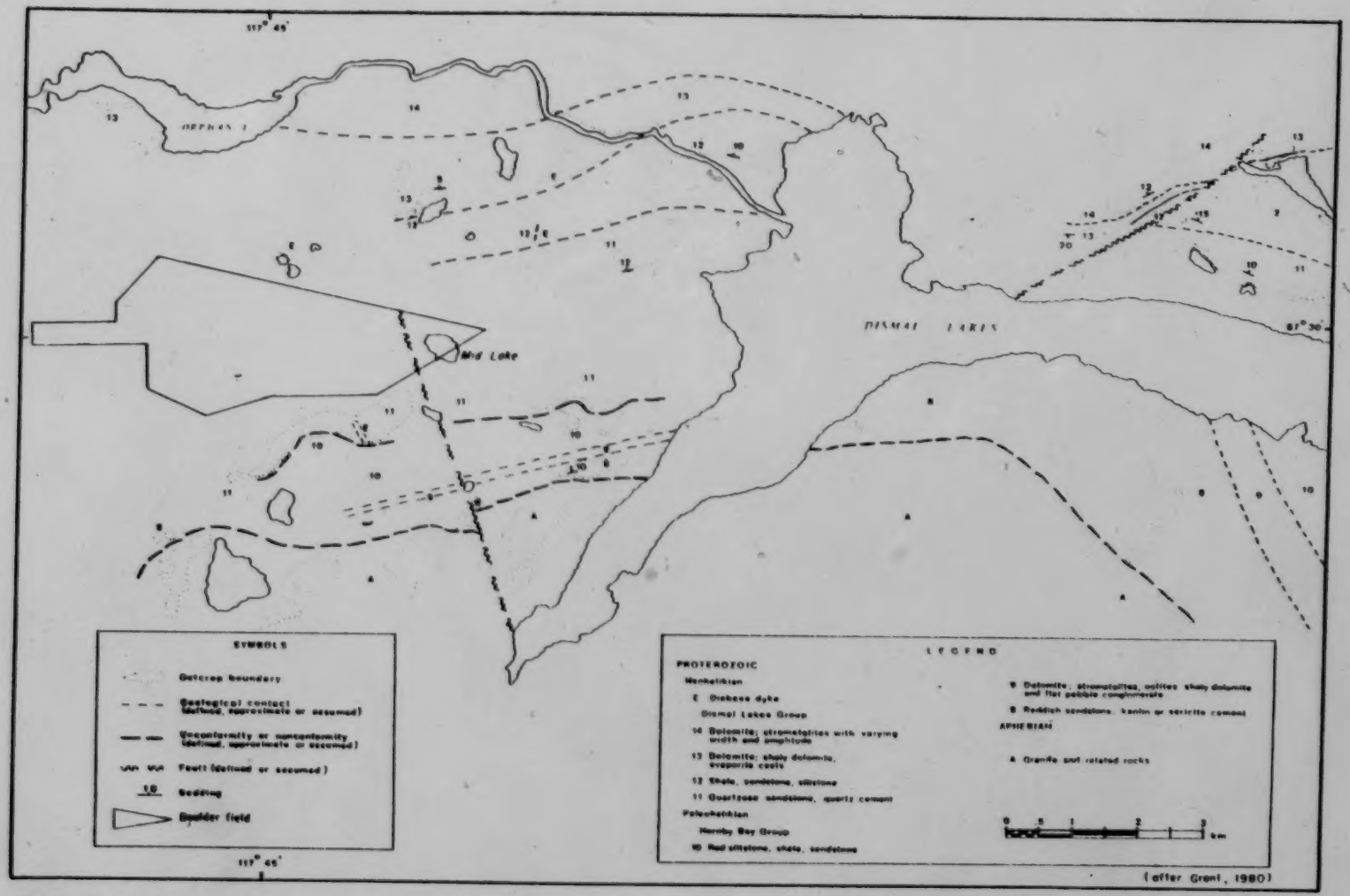

Figure 2. Bedrock geology - west Dismal Lakes

in the west Dismal Lakes area are in glacial drift believed to be underlain by Unit 11 strata. Dismal Lakes Group Units 12 through 16 outcrop northwest of Dismal Lakes. Shale, sandstone and siltstone of Unit 12 grade into shaly dolomite (Unit 13), then into dolomite (Units 14 to 16). Unit 14 dolomite forms extensive cliffs immediately north of Orphan Lake.

Two diabase dikes (Unit E) intrude Dismal Lakes Group strata at west Dismal Lakes. The dikes are medium grained black-green pyroxene diabase (King *et al.*, 1979). Two major faults have been mapped in the area. Baragar and Donaldson (1973) mapped a north-northwest trending fault bisecting the west Dismal Lakes area, passing immediately west of Mid Lake. Grant (1980) believed a fault which exists on the north shore of Dismal Lakes extends beneath the southwest arm of Dismal Lakes.

H. ECONOMIC GEOLOGY

Exploration in the Dismal Lakes area for copper and uranium has occurred in separate phases. The occurrence of native copper in the Coppermine River area was known as early as 1708 (Kindle, 1972). Between 1771 and 1912 a number of expeditions confirmed the presence of copper bearing rocks. Exploration companies worked the area between the Coppermine River and Dismal Lakes intermittently from 1929 until 1966, when new copper discoveries created an intense revival of interest. Exploration resulted in the location of a number of copper occurrences in the Hope Lake area, 15 km northeast of Dismal Lakes (Figure 1). Copper mineralization occurs in flood basalts of the Coppermine Creek Formation (Unit 17). The largest deposit has been outlined as a 3.5 million ton body averaging 3.44 % copper (Kindle, 1972). The deposit is uneconomic at the present time. Exploration for copper was practically at a standstill by 1970.

The second phase of mineral exploration in the Dismal Lakes area was for uranium in Helikian sandstones of the Hornby Bay Basin. In 1969, Aquitaine Company of Canada Limited conducted an airborne radiometric survey over the Hornby Bay Basin from Great Bear Lake to the Coppermine River basaltic flows. The company discovered uranium occurrences west of the Teshierpi River, about 10 km south of Dismal Lakes, during follow-up work (Salat and Arnaud, 1970).

Trigg, Woollett, Olson Consulting Ltd., exploring on behalf of Esso Minerals Canada, discovered radioactive boulders immediately north and west of the PEC claim group in 1972. The YUK claims were staked to cover the boulders and their presumed source. Subsequent exploration resulted in the discovery of the PEC uranium deposit. Drill holes intersected uraniferous zones that grade greater than 0.1 % U_3O_8 over 1.0 m. The most uraniferous interval assayed 5.19 % U_3O_8 over 0.9 m. The small size and remote location of the PEC uranium deposit makes it uneconomic at the present time.

I. EXPLORATION HISTORY OF WEST DISMAL LAKES AREA

The first exploration work in the west Dismal Lakes area was performed by Hudbay Uranium Company. The SAN and MAL mineral claims were staked in 1977 immediately south of the west Dismal Lakes boulder field. During the 1977 and 1978 summer field seasons, geological mapping and prospecting, airborne radiometric surveying, lake bottom geochemistry, IP surveying, and airborne and ground EM surveying were implemented. No significant uranium occurrences or anomalies were discovered on the claims. The Hudbay Uranium Company did no further work in the area and the claims lapsed.

Since Hudbay's withdrawal, exploration at west Dismal Lakes has been carried out solely by Trigg, Woollett, Olson Consulting Ltd. for Esso Minerals Canada. Work has concentrated upon locating the source of uraniferous sandstone boulders initially discovered in 1978 by ground radiometric prospecting (Ahuja, 1978). In addition to detailed radiometric prospecting (Grant and Woollett, 1979; Grant, 1980; Pawliuk and Trigg, 1981), a number of other exploration projects have been performed.

(1) The WD mineral claims covering the boulder field were staked (Grant and Woollett, 1979; Pawliuk and Trigg, 1981).

(2) Aerial photographs were reviewed for surficial geology data (Vagners, 1979).

(3) The bedrock geology was mapped in detail (Grant, 1980).

(4) A number of radioactive boulders were assayed (Grant, 1980).

(5) The angularity of some uraniferous sandstone boulders was measured and plotted (Grant, 1980).

(6) A radon in soil gas survey which used thirty Track-Etch© cups was performed (Grant,

1980).

(7) Very low frequency electromagnetic surveys were carried out (Grant, 1980; Pawliuk and Trigg, 1981).

(8) A petrographic study comparing radioactive sandstone boulders of the west Dismal Lakes and PEC areas was completed (Grant, 1980).

(9) A limited amount of diamond drilling was undertaken (Pawliuk and Trigg, 1981).

No exploration work, except field work for this study, was performed in the west Dismal Lakes area during 1982 or 1983.

II. PURPOSE AND METHODOLOGY

The west Dismal Lakes study was divided into three main components: investigations of (1) glacial geology, (2) the distribution of uraniferous sandstone boulders and (3) till geochemistry. All three investigations involved field work performed between July 2 and August 14, 1981 and on July 10, 1982.

A. GLACIAL GEOLOGY

The glacial geology study was undertaken to provide a base for the interpretation of boulder field and till geochemistry data. The investigation was subdivided into three parts: (1) determination of the direction(s) of ice movement, (2) mapping of the surficial sediments in the west Dismal Lakes area and (3) reconstruction of the last glacial and post glacial geologic history, with respect to the uraniferous sandstone boulders and west Dismal Lakes valley sediments.

The ice flow direction was determined from a compilation of various data. Glacial striae and chattermarks were mapped at selected outcrops up to 15 km from the west Dismal Lakes area. Mapping was concentrated at outcrops near the boulder field. Aerial photographs at a scale of 1:59,400 were studied with emphasis on landforms streamlined by glacial ice, for example, molded bedrock outcrops, drumlinoid features and flutings. Till fabric measurements were taken from 11 sites; 8 sites are in the west Dismal Lakes area (Compilation map) and 3 sites are west of the PEC uranium deposit. Pebble counts of 100 clasts were taken at the 11 till fabric sites. The pebble lithologies were identified in an attempt to define the last ice flow direction. Finally, the distribution of uraniferous sandstone boulders , and the shape and location of geochemically anomalous till areas were studied for trends indicating the last ice flow direction.

The mapping of surficial sediments was carried out in three phases : (1) preliminary office examination of aerial photographs and literature review, (2) field work and (3) mapping on aerial photographs at a scale of 1:59,400. Field work included the examination of geochemical sample holes, 0.2 m deep till fabric pits, and natural exposures; and the assessment of landforms. The natural exposures examined were

scattered sections along creeks flowing into Dismal Lakes and three sections along the river draining Orphan Lake (Compilation map). These sections were less than 3.0 m in thickness and poorly exposed, often due to active layer slumps. At each section, after preparing a fresh surface, the structure, texture, and thickness of each sedimentary unit was described and tentatively assigned an origin. Samples were collected at the 11 till fabric / pebble count sites and returned to the laboratory for analyses.

Laboratory studies were performed to obtain data useful in the reconstruction of the geologic history and in the interpretation of geochemical data. Grain size data was obtained using standard sieving and hydrometer techniques (American Society Testing and Materials, 1964).

The reconstruction of the last glacial and post glacial geologic history of the west Dismal Lakes area was based upon the study of ice movement direction indicators, surficial sediment mapping and published reports.

B. BOULDER FIELD

Boulder field investigations were carried out to locate the bedrock source of the boulders by: (1) estimating the distance of transport of the uraniferous sandstone boulders from their bedrock source to their present location and (2) determining whether the boulder field shape indicates the direction of last ice movement and / or a possible bedrock source for the boulders.

The distribution of uraniferous sandstone boulders in the west Dismal Lakes field had been mapped previously by Trigg, Woollett, Olson Consulting Ltd. personnel. In addition, the volume, angularity and radioactivity had been previously recorded for some of the boulders. In this study the distribution of boulders by volume and radioactivity, and the distribution of all boulders in the field, were assessed with respect to a train or fan shape typical of glacial dispersion from a point source. Linear regression analysis of boulder angularity versus distance in the direction of ice flow was performed to estimate the transport distance of the boulders.

The data on radioactive boulders derived from the PEC uranium deposit were used as a comparison with the west Dismal Lakes boulders. The distribution of radioactive boulders in the PEC area was previously mapped by Trigg, Woollett, Olson Consulting Ltd..

In this study the PEC boulders were assessed with respect to field shape and to distance of transport from their source at the PEC uranium deposit. Forty six radioactive boulders were measured for angularity following the technique of Bayrock (1980). This technique involves measuring the length of the curved edge between two perpendicular flat faces of a boulder. Linear regression analysis of angularity versus distance of transport from the PEC uranium deposit was then performed. Angularity data was also used to assess Bayrock's (1980) formula, which relates the degree of boulder rounding to the distance of boulder transport from its bedrock source.

C. TILL GEOCHEMISTRY

The primary objective of the till geochemistry study was to obtain an indication of the location of the bedrock source of the uraniferous boulders, from the shape and location of geochemically anomalous areas of till. Geochemically anomalous areas, for this study, are defined as areas which have geochemical values greater than or equal to one standard deviation above the arithmetic mean. Secondary objectives were:

(1) to compare the distribution of uranium in the till matrix with the distribution of uraniferous sandstone boulders;

(2) to determine which size fraction of the till matrix contains the most uranium;

(3) to assess if the shape of geochemically anomalous areas indicates the direction of the last ice flow;

(4) to investigate whether other elements have similar distribution patterns as uranium in the till matrix;

(5) to assess whether elements present at the PEC uranium deposit are present in the west Dismal Lakes area; and

(6) to compare geochemical values for the west Dismal Lakes and PEC areas.

Two hundred and eighteen till samples were collected: 205 from a detailed grid which covered the west Dismal Lakes boulder field and extended east to Dismal Lakes, and 13 samples from a line extending west from the PEC uranium deposit. Mudboil samples were collected where possible. At the 29 sampling stations where a mudboil was not within 10 m, a till sample was taken.

Mudboils are round to elongate 0.5 to 3.0 m diameter bare soil patches that form on perennially frozen till, or any poorly sorted sediments that contain significant fines. Mudboils have been referred to in the literature by various names including frost boils, sorted and non-sorted circles and tundra craters.

Mudboils were chosen as the sampling target for three reasons.

(1) Mudboils have developed exclusively in till at west Dismal Lakes, therefore sampling mudboils confirmed that till was being collected. Till is the most desired surficial material for analysis because it is the first derivative of bedrock and as such it is easier to relate analytical results with the bedrock geology.

(2) Mudboils provide the freshest till sample for the least amount of digging. This is because mudboils are diapiric features caused by the confinement of liquified sediment between the permafrost table and a carapace (Shilts, 1978). This action moves less weathered sediment closer to the surface, where it can be sampled.

(3) Sampling mudboils is quick due to the lack of a vegetation mat, therefore the number of samples collected can be maximized for the time available.

Mudboil samples were taken at a depth of approximately 30 cm from the middle of the non-vegetated area. Two kilogram samples were taken; large rock clasts and organic material were removed from the samples.

The tracing of mineralized material, including both boulders and small fragments in till matrix, has provided data on how glaciers disperse material from a point source. Shilts (1976) proposed that glaciers disperse material in the form of a negative exponential curve, or in other words, there is an exponential decline of material away from the source. He divided the dispersal curve into two components: (1) a rapid decrease in concentration or "head" over and/or close to the source, and (2) a more gradual decrease or "tail" at greater distances. The sample spacing used at west Dismal Lakes is presumed to permit delineation of the "head" of a dispersal fan, if one exists.

Klassen and Shilts (1977a) and Shilts (1972, 1976, 1977) conclude that the clay size fraction of till matrix gives the best background to anomalous value contrast for uranium analyses. Therefore, in this study all samples had the clay size fraction (-2 μm) analyzed whereas only selected samples had the 2-60 μm and 60-250 μm fractions analyzed. The following assumptions are inherent in clay size fraction analysis. The coarser

fractions contain mostly quartz and feldspar and have a low metal content after weathering. The -2 μm fraction contains phyllosilicates, iron oxides, and manganese oxides which adsorb cations in proportion to those released during post glacial weathering of labile minerals that were originally physically dispersed by glacial action (Shilts, 1977). The -2 μm till fraction is less diluted by erratic amounts of quartz and feldspar than coarser till fractions. Analysis of the -2 μm fraction eliminates texture dependent geochemical variations among samples. The validity of some of these assumptions for the west Dismal Lakes area is discussed in Chapter III.

The laboratory procedure for the till geochemical samples was thoroughly discussed with W. W. Shilts (personal communication, 1981), Geological Survey of Canada. Shilts has extensive experience with geochemical surveys utilizing mudboils as the sampling medium (Shilts, 1972; Ridler and Shilts, 1973; Klassen and Shilts, 1977a). Till geochemical samples were processed in the following sequence:

(1) The samples were oven dried at 60°C and sieved to -250 μm through brass screens at the University of Alberta.

(2) The samples were then separated into three size fractions (-2 μm, 2-60 μm, 60-250 μm) at the Geological Survey of Canada laboratories in Ottawa. The procedure followed is outlined in Appendix A.

(3) The samples were transferred to Bondar-Clegg & Company Ltd., Ottawa, where fluorometric and Atomic Absorption Spectrometry (AAS) analyses were performed. The same procedures as used for the samples of Klassen and Shilts (1977a) were followed (Appendix B). For all 218 samples, the -2 μm fraction was analyzed for uranium by the fluorometric method. In addition, for 37 samples from the boulder field area, the 2-60 μm and 60-250 μm fractions were analyzed for uranium. Nine -2 μm fraction samples were renumbered and returned for reanalysis. All 218 samples were analyzed by AAS on the -2 μm fraction for copper, lead, zinc, manganese and chromium. In addition 202 samples, including the 13 from the PEC area, were analyzed by AAS on the -2 μm fraction for cobalt, nickel, molybdenum and iron.

(4) In an effort to check the results obtained by uranium fluorometric analysis, the -2 μm fraction of 117 west Dismal Lakes samples was analyzed for uranium by Delayed Neutron Counting (DNC). The SLOWPOKE reactor facility at the University of Alberta was used. The

DNC technique using a SLOWPOKE reactor is outlined by Boulanger *et al*. (1973). The procedure used for this study is outlined in Appendix C.

(5) To aid in the evaluation of geochemical data, twelve -2 μm fraction samples were analyzed by X-ray diffraction. The methodology followed is given in Appendix D.

D. NUMERICAL ANALYSIS TECHNIQUES

In this study most numerical data are presented in the form of contour maps and a trend surface plot. These were produced using the SURFACE II Graphics System (Sampson, 1975). Contour maps were used in the interpretation of boulder field data and till geochemistry results. The trend surface plot aided in the assessment of till geochemistry results.

The contour map plotting process involved two steps; the calculation of a data grid and the construction of contours. In the calculation of the data grid, the value at a grid point is a distance weighted average ($1/D^2$) of either the projections of dips of the surfaces at nearby data points (Method A), or the nearby data points (Method B). In the construction of the contours, a smoothing algorithm called piecewise Bessel interpolation (Sampson, 1975) was used. Because of this process, lack of data points along the map boundaries produced some distortion.

While contouring emphasizes local variations, trend surfaces illustrate regional patterns. A trend surface is defined as a linear or polynomial function of the geograhic coordinates of a set of observations so constructed that the squared deviations from the trend are minimized (Davis, 1973). A trend surface illustrates both the amount and direction of any trend in data values. Trend surface analysis assumes that the mapped variable can be decomposed into two components: (1) a regional component operating over a large area; and (2) a local component, or residual, which can be defined as apparently non-systematic fluctuations that are superimposed on the large scale pattern (Krumbein and Graybill, 1965). In this study only the regional component was studied. The coefficient of determination, or goodness of fit, records the proportion of variation in the independent variable (geographic coordinates) accounted for or due to the fitting of a trend surface on the dependent variable (copper concentration for this study).

When geochemical data points do not extend past the boundaries of the plot area, almost no constraints exist on the form of the trend surface along the edges of the plot. Whatever slope exists in the region of control is extrapolated to the plot boundaries, creating "edge effects". "Edge effects" occur on all trend surface plots but the effect increases with the degree of trend surface being fitted (Davis, 1973). Thus, trend surface patterns along the edges of plots should be interpreted with caution. When data points are distributed along a narrow band the form of the fitted trend surface becomes distorted parallel to the data point pattern. The data point pattern causes some distortion in the southern third of the west Dismal Lakes till sampling area.

III. RESULTS AND DISCUSSION

Results and discussion are presented for each of the study's three main components: glacial geology, boulder field analysis and till geochemistry. A compilation map containing results and discussion from Chapters III and IV, and the likely source area of the uraniferous sandstone as proposed in Chapter V, is located in the map pocket.

A. GLACIAL GEOLOGY

ICE FLOW DIRECTION

A knowledge of past ice flow directions is fundamental in the tracing of glacially transported boulders to their source. Ice flow directions are also a major contribution to the reconstruction of the last glacial history.

RESULTS

(a) Striae, chattermarks and friction cracks - Chamberlain (1888) noted that glacial striae are only preserved on certain rock types; this is the situation at west Dismal Lakes. Chattermarks, crescentic-cross fractures, lunate fractures and well developed striae are often preserved on Unit 11 sandstone. Granitic rocks (Unit A) and Unit 8 sandstone have moderately to poorly developed striae preserved. Occasionally, quartz veins crossing the granitic rocks have moderately well developed striae preserved. Poorly developed striae were measured on diabase dikes. In all cases the best striae have been recently exposed, having been previously protected by boulders or thin drift. No ice flow direction indicators are present on the numerous dolomite outcrops which are immediately north of the boulder field because the outcrop surfaces are deeply pitted by weathering. Glacial grooves in the west Dismal Lakes area parallel bedrock bedding planes and are not reliable direction indicators.

Striae on Unit 11 sandstone range from 3 to 15 cm in length, and are less than 5 mm in width and depth. Chattermarks and crescentic-cross fractures are emphasized by lichen growth. Glacial striae are plotted by elevation on Figures 3 and 4. On many outcrops

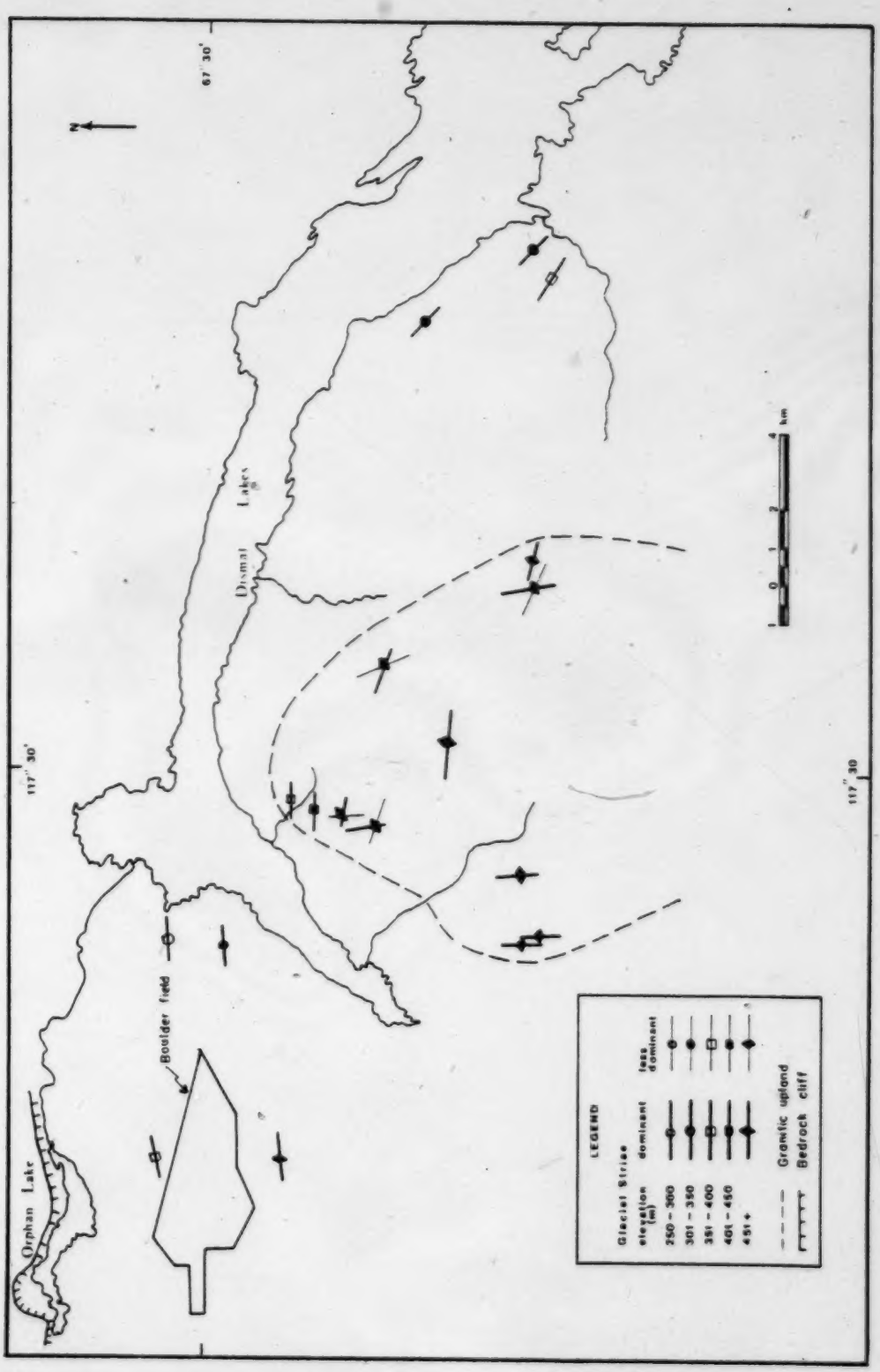

Figure 3. Glacial striae - Dismal Lakes area

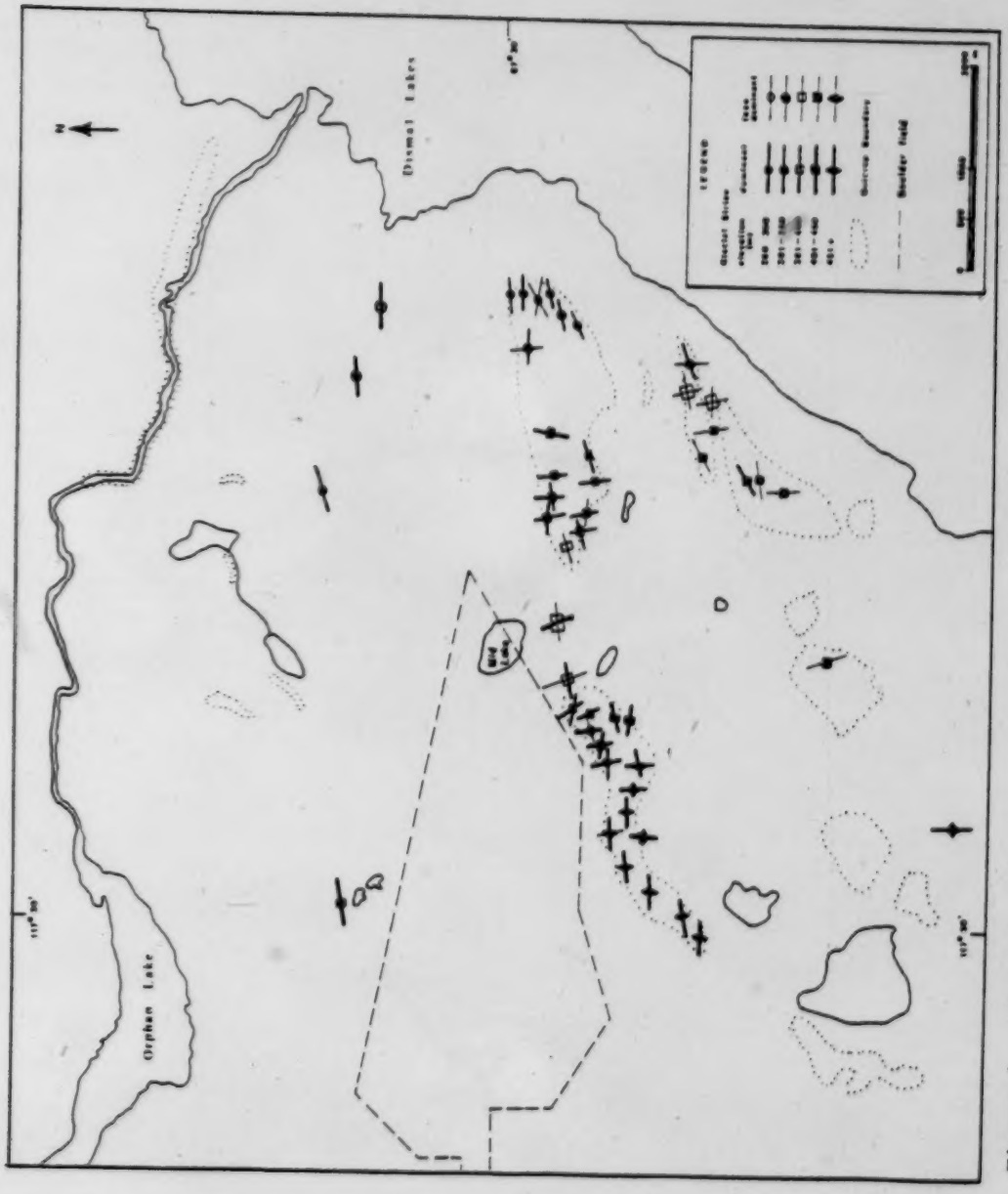

Figure 4. Glacial striae - west Dismal Lakes

striae in more than one direction were observed. At an outcrop, the most recent ice flow direction was determined from cross-cutting striae. Most of the striae measured only indicate the orientation and not the direction of ice flow. In this study, for ease of presentation, striae orientations are given between 180 ° and 360 ° azimuth.

Striae below 350 m asl at west Dismal Lakes are dominantly oriented westerly, averaging 263 °. Further east in the Dismal Lakes valley, striae at this elevation are northwesterly, parallel with the Dismal Lakes valley. Above 350 m asl at west Dismal Lakes two orientations of striae were frequently observed; one set of striae had an average orientation of 263 ° and the other 352 °.

On the granitic upland at 650 m asl, within a few metres of the maximum elevation in the region, striae are oriented at 277 °. Along the eastern edge of the upland, striae are oriented either at 287 ° or less often at 347 °. Along the southwestern margin of the upland, striae are oriented at 352 °.

In the west Dismal Lakes valley, small outcrops of Unit 11 sandstone and diabase have poorly preserved striae. Measured striae are oriented at 258 °, 260 °, 266 ° and 268 °. At the outcrops nearest the boulder field, a Unit 11 sandstone exposure has well developed striae at 264 ° and a diabase dike has poor to moderately developed striae at 260 °. On the two large Unit 11 sandstone outcrops southeast of the boulder field, the most abundant and best developed striae were observed at the east end of the outcrops. This was a function of the large areas of exposed polished bedrock on the eastern slopes.

(b) Landforms - Drumlinoid forms, flutings, molded bedrock outcrops and eskers can be used as secondary evidence of the last ice flow direction (Figure 5). Three drumlinoid forms, oriented at 315 °, are located at the southeast end of Dismal Lakes in the Kendall River valley. These elongated hills are approximately 1500 m in length, 300 m in width and 10 m in height. Flutings in the area comprise bedrock and/or drift molded into long linear ridges; most are poorly developed. At the southeast end of Dismal Lakes flutings are aligned at 319 °. North of Dismal Lakes numerous ridges covered by thin drift are oriented at 317 °. Five kilometres north of the boulder field faint linear depressions and ridges in thin drift are aligned at 271 °. In all cases the flutings parallel, or nearly parallel, the strike of bedrock bedding planes.

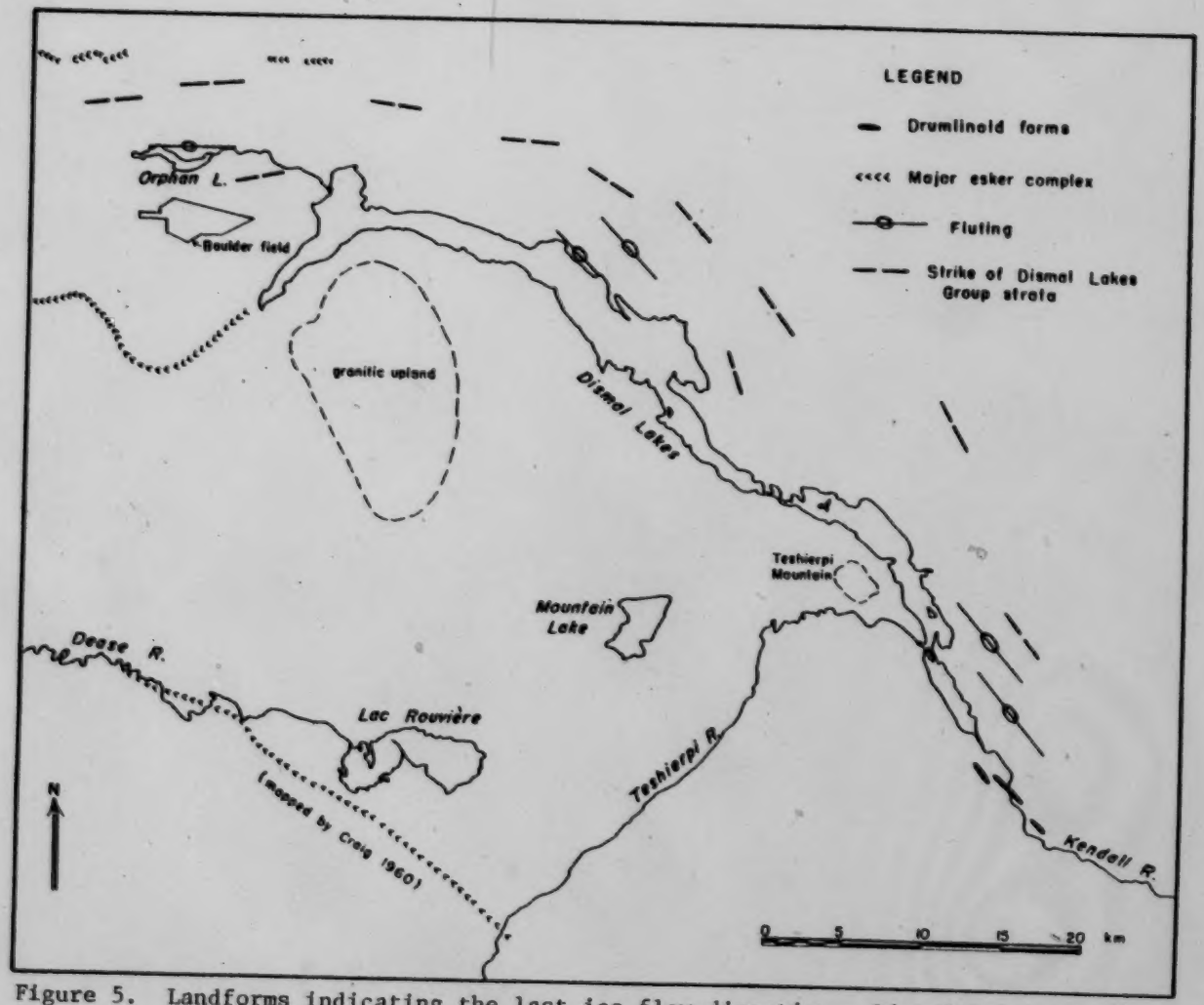

Figure 5. Landforms indicating the last ice flow direction - Dismal Lakes area

The strike of Dismal Lakes Group strata shifts from northwesterly, north of Dismal Lakes, to westerly north of Orphan Lake. Where the direction of ice movement parallels the strike of bedding, the topography consists of sharp ridges with valleys between, in other areas the terrain is variable.

In the area of the boulder field, Unit 11 sandstone outcrops are more exposed and polished on the northeast and east slopes. In addition, the drift covered slopes on the west and northwest sides of bedrock knobs are more gentle than those on the east and southeast. Where a northerly trending diabase dike is exposed immediately east of the boulder field a well defined scarp is evident along the east side of the dike whereas the west side is covered by gently sloping drift.

Where the orientation of major esker complexes in a region broadly coincide, their orientation can be used as secondary evidence for the last ice flow direction (Sugden and John, 1976). There are three major esker complexes in the Dismal Lakes region. An esker located 9 km north of the boulder field is oriented east-west, an esker 5 km southwest of the boulder field is aligned east-west for the majority of its length, and 24 km south of the granitic upland an esker is aligned northwest-southeast.

(c) Till Pebble Lithologies - Till pebble lithologies reflect bedrock units in the direction opposite to glacial flow. In order to provide evidence of ice flow direction, till pebble lithologies in the area of the west Dismal Lakes boulder field were identified. In percentages, the lithologies are: sandstone 42, quartzite 24, dolomite 10, granitic rocks 9, shale 8, other igneous and metamorphic rocks 6 and other rocks 1. The data for till pebble lithologies and bedrock units in the direction opposite to glacial flow appear in Appendix E.

(d) Till Fabric - The combined till fabric for five sample sites at or near the boulder field centre (20E, 10N) and all within 250 m of each other is plotted in Figure 6. A spherical probability density distribution was applied to this data (Mark, 1973). In this procedure, data is in the form of a 3x3 matrix, and the elements of the matrix can be regarded as defining points lying on a 3-dimensional ellipsoid. The eigenvectors of the matrix yield the directions of the principal axes of the ellipsoid and the eigenvalue represent the length of

EIGENVECTORS TREND	PLUNGE	EIGENVALUE	NORMALIZED EIGENVALUE
216.9°	8.5°	107.61	0.43
125.2°	11.2°	87.60	0.35
343.3°	75.9°	54.78	0.22

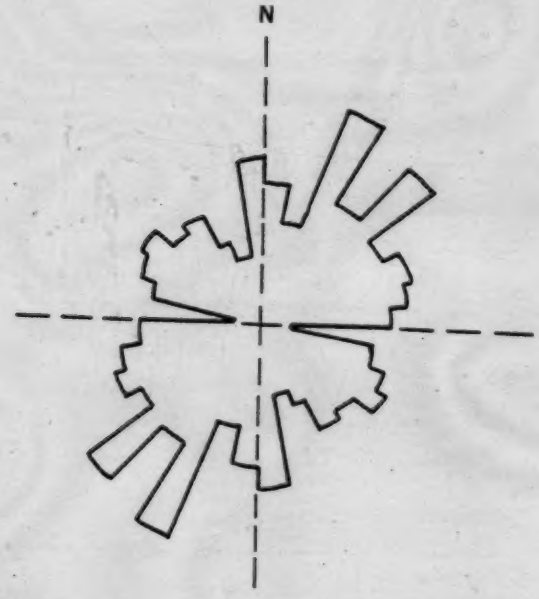

N = 250

Note: combined from 5 sample sites at or near the boulder field centre (20E, 10N), all sites are within 250m of each other

Figure 6. Combined till pebble fabric - west Dismal Lakes

these axes (Cubitt and Henley, 1978). The axes of maximum and minimum clustering are the eigenvectors associated with the largest and smallest eigenvalues, respectively, of a particular 3x3 matrix (Mark, 1973). Normalization produces an eigenvalue of unit length. The principal eigenvector has an azimuth of 217 °. The plunge of the pebbles ranges between 0 ° and 82 ° from the horizontal, with a principal eigenvector of 9 °. The normalized eigenvalues, used to measure the strength of the preferred orientation, are 0.43, 0.35 and 0.22. The pebbles measured were between 15 cm and 20 cm below the ground surface.

DISCUSSION

Published maps (Craig, 1960; Craig and Fyles, 1960; Prest *et al.*, 1968; St-Onge, 1980) indicate a regional northwesterly ice flow for the last ice in the area between Great Bear Lake and Coronation Gulf. In the Dismal Lakes area, the granitic upland is the highest topographic feature by at least 100 m. The direction of ice movement over the top of the upland was not influenced by topography. Striae on the upland indicate that the dominant ice flow direction was westerly during the last glaciation (Figure 3). The esker complexes in the Dismal Lakes region, which generally trend westerly, also indicate a westerly ice flow (Figure 5).

The flow pattern of the last ice in the west Dismal Lakes area was influenced by bedrock topography. The ice moved northwest in the central Dismal Lakes valley, parallel with the valley and the strike of the Dismal Lakes Group strata, and was diverted west and southwest at west Dismal Lakes. Ice was funnelled between the granitic upland south of Dismal Lakes and the bedrock cliffs north of Dismal Lakes (Figure 3). In addition, ice was diverted around the southern margin of the granitic upland. In the immediate area of the boulder field the direction of the last glacial advance was along a line of 260 ° azimuth (Figure 4). The best evidence for this orientation is provided by striae in the west Dismal Lakes valley and dominant striae on the two large Unit 11 sandstone outcrops immediately southeast of the boulder field (Figure 4).

Striae at low elevations provide the best evidence for the flow pattern along Dismal Lakes and in the west Dismal Lakes valley. Striae at higher elevations illustrate the

divergent flow around the granitic upland.

Drumlinoid forms at the southeast end of Dismal Lakes and flutings east and north of Dismal Lakes provide evidence that the last ice moved northwest along the Dismal Lakes valley (Figure 5). North of Orphan Lake flutes trend westerly, indicating ice flow had been diverted west. Bedrock bedding planes are a major influence on local bedrock topography west, north and east of the Dismal Lakes. The flow direction of the last ice likely was controlled by bedrock topography because all flutes in the area parallel or nearly parallel the strike of bedrock bedding planes.

Small scale features in the boulder field area support a westerly flow for the last ice. The largest areas of polished rock occur on the eastern and northeastern sides of large outcrops. Also, several bedrock knobs which have gentle slopes of drift on the western side are crude crag and tail features.

Clasts in till reflect bedrock units in the direction opposite to glacial flow and therefore may be useful indicators of ice flow direction. Clasts in the centre of the boulder field are dominated by sandstones and quartzites of local origin. Shale clasts are likewise of local origin. Dolomite and granitic clasts may provide an indication of ice flow direction. Dolomite outcrops exist north and northeast of the boulder field; the dolomite was easily weathered as evidenced by resistant quartz veins raised above a deeply pitted dolomite surface. The solution weathering of the dolomite indicates that it is soft and not resistant enough to be glacially transported far or reworked from older drift. Granitic rock outcrops form resistant highland areas south and southeast of the boulder field. One possible explanation of the dolomite and granitic clast abundances is that the dolomite clasts are from local outcrops, whereas granitic clasts are either far travelled or reworked from older drift. This explanation requires that the last ice in the boulder field area advanced from the east-northeast.

Additional evidence for west-southwest movement of the last ice in the boulder field area is provided by geochemically anomalous areas of till and the uraniferous sandstone boulder distribution. Till geochemistry results indicate that the highest uranium and copper values occur in the northeast, with values decreasing to the west-southwest. Detailed prospecting has delimited the boulder field to a north-south distance of 2 km and an east-west distance greater than 5 km. These elongated east-west patterns parallel the

last ice flow direction.

The random orientation of till pebbles at west Dismal Lakes (Figure 6), as evidenced by all three normalized eigenvalues being approximately equal, and the wide range of pebble plunges, indicates that no fabric exists at 20 cm depth. No pebbles were measured below this depth because the watertable exists at 20 cm depth and permafrost starts at < 1 m depth. It is believed that a fabric was originally present in the till, but that post glacial processes including, frost heave, gelifluction, cryoturbation and water movement over the permafrost, destroyed the fabric. Till pebble fabrics are not a useful method of determining ice flow directions in the west Dismal Lakes area.

An earlier glacial advance moved north-northwesterly over the area west of Dismal Lakes. Cross-cutting striae, generally at high elevations, are the evidence for this advance. Although erosional features from this earlier glaciation are present, no deposits produced by the earlier glaciation were identified in the field.

SURFICIAL SEDIMENTS

Knowledge of the types and distribution of surficial sediments is now becoming recognized as an integral part of boulder tracing and mineral exploration. If exploration concentrates solely on trying to see through the drift cover, without examining it for clues to locating mineral deposits, a great deal of information is missed (Vanderveer and Sparkes, 1982). Mapping at west Dismal Lakes was undertaken for three specific reasons.

(1) To determine in which sediment type the uraniferous sandstone boulders are contained, so that the depositional environment of the boulders can be reconstructed.

(2) To know the areal extent of the surficial units, particularly till, so that only one unit was sampled for the geochemical study. Sampling different units may explain some geochemical irregularities.

(3) To provide basic data for the reconstruction of the last glacial and post glacial history. Knowledge of past glacial and post glacial processes aids in the explanation of the boulder distribution and geochemical results.

Table 1 is a list of the surficial units for the west Dismal Lakes area, and Figure 7 illustrates their distribution.

Eon	Era	Period	Epoch	Map-Unit	Lithology
PHANEROZOIC	CENOZOIC	QUATERNARY	HOLOCENE	7	Block field ; freeze and thaw effects
				6	Area affected by mass wasting ; mostly till
				5	Alluvium and deltaic deposits ; silt, sand, gravel
			PLEISTOCENE	4	Glaciofluvial outwash ; gravel , sand
				3	Ice-contact stratified drift (esker and esker complexes), gravel , sand , some till
				2	Till ; clayey sand to sand ; 2a reworked and/or eroded
UNCONFORMITY					
PROTEROZOIC	APHEBIAN AND HELIKIAN			1	Bedrock

Table 1. Surficial geology units - west Dismal Lakes

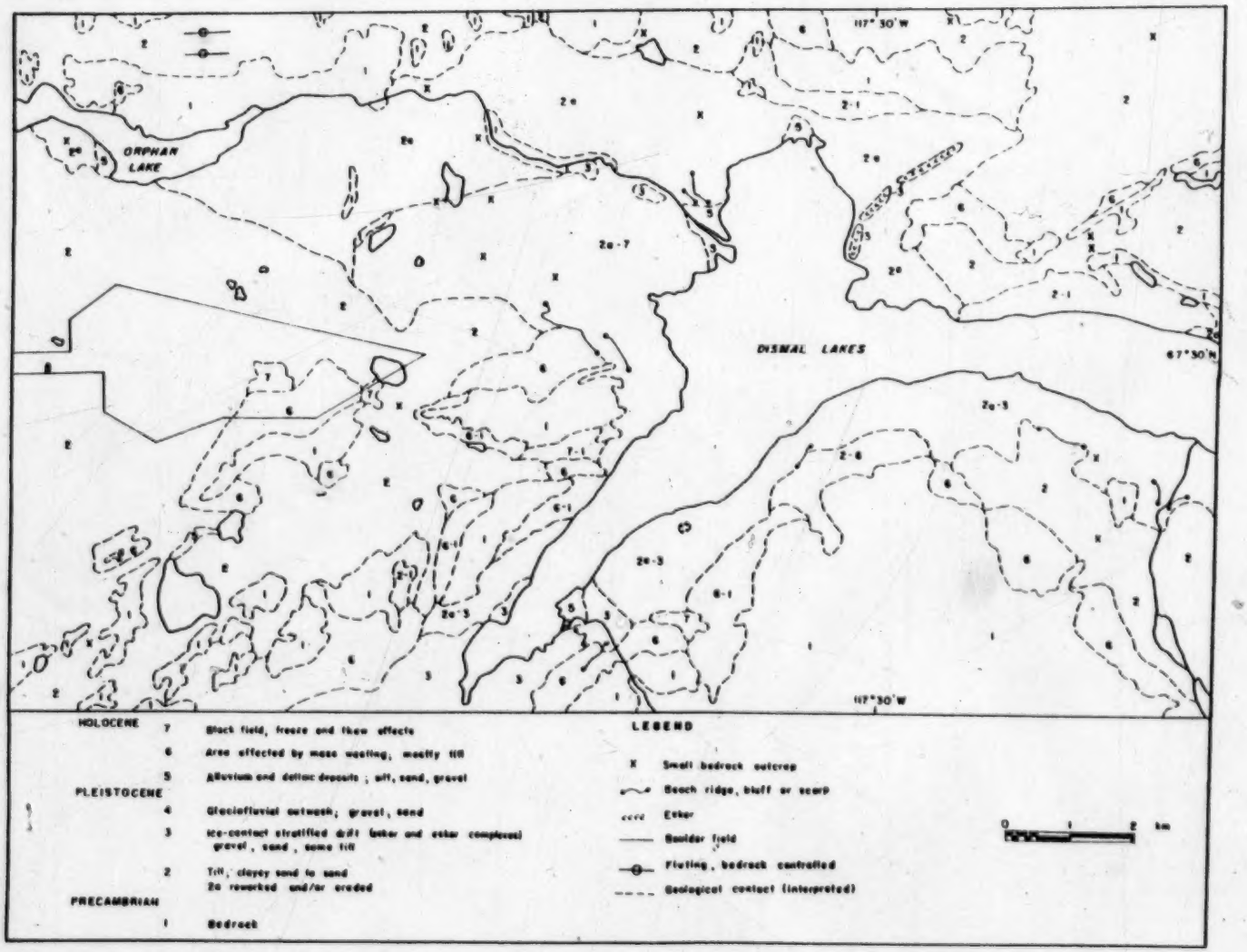

Figure 7. Surficial geology - west Dismal Lakes

(a) Bedrock (Unit 1) - Exposed bedrock and areas where drift is less than one metre in thickness are included in this unit. Bedrock outcrops have been rounded and streamlined by glacial action, although the orientation of the outcrops is largely controlled by regional structure. Exposed bedrock for the most part is smooth and lichen covered. However, dolomite outcrops north of the boulder field have a pitted weathered surface. Pebbles, cobbles and boulders commonly rest on bedrock. The contact between scattered clasts and thin till veneer is usually distinct; the contact is locally gradational.

(b) Till (Unit 2) - Till is defined for this study as "a sediment that has been transported by and subsequently deposited by or from glacier ice, with little or no sorting by water" (Dremanis, 1982). Till is the surficial unit of greatest interest for this study as most uraniferous sandstone boulders and all geochemical sampling sites are located in it.

Till is the most common surficial sediment and occurs as till plains. Generally the till lies directly on glacially striated bedrock. In many places the till is sufficiently thick to mask the underlying bedrock topography, as in the boulder field area.

Typical till in the Dismal Lakes area is boulder rich with a fine to medium sand matrix, which locally may be silty or clayey. The till is loose and massive with occasional fissility. All till investigated was unfrozen, within the active layer, and often was water saturated.

The texture and colour of the till matrix are directly related to local bedrock composition. At west Dismal Lakes, eight till samples (for locations see compilation map) underlain by Unit 11 sandstone average 19 % clay, 34 % silt and 47 % sand (Figure 8). The colour of till across the boulder field area was generally light brown (7.5YR 6/4 dry). In the PEC area, three till samples collected over dolomite subcrop average 23 % clay, 30 % silt and 47 % sand. Till at PEC is light yellowish brown (10YR 6/4 dry). At an exposure approximately 20 km east of the west Dismal Lakes boulder field, the till matrix becomes clay-rich with a distinct red hue less than 0.5 km in the direction of glacial flow from an interpreted contact between quartzose sandstone and red shale bedrock.

The till at west Dismal Lakes contains abundant pebbles, cobbles and boulders. Clasts up to 0.5 m in diameter exist; most are from 3 to 5 cm in diameter. The till clasts are mainly subangular, but range from angular to rounded. The roundness of clasts is partly

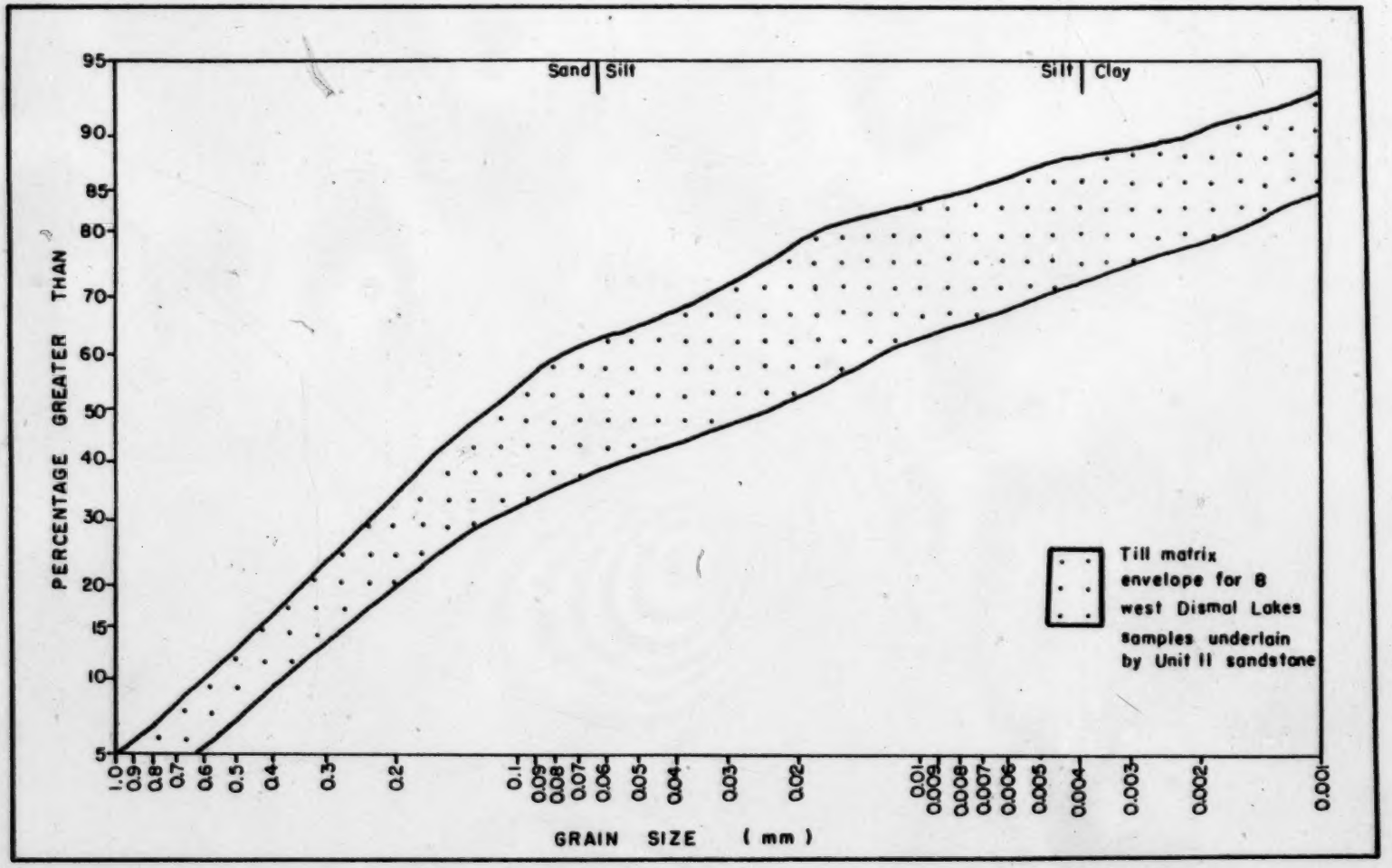

Figure 8. Till matrix envelope - west Dismal Lakes

a function of lithology. In general, shales are angular, sandstones and quartzites are angular to subrounded, and other lithologies are subangular to rounded. Boulder densities on the till surface average five boulders per square metre, which is consistent with that recorded in the PEC area (Vagners, 1977).

Reworked and/or eroded till (Unit 2a) occurs along the shore of Dismal Lakes. Limited exposures, mostly along interpreted beach ridges, indicate the removal of fines and the concentration of sands and gravels. Beach ridges occur at elevations up to 320 m asl in the Dismal Lakes region. All beach ridges have clast littered slope faces.

Beach ridges at west Dismal Lakes occur at elevations between 300 and 320 m asl, and range in height from 2 m to greater than 11 m. The ridges consist of extremely sandy and gravelly washed till or very poorly sorted gravelly sand. The matrix is dominated by coarse sand and granules. Subrounded to angular clasts, up to 40 cm in longest dimension, account for approximately 30 % of the material. Beach ridges north and east of the granitic upland, at elevations of 290 to 300 m asl, are approximately 3 m in height. A sandy till ridge north of the granitic upland contains numerous clasts up to 30 cm in length. A ridge east of the granitic upland consists of coarse sand and gravel, similar to ridges at west Dismal Lakes.

Six exposures of surficial sediments below 320 m asl were examined at west Dismal Lakes. Three are beach ridges. The other three sites, all along the river flowing between Orphan and Dismal Lakes, have a 20 to 60 cm thick surface layer of sand over till. The sand is moderately clean with some granules and larger clasts. The till matrix appears to become more clay-rich with increasing depth.

A network of poorly developed runoff channels indicates that an area of till at west Dismal Lakes has been eroded. The drainage pattern is braid-like in the eroded area, while horse-tail drainage (French, 1976) has developed on uneroded till with similar slopes.

(c) Ice-contact stratified drift (Unit 3) - During deglaciation of the area, meltwater drainage towards the glacier margin resulted in the deposition of ice-contact stratified drift. Glaciofluvial sand and gravel occur within the area as eskers and esker complexes.

A major esker complex is located approximately 6 km southwest of the boulder field (Figure 5). It extends 7 km from the southwest arm of Dismal Lakes where it is

diverted west. The esker complex is best preserved southwest of the boulder field where the complex is approximately 20 m high and between 200 and 500 m across. The main crest can be traced for 9 km. Evidence suggests that the esker extends northeast and is covered by Dismal Lakes water. Drilling through the ice (Pawliuk and Trigg, 1981) encountered a minimum of 20 m and possibly up to 75 m of sand and gravel under the water of the southwest arm of Dismal Lakes. Remnants of sand and gravel, often eroded to beach ridges, occur along the shoreline of the southwest arm.

A small, narrow, discontinuous and sinuous esker exists on the north shore of Dismal Lakes (Figure 7). In addition, minor exposures of stratified sand and gravel were observed along the river east of Orphan Lake.

(d) Glaciofluvial outwash (Unit 4) - Proglacial meltwater, draining from a glacial lake, has the capability to erode ice-contact stratified drift and deposit a stratified sand and gravel plain. This has occurred south of the southwest arm of Dismal Lakes where a large meltwater channel was incised into an esker complex. The reworked sand and gravel was deposited in a broad plain immediately south of the channel.

(e) Alluvial and deltaic deposits (Unit 5) - Within the west Dismal Lakes area, minor accumulations of alluvium occur along streams, but the major deposits are deltas. Alluvial and deltaic deposits consist of silt, sand and gravel.

(f) Areas affected by mass wasting (Unit 6) - In the study area, gelifluction terraces between 25 and 40 cm in height occur in till on slopes greater than 1.5 °. In general a distinct terrain surface change occurs at 3 ° slope. On slopes greater than 3 ° gelifluction terraces dominate, whereas on slopes less than 3 ° hummocks and surface boulders are common.

Material affected by gelifluction at west Dismal Lakes has a preferred down slope alignment of pebbles (Figure 9). The principal eigenvector has an azimuth of 151 °, which lies close to the orientation of the slope at 137 °. The principal normalized eigenvalue is high (.81). Local scars, indicative of rapid mass movement, exist in the Dismal Lakes area. Small, shallow active layer slumps occur in till on the slopes of the granitic upland and

EIGENVECTORS TREND	EIGENVECTORS PLUNGE	EIGENVALUE	NORMALIZED EIGENVALUE
151.0°	8.1°	40.45	0.81
59.8°	8.2°	7.17	0.14
285.0°	78.4°	2.38	0.04

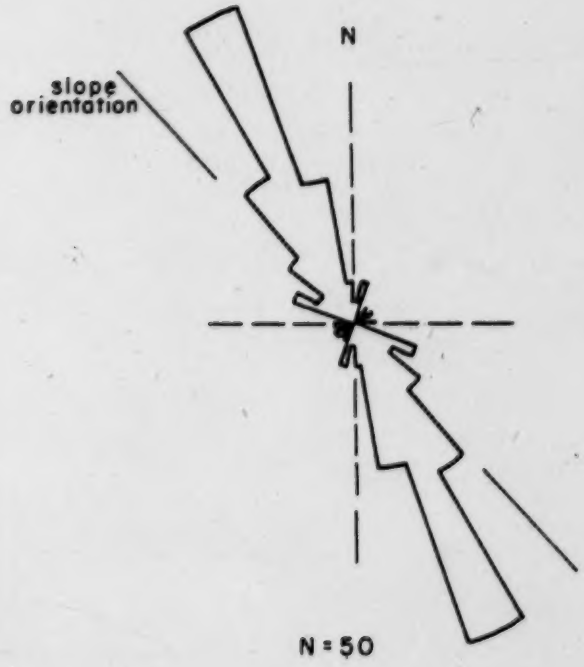

Figure 9. Pebbles oriented by gelifluction

along stream embankments.

(g) Block fields (Unit 7) - Block fields are usually level areas covered with angular blocks of rock. Block fields are common in periglacial areas underlain by sandstone or shale. In the west Dismal Lakes area small block fields are associated with Unit 11 sandstone. The blocks which range in size from 0.3 to 2.0 m across their largest dimension, are extremely angular and are randomly oriented. The block fields have an open-work texture at the surface; infilling between blocks by finer sediment often does not occur until a depth of 1.0 m.

In many locations the closest bedrock outcrop is over 0.5 km from a block field. In spite of this, the dense packing, extreme angularity and large size of boulders indicates the frost wedged blocks formed "in situ" and are close to bedrock.

DRIFT THICKNESS

Drift thickness, particularly in the west Dismal Lakes valley, is used in the reconstruction of the erosion and deposition of the uraniferous sandstone boulders and associated till. Drift thickness was estimated from bedrock outcrops, block fields, three drill holes, exposures along creeks, and landforms. Away from these control points interpreted drift thickness is highly speculative.

In most areas drift thickness is 5 m or less, with the bedrock surface controlling the topographic surface. Bedrock outcrops commonly project through the drift cover or are thinly mantled by drift. The bedrock surface below drift is believed to be highly irregular. This can be best illustrated near the PEC uranium deposit where drift thickness between holes at the same elevation and less than 150 m apart can vary by 35 m. Drift filled depressions, several metres deep, exist within areas covered by generally thin drift.

An estimated drift thickness of less than 5 m exists in the west Dismal Lakes valley within 7 km of Dismal Lakes. This interpretation is based upon scattered bedrock outcrops and block fields throughout the area, three drill holes west of Mid Lake which encountered a maximum of 6 m of drift (Pawliuk and Trigg, 1981), and three exposures of less than 2.5 m of drift along the river between Orphan and Dismal Lakes.

Data does not exist on the drift thickness of the till plain on which the boulder field is located. The flat nature of the area may imply a significant thickness of drift, however similar topography south of Dismal Lakes has only 2.5 m of drift. Because the regional dip of the bedrock is approximately 10 ° north, the greatest drift thickness is expected near the northern edge of the till plain. It is estimated the till plain consists of drift up to 10 m in thickness.

B. URANIFEROUS BOULDER FIELDS

WEST DISMAL LAKES BOULDER FIELD

West Dismal Lakes uraniferous sandstone boulders were examined. The distribution of the boulders by location, volume and radioactivity was analyzed to determine whether the direction of the last ice flow and / or a possible bedrock source for the boulders was indicated. The angularity, lithology, mineralogy and size of the boulders were examined with the aim of obtaining data on: the distance of boulder transport; the mechanisms of boulder erosion, transport and deposition; and / or the bedrock source of the boulders.

RESULTS

(a) Boulders - Trigg, Woollett, Olson Consulting Ltd. personnel have discovered over 500 uraniferous boulders by ground radiometric prospecting using SPP2N scintillometers. Approximately 95 % of these boulders are sandstone. Grant (1980) states that the uraniferous sandstone boulders are generally grey to cream, fine grained, hematitic and / or limonitic, pyritic, highly siliceous quartzose sandstone. Approximately 5 % of the boulders are grit to pebble conglomerates. Two uraniferous sandstone boulders from the west Dismal Lakes boulder field assayed 0.30 % uranium oxide and 0.28 % copper, and 3.30 % uranium oxide and 0.60 % copper, respectively (Grant and Woollett, 1979). A petrographic study (Grant, 1980) indicated that the west Dismal Lakes boulders are mineralogically different from boulders derived from the PEC uranium deposit. All boulders discovered are on surface or are covered by less than 15 cm of glacial drift and

organic material.

(b) Boulder field shape - The distribution of uraniferous boulders at west Dismal Lakes is presented in Figure 10; exact boulder coordinates are listed in Appendix E. Not all areas containing boulders were prospected at the same grid spacing; prospecting grids are plotted in Figure 11. Reliable statistical interpretations cannot be made from an area prospected at different grid spacing. Since most boulders are within the area prospected at 10 m grid spacing, this area was analyzed in detail (Figure 11). Outside this area, the locations of uraniferous sandstone boulders were used in determining the general shape and boundaries of the boulder field.

Detailed prospecting along grid line 20E has delimited the main field to a width of approximately 2.2 km, from 0N to 22N. Sharp north and south boundaries occur at grid line 20E. The east and west boundaries are much less distinct; the field is at least 5.0 km long. Although the number of boulders decreases west of 10E, it is believed that the boulder field extends past the western limit of prospecting. The eastern limit of the field in the detailed study area is at 47E, however prospecting south of 10N resulted in the discovery of six boulders between 49E to 58E and 10N to 1S. A boulder at 67E, 11N is the most easterly boulder in the west Dismal Lakes area.

A contoured plot of boulder distribution in the detailed study area is presented in Figure 12. The plot is derived from 522 data points, each representing 1 ha. In the calculation of the data grid, Method B was used (see Chapter 2) (Figures 13 and 14 were obtained by the same procedure). Contouring filters out isolated boulders and provides a clearer picture of the shape of a portion of the boulder field. The area of greatest boulder concentration is elongated along 11N; a secondary elongation occurs along 21E. The greatest boulder concentration is located at 10N, 20E; this location is referred to as the boulder field centre.

(c) Boulder size - Uraniferous sandstone boulders range in volume from 252,000 cm^3 to less than 1,000 cm^3, while the average volume is approximately 19,000 cm^3. Dimensions of the boulders commonly have the ratio 4:3:2, though dimensions range from 1:1:1 to 3:1:1 to 2:2:1. The largest single dimension measured is 110 cm.

The distribution of uraniferous sandstone boulders by volume within the detailed study area is plotted in Figure 13. The largest boulder was located at the extreme western

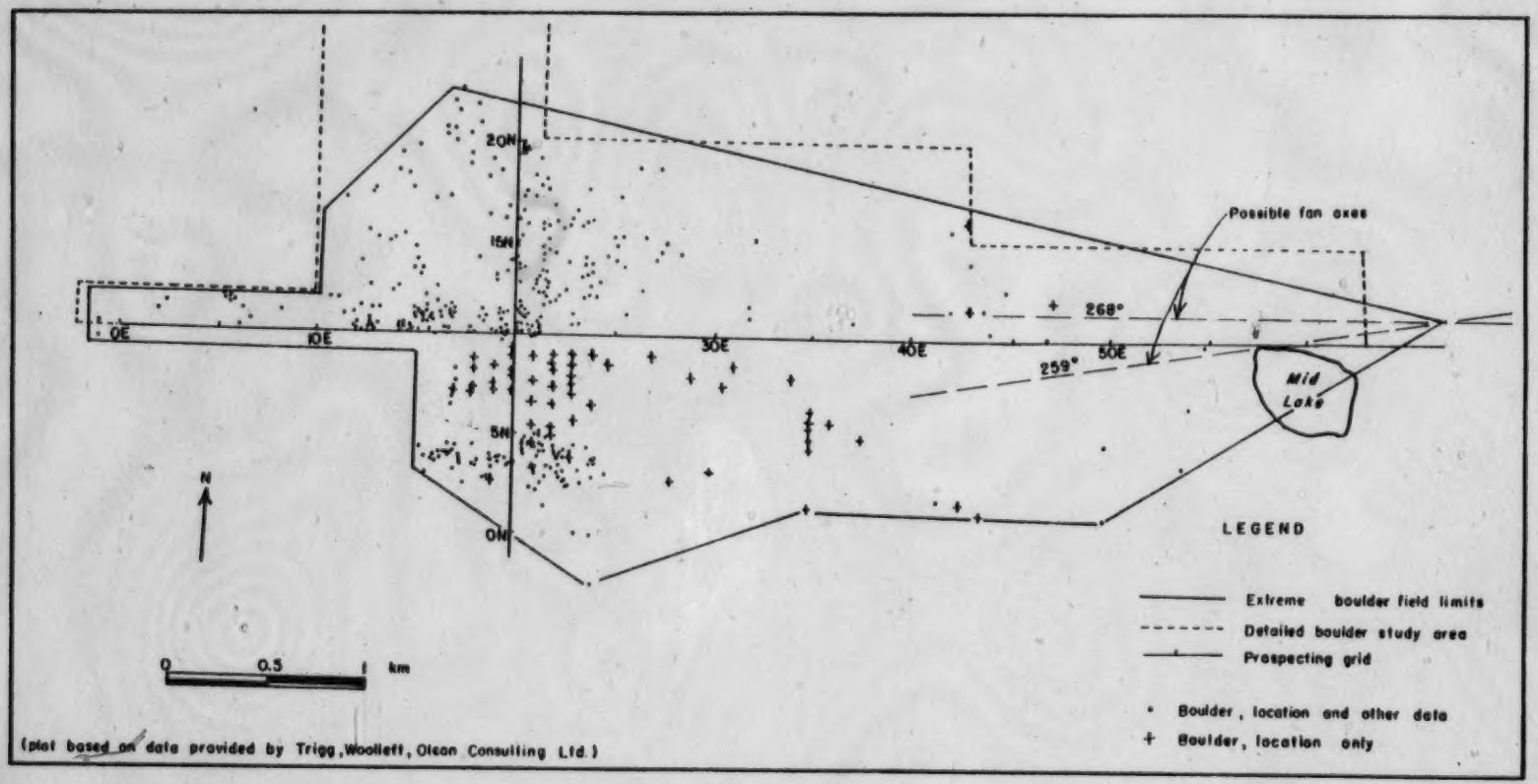

Figure 10. West Dismal Lakes boulder field

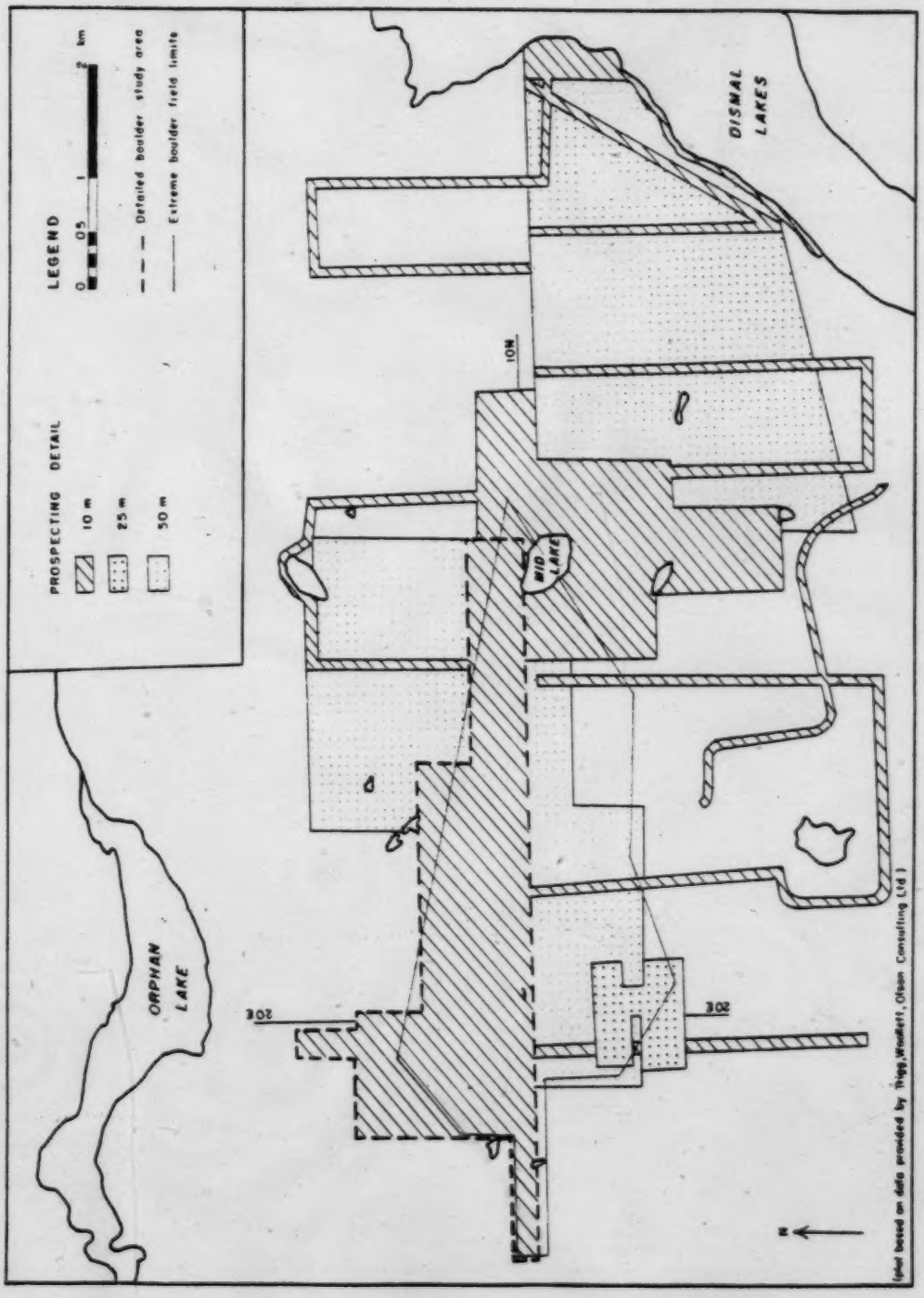

Figure 11. Prospecting grids - west Dismal Lakes

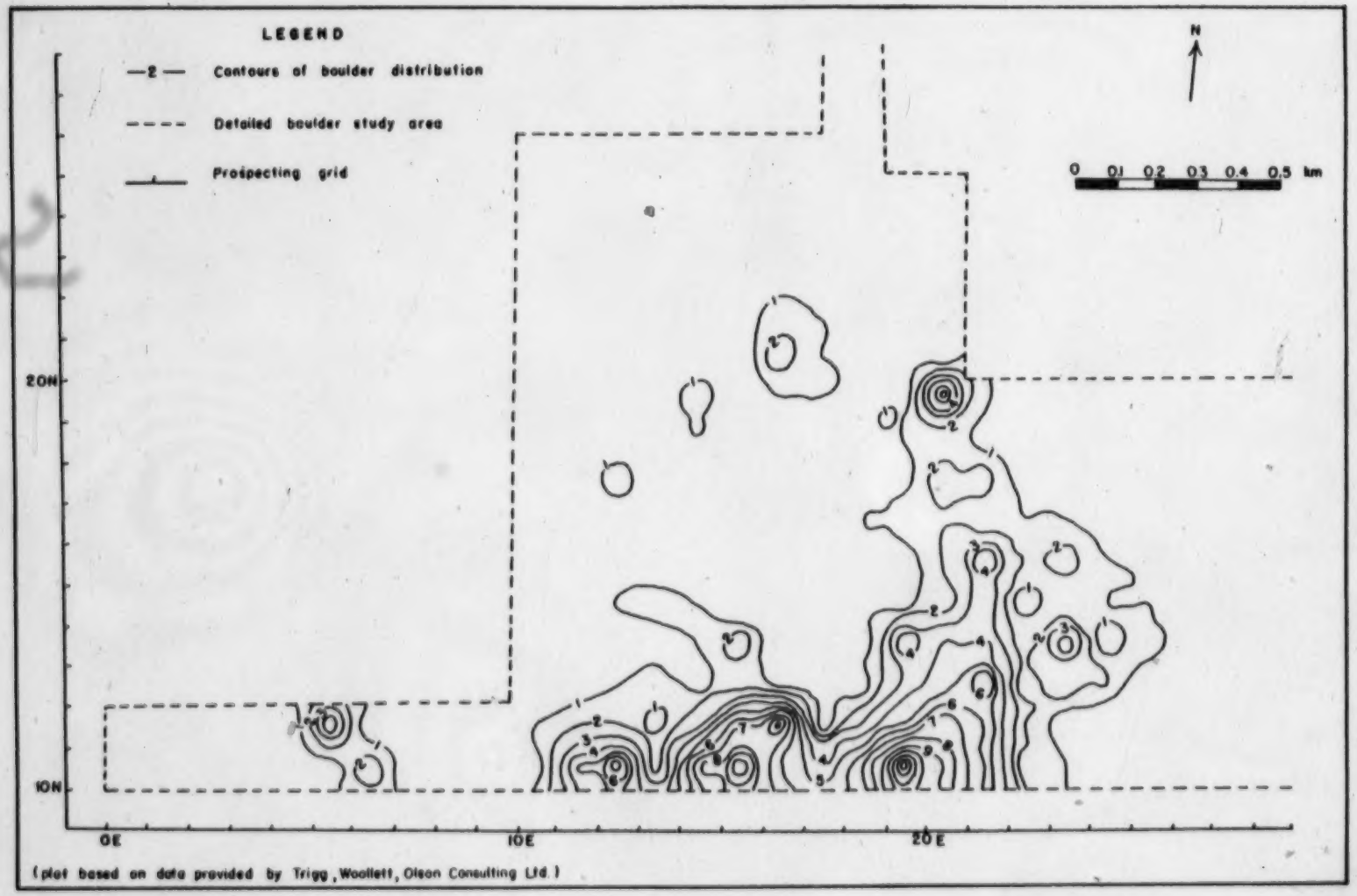

Figure 12. Contoured plot of boulder distribution

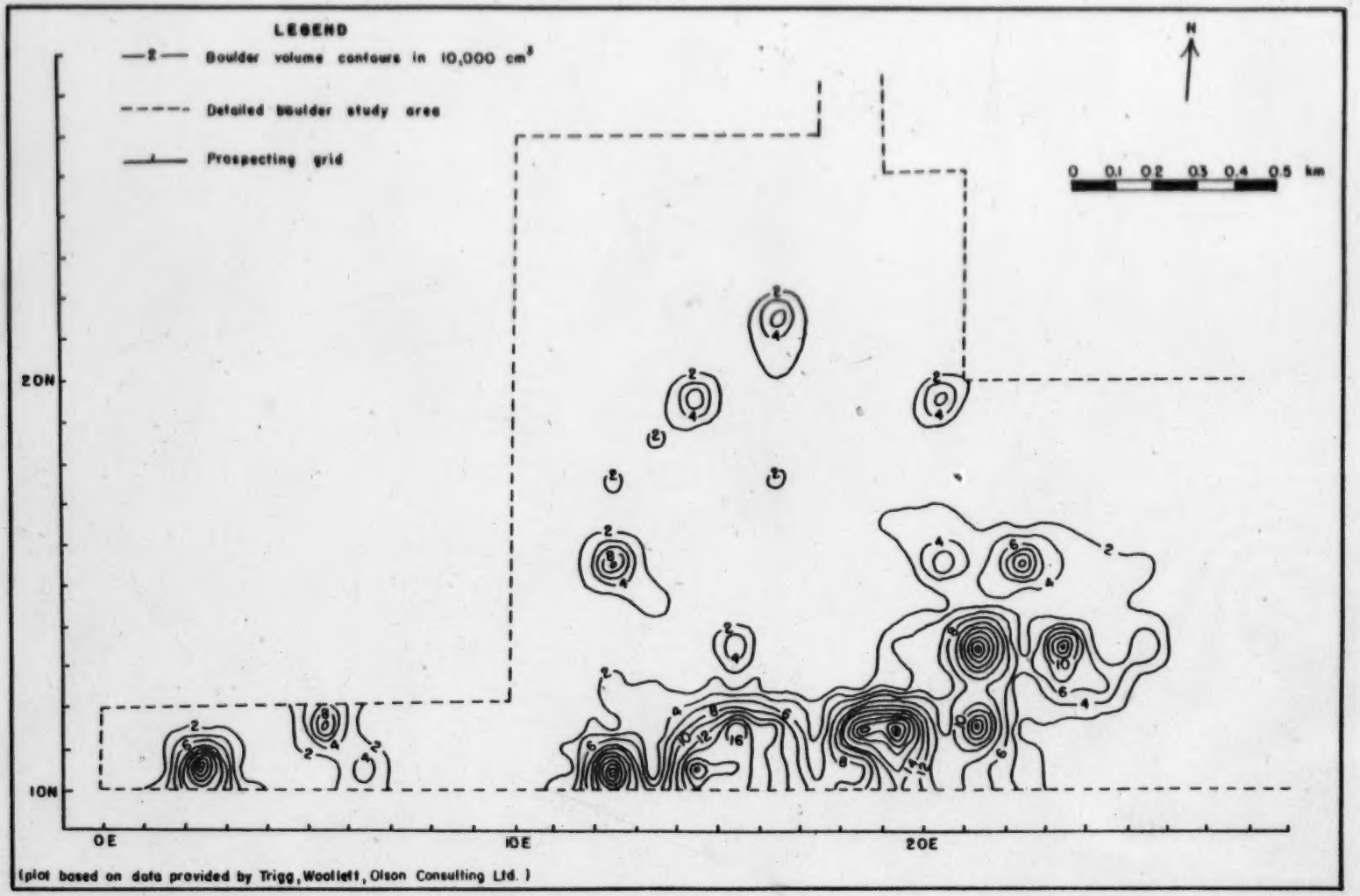

Figure 13. Contoured plot of boulder volume

edge of the mapped boulder field (2E, 11N).

(d) Boulder Radioactivity - Radioactivity produced by the boulders ranges from less than 1,000 cps to greater than 15,000 cps, the maximum which can be measured using a SPP2N scintillometer. Most of the uraniferous sandstone boulders in the detailed study area produced radioactivity between 1,000 and 5,000 cps; the average was approximately 4,000 cps. Volume and radioactivity of the uraniferous sandstone boulders are not related; the largest boulder (252,000 cm^3) produces radioactivity of 2,000 cps, and many boulders with radioactivity greater than 15,000 cps are smaller than 1,000 cm^3.

The distribution of radioactivity of uraniferous sandstone boulders in the detailed study area is plotted in Figure 14. The highest radioactivity is concentrated along line 10N between 12E and 21E. A secondary high occurs at approximately 20E, 20N.

(e) Boulder Angularity - Boulder angularity, for this study, is defined as the length of the curved edge between two perpendicular faces of a clast measured in centimetres (Bayrock, 1980). Therefore, the larger the angularity value the more rounded the clast. The angularity of the uraniferous sandstone boulders ranges from 1 to 11; the angularity mean and mode are 5. Angularity measurements were obtained by Grant (1980) from 71 boulders in the detailed study area and from 3 boulders southeast of this area. Grant believes the measured boulder edges resulted from glacial action and were not caused by failure along structural planes in the rock or post glacial weathering.

Angularity data can sometimes be used to determine the distance of boulder transport. A scatter plot of angularity versus distance west of 67E, the location of the easternmost uraniferous sandstone boulder, is given in Figure 15. Regression analysis of boulder angularity on the distance west of 67E was performed. The coefficient of determination, or the proportion of variation in the dependant variable (angularity) accounted for by the independant variable (distance west from 67E) is very small, 0.053. In other words, knowledge of the distance west from 67E improves our prediction of angularity by only 5.3 % from randomness.

Bayrock (1980) relates the degree of boulder rounding to the distance from the boulder source. The approximate distance to the source is determined from the formula $D=KS^2$, where D is the distance to the source in metres, K is a constant having a value between 60 and 100, and S is angularity in centimetres. D is the minimum distance of

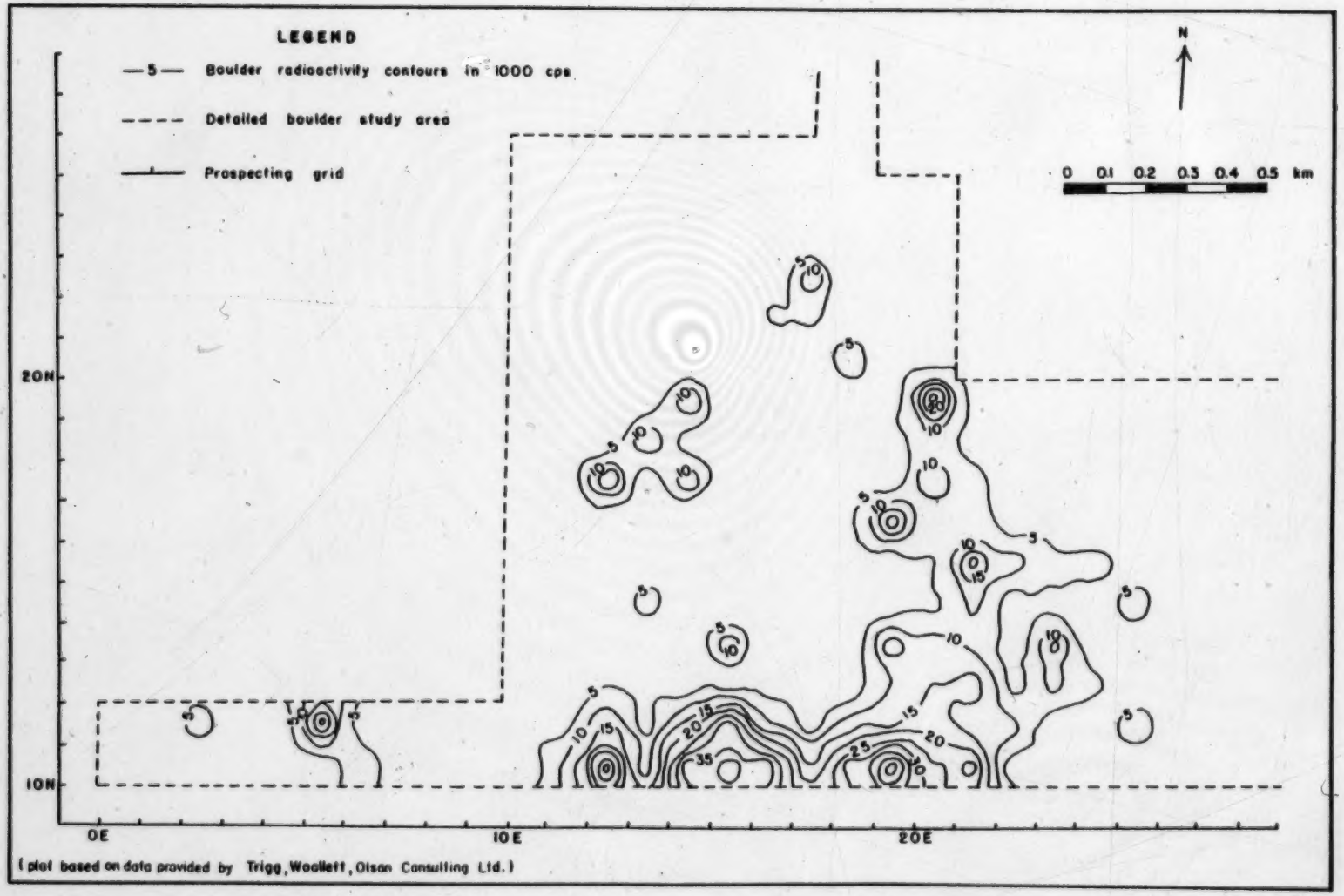

Figure 14. Contoured plot of boulder radioactivity

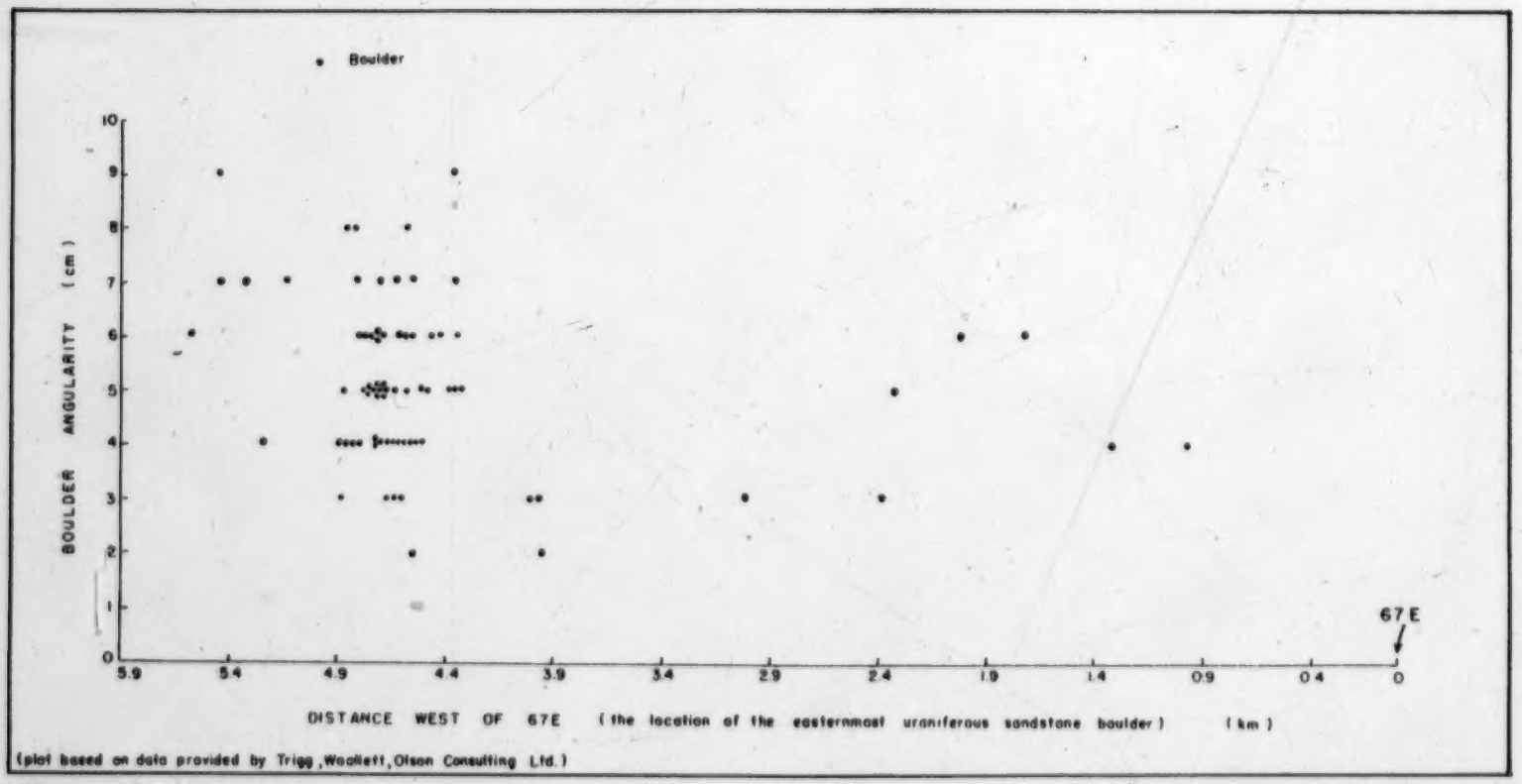

Figure 15. Plot of boulder angularity versus distance west of 67E

transport, assuming the boulder travelled in a basal position within the ice. If basal material is moved above the basal zone in the ice, D will be less than the distance of transport. The constant K is dependent upon boulder lithology. Bayrock suggests K values of 60 for well cemented sandstone, 80 for granite and 100 for orthoquartzite. The west Dismal Lakes boulders are well indurated quartz cemented sandstone, and therefore would have a large K value. In applying the formula using a K value of 100 and the mean angularity of 5, the calculated minumum distance of basal position transport of the boulders is 2.5 km.

DISCUSSION

(a) Fan and Train Defined - A boulder fan is an accumulation of boulders with distinct lithology and / or mineralogy which have been deposited by glacial action within a V-shaped area with 5 ° to 15 ° between the sides and which is more or less parallel with glacial movement. This definition was derived from boulder field descriptions by Bayrock (1980; personal communication January 19, 1983), Minell (1978), Hyvarinem *et al*. (1973), Dreimanis (1958) and Shilts (1976). If the angle formed by the sides is close to 0 °, then the fan is called a boulder train (Bayrock, 1980). The proximal end of a boulder fan (apex) or train may coincide with the bedrock source of the boulders or there may be a gap. Bayrock (1980) reports the former is more typical than the latter. In the ideal situation the concentration of boulders decreases exponentially away from the bedrock source (Shilts, 1976). In reality, the concentration of boulders often increases away from the bedrock source before it begins to decrease (Bayrock, personal communication January 19, 1983). The center line of a boulder fan or train is called the axis. The concentration of boulders typically is higher along the axis and falls off toward the sides. The axis may have a slightly different orientation than glacial directions obtained from striae and other indicators. Variations of up to 15 ° may be encountered, though Bayrock (personal communication January 19, 1983) estimates that 50 % of the time, axis and striae coincide.

(b) Proposed Fan - The west Dismal Lakes boulder field has neither an ideal fan nor train shape. The extreme boulder field limit (Figure 10), which enclose all mapped boulders

in the field, is elongated approximately east-west and has a crude fan shape centred on the easternmost boulder. Although no sharp northern fan boundary exists, one may argue that a line between 11N, 67E and 22N, 18E is a crude boundary (Figure 10), as no boulders have been mapped north of this line. The main boulder concentration (Figure 12) is elongated east-west along grid line 11N. Along grid line 20E detailed prospecting revealed the boulder field extended from 0N to 22N; bisecting this distance is grid line 11N. This line may be the axis of the boulder fan, it deviates by about 8 ° from the 260 ° direction of the last glacial advance through the boulder field area. However, the line bisecting the arc subtended by the fan's apex is oriented 259 °. This line, almost exactly coinciding with the last ice flow direction, may also be considered as the boulder fan axis.

The fan has an arc of 43 °. Although this angle is large compared to that of most fans produced by one glacial advance, it is smaller than that of fans produced by two or more separate glacial advances (Hyvarinen *et al.*, 1973).

It must be emphasized that many of the boulders used to construct the extreme boulder field limit are located in areas prospected with grids greater than 10 m (Figure 11). Tight control does not exist on the boulder fan outline in these areas. The generalized form of the boulder fan should only be used to interpret broad trends.

Length and Dispersion - The distribution of boulders is well known in the northern half of the proposed fan. Analysis of this distribution provides insight on the processes which formed the boulder fan. The number of boulders in 100 m wide swaths west of 67E and north of 11N is plotted in Figure 16. With increasing distance away from the source the concentration of boulders initially increases and then subsequently decreases (Figure 16(a)). Bayrock (personal communication January 19, 1983) and Minell (1978) have observed similar boulder distributions. Bayrock suggests that this boulder distribution is a modification of the ideal dispersion curve (Figure 17).

The west Dismal Lakes boulder dispersion curve may be represented by the outlined portion of Bayrock's modified dispersion curve (Figure 17). The general shape of both curves are similar; the maximum accumulation of boulders occurs in the central portion of the curve and the portion of the curve furthest away from the source has a more gradual slope than the portion between the crest and the source. If Bayrock's modified dispersion curve is used it predicts the source area for the boulders is

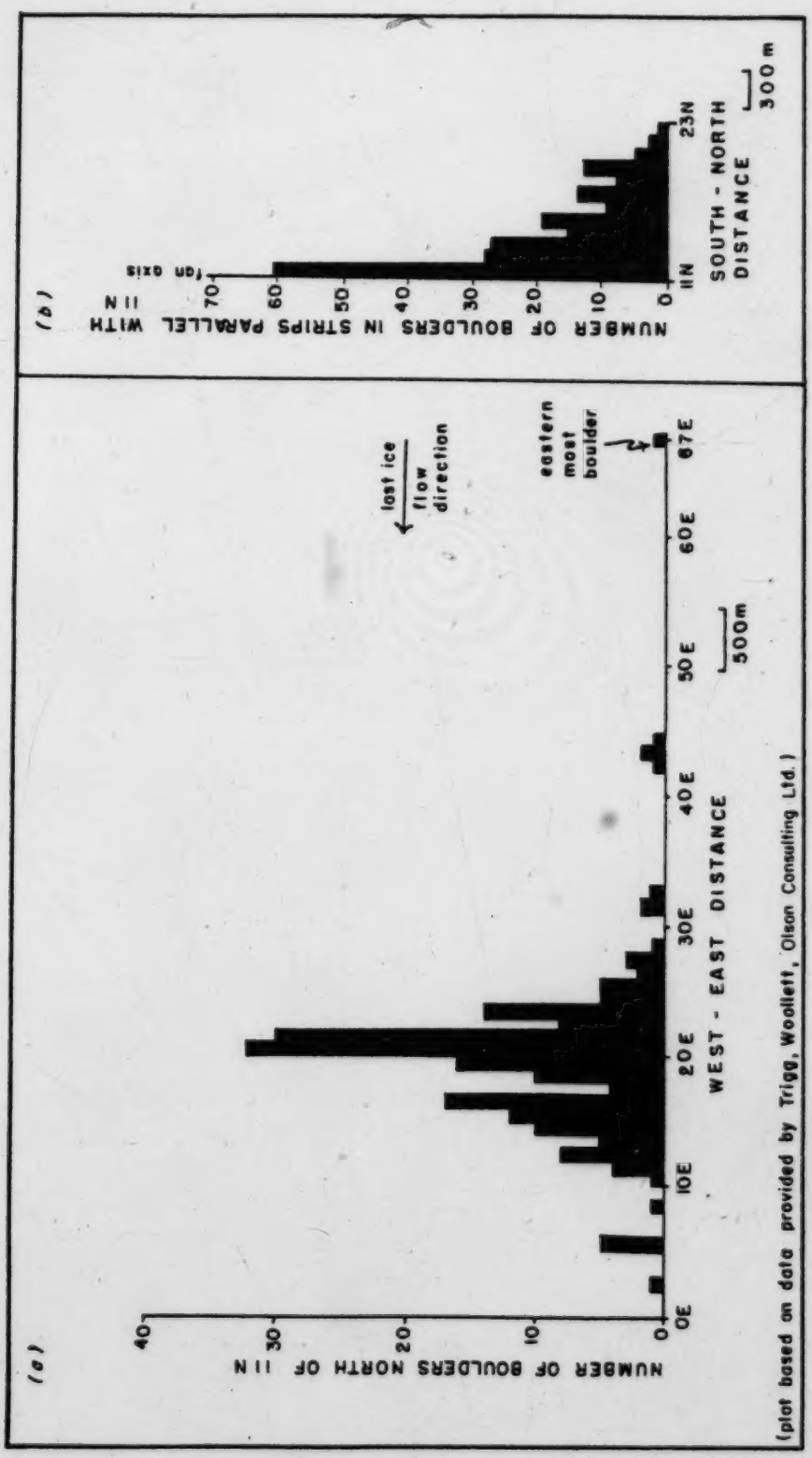

Figure 16. Boulder distribution away from 67E and 11N

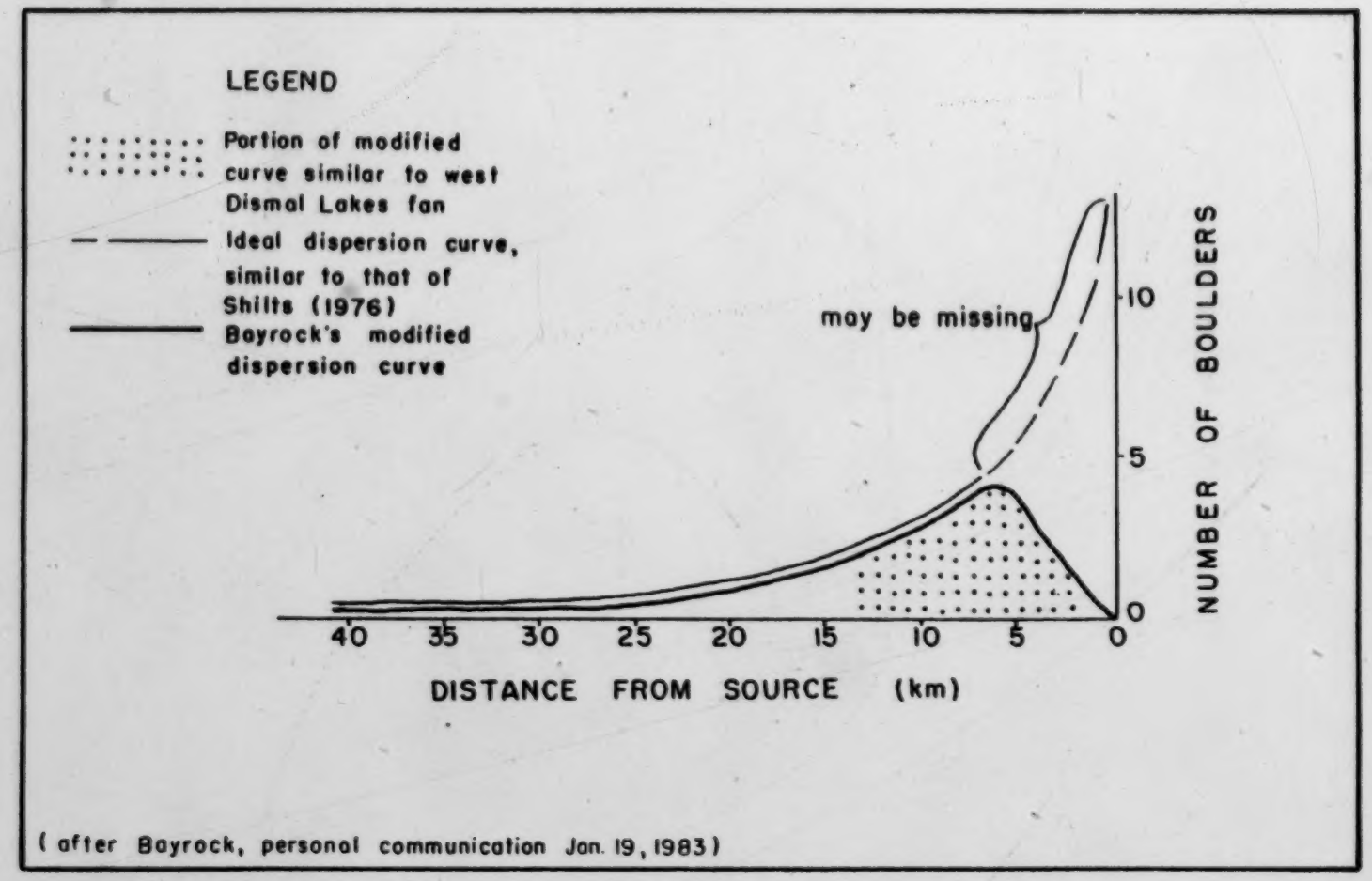

Figure 17. Glacial dispersion curves

approximately 5 km east of the main boulder concentration and shows that the greatest accumulation of boulders is not immediately west from the source. However, Bayrock does not provide an explanation of the processes leading to the dispersion pattern. Possible explanations are presented in the next chapter, after ice sheet conditions during erosion, transport and deposition of the uraniferous sandstone boulders are discussed.

Width and Dispersion - The only characteristic of the proposed fan which is in agreement with the ideal dispersion model is the decrease in boulder concentration away from an axis (using 11N in this case) (Figure 16(b)). The sharp decline away from 11N provides further evidence that the fan results from only one glacial advance (Bayrock, 1980).

(c) Patterns Within the Boulder Field - The main concentration of boulders (Figure 12) forms a crude V-shaped pattern pointing eastward. This may indicate a fan with an east-west axis.

Volume and Radioactivity - The plots of boulder distribution, volume and radioactivity (Figures 12, 13 and 14), all of which were derived by the same method, have the same general outline of the main boulder concentration. In addition, the major trends within the main boulder concentration are consistent between the three plots. Some differences between plots exist, such as the extreme value on the volume plot at 2E, 11N which results from two boulders, one of which is the largest mapped at west Dismal Lakes. It is concluded that only boulder locations need be analyzed, as boulder volume and radioactivity data do not provide any significantly different information from that of boulder distribution.

Boulder Angularity and Transport Distance - According to Powers' (1953) chart for visual estimation of rounding, the west Dismal Lakes boulders are angular. Boulder shape is believed to be largely a result of glacial processes. Even though climatic conditions necessary for frost shattering have occurred during the post glacial period, the lack of rock fragments near the boulders indicates that the process has not acted on the boulders.

Statistically, the angularity of west Dismal Lakes boulders apparently does not change away from the source because the coefficent of determination of 0.053 is not

significant. A slight increase in rounding away from the source may be interpreted visually from the scatter plot (Figure 15) when comparing boulders in the vicinity of 4.0 km west of 67E with those west of the main boulder concentration. However, this trend can not be seen within the main boulder concentration.

The angular nature of the boulders is not consistent with boulder transport in the basal zone. In such cases, roundness is a function of transport distance because of grinding of the boulders against the substrate and other debris. Transport of the boulders above the base of the ice sheet would best explain the angularity of west Dismal Lakes boulders. In such a situation the angular nature of the boulders results from quarrying and plucking processes. The crude, visually inferred trend of roundness increasing away from the source, probably results from the occasional contact between boulders while in transport above the ice sheet base.

Bayrock's (1980) formula which relates boulder angularity to the distance from the boulder source assumes basal transport of boulders. It is inappropriate to strictly apply his formula to the west Dismal Lakes boulders because the boulders were probably transported above the ice sheet base. However, the formula can provide an absolute minimum distance of transport, since abrasion is assumed to be less between boulders than between boulders and the substrate. The calculated distance of transport for the average boulder in the main boulder concentration is 2.5 km.

Shilts (1973b) traced granodioritic glacial erratics which occur on the ground surface in southeastern Quebec. Cobbles had maximum concentrations at 9 km and 18 km, and pebbles had maximum concentration 18 km, away from the source. He proposes that the boulders were eroded subglacially, transported above the ice sheet base, and deposited by melt-out. A similar mechanism is believed to have caused the west Dismal Lakes boulder field. However, the source at west Dismal Lakes probably is not as topographically prominent as that in Shilts' area, and therefore, the boulders were likely transported closer to the ice sheet base. The result is that the distance of transport of west Dismal Lakes boulders is probably less than 9 km.

Boulder angularity data indicate that the west Dismal Lakes boulders travelled greater than 2.5 km from their source (Bayrock, 1980). Comparisons with boulders with similar transport mechanisms (Shilts, 1973b) indicate the west Dismal Lakes boulders

travelled less than 9 km. In general, 80 % of all material transported by glacial ice is deposited within 10 km of its source. This is based on numerous descriptions of dispersal fans and trains in the mineral tracing literature, including Dreimanis (1958) and Hyvarinem *et al*. (1973). All of these distances are consistent with Bayrock's (personal communication January 19, 1983) modified curve which indicates that the west Dismal Lakes boulders have been transported approximately 5 km.

PEC BOULDER FIELDS

Boulder tracing was an intergal component in the discovery of the PEC uranium deposit. Over 4,000 radioactive boulders were discovered and mapped west and northwest of the deposit by Trigg, Woollett, Olson Consulting Ltd. personnel. Included in this number is the Uke Lake boulder train, the axis of which intersects the PEC uranium deposit (Ahuja, 1974) (Figure 18). For this study, the Uke Lake train and boulders were analyzed to determine if similarities between the Uke Lake train and the west Dismal Lakes field exist, and whether these similarities could provide information which would ultimately lead to the bedrock source of the west Dismal Lakes boulders.

RESULTS

The Uke Lake radioactive boulder train contains over 1,100 boulders. Most are Dismal Lakes Group Unit 11, either sandstone (42 %) or conglomerate (49 %) (Ahuja, 1974). The boulders are on the surface or covered by less than 40 cm of till (Vagners, 1977). Drift thickness in the vicinity of the boulder train, in spots, exceeds 25 m (Ahuja, 1974).

The Uke Lake boulders occur in two boulder trains (Figure 18). The trains, 325 m apart, are oriented at an azimuth of 265 °. The north train was traced from 1,450 m east of Uke Lake to 600 m west of Uke Lake. The limits of the south train were not delineated because a major portion of the train is on another company's claims (PEC claims).

For 60 % of its length, the north train is less than 120 m wide. Both north and south boundaries of the train are distinct. The first radioactive boulder is 2,830 m west of the PEC uranium deposit. Boulders are most abundant between 3,160 and 3,930 m west

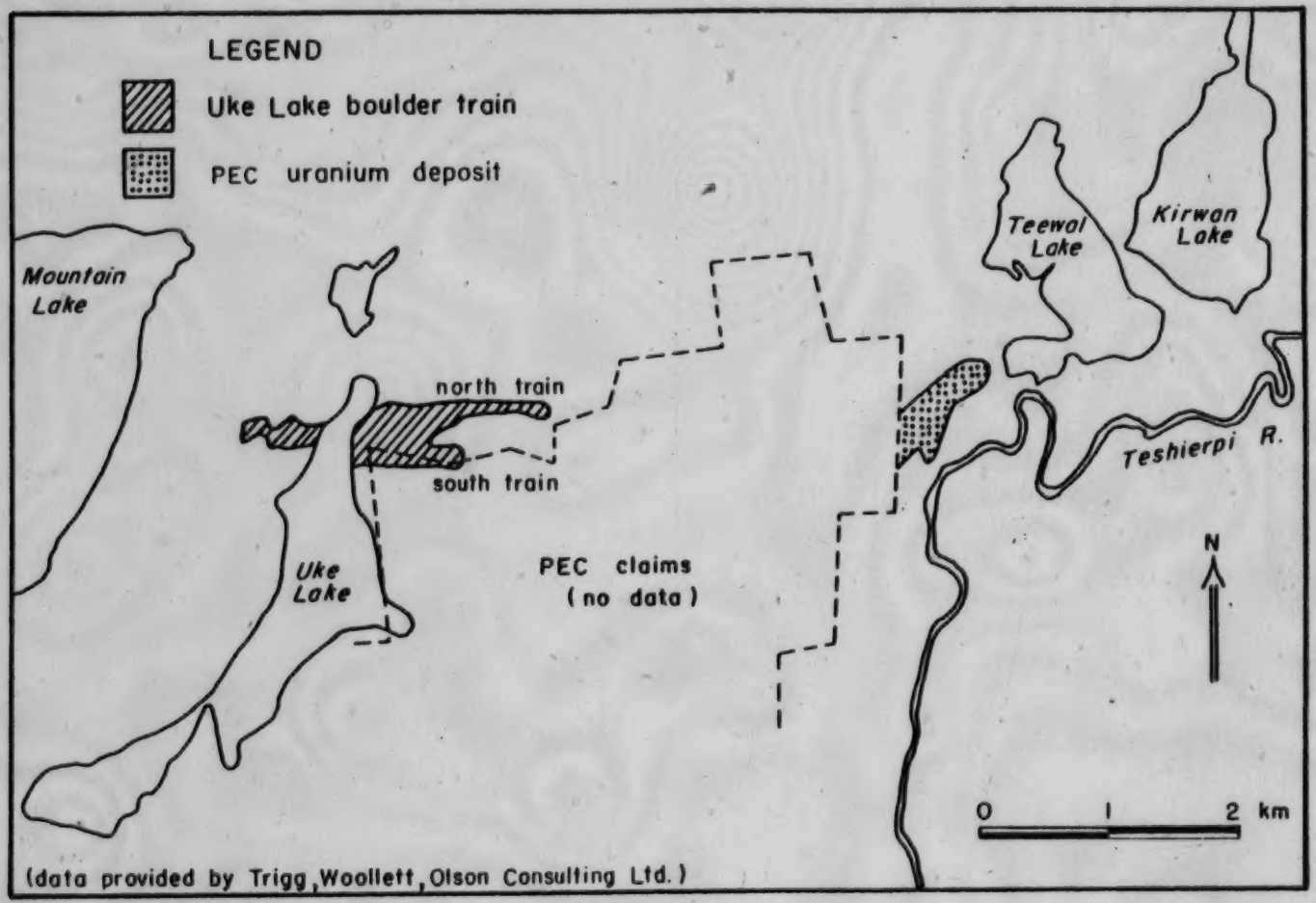

Figure 18. Uke Lake boulder train

of the PEC uranium deposit; west of this zone the number of boulders decreases significantly.

Most radioactive boulders have maximum size dimensions between 15 and 60 cm (Ahuja, 1974). Radioactivity produced by the boulders ranges from less than 1,000 cps to greater than 15,000 cps, with an average of 4,150 cps (Ahuja, 1974). Boulder radioactivity reaches a maximum between 3,180 and 3,930 m west of the PEC uranium deposit.

The angularity of 46 boulders from the north Uke Lake train was measured in order to investigate the relationship of boulder angularity versus distance of transport from a known source. The Uke Lake boulders appear more angular than those of the west Dismal Lakes field. The mean angularity of the Uke Lake boulders is 4.1 cm, the mode is 2.0 cm.

A scatter plot of boulder angularity versus distance west of the PEC uranium deposit is presented in Figure 19. Regression analysis on this data proved that no statistical trend exists (coefficient of determination of 0.064). No trends were noticed on visual inspection of the data.

Bayrock's (1980) formula $D=KS^2$, which relates the degree of boulder roundness to the distance from their source, was investigated; the results are presented on Figure 19. With known distance and K (100 would probably be best for the quartzose sandstone of the PEC area), angularity for basally transported boulders was calculated. There is a discrepancy between the actual and calculated boulder angularities.

DISCUSSION

Comparing Uke Lake and west Dismal Lakes boulder fields may provide one of the few sources of data on the ice transport distance of the west Dismal Lakes boulders. Table 2 presents a comparison of the two fields. The similarities include: (1) lithologies of the boulders, (2) the number of boulders in the fields, which may indicate comparable volumes of bedrock were eroded, (3) the narrow eastern end of the fields, indicating both fields have a point source, and (4) boulder size and angularity, suggesting similar ice erosion, incorporation, transport and deposition mechanisms.

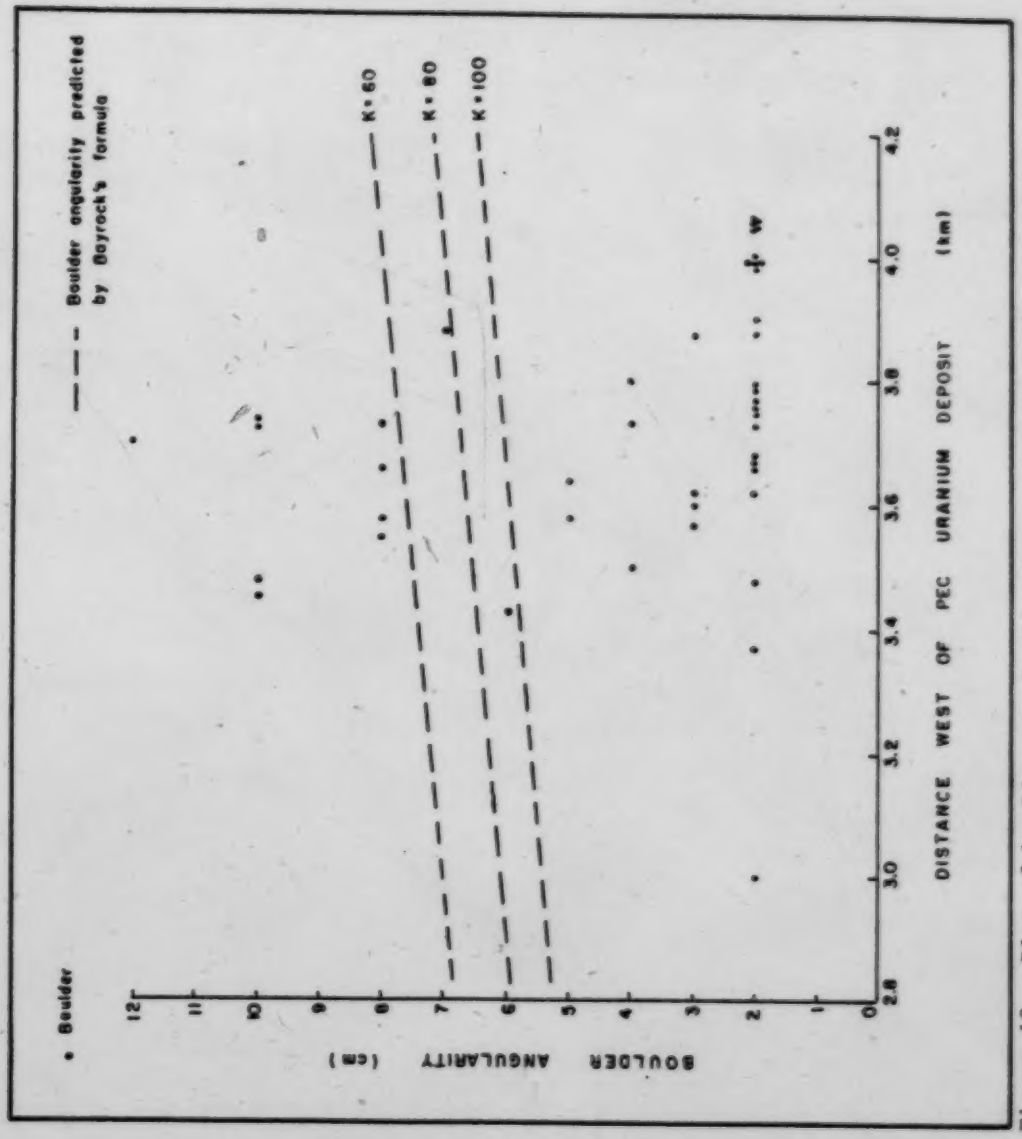

Figure 19. Plot of boulder angularity versus transport distance - PEC

	Uke Lake	West Dismal Lakes
Number of boulders	1100	500+
Lithology of boulders	Unit 11 42 % sandstone 49 % conglomerate	Unit 11 95 % sandstone 5 % conglomerate
Drift thickness	25 m	10 m *
Field shape	2 parallel linear trains	crude fan
Field length	3000 m	5000+ m
Field width	120 m	2000 m
Orientation of long axis of field	265°	260°
Topography	lee side of gentle 50 m high bedrock outcrop, northwest slope	generally flat, slight northwest slope
Distance - main boulder concentration to bedrock source	3160 m	5600 m *
Distance - closest boulder to bedrock source	2830 m	1500 m *
Maximum boulder size	60 cm	110 cm
Average boulder radioactivity	4150 cps	4000 cps
Boulder angularity		
mean	4.1 cm	5.0 cm
mode	2.0 cm	5.0 cm

* estimated

Table 2. Comparison of west Dismal Lakes and Uke Lake boulder fields

Visual and regression analyses for both fields showed essentially no increase in boulder roundness with increasing distance of transport. Therefore, angularity data cannot be used as an indicator of transport distance. We cannot apply Bayrocks' (1980) formula because the boulders likely were not transported at the base of the ice sheet and/or the formula does not work for the Dismal Lakes area.

The first boulder in the Uke Lake train was deposited 2,830 m west of the PEC uranium deposit, and the main concentration of boulders was deposited 3,160 m west. When compared to the Uke Lake train, a transport distance of 5 km for the majority of west Dismal Lakes boulders seems reasonable.

C. TILL GEOCHEMISTRY

WEST DISMAL LAKES GEOCHEMICAL SAMPLES

The purpose of the till geochemistry study at west Dismal Lakes was to obtain an indication of the location of the bedrock source of the uraniferous boulders from the shape and location of geochemically anomalous areas. The distribution of large uraniferous material (boulders) dispersed by the glacial ice was analyzed in the previous section. In this section, the distribution of the smallest material, the -2 μm fraction of the till matrix, dispersed by the glacial ice is examined. The ease of multi-element analyses on this size fraction allows determination of which, if any, other elements have a similar distribution pattern as uranium, and thus whether they can be used as indicators of uranium. A detailed sampling grid was used.

RESULTS

Till samples from west Dismal Lakes area were analyzed for uranium and nine other elements. Till sampling stations are illustrated in Figure 20. Anomalous areas, for this study, are defined as areas which have geochemical values greater than or equal to one standard deviation above the arithmetic mean. The maximum, minimum, mean, standard deviation and detection limit for each of the data sets is given in Table 3. A complete listing of all geochemical values is contained in Appendix G. On the geochemical plots, anomalous

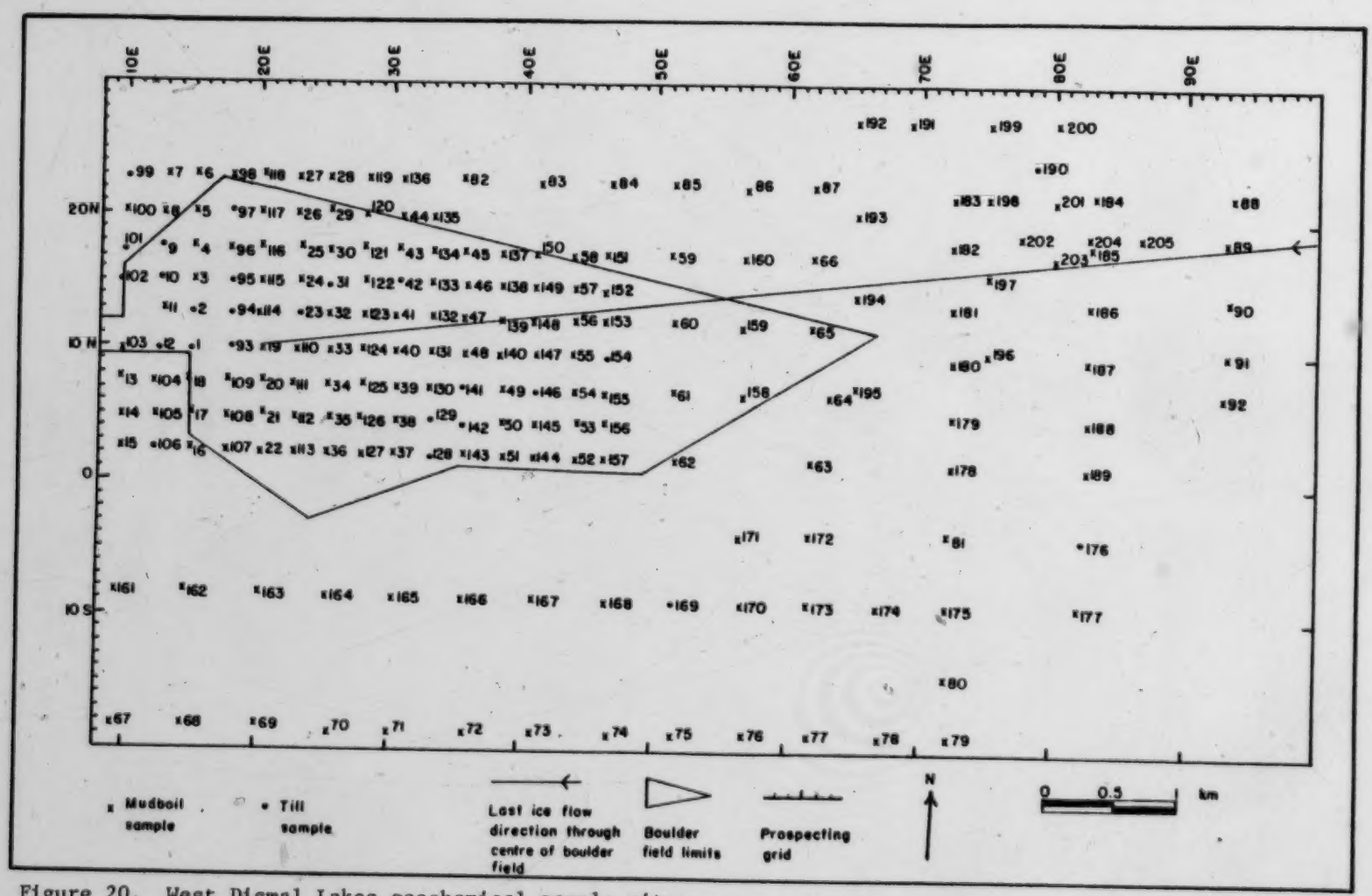

Figure 20. West Dismal Lakes geochemical sample sites

VARIABLE	UNIT	N	MINIMUM	MAXIMUM	MEAN*	STANDARD DEVIATION	DETECTION LIMIT
U -2	PPM	205	0.3	5.6	1.21	0.72	0.1
U -60	PPM	37	0.2	2.5	0.61	0.38	0.1
U -250	PPM	37	0.3	1.8	0.63	0.32	0.1
U DNC	PPM	117	2.57	6.64	3.65	0.82	0.12
Fe	%	189	2.5	7.3	4.5	0.8	0.1
Cu	PPM	205	58	230	134	35	1
Pb	PPM	205	6	44	17	5	2
Zn	PPM	205	28	250	99	26	1
Co	PPM	189	10	24	16	2.5	1
Ni	PPM	189	24	70	39	6.9	2
Cr	PPM	205	28	95	51	11.5	2
Mo	PPM	189	1	5	1.7	0.9	1
Mn	PPM	205	125	1460	560	204	1

* arithmetic

Table 3. West Dismal Lakes geochemical results - Descriptive measures

areas at approximately one and two standard deviations above the mean are highlighted. Anomalous areas resulting from only one data point are also indicated.

URANIUM

(a) Uranium fluorometry analysis - Three size fractions (-2 μm, 2-60 μm, and 60-250 μm) of till were analyzed by fluorometry by Bondar-Clegg & Company Ltd.. The detection limit for the fluorometric analyses is 0.1 parts per million (PPM) uranium. The accuracy of a result is its closeness to the actual amount present, and the precision of a result is its reproducibility. As an accuracy check during fluorometric analyses, one of every twenty samples processed was an internal laboratory standard. For precision, one of every ten samples was reanalyzed. Bondar-Clegg & Company Ltd. had precision tolerances of: ±100 % at the detection limit, ±25 % at 10 times the detection limit, and ± 10 % at 100 times the detection limit. Nine -2 μm fraction samples were renumbered and resubmitted for uranium analyses. The results are presented in Table 4. For seven of the nine samples, the reanalyzed uranium values were within the precision tolerance range.

Uranium values for the -2 μm fraction of 205 till samples from west Dismal Lakes range from 0.3 to 5.6 PPM, with a mean of 1.2 PPM. Figure 21 contains the contoured results. The plot was derived from 205 data points. Method A was used in the calculation of the data grid, which had 125 m between rows and columns. The anomalous area in the southeast occurs in shallow drift over granitic bedrock. Sporadic anomalous areas occur near the boulder field, though the area with the greatest concentration of boulders is not anomalous. The two most pronounced anomalous areas occur in the northeast corner of the sampled area.

To determine which size fraction of the till contained the most uranium, the 2-60 μm and 60-250 μm fractions of 37 samples from the vicinity of the boulder field were analyzed . The 2-60 μm fraction has a mean uranium value of 0.61 PPM. The 60-250 μm fraction has a mean uranium value of 0.63 PPM. For the 37 samples analyzed, the 2-60 μm fraction has more uranium than the 60-250 μm fraction in 10 samples, less in 18 and the same in 9 samples. No significant difference in uranium values between the two size fraction exists. However, when compared to the -2 μm fraction, both the 2-60 μm and 60-250 μm fractions have significantly lower uranium values. In 35 of the 37 samples, the largest uranium values are from the -2 μm fraction. For the other 2 samples, the largest

Sample number	Run # 1			Run # 2		
	Value (PPM)	Tolerance ± (%)	(PPM)	Value (PPM)	Tolerance ± (%)	(PPM)
1	2.1	13	0.3	1.7	15	0.3
2	3.0	13	0.4	3.2	12	0.4
11	1.4	18	0.3	0.2	80	0.2
19	1.8	14	0.3	1.2	22	0.3
66	4.3	12	0.5	4.0	12	0.5
93	1.4	18	0.3	1.0	25	0.3
114	1.4	18	0.3	1.1	23	0.3
182	0.6	41	0.3	0.1	100	0.1
185	5.6	11	0.6	5.1	12	0.6

Table 4. Reanalyzed fluorometry U results

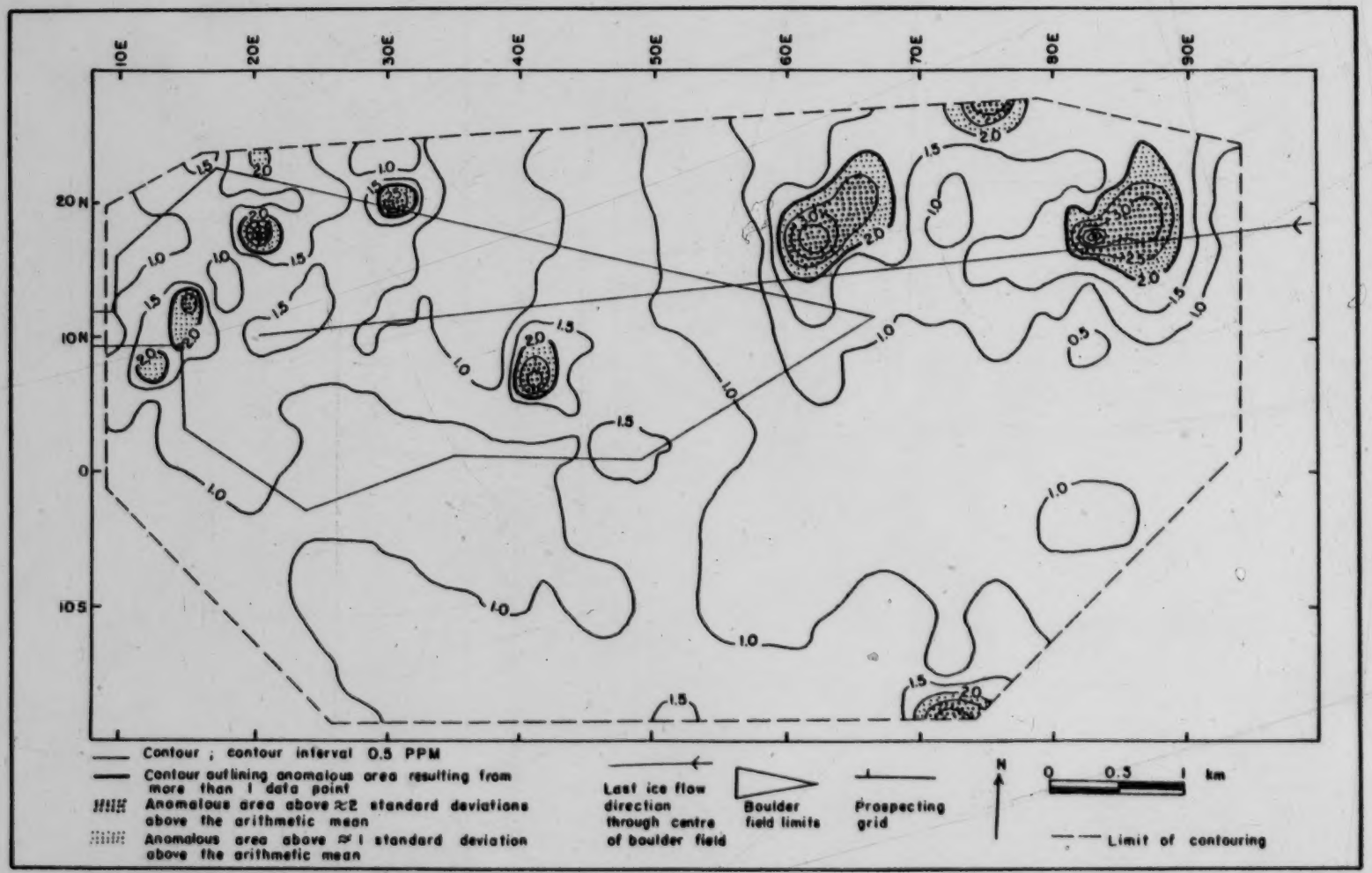

Figure 21. Contoured uranium by fluorometry results

uranium values are from the 60-250 μm fraction.

(b) Uranium by delayed neutron counting (DNC) - The -2 μm size fraction of 117 till samples from the west Dismal Lakes area was analyzed by DNC. The detection limit for uranium by DNC is 0.12 PPM in a 5 g sample. The system used gave a sensitivity of 51.2 ±1.6 cts/μg natural uranium. The accuracy of the method was assessed by analyzing 12 reference standards against the calibration standard Canadian radioactive reference ore BL-1. All reference standards, except one, are within the recommended limits (Duke *et al.*, 1982), even without a thorium content correction. With the correction all results are within the recommended uranium limits. During till sample analyses, one of every seven samples was the calibration standard BL-1. The precision of the method is largely controlled by counting statistics. With the equipment used, concentrations of 2.57 to 6.64 PPM uranium in a 5 g sample were determined with a precision of better than ±7 %. As a precision check 59 samples were analyzed twice. The uranium values are in agreement within one standard deviation for 55 of these samples. The remaining 4 samples are in agreement after a third analysis.

The DNC uranium values from west Dismal Lakes range from 2.57 to 6.64 PPM, with a mean of 3.65 PPM. Figure 22 contains the contoured uranium values. The plot was derived from 117 data points using the same process as for Figure 21. The only anomalous area resulting from more than one data point is in the northeast corner of the map. No definite trends occur over the boulder field.

Instrument Neutron Activation Analyses (INAA) were performed on four -2 μm fraction samples to determine uranium and thorium values. INAA results are presented in Table 5. Uranium values by INAA range from 5 to 14 % lower than those by DNC, and 41 to 164 % higher than those by fluorometric methods. The thorium/uranium ratios from the INAA results range from 2.2 to 3.8. Duke *et al.* (1982) advise that thorium interference in the DNC method need only be considered significant when the thorium/uranium ratio is greater than 5. Similarly, Stuckless *et al.* (1977) conclude that DNC results are generally precise within ±5 % when thorium/uranium ratios are between 2 and 8. It was concluded that thorium interference in the DNC uranium results is not significant. This was confirmed by the relative close agreement between INAA and DNC uranium values.

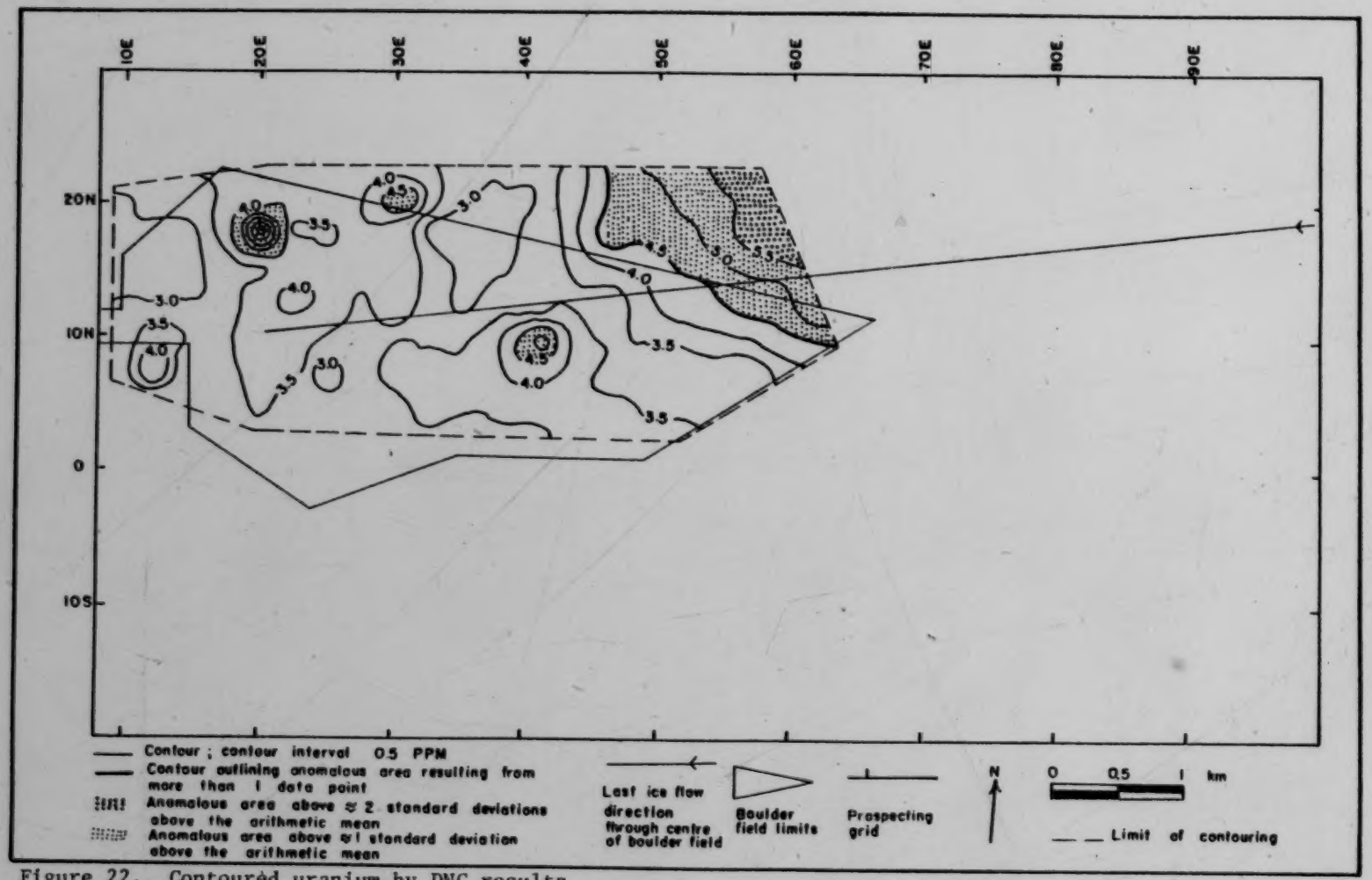

Figure 22. Contoured uranium by DNC results

Sample number	116	114	99	44
U INAA (PPM)	6.19 ± 0.19	3.70 ± 0.18	3.82 ± 0.16	4.92 ± 0.19
U DNC (PPM)	6.64 ± 0.35	4.05 ± 0.23	4.37 ± 0.25	5.19 ± 0.28
U fluorometry (PPM)	3.8 ± 0.5	1.4 ± 0.3	1.8 ± 0.3	3.5 ± 0.5
U DNC/INAA	1.07	1.09	1.14	1.05
U INAA/fluorometry	1.63	2.64	2.12	1.40
Th INAA (PPM)	13.6 ± 5.1	13.9 ± 5.1	11.8 ± 4.8	13.6 ± 4.9
Th/U INAA	2.2	3.8	3.1	2.8

Table 5. INAA results

(c) Fluorometry and DNC uranium results - One hundred and seventeen till samples from the west Dismal Lakes area were analyzed for uranium by both fluorometric and DNC methods. For these samples, a comparison of descriptive measures is presented in Table 6. Fluorometry values are from 29 to 93 %, with a mean of 73 %, lower than DNC values. DNC values are 63 to 79 % higher than those obtained by fluorometry for 95 of the 117 samples. A scatter plot of DNC and fluorometry uranium values is presented in Figure 23. The sample correlation coefficient is 0.486, or in other words 24 % of the variability in DNC values may be explained by the linear relationship they have with fluorometry values. For this correlation, with 115 degrees of freedom the 99 % and 95 % confidence levels are 0.24 and 0.18, respectively.

Low fluorometry values may be caused by quenching. Quenching is any process occurring within a fluorescent substance that decreases the observed intensity of the fluorescence (Price *et al*., 1953). A number of quenchers which decrease fluorometry uranium values have been suggested. The one most mentioned is manganese, others include chromium, iron, cobalt, lead, nickel, thorium, platinum, titanium, gold, cerium, praseodymium and neodymium (Grimaldi *et al*., 1954; Kolthoff *et al*., 1962; Stuckless *et al*., 1977). Since the degree of quenching depends only on the concentration of the quencher, and not on the ratio of the quencher concentration to uranium concentration, it is possible to reduce quenching to a negligible factor by using sufficiently small samples. Grimaldi *et al*. (1954) suggests a few micrograms of sample should be used when a strong quencher such as manganese is present.

Quenching may have reduced uranium values obtained by fluorometry because manganese is present and 0.1 g samples were analyzed. A scatter plot of manganese versus a ratio of DNC / fluorometry uranium values was constructed. If manganese was quenching, the DNC / fluorometry ratio would increase with increasing manganese content. This is not the case; the scatter plot has a correlation coefficient of -0.075 indicating no linear relationship. Therefore manganese quenching does not account for the lower fluorometry uranium values relative to DNC and INAA results.

OTHER ELEMENTS

(a) General - The -2 μm fraction of the 205 till samples from the west Dismal Lakes area was analyzed for nine elements in addition to uranium. Grant (1980) examined over

Variable	Minimum	Maximum	Mean
U by DNC (PPM)	2.57	6.64	3.57
U by fluorometry (PPM)	0.3	3.8	1.06
Mn by ASS (PPM)	200	1230	527
U DNC/fluorometry	1.41	14.63	3.72

Table 6. Comparison of U by fluorometry and DNC

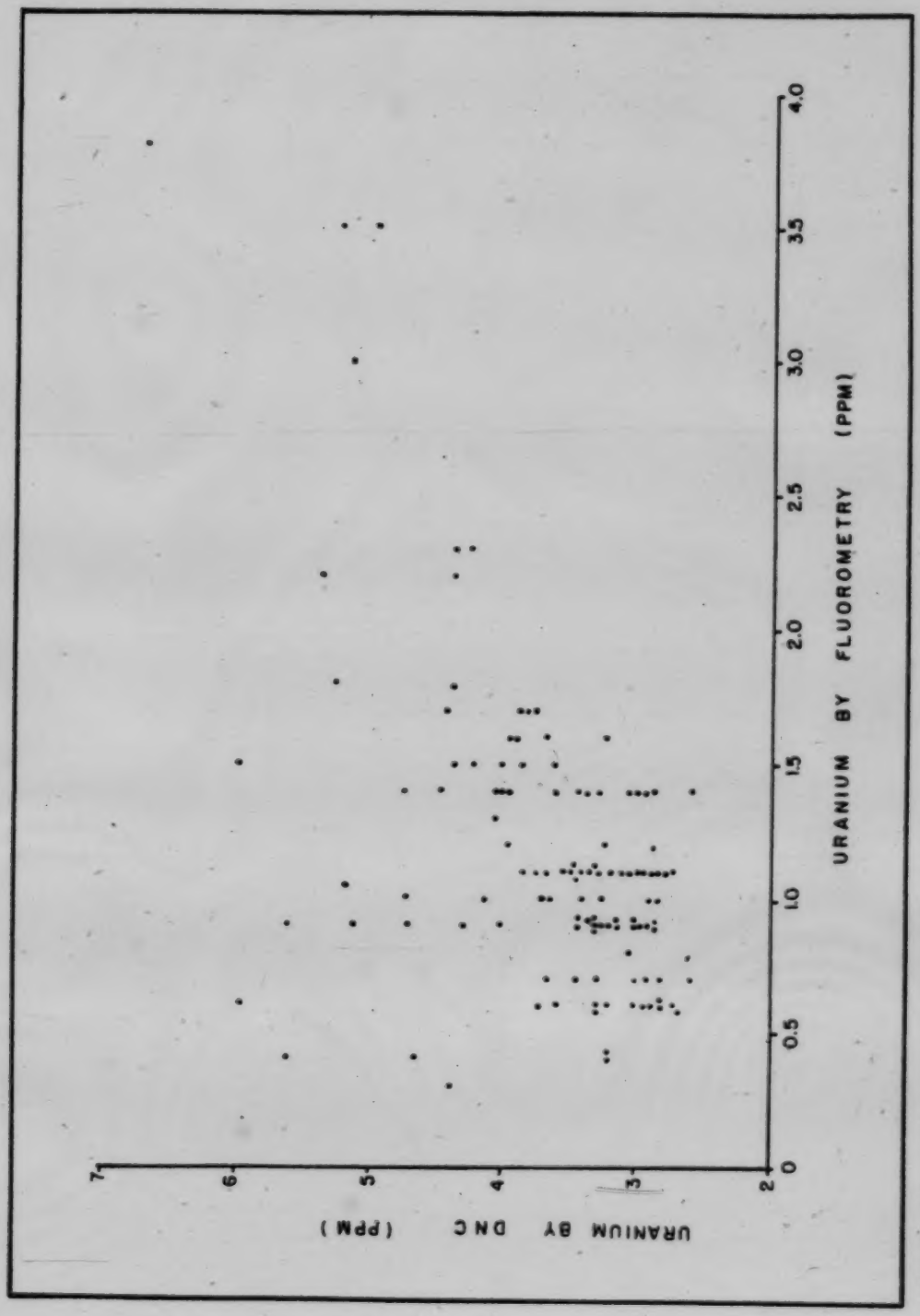

Figure 23. Plot of uranium DNC and fluorometry values

300 west Dismal Lakes radioactive sandstone boulders. He identified secondary minerals containing iron, copper, nickel and cobalt. If the source of the west Dismal Lakes boulders is geochemically similar to the PEC uranium deposit, then some of the following elements may be associated with west Dismal Lakes boulders and related glacial debris: chromium, molybdenum, iron, cobalt, nickel, copper, zinc and lead (Boyle, 1974). These elements, plus manganese, were analyzed by Bondar-Clegg & Company Ltd. using Atomic Absorption Spectrometry (AAS). The detection limit for each element is given in Table 3. Bondar-Clegg & Company Ltd. had the same precision and accuracy checks and tolerances for AAS as for fluorometry.

Contoured plots showing element geochemical patterns are presented (Figures 24 and 26, Appendix H). Each plot was derived from the same 205 data points as uranium, except the plots of cobalt, nickel, molybdenum, and iron where 189 data points were used (eliminate sites 190 through 205 on Figure 20). The plotting process was the same as that for uranium.

(b) Copper - Copper ranges from 58 to 230 PPM. Anomalous areas are concentrated in the north half of the map, especially within the northeast quadrant (Figure 24). Over the northern half of the main boulder concentration, copper values are above the mean, but anomalous areas result from only one data point.

A third degree trend surface, fitted to the same data as contoured in Figure 24, is presented for copper (Figure 25). The goodness of fit for the trend surface is 20 %. The surface has a high in the northeast which narrows and lowers to the west. The area of high copper values in the northeast corresponds with high fluorometric uranium values (Figure 21).

(c) Lead and zinc - Lead values range from 6 to 44 PPM. Zinc values range from 28 to 250 PPM. Anomalous areas are coincident and concentrated over and west of the main boulder concentration (Figure 26). Small areas of values between one and two standard deviations above the mean occur sporadically throughout the west Dismal Lakes area; a number of these represent one data point. The lowest lead and zinc values are located in the vicinity of 75E, 10N.

(d) Chromium, nickel, cobalt, molybdenum, manganese and iron - Geochemical plots of these elements consist of isolated and sporadic anomalous areas, each representing

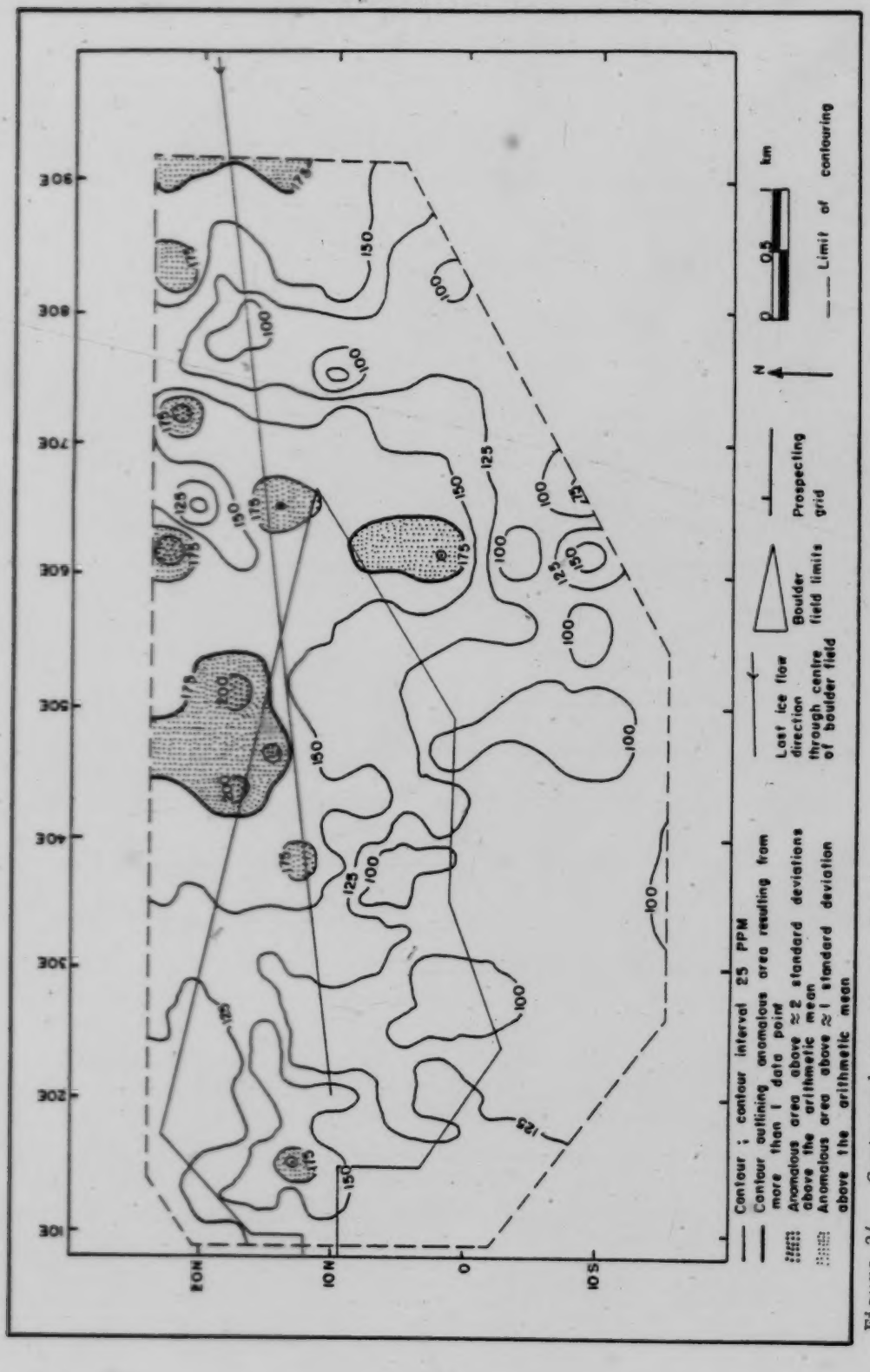

Figure 24. Contoured copper results

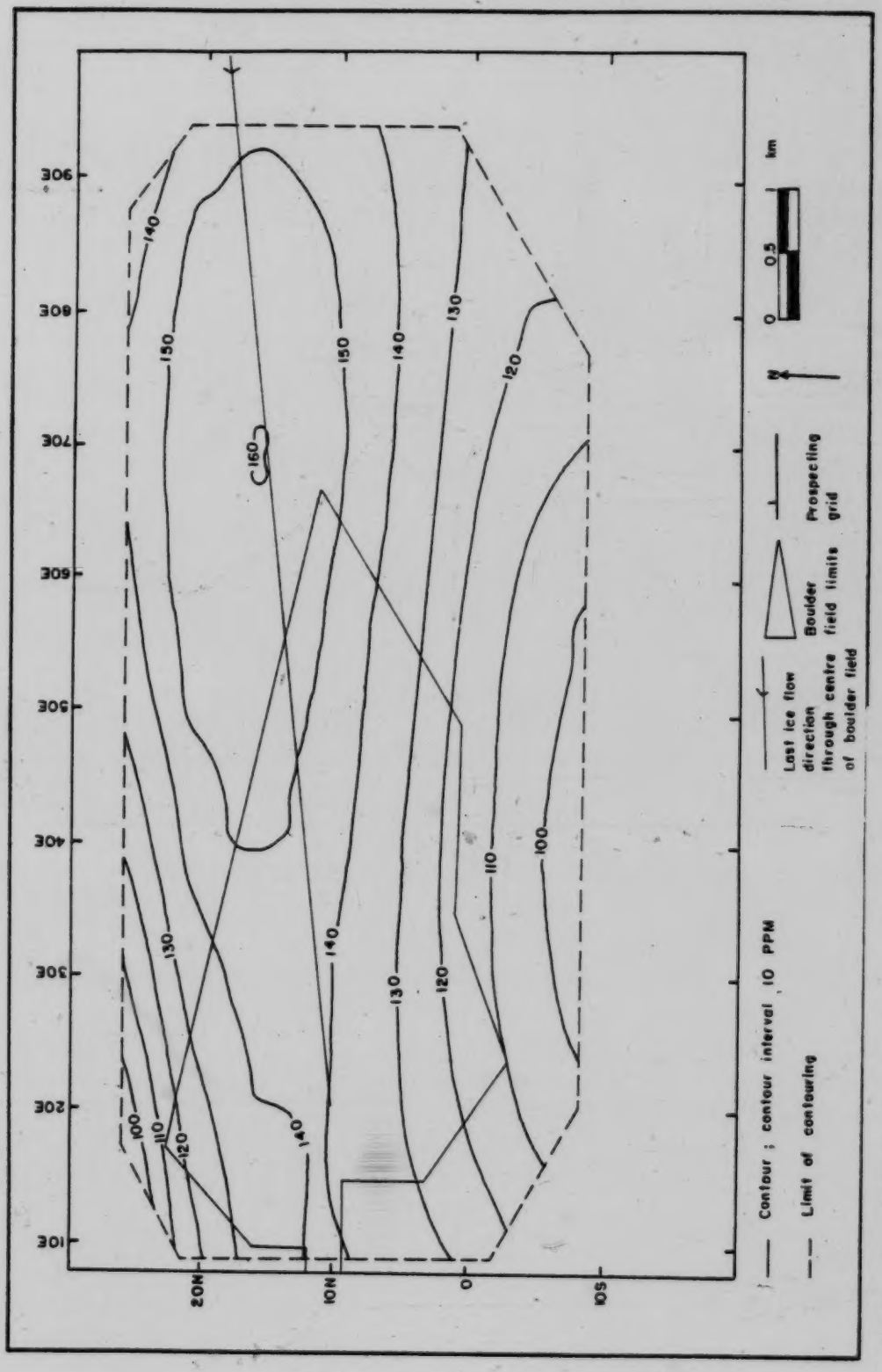

Figure 25. Copper trend surface, third degree

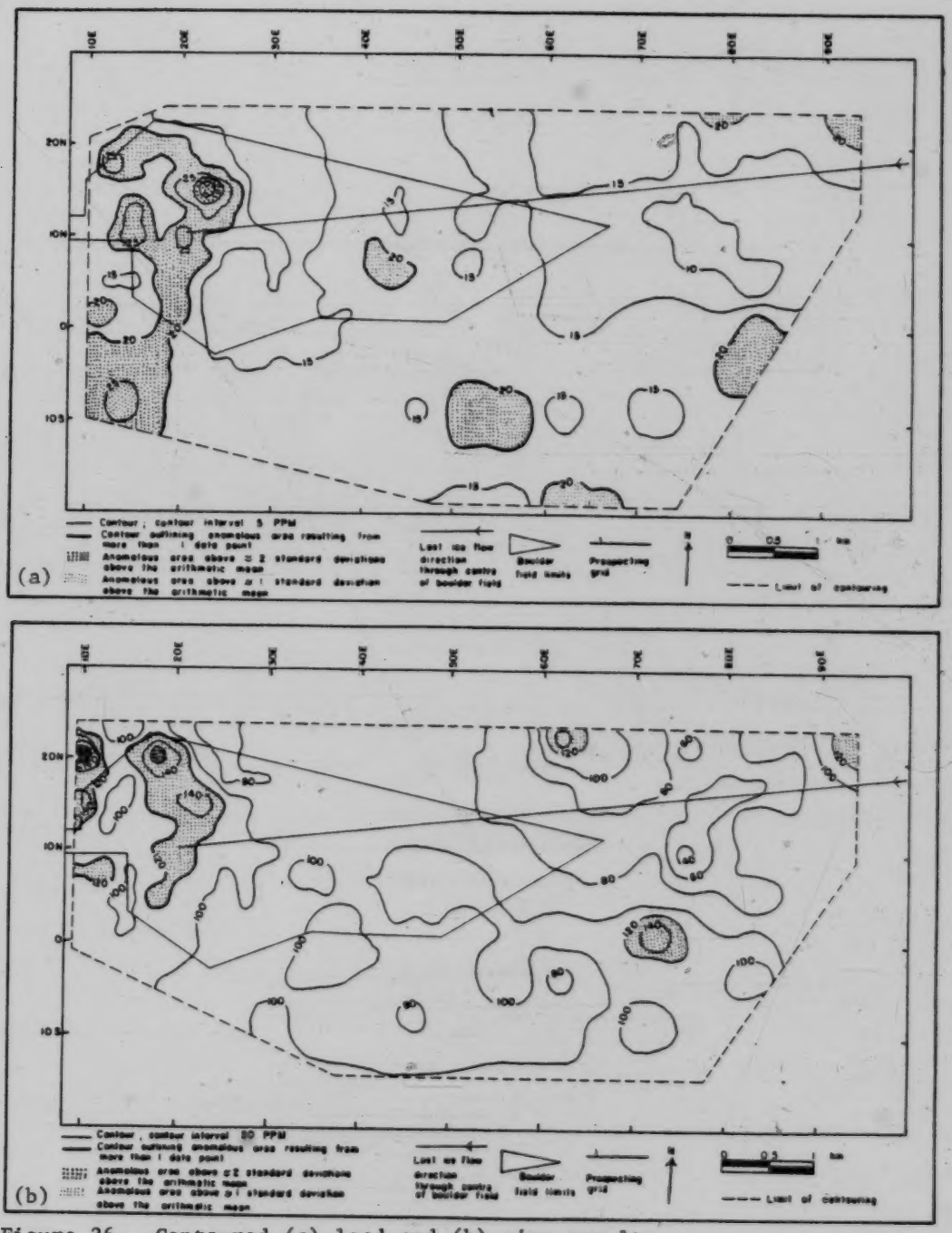

Figure 26. Contoured (a) lead and (b) zinc results

one data point. Contour maps (Appendix H) and trend surface plots do not reveal any trends.

(e) Elemental relationships - Relationships between the analyzed elements are illustrated by means of a correlation matrix (Table 7). The null hypothesis that there is zero correlation was tested. For the 99 % and 95 % confidence levels the critical values are .19 and .14 respectively for 187 degrees of freedom. When the absolute value of a correlation coefficient exceeds the critical value the null hypothesis is rejected; in other words some degree of correlation exists. This test assumes that the data are a random sample from a multivariate normal distribution. For large samples, such as used in this study, the assumption is not critical (Elementary Statistics Using MIDAS, 1976). Significant correlation coefficients are highlighted in the matrix.

DISCUSSION

URANIUM

The greatest number of till samples collected over the largest area at west Dismal Lakes were analyzed for uranium by fluorometry. Therefore fluorometric results for the -2 μm till fraction are used to interpret the distribution of uranium within the till. After eliminating anomalous areas resulting from only one data point, remaining anomalous areas are either (1) along a line oriented 260 ° which extends northeast from the main boulder concentration and parallels the direction of the last glacial flow over the area, or (2) over the boulder fan (Figure 21).

The two most pronounced anomalous areas are located at, or just northeast of, the boulder fan's apex. Both lie very close to the line of last ice flow through the centre of the field. The anomalous areas are 4 and 6 km from the centre of the boulder field. These distances broadly agree with the previously suggested boulder transport distance of 5 km. From this, it is proposed that these anomalous areas are associated with, and are over or slightly west of the uranium-bearing source of the boulders. The following points support this hypothesis.

(1) Uranium in the oxide state is very mobile (Earle, 1980). The chemical weathering of mineralized bedrock released uranium, which was subsequently scavenged by clays and

N = 189 Degrees of freedom = 187 R@ 95 % =.1428 R@ 99 % =.1869

U	1.0000									
Cu	-.0587	1.0000								
Pb	.1614	.1488	1.0000							
Zn	-.0391	.0145	.4492	1.0000						
Co	-.0812	.3036	.2902	.2958	1.0000					
Ni	-.1390	.0457	.3037	.3901	.5029	1.0000				
Cr	.1193	-.0339	.4736	.6019	.3128	.4670	1.0000			
Mo	-.0101	-.0842	-.0067	-.0339	-.0088	-.0237	.0482	1.0000		
Mn	-.1722	.1095	.2937	.2691	.4734	.2697	.0818	-.0067	1.0000	
Fe	.0104	-.0805	.4624	.5467	.4359	.5656	.7732	.0123	.2172	1.0000
	U	Cu	Pb	Zn	Co	Ni	Cr	Mo	Mn	Fe

Table 7. Correlation matrix of geochemistry results

iron and manganese oxides in the -2 μm fraction of the till in the vicinity of the uranium source.

(2) Minell (1978) documented an example where the uranium anomalous area in till was closer to the bedrock source than the mineralized boulders. DiLabio (1979) and Bjorklund (1976b) also found that the largest uranium values in the fine size fractions of till were directly over and/or a small distance in the direction of ice flow from the bedrock source.

(3) The anomalous area with the largest uranium values is just east of a north-south trending diabase dike which outcrops as a ridge. This ridge may have acted as a ramp to move debris, eroded from uranium bedrock source, above the base of the ice sheet. The result is a gap between the bedrock source and the glacially transported mineralized debris.

Although a few anomalous areas and slightly higher than background values occur over the boulder fan, there is no obvious correlation of boulder concentration with the concentration of uranium in the finest size fractions of till. In general this agrees with Bjorklund (1976b), who reported that till in a boulder field had only background uranium values away from the bedrock source. The reason for the lack of correlation may be chemical weathering in the surface layer, which leached away the mobile uranium (Bjorklund, 1976a).

The pattern of the -2 μm uranium values is not conclusive and is difficult to explain without other evidence. However, when taken in combination with such evidence as probable zones of increased erosion, ice flow direction indicators, the distribution of the boulders and the location of the boulder fan's apex, the pattern indicates the region with the two most pronounced anomalous areas contains the bedrock source of the uranium.

Uranium values from the 2-60 μm and 60-250 μm fractions were only used to determine which size fraction of west Dismal Lakes till contains the most uranium. The mean of uranium values within the -2 μm fraction is almost double the means of uranium values within the other fractions. This, combined with the fact that for 35 of the 37 samples analyzed the -2 μm fraction has the largest uranium value, proves the initial assumption that the -2 μm fraction, which is dominated by phyllosilicates and iron and manganese oxide scavengers, is the most likely to contain uranium.

It is concluded that for uranium, the -2 μm fraction is the most suitable to analyze at west Dismal Lakes. The concentrating of scavenging components by eliminating the non-scavenging mineral grains (+2 μm) increases the background to anomalous area contrast, eliminates granulometric variations between samples (Klassen and Shilts, 1977b), permits more accurate comparisons between samples and allows better outlining of glacial indicator trains (Shilts, 1975).

At west Dismal Lakes 117 till samples were analyzed for uranium by DNC, and 205 by fluorometry. Because the DNC data base is smaller, DNC results are only used to supplement fluorometric data. All the DNC samples are from, or near, the boulder fan (Figure 22). Consequently, there is a problem in determining the background uranium concentration, which makes it difficult to locate anomalous areas. The only anomalous area, after eliminating those resulting from only one data point, occurs north of the boulder fan's apex. This anomalous area broadly coincides with the second largest fluorometric anomalous area. In general, the DNC results are consistent with those of fluorometry. The explanations proposed for the fluorometric results can also be used for the DNC results.

For this study, the DNC method of uranium analysis was superior to the fluorometric method. DNC precision was better and DNC values were consistently higher than those by fluorometry. Klassen and Shilts (1977a) found INAA and fluorometric analyses in close agreement for till samples from the Baker and Kaminak Lakes areas, N.W.T.. In this study INAA and DNC analyses are similar, but significantly larger than, analyses done by fluorescence. The reason for the lower fluorometry values is not known. Manganese quenching has been shown, in this study, not to lower fluorometry values. No quenching was caused by cobalt, chromium, lead and nickel, given the lack of correlation with uranium in Table 7. Thorium values, determined by INAA, were not large enough to affect DNC uranium values.

The low correlation coefficient for DNC versus fluorometry uranium results (0.486) may be explained by the lower precision of the fluorometric method. The lower precision is a result of the small amount of sample analyzed (0.1 g for fluorometry versus 5.0 g for DNC). Levinson (1974) states that precision and accuracy for a 0.1 g sample are significantly lower than that for a 1.0 to 5.0 g sample.

Despite the lower values and precision compared to DNC, fluorometry uranium results were interpreted because (1) of the greater number of samples, (2) the samples cover a larger area and (3) the general agreement in trends with DNC results. However, if this type of sampling is performed in future at west Dismal Lakes, uranium analyses should utilize DNC.

OTHER ELEMENTS

At west Dismal Lakes, copper ranges from 0.28 % to 0.60 % in the boulders assayed (Grant and Woollett, 1979) and chalcopyrite and malachite were major secondary minerals identified in the boulders (Grant, 1980). Therefore, some relationship between copper and uranium may exist. Also, if the west Dismal Lakes uranium source is geochemically similar to the PEC uranium deposit, which Geldsetzer (1974) suggested to be a uranium-vanadium-copper stratiform deposit, then a uranium-copper relationship probably exists at west Dismal Lakes.

Copper values in till have no obvious patterns, though a crude trend with the largest copper values occurring northeast and east of the boulder fan does exist (Figure 24). Areas of anomalous copper and uranium values in till do not coincide. The copper third degree trend surface (Figure 25) has a goodness of fit of only 20 %. It shows three general patterns: (1) the area of largest copper values is northeast of the boulder fan, similar to the largest uranium values, (2) the copper high is elongated east-west, only 10 ° different from the flow direction of the last ice, and (3) the area of largest copper values is centred on a line oriented 260 ° (parallel to the flow of the last ice) which extends northeast from the main boulder concentration. From these, it is concluded that copper anomalous areas in till (1) can give an indication of last ice flow direction, (2) have no association with the boulders, and (3) have a crude spatial association with uranium anomalous areas in till, but have no statistical correlation with uranium on a sample by sample basis. If the apparent coincidence of uranium contoured results (Figure 21) and copper trend surface (Figure 25) highs is real, the uranium source may be below the highs. This is the case at Kazan River, N.W.T., where uranium and copper values from -2 µm till samples are largest over a uranium occurrence (DiLabio, 1979). If future till geochemistry work is performed at west Dismal Lakes, tills should be analyzed for copper to determine if a copper-uranium relationship exists.

Although zinc and lead till geochemistry patterns (Figure 26) are not well developed, a trend is apparent; the smallest lead and zinc values are in the vicinity of the largest uranium values and the probable area of the uranium source. No relationship exists between uranium and lead and / or zinc in till or boulders at west Dismal Lakes. When comparing contour plots both lead and zinc appear to have a negative spatial relationship with uranium in till; this is not apparent, however, from the sample to sample correlation matrix (Table 7) and conflicts with the findings of Shilts and Cunningham (1977) at other areas.

Molybdenum and cobalt occur with uranium at the PEC deposit (Abercrombie and Trigg, 1980). Grant (1980) identified annabergite and erythite as secondary minerals in the west Dismal Lakes uraniferous sandstone boulders. Therefore, the following elements may be related at west Dismal Lakes: molybdenum and uranium, cobalt and uranium, cobalt and molybdenum, nickel and uranium, and nickel and cobalt. Only nickel and cobalt have a significant coefficient in the correlation matrix (Table 7). Chromium, nickel, molybdenum, cobalt, iron or manganese can not be used as tracers for uranium at west Dismal Lakes. This is in agreement with the findings of Klassen and Shilts (1977b) for -2 µm till samples at Kaminak Lake, N.W.T., where there is no clear association between uranium and nickel, cobalt, manganese, molybdenum or iron. Shilts and Cunningham (1977) also have no nickel, cobalt or manganese enrichment corresponding to anomalous uranium areas in -2 µm till samples from the Baker Lake area, N.W.T.. However, they do have coinciding enrichment of molybdenum and iron with uranium.

In general, the correlation coefficients between lead, zinc, cobalt, nickel, chromium, manganese, and iron are significant (Table 7). Uranium, copper and molybdenum generally do not have significant correlation coefficients. It may be that the former six elements are all at, or near, regional background concentrations in the west Dismal Lakes area. This would explain the lack of, or poorly developed, trends in the contoured maps for these elements. Molybdenum values in the area are low; approximately 25 % of the samples have molybdenum values below the AAS detection level. The recording of molybdenum values below the detection level probably caused the lack of correlation between molybdenum and other elements. Copper and uranium likely exist at the west Dismal Lakes uranium source, therefore copper and uranium values in tills should vary

throughout the west Dismal Lakes area depending on their proximity to the source and the glacial dispersion path. The copper and uranium values would therefore not be expected to correlate with the background values of the other elements.

If copper and uranium in the drift had identical movement by glacial ice and postglacial hydromorphic processes, then they would be expected to have significant correlation. Since the correlation coefficient is not significant, they either have different sources or non-identical movement. The latter seems the more likely since copper and uranium anomalous areas are in the same general vicinity.

X-RAY DIFFRACTION

To aid in the evaluation of geochemical results, the mineralogy of the -2 μm fraction of 12 west Dismal Lakes till samples was determined by X-ray diffraction. The X-ray diffraction study had two objectives.

(1) The data were to confirm or refute the assumption that the -2 μm fraction of till is composed mainly of phyllosilicates with some quartz and feldspar. This is important because phyllosilicates, in addition to iron and manganese oxides, readily scavenge and adsorb cations released during post glacial weathering. Therefore, phyllosilicates in the till keep mobile uranium cations in the general locality where they were dispersed by glacial ice. The phyllosilicates prevent postglacial hydromorphic dispersion. The scavenging and adsorption processes also concentrate elements, resulting in easier detection and greater contrast between background and anomalous concentrations.

(2) Sample mineralogies, in semi-quantitative form, were compared to determine if significant differences existed. Large differences between samples in the quartz / feldspar content compared to the amount of phyllosilicates would make comparisons of the geochemical results unreliable due to the great adsorption capacity of phyllosilcates and the lack of adsorption by quartz and feldspar.

X-ray diffraction results confirmed the assumption that the major constituents of the -2 μm fraction are clay minerals, quartz and feldspar. The main minerals detected are illite, chlorite, quartz, microcline and albite. These five minerals are present in all samples. Kaolinite is present in 11 samples and smectite is present in one sample. X-ray diffraction results are presented in Appendix I.

Semi-quantitative clay mineral percentages were calculated using the area under the peak method, with form factors of 4 for illite and 2 for chlorite and kaolinite. The quartz peak height (d=4.2) provides a relative measure of quartz between samples. Analyses show that the -2 μm fractions of west Dismal Lakes till samples have similar mineralogy. The comparison of geochemical results is not affected by mineralogical differences between samples.

MUDBOIL VERSUS TILL SAMPLES

Even though mudboils occur exclusively on till at west Dismal Lakes, the processes forming mudboils may have produced geochemical differences between till from mudboils and samples of undisturbed till. This possibility was investigated.

Of the 205 till samples collected at west Dismal Lakes, 180 are mudboil samples and the remaining 25 are samples of undisturbed till. The mean uranium value for the undisturbed till samples versus mudboil samples is lower for DNC analyses but higher for fluorometric analyses (Table 8). For both DNC and fluorometry, the maximum and minimum values for the smaller undisturbed till sample set are within those of the larger mudboil sample set. It appears that for uranium values at west Dismal lakes, no significant geochemical difference resulted from the sampling of undisturbed till as opposed to mudboils. This conclusion was also reached for the other nine elements analyzed after visual examination of the data.

PEC GEOCHEMICAL SAMPLES

PEC geochemical till samples, collected west from the PEC uranium deposit, were intended to provide a model of glacial dispersion in the Dismal Lakes region. This model or dispersion pattern could then be applied to the west Dismal Lakes geochemical results.

		Minimum (PPM)	Maximum (PPM)	Mean (PPM)	Number
Uranium by fluorometry	Mudboils	0.3	5.6	1.2	180
	Undisturbed till	0.4	3.9	1.4	25
Uranium by DNC	Mudboils	2.57	6.64	3.66	102
	Undisturbed till	2.83	4.37	3.53	15

Table 8. Comparison of uranium values between mudboil and undisturbed till samples

RESULTS

Uranium values were determined for 13 till samples from the PEC area. Values for nine other elements were determined for 12 of the samples. The samples were processed in the same manner as the west Dismal Lakes samples. All analyses were performed on the -2 μm fraction. The sampling stations are situated on an east-west line which begins 1.5 km and terminates 4.1 km west of the PEC uranium deposit. The sampling interval is illustrated on Figure 27. At the four easternmost sample stations undisturbed till samples were taken. This area has a thin drift cover and is underlain by Unit 8 sandstone. At the nine westernmost stations, mudboils developed in several metres of till were sampled. This area is underlain by Unit 9 dolomite.

Uranium was determined by fluorometric methods. The uranium values range from 0.3 to 2.6 PPM with a mean of 1.1 PPM. Lowest uranium values are from the mudboil samples (Figure 27). The highest uranium values are from the four undisturbed till samples collected nearest to the PEC uranium deposit. The samples with the highest uranium values do not occur near the radioactive boulders (Figure 27).

The maximum, minimum and mean values for copper, lead, zinc and manganese are given in Table 9. PEC and west Dismal Lakes values are similar for copper, lead and zinc but manganese values from PEC are higher. The patterns of zinc and manganese values along the PEC sampling line are similar to that of uranium (Figure 27). Copper and lead values, along with the other elements analyzed for, show no trends.

DISCUSSION

For the PEC geochemical samples, the location of the highest uranium values is believed to be mainly a function of the thin till cover in that area. The extremely large manganese values within the undisturbed till indicate that the undisturbed till was much more weathered than the mudboil material. The high uranium values result from the concentration of mobile uranium by manganese oxide and other scavengers in the weathered till (Figure 27). The high uranium values are not believed to be a function of the sampling of undisturbed till as opposed to mudboils. The high uranium values may be

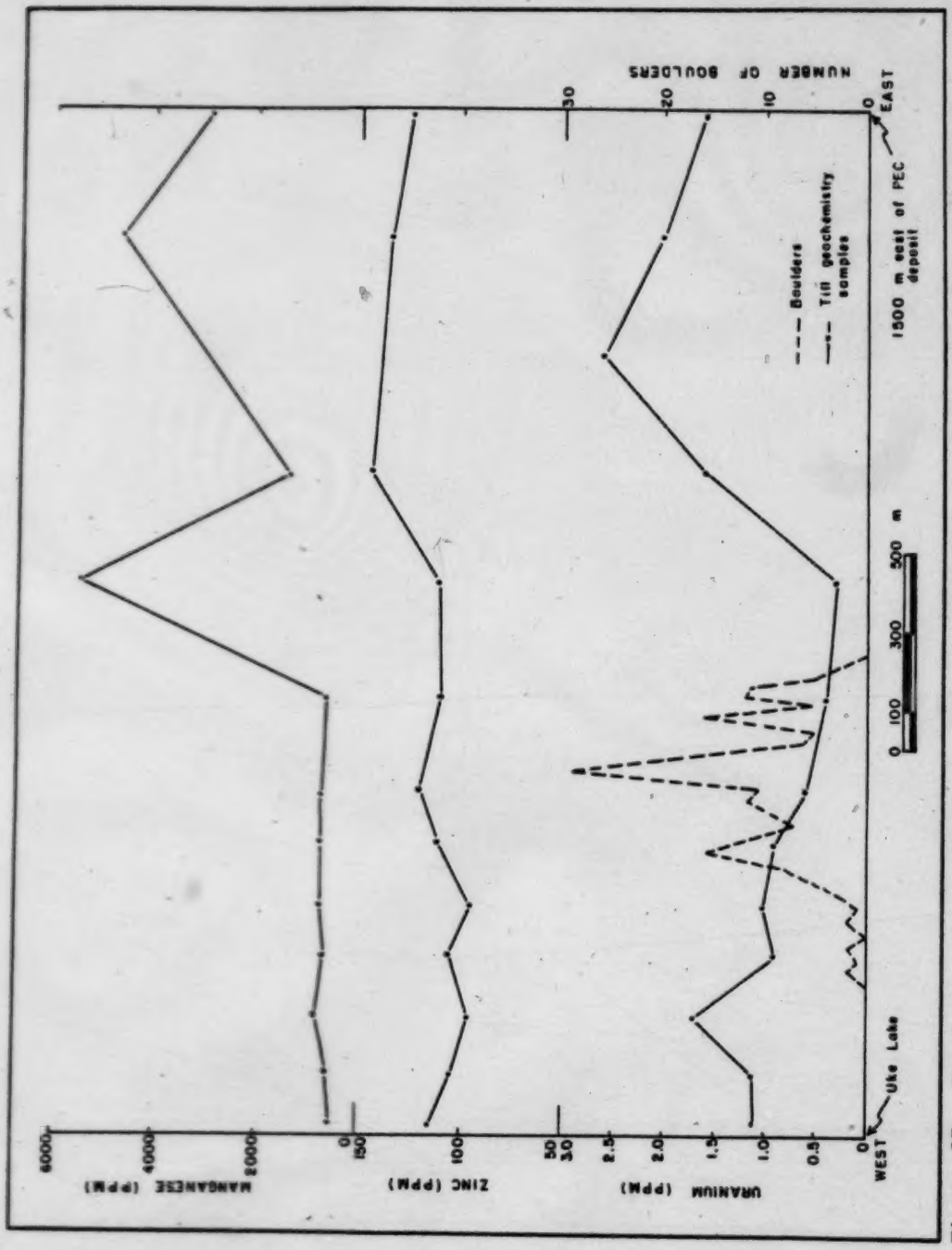

Figure 27. Uranium, manganese and zinc values at PEC

Variable	Unit	Minimum	Maximum	Mean
Cu	PPM	60	260	138
Pb	PPM	10	29	18
Zn	PPM	96	144	113
Mn	PPM	490	5800	1114

Table 9. PEC geochemistry results - Descriptive measures

partially a function of (1) sandstone bedrock beneath the samples (versus dolomite beneath the lower uranium values) and/or (2) closer location to the PEC uranium deposit. Zinc values are also elevated in the highly weathered samples (Figure 27); this is consistent with the findings of Miller (1979) in the Bathurst Inlet area, N.W.T..

Few correlations or trends between PEC and west Dismal Lakes data are apparent. There is agreement that high uranium values are obtained from areas of thin (<0.3 m) and therefore, highly weathered till. Since the PEC geochemical data are not reliable due to the collection of non-uniform samples, the apparent correlation of (1) the highest uranium values at west Dismal Lakes near the proposed source with (2) the highest uranium values at PEC being closest to the deposit, may not be real.

In conclusion, PEC geochemical sample results do not provide a dispersion model nor any significant trends which may be compared to results from the west Dismal Lakes area. A major reason the PEC geochemistry study did not provide useful results was that a discontinuous till cover necessitated the collection of non-uniform samples. At west Dismal Lakes the till cover is more uniform; it is assumed the geochemistry results from that area are more reliable. The PEC samples do show that comparisons should not be made between samples from areas with <0.3 m of drift and >0.3 m of drift. The sampling of thin till over bedrock provides the highest geochemistry values. These samples are probably the most representative of the underlying bedrock. However, since areas of thin drift cover in the Dismal Lakes area are small and sporadic, it is best to avoid this type of terrain in future till geochemistry surveys.

IV. THEORETICAL DISCUSSIONS OF GLACIAL ICE CONDITIONS AND POST GLACIAL PROCESSES

A. GLACIAL ICE CONDITIONS

A reconstruction of the ice conditions which existed during the erosion, transport and deposition of the uraniferous sandstone boulders and associated debris at west Dismal Lakes would provide valuable information in tracing the bedrock source of the boulders. Unfortunately published material on the Laurentide ice sheet profile, thickness, flow dynamics and flow patterns is scarce and highly speculative. Reconstruction of the history of the Laurentide ice sheet has concentrated on ice frontal positions, especially along the southern margin. Little reconstruction work has been carried out on the northwest quadrant of the ice sheet. Therefore, although the following proposed ice reconstruction for the Dismal Lakes area is a theoretical approximation, it will provide ideas which future studies can refine. Parts of the reconstruction rely on published works from the Antarctic and Greenland ice sheets and from valley glaciers (Boulton, 1974, 1978; Gow *et al*., 1979; Hallet, 1979; Lawson, 1979; Nye, 1952; Robin and Millar, 1982; Rothlisberger, 1968; Sugden, 1977). Use of these ice masses as analogues for the Laurentide ice sheet may be inadequate. Although the data base for the reconstruction is small, it is believed that the ice reconstruction is reasonable within the present knowledge of glacier and ice sheet dynamics.

(a) Ice Front Position - The exact position of the ice front during the period of uraniferous sandstone erosion and boulder deposition is not known. Two possibilities exist, the ice front was either in the immediate Dismal Lakes area or was hundreds of kilometres beyond. If erosion and deposition of the uraniferous sandstone occurred at the ice margin, they must have taken place during a minor ice readvance within the general retreat of the ice sheet. They did not occur during the initial ice front advance over the area since the following evidence is not in agreement with lodgement deposition which is the only possible mechanism of debris deposition for that situation. The sharp northwest boundary of the boulder field indicates a rapid stoppage of deposition in contrast to the thin continuous deposition of debris by lodgement in an area of flat topography. The loose

nature of the till within which the boulders are found is not characteristic of material deposited by the lodgement mechanism. The boulders are not striated, indicating minimal transport of the boulders at the ice sheet base and therefore minimizing the chance for lodgement deposition. In addition, if the boulders had been eroded by the initial ice front advance and soon after deposited by lodgement, it seems likely that the boulders would have undergone some subsequent erosion and disbursement by the large volume of ice which moved across the area before the glacial maximum.

The possibility exists that the uraniferous sandstone was eroded and deposited by a late stage minor readvance of ice flowing northwest and then diverted west in the Dismal Lakes valley. Glacial striae in the valley indicate ice flow controlled by local topography. These striae may have been eroded by a late stage readvancing ice lobe. This ice lobe, if it existed, must have been less than 300 m thick as striae near the top of the granitic upland are oriented parallel with the regional ice flow direction.

Extreme forces were required to fracture the uraniferous sandstone. Three points in support of this statement are presented. The volume (greater than 10 m^3) of uraniferous sandstone eroded, from what is believed to be a small area of bedrock, required large and concentrated fracturing and plucking forces. Secondly, the highly silicified uraniferous sandstone is very resistant to erosion. The topographically prominent, smooth and highly polished Unit 11 sandstone outcrops southeast of the boulder field provide proof of the sandstone's resistive nature. Thirdly, the massive nature of the these outcrops indicate that the joint system within Unit 11 sandstone was not of primary importance to the fracturing mechanism. Probably, the primary fracture mechanism was large pressure and stress gradients induced in the sandstone by overriding ice. When large forces were attained, the sandstone fractured where the strong grain to grain cohesion could be overcome, this was often along joint planes.

Though ice velocities across the area are not known, from a theoretical model Boulton (1974) suggests that much greater than 300 m of ice would be required to suppress cavitation in the lee side position of bedrock knobs of about 50 m in length. This size of bedrock protuberance presently exists in the west Dismal Lakes valley, and similar size ones probably were present to be eroded by the last ice sheet. Since extreme forces were required to fracture the uraniferous sandstone and greatest fracturing potential

occurs when cavitation is just suppressed (Boulton, 1974), the thin ice of a readvancing lobe (< 300 m) probably was insufficient to erode the uraniferous sandstone. Ice of greater thickness, and therefore able to produce greater normal pressure, likely was required to fracture the uraniferous sandstone.

To have greater than 300 m of ice over the west Dismal Lakes area, the ice front must have been a considerable distance beyond the Dismal Lakes area. Three lines of evidence indicate that the ice front was much greater than 100 km northwest of Dismal Lakes.

(1)The highly silicified uraniferous sandstone in the west Dismal Lakes boulder field required extreme fracturing and plucking forces. It is assumed that the boulders were excavated during the period of maximum erosion for the Dismal Lakes area. Robin (1972) notes that erosion by polar ice sheets can be influenced by basal warming as the ice thickness increases. He proposes that maximum erosion coincides with thick ice, and possibly with the maximum thickness, and therefore, maximum extent of the ice. Sugden (1978) assumes that the majority of glacial erosion occurs during maximum ice conditions. The maximum Pleistocene extent and the maximum late Wisconsinan extent of the Laurentide ice sheet in the vicinity of the Mackenzie River delta and the Beaufort Sea coast broadly coincide (Sugden, 1977; Hughes, 1973; Prest *et al*., 1968)(Figure 28 - maximum concept). At the ice sheet's maximum thickness and extent the ice front was approximately 400 km northwest of Dismal Lakes (Sugden, 1977).

(2) With the ice sheet at its maximum extent Sugden (1977) postulated the Dismal Lakes area was in a zone of a warm basal freezing thermal regime. This zone is equivalent to Boulton's (1972b) zone C. Boulton believed that the amount of erosion in the zone of warm freezing was not surpassed by any other basal thermal regime beneath the Laurentide ice sheet. In addition, the warm freezing zone has the most efficent mechanisms for debris entrainment, due to regelation and plastic ice flow. Sugden (1978) went one step further and postulated that the zones of most intensive glacial erosion and warm basal freezing conditions coincide. For the Dismal Lakes area to have had warm basal freezing conditions and maximum erosion, the ice front likely was a significant distance away and at or near its maximum position.

(3) The geomorphology of the Dismal Lakes area does not indicate a nearby ice front

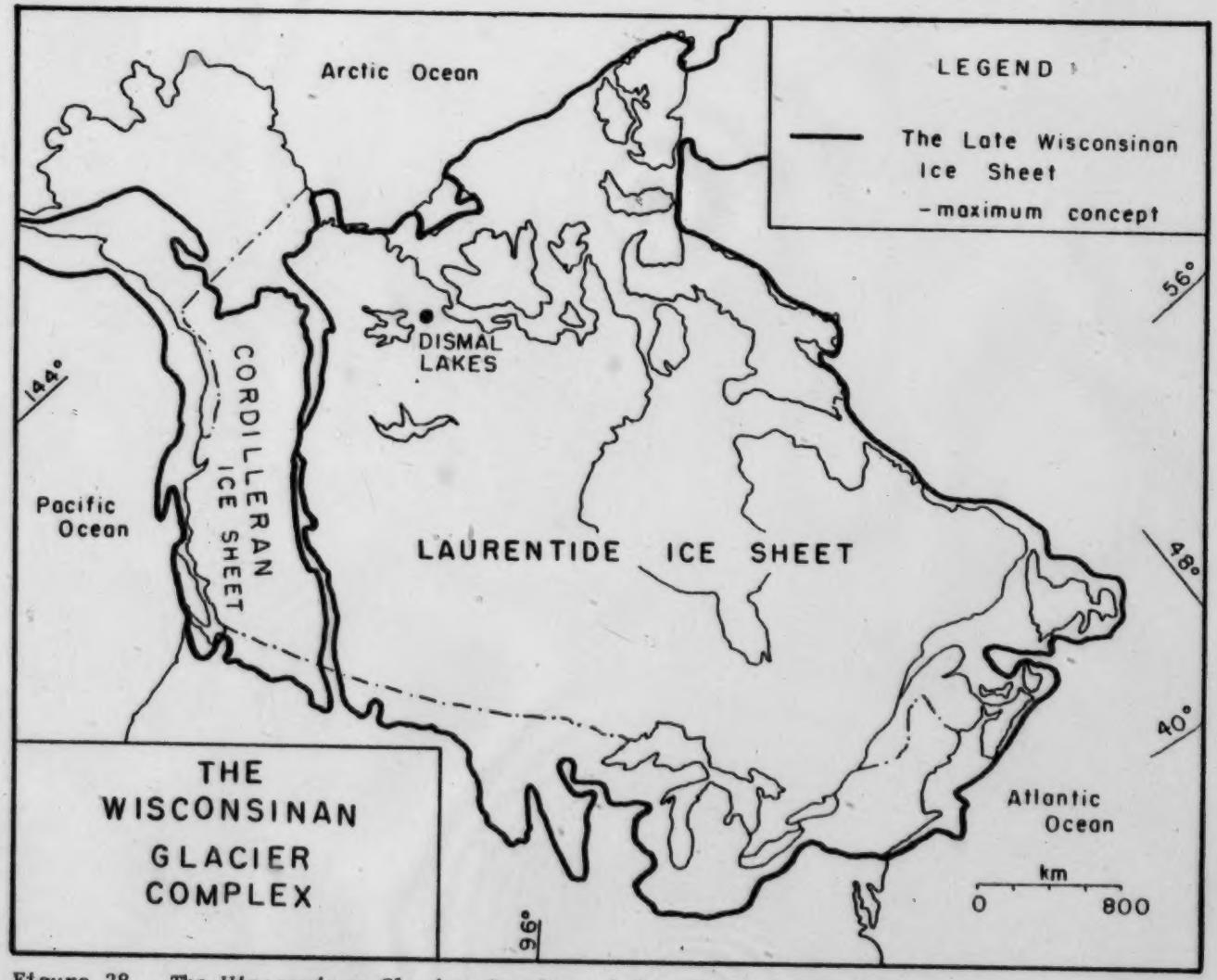

Figure 28. The Wisconsinan Glacier Complex (after Prest, in press)

position. The area lacks terminal or hummocky moraines and crevasse fills; features that are commonly associated with terminal or major recessional ice fronts. Drift cover in the west Dismal Lakes valley is sufficiently thick that the overriding ice was not debris poor. If an ice front stagnated in the area, terminal or recessional ice front sediments should have been deposited. While working on this study, no evidence was gathered for the ice front position which St-Onge (1983) mapped in the west Dismal Lakes valley. The extensive areas of till plain and single crested eskers indicate, furthermore, that during their deposition the ice front was not nearby (Sugden and John, 1976).

Thus, evidence from the Dismal Lakes area has some agreement with conclusions in published works which postulate that the Laurentide ice sheet was at or close to its maximum extent during the period of maximum erosion in the study area. For the remainder of this study, the idea that maximum erosion conditions were necessary for the erosion of the uraniferous sandstone which created the boulder field is used.

(b) Ice Thickness - Sugden (1977) modeled the morphology of the Laurentide ice sheet at its maximum extent. His model utilizes an ice surface profile adapted from a selection of profiles calculated for the East Antarctic and Greenland ice sheets. At the glacial maximum Sugden estimates the maximum ice thickness for the Laurentide ice sheet at 4,244 m, and ice over the Dismal Lakes area was approximately 2,800 m thick. These values may be moderately over estimated because Paterson (1972) calculated a maximum Laurentide Ice Sheet thickness of 3,600 m. However, both models indicate at least 2,000 m of ice was over the Dismal Lakes area during the period of maximum erosion.

(c) Ice Flow - A model of ice flow dynamics for the west Dismal Lakes area during the glacial maximum would assist the ice sheet reconstruction and drift prospecting. Dynamics of present day ice sheets are used as analogues in the model.

Ice sheets flow by the processes of internal deformation and basal sliding. These processes are reviewed in detail by Paterson (1981) and summarized in Sugden and John (1976).

Ice sheet flow by internal deformation is in response to stresses set up in the ice mass by the force of gravity. Stress can be divided into two components: hydrostatic

pressure and shear stress. Hydrostatic pressure is caused by the weight of the overlying ice and is equal in all directions. Shear stresses are related to the weight of the overlying ice and the ice surface slope, and result in ice crystals slipping past one another. Shear stresses increase with increasing ice sheet thickness and ice surface slope. The strain rate, or rate of deformation of polycrystalline ice, quickly attains a steady value when a constant stress is applied to ice (Glen, 1955). This relationship (Glen's flow law) demonstrates that the strain rate is highly sensitive to the shear stress and ice temperature. For ice sheets, Glen's flow law requires that (1) most internal deformation occurs at the base and that the movement of surface layers is largely a result of being carried forward on the lower layers and (2) the thicker the ice and the higher the basal temperature, the greater the velocity of ice flow. Glen's flow law oversimplifies real ice sheet conditions; however, it provides a useful explanation of the basic processes of internal deformation of ice. In reality, the non-uniform composition of the ice sheet and uneven ice sheet surfaces cause deviations from Glen's flow law.

Ice sheet flow by basal sliding can be divided into three main processes. Enhanced basal creep, an extreme type of internal deformation, occurs within the lowest ice layers and is most effective in warm basal conditions. The other two processes, pressure melting and slippage over a thin water layer, act at the ice/rock interface and only occur beneath warm based ice. Weertman (1965) concludes that a basal water layer only a few millimetres thick can increase sliding velocities by 40 to 100 % due to the reduced area of friction between the ice and rock. Basal sliding is a jerky stick-slip movement. When it does occur, basal sliding can account for up to 90 % of the total ice sheet movement (Sugden and John, 1976). Maximum basal sliding occurs near the ice sheet equilibrium line that separates the accumulation and ablation zones.

Ice flow at west Dismal Lakes was modified by bedrock topography. The maximum relief in the area is 430 m. More than 2,000 m of ice covered the area during the glacial maximum. Combining this data, two ice units each with different ice flow dynamics likely existed during the glacial maximum over the Dismal Lakes area. The two units were (1) an upper unit of sheet flow and (2) a lower unit where flow was diverted by bedrock topography.

Ice sheets with thick upper and lower units that have different flow dynamics, have not been observed. However, Robin and Millar (1982) modeled such a condition based upon radio-echo layering data obtained from the Antarctic ice sheet. Their model of ice sheet flow indicates a change of ice flow type along a gradational boundary between rigid cold upper ice and more plastic warmer lower ice. Bedrock topography has considerable influence on the stress and strain of the lower layer. The authors advocated that this lower layer accounts for 5 to 25 % of the ice thickness. The dominant influence on the upper layer is the regional ice surface slope.

The ice sheet conditions presented in the above model are the most likely explanation of ice flow dynamics over west Dismal Lakes during the glacial maximum. A lower layer, probably in the vicinity of 500 m thick, had flow modified by the local bedrock topography. Ice was diverted around and over the largest bedrock uplands and knobs, creating zones of converging and diverging flow. Depending on the basal thermal regime, flow was either by deformation and basal sliding or solely by deformation. The thermal conditions of the lower layer were highly influenced by the basal thermal regime of the ice sheet. The upper layer moved west as a sheet following regional flow lines. Flow in the upper layer was by internal deformation. The regional ice surface slope influenced the rate of flow. Only the largest bedrock protuberances modified the horizontal flow lines of the upper layer, flow lines were broadly arched over these protuberances. The thermal conditions of the upper layer were most influenced by temperatures at the ice sheet-air surface interface.

(d) Basal Temperature - The Laurentide ice sheet in the Dismal Lakes area during the period of maximum erosion probably was warm based because the volume of uraniferous sandstone excavated in the creation of the boulder field cannot be explained by the limited erosion capabilities of a cold based ice sheet. Warm based ice does not imply the air or ice surface temperatures were above the freezing point, as a net amount of heat can be produced at an ice sheet bottom (Weertman, 1957). For the Dismal Lakes area during maximum ice conditions Sugden (1977) suggested a surface mean annual temperature of -35 °C. To keep the Laurentide ice sheet bottom near Dismal Lakes at the pressure melting point various heat sources were needed. Heat could have been produced by (1) friction in

the processes of internal deformation of ice, basal sliding and meltwater circulation, (2) pressure melting, (3) the release of geothermal energy, and (4) the release of the latent heat of fusion during refreezing of meltwater.

Heat produced by friction in the processes of internal deformation of ice and basal sliding of ice over bedrock was considered by Sugden (1978) to be the most important influence on warm conditions at the base of an ice sheet. Both processes increase with an increase in shear stress and / or ice velocity. The amount of shear stress is a function of ice thickness and the slope of the ice surface. The entire Dismal Lakes area experienced a great thickness of overriding ice at the glacial maximum and therefore significant heat was probably produced by friction. Ice velocity increases significantly in zones of converging flow. The east end of the west Dismal Lakes valley experienced converging flow and this area may have had warmer basal temperatures due to friction. Rothlisberger (1968) considered friction resulting from meltwater circulation at the base of an ice sheet as another source of heat. With warm basal conditions, meltwater flowed through the Dismal Lakes area and contributed to the maintenance of basal temperatures at the pressure melting point.

The likelihood of warm basal ice conditions increases with ice thickness, since ice temperatures increase with depth due to pressure melting (Boulton, 1972b; Sugden, 1977). The ice thickness over the Dismal Lakes area during the glacial maximum was in excess of 2,000 m. Warm basal conditions often exist beneath ice thicknesses of this order for present ice sheets (Gow *et al.*, 1979). It is assumed the > 2,000 m of ice contributed to the warm basal conditions in the Dismal Lakes area. Geothermal energy in the form of heat is supplied to the bottom of all ice sheets, and this may also have contributed to the warm basal conditions in the Dismal Lakes area.

Sugden (1977) postulated that the Dismal Lakes area was in a zone of warm basal freezing conditions during the glacial maximum. In this zone, water derived from warm melting regions near the ice sheet centre, refreezes to the ice sheet bottom. The latent heat of fusion is released during refreezing. Sugden (1977) believed the maximum extent of warm basal conditions coincided with the maximum distance of basal meltwater flow outwards from the central zone of warm melting. Therefore, he considered the latent heat of fusion released during the refreezing of meltwater as the primary heat source to the

basal thermal regime in the zone of warm freezing.

During the period of maximum erosion, the above heat sources combined to produce basal temperatures at or slightly above the pressure melting point in the Dismal Lakes area.

(e) Mechanisms of Erosion and Debris Entrainment - Knowledge of the mechanisms of erosion and debris entrainment makes a significant contribution to the tracing of mineralized drift. The basic processes of glacial erosion are abrasion and quarrying; the former is responsible for the ground material found in till matrix, while the latter produces boulders and till clasts. The processes of debris entrainment are directly linked to the erosion mechanisms.

Abrasion - Abrasion is the process where bedrock is scoured by debris carried in the basal layers of the glacier. Abrasion was active at west Dismal Lakes, as evidenced by striae, chattermarks, molded bedrock outcrops and the large quantities of till containing rock flour.

The following points are included in a summary by Sugden and John (1976) of variables affecting abrasion. (1) The faster the sliding velocity of the ice, the greater the abrasion. Increased velocity can be achieved by having a thin water layer at the ice/rock interface. (2) Material must be continually transported to the glacier sole to renew the abrasive material. This is accomplished by either melting at the glacier base and thus the lowering of incorporated debris, or by the thinning of the basal layer as ice diverges around obstacles. (3) The removal of rock flour from the ice/rock interface makes the abrasion process more effective. Meltwater is a good agent in the removal of rock flour. The conditions just outlined require water at the glacier sole and hence warm based glacial conditions. This supports the belief that warm based ice occurred at west Dismal Lakes at some period during the last glacial event.

The rock flour generated by abrasion, and initially moved by meltwater, either settled in ponds near the source area, was carried away by meltwater streams or became incorporated into the ice. Erosion by abrasion is most effective in specific environments beneath the ice sheet. Maximum abrasion likely occurs in areas of maximum overlap of the following conditions. Areas with large basal ice velocities, such as zones of converging

flow (Clayton and Moran, 1974) and/or extending flow (Hallet, 1979) can experience intense abrasion. Valley bottoms experience enhanced abrasion due to increased vertical pressure from a greater ice thickness. On a local scale the stoss sides of bedrock protuberances encounter strong abrasive action due to the higher effective normal pressure exerted by diverging and overridding ice. Areas with rapid basal melting often encounter strong abrasion since new abrasive material is transported to the ice/rock interface and rock flour is quickly removed. Finally, a change to a softer bedrock lithology can significantly increase the amount of abrasion (Boulton, 1974).

Quarrying - The explanation of the dense concentration of boulders in the west Dismal Lakes field must include processes of erosion, ice transport and deposition which kept the boulders concentrated. Quarrying of a large quantity of uraniferous sandstone from a small area is the only erosion process capable of supplying the quantity of uraniferous sandstone in the boulder field and keeping the boulders concentrated. Quarrying comprises the combined processes of fracturing and loosening of bedrock into blocks, and plucking of the blocks from the ice/rock interface. Since both fractured and abraded bedrock material are removed by plucking, the mechanisms of plucking are discussed later in this section.

Fracture of the uraniferous sandstone was by subglacial processes since it is believed to have occurred at or near the glacial maximum. The rock available for subglacial fracture was resistant, highly silicified sandstone, which, in general, was massive. Any preglacial, periglacial sandstone block fields, or jointed and weak sandstone would have previously been removed by the erosion processes which acted as the ice sheet front crossed over the area. A number of rock fracturing processes which operate subglacially and can produce blocks for basal entrainment have been suggested.

(1) Temporary changes in pressure and stress gradients, induced in subglacial bedrock protuberances by the jerky stick-slip motion of debris-rich ice, can lead to bedrock fracturing in the lee side position (Boulton, 1974). Boulton's model has the zone of maximum stress in the bedrock protuberance and the zone of minimum normal pressure coinciding. This overlapping zone is the area with the greatest tendency for rock fracture. It occurs just before the point of cavity closure on the lee side of a protuberance.

(2) Boulders in traction in basal ice have been observed to induce fracturing on the lee

sides of bedrock protuberances where pressure and rock strength are reduced (Boulton, 1978).

(3) The unloading of bedrock, due to ice sheet thinning and the removal of erosion products, may cause dilation joints in bedrock parallel to the ice sheet base by the release of stored strain energy.

(4) For basal ice at or near the pressure melting point, regelation of meltwater in joints along the lee side of bedrock protuberances may cause bedrock fracturing by the 9.2 % volume expansion of water on freezing (Carol, 1947).

The first two processes are more probable for the fracture of large quantities of bedrock (Boulton, 1979; Sugden and John, 1976), and are believed to be the primary mechanisms that were operative at west Dismal Lakes. The last two processes are judged to be minor and local in extent and, although they may have aided in the fracture of uraniferous sandstone at west Dismal Lakes, they are not considered primary mechanisms.

The process where temporary changes in pressure and stress gradients caused by ice moving over an irregular bedrock topography result in bedrock fracture probably was significant at west Dismal Lakes. The present bedrock surface is irregular on a local scale, even after at least two glacial advances have streamlined the topography. It is assumed that more bedrock protuberances existed before the last glaciation. Glacial striae show that ice flow was locally modified by bedrock topography, with ice flow over and around bedrock highs. Ample opportunity existed for ice induced changes in pressure and stress. Therefore, conditions favourable for the fracturing processes described by Boulton (1974, 1978) were present at west Dismal Lakes.

Fracturing, by the processes described by Boulton (1974, 1978), is most effective in specific environments, and maximum fracturing probably occurs where the following environments overlap. The lee side of bedrock protuberances is the preferred location for fracturing; ideally with a cavity between the ice and bedrock at this position (Boulton, 1974). An irregular bedrock surface with small protuberances increases the number of lee side positions within an area, and hence increase the probability of fracturing (Boulton, 1974). Protuberances with high amplitudes in combination with large basal ice velocities increase the likelihood of cavities at the lee side. The largest basal ice velocities occur in the middle of valleys oriented parallel with the regional ice flow direction (Sugden and

John, 1976), and where ice flow is converging and / or extending. Local zones with increased frequency of planes of weakness can enhance fracturing (Boulton, 1974). Planes of weakness can include joints, dilation fractures, bedding planes and rock contacts. Although fracturing can occur beneath cold based ice, it can be more intense under warm ice when a thin basal water layer reduces pressures in lows (lee side cavities). Large clasts in the basal ice may augment fracturing by increasing pressure on stoss sides of bedrock protuberances (Boulton, 1978; Sugden and John, 1976).

Plucking - After abrasion and fracturing, plucking removes the debris from the ice / rock interface and incorporates it into the basal zone of the ice sheet. A number of subglacial plucking mechanisms can incorporate abraded and fractured glacial debris into basal ice.

(1) Plastic flow of ice around loosened fragments resting on bedrock can incorporate debris into the ice (Boulton, 1974). Boulton observed that boulders lying on the rock floor in a lee side cavity of a bedrock protuberance were encased by "eddy" ice flow during the closure of the cavity and were removed. The formation and closure of cavities resulted from ice thickness and basal ice velocity fluctuations caused by plastic ice flow around bedrock protuberances. Boulton suggested that where a bedrock protuberance is longer than its width, ice flow into the lee side position from the lateral flanks produces a point where ice movement is directed away from the rock surface and fragments are plucked.

(2) Regelation, the refreezing of water which has melted under pressure, can incorporate subglacial debris into basal ice. Two processes of regelation have been suggested. Kamb and LaChapelle (1964), Boulton (1970a), and Rothlisberger and Iken (1981) described water, which was derived from pressure melting on the stoss side of bedrock protuberances, that refreezes on the lee side and embeds debris in the glacier sole. The regelation layers which form tend to be destroyed by pressure melting at the next bedrock protuberance of comparable size. For this reason debris is removed in relatively thin layers, less than 0.5 m in thickness (Sugden and John, 1976).

A second regelation process has been described by Weertman (1961) and Boulton (1972b). When an ice sheet has a warm, melting base beneath its centre and basal freezing conditions near its margin, net freezing of interior derived meltwater onto the ice sheet sole can incorporate subglacial debris. Meltwater tends to be concentrated at low points

of the bedrock surface, and most freezing and, therefore, incorporation of debris takes place at such points. This process requires sensitive thermal conditions which allow a change from basal melting to freezing. Far greater volumes of ice and debris can be frozen on to an ice sheet sole by this regelation mechanism compared to the first. In fact Gow *et al*. (1979) from work in Antarctica, believe that freezing of interior derived meltwater to the base of the ice sheet is the major debris incorporation mechanism for polar continental ice sheets.

(3) A freeze-on mechanism of plucking for cold based ice sheets has been described by Boulton (1972b) and Hughes (1973). Boulton (1972b) described the process "if the depth of freezing in subglacial materials coincides with major joints or planes of weakness along which the frictional resistance is reduced by the high pore-water pressures likely to occur at this point, then the material may be carried forward by the glacier as long as there is no obvious hindrance to forward movement of the block". The terms used by Boulton (1972b) such as "the plucking of very large erratics" and the plucked "mass", suggest that this mechanism was proposed for the incorporation of bedrock pieces much larger than boulders. Since the uraniferous sandstone in the boulder field occurs in boulder or smaller size fragments, the highly silicified uraniferous sandstone contains no known major horizontal plane of weakness and the uraniferous sandstone was likely fractured and plucked during warm based ice conditions; the freeze-on mechanism is not considered further in this study.

It has been observed that plastic flow is most effective for the plucking of boulder size fragments and regelation is favoured for smaller particles (Boulton, 1974; Sugden and John, 1976). At west Dismal Lakes, plucking of the uraniferous sandstone boulders was likely accomplished by plastic ice flow or regelation in a region of warm freezing base, or a combination of the two. The irregular bedrock surface and the evidence of basal ice flow diverted by bedrock protuberances, indicate that the conditions necessary for plucking by plastic flow existed. Boulton (1972b) and Sugden (1977) both theorized that continental ice sheets had changing basal thermal conditions outwards from their centre. The progression had melting beneath the centre, through a zone of basal freezing of meltwater, to a frozen base nearer the ice sheet margin. Sugden (1977) in a schematic map places the Dismal Lakes area, at the glacial maximum, in the zone of warm basal

freezing, where interior derived meltwater froze to the ice sheet sole. Thus, the conditions for Weertman's (1961) and Boulton's (1972b) regelation plucking process may also have existed at west Dismal Lakes during the period of maximum erosion.

Plucking of abrasion products was likely accomplished by a combination of the two regelation mechanisms. Plastic flow of ice likely was a minor component in the plucking of rock flour.

Zones of Increased Erosion and Plucking at West Dismal Lakes - The factors controlling the areas of increased abrasion, fracturing and plucking at west Dismal Lakes are listed in Table 10. After each of the factors are discussed individually, they are combined to outline the probable zone of erosion and plucking of the uraniferous sandstone.

With the basal ice flow influenced by bedrock topography, ice was funnelled through valleys parallel with the regional ice flow direction. In the west Dismal Lakes valley, funnelling created a zone of convergent and compressive flow as ice entered the valley, and a zone of divergent and extending flow as the valley widened. Increased erosion is expected in: (1) the main valley bottom parallel to the regional ice flow direction, (2) the zone of convergent flow, and (3) the zone of extending flow. These zones are roughly outlined on Figure 29. The zones do not overlap, except in a triangle northeast of Mid Lake where two of the zones coincide.

Bedrock areas with joints and/or faults are difficult to map at west Dismal Lakes due to the drift cover. Two faults are shown on Figure 29. It has been speculated that the easternmost fault extends beneath the southwest arm of Dismal Lakes. Block fields are believed to indicate jointed bedrock at or close to the surface. Block fields of Unit 11 sandstone are outlined on Figure 29. Increased fracturing is likely in bedrock areas with planes of weakness, such as block fields. Plucking is likely to be greater in areas of fracturing. Erosion may be enhanced, due to increased debris load in the basal ice, in the direction of ice flow from zones of plucking.

Outcrops of diabase indicate a dike crosses the west Dismal Lakes valley east of the boulder field (Figure 29). These outcrops are topographic highs and illustrate the resistant nature of diabase compared to the surrounding sandstone. West of the dike, diabase debris in the ice may have increased erosion.

For the west Dismal Lakes area, increased abrasion, fracturing and plucking are expected in the following environments.

	Abrasion	Fracturing	Plucking
1. In valley bottoms parallel to the regional ice flow direction	X	X	
2. In zones of converging ice flow	X	X	
3. In zones of extending ice flow	X	X	
4. Along the stoss and lateral sides of bedrock protuberances	X		
5. Along the lee sides of small but high bedrock protuberances		X	
6. In zones with many bedrock joints and/or faults		X	
7. Down ice from zone of plucking	X	X	
8. Down ice from a change to a less resistant bedrock lithology	X	X	
9. Along the lee side of bedrock knobs which have a greater length than width			X
10. In bedrock lows			X

Table 10. Factors controlling areas of increased abrasion, fracturing and plucking

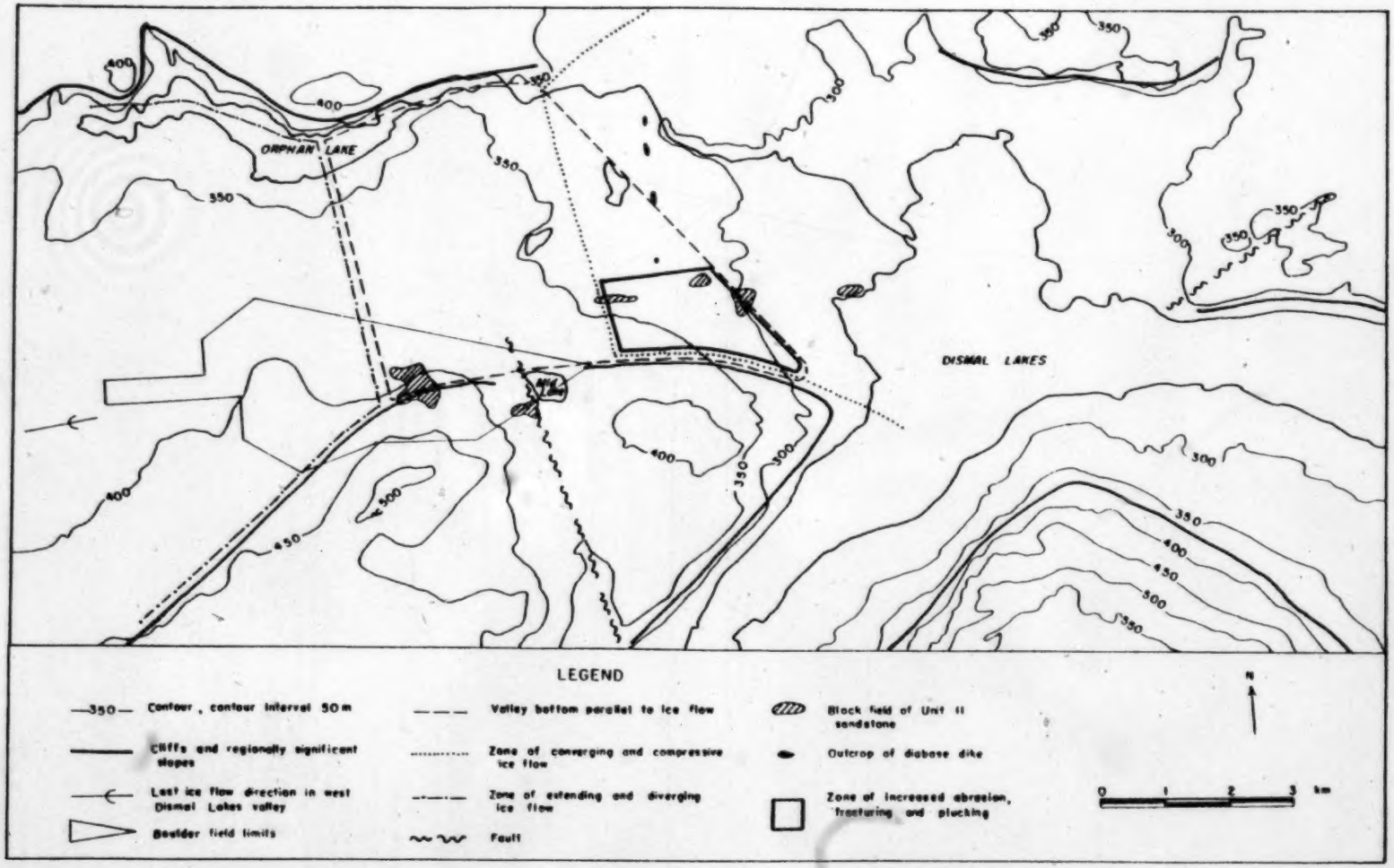

Figure 29. Zones of increased erosion and plucking

Bedrock protuberances cannot be mapped at west Dismal Lakes due to the drift cover. However, it is believed that numerous protuberances large enough to enhance erosion and plucking existed prior to the last glacial advance and may still exist beneath the drift. This interpretation is based on the irregular bedrock surface mapped further east in the Dismal Lakes valley.

After compiling the above data, outlined on Figure 29 is the proposed zone of increased abrasion, fracturing and plucking of Unit 11 sandstone between the boulder field and Dismal Lakes. It is the area of greatest overlap of the environments where increased erosion and plucking are expected. The north boundary of the outlined area is the contact between Unit 11 sandstone and Unit 12 shale. The south boundary coincides with the southern edge of the main valley. The west and east boundaries are more interpretive; the west boundary is the western limit of basal ice converging into the valley and the east boundary is the eastern limit of the valley bottom which is parallel to the last ice flow. Within the outlined area, abrasion is expected to dominate on the stoss and lateral sides of bedrock protuberances, and fracturing and plucking are the dominant process expected on the lee sides. Also within the proposed area, localized increased erosion and plucking probably occurred west of the diabase dike and / or in areas where block fields presently are.

(f) Transport - Subglacially derived debris is usually carried in the lowest level of the basal transport zone of an ice sheet. This level is called the stratified facies by Lawson (1979) and the traction zone by Boulton (1975). Occasionally processes occur within this level, often in response to bedrock topography or changing basal thermal conditions, which allow debris to be moved upward into the upper basal or englacial transport zones. On rare occasions, these processes carry basally derived debris to the supraglacial transport zone (Boulton, 1978).

Since the glacial debris at west Dismal Lakes sourced at the ice sheet base, one would expect that the debris was transported low in the basal zone of the ice sheet (Lawson, 1979; Boulton, 1975). However, the angular nature of, and the lack of striae on, the uraniferous sandstone boulders is not consistent with transport where debris is in contact with the bedrock and other debris.

If the debris, including the boulders, was not transported in the lowermost basal ice, it is likely the debris was carried either in the upper level of the basal transport zone (dispersed facies of Lawson, 1979; suspended zone of Boulton, 1975) or the lower level of the englacial transport zone (diffused facies of Lawson, 1979). A number of mechanisms which move basally incorporated debris higher in an ice sheet have been proposed; most involve ice thrusting, or in other words the formation of a series of low angle shear planes within the ice.

Three mechanisms have been proposed to initiate a series of shear planes. (1) Nye (1952) postulated that shear planes can occur when the bedform beneath the ice sheet becomes concave. Such areas have compressive flow with a resulting decrease in flow rate in the direction of ice flow. This idea was further refined by Moran (1971) and Clayton and Moran (1974). (2) Boulton (1972b) proposed that at the boundary between warm interior and cold more marginal basal thermal conditions , shear planes, folding and other deformation can occur. The change in flow dynamics including a decrease in flow rate in the direction of ice flow, cause longitudinal compression and high stress which generate discrete shear planes. (3) The movement of ice over bedrock protuberances , faults or dikes perpendicular to the ice flow direction, can result in shear planes (Boulton, 1970a) and/or folding (Whillans, 1978; Boulton, 1974). The deformation is in response to localized changes in the basal thermal regime, pressure gradients, and stress gradients as the ice flowed over the protuberance. In all mechanisms, shear planes cannot incorporate or pluck debris, they only move debris to a higher transport zone within the ice (Boulton, 1970a; and 1972b).

Two mechanisms which do not involve shear planes have been proposed. Rothlisberger (1968) noted that differential movement between basal debris layers can cause debris to rotate and rise within an ice sheet. Boulton (1978) speculated that if an extreme amount of basal freezing of meltwater derived from the ice sheet interior occurred, then debris could be moved a large distance away from the ice sheet base.

At west Dismal Lakes, the bedrock topography is presently irregular and it is believed to have been even more irregular prior to the last ice advance. The easternmost 3 km of the west Dismal Lakes valley has a slight concave profile. Sugden (1977) speculated that the Dismal Lakes area was near the boundary between warm freezing and cold frozen

basal conditions at the glacial maximum, the period when erosion of the uraniferous sandstone is believed to have occurred. With these three conditions, the west Dismal Lakes area had the environmental requirements for the movement of debris into higher transport zones by a series of shear planes.

The lowest ice layer, west from the zone of erosion and plucking of the uraniferous sandstone, was debris-rich. The debris increased the ice viscosity, shifting the ice closer to brittle behavior, in contrast to the plastic-like behavior of debris-poor ice. This, in combination with suitable environmental requirements, enabled shear planes to occur beneath the ice sheet in the west Dismal lakes area. The shear planes would have been similar to those illustrated by Moran (1971) and discussed theoritically by Hambrey and Muller (1978).

In proposing the location of the shear zone one should note (1) the distribution of the uraniferous sandstone boulders, (2) the area which has been proposed for increased erosion and plucking of Unit 11 sandstone, and (3) the anomalous areas of uranium in the geochemical plots. All these point to the west Dismal Lakes valley east of the boulder field as the probable source region. In this area, there is no change in valley profile and the former ice sheet would have had the same basal thermal regime, therefore a locally prominent topographic high likely initiated the shear planes. The most prominent topographic protuberance within the valley is the diabase dike. The dike could have acted as a ramp for the uraniferous sandstone boulders. If so, the boulder's source area is east of the dike and probably in the zone of increased erosion and plucking.

In view of the angularity and distribution of the uraniferous sandstone boulders, it is believed that shear planes in close proximity to the zone of plucking moved the boulders away from the ice/rock interface. This prevented significant rounding and dispersal of the boulders. Large scale freezing of meltwater from the ice sheet interior may have aided in moving the boulders and other debris away from the ice sheet base. Transport of the uraniferous debris was probably in the upper level of the basal transport zone and/or the lower level of the englacial transport zone.

(g) Deposition - All west Dismal Lakes till examined was within the active layer, therefore, structure and other properties may have been altered by frost and water

processes and no conclusion on the exact depositional environment of the till can be made. This is a problem when areas have no vertical exposures / sections and only surface sampling is possible. However, for situations when till is well exposed the following is a theoretical discussion on the deposition and classification of till on the Canadian Shield including some speculation with regards to west Dismal Lakes till. Explorationists should be able to apply the till classification scheme presented. Till is classified according to the process of deposition and associated position with respect to the ice mass. The genetic classification of tills by Haldorsen (1982) is used in this study. The four basic till types are lodgement, subglacial melt-out, supraglacial melt-out and flow (Table 11). The first two are deposited subglacially, the last two supraglacially. Only lodgement till is deposited directly from active ice, though subglacial melt-out can be deposited in the active ice zone.

Lodgement till is deposited by the lodging and plastering of material from basal sliding ice by pressure melting and other mechanical processes (Haldorsen, 1982; Dreimanis, 1982). When the frictional drag between the substrata and the debris of the basal traction zone equals the tractive force exerted on the debris by the advancing glacier, the debris no longer moves and becomes lodged.

Melt-out till is deposited by a slow release of glacial debris from stagnant ice by melting and / or sublimation, without internal sliding or deformation (Dreimanis, 1982). Melting can take place either at the surface or at the base of the glacier, while sublimation can only occur at the surface (Shaw, 1977). The glacier ice is stagnant as a result of either general stagnation of the glacier, or local stagnation of ice blocks beneath active ice (Lawson, 1981a). Subglacial melt-out till may form beneath marginal positions of cold based glaciers (Haldorsen, 1982; Shaw, 1979), beneath thick active warm based glaciers where pressure melting and basal stagnation occurs in zones of concentrated subglacial debris (Haldorsen, 1982; Boulton, 1970b), or by the melting of buried, debris-rich basal ice remnants associated with stagnant ice during final deglaciation (Haldorsen, 1982). Supraglacial melt-out till is deposited by the processes of melt-out and lowering of surrounding and underlying ice, at or near the ice front.

Flow till or sediment flow deposits (Lawson, 1979) result from the down slope transport of sediment-water mixtures on ice marginal slopes under the force of gravity. The sediment in the flows is debris released through melt-out processes. Each till type has

till type	A LODGEMENT	B SUBGLACIAL MELT-OUT	C SUPRAGLACIAL MELT-OUT	D FLOW
location of deposition	subglacial	subglacial	supraglacial	supraglacial
ice zone of deposition	active	stagnant or active	stagnant	stagnant
typical characteristics	1. fissility 2. dense, over consolidation 3. striated clasts 4. high proportion of fine grained matrix material (Boulton et al., 1979) 5. bullet nosed boulders with truncated distal ends (Boulton, 1978; Kruger, 1979) 6. abraded, subrounded clasts 7. shear planes 8. resting on bedrock 9. in areas of irregular bedrock topography 10. massive 11. clasts are dominated by local lithologies (Shaw, 1977) 12. lacking meltwater features	1. subangular clasts (Boulton, 1978) 2. massive or occasional stratifications (Lawson, 1979) 3. loose, normal consolidation (Lawson, 1979) 4. clasts are dominated by local lithologies (Shaw, 1979) 5. in areas of irregular bedrock topography 6. lacking meltwater features 7. high proportion of coarse material (Haldorsen, 1982)	1. massive (Lawson, 1979) 2. coarse material (Eyles, 1979; Lawson, 1979) 3. clasts lack striae 4. angular boulders (Boulton, 1978) 5. loose, normal consolidation (Lawson, 1979) 6. laterally extensive sheet deposits (Lawson, 1979) 7. sorted and stratified sediments within or interstratified with till (Haldorsen and Shaw, 1982) 8. large unlithified clasts of sediment derived from subtill deposits (Haldorsen and Shaw, 1982)	1. graded bedding 2. thin laminated units 3. rip-up clasts 4. reworked sediment 5. loading structures 6. linear flow structures on tops and bottoms of individual flows 7. shortage of boulder or larger size material 8. associated with fluvial and lacustrine deposits

Table 11. Till types and typical characteristics

typical characteristics associated with it, though few characteristics are diagnostic of a particular till. Till of a given process can be identified only by using an assemblage of characteristics (Table 11).

At west Dismal Lakes the uraniferous sandstone boulders and associated glacial debris were likely transported in the upper level of the basal transport zone and/or in the lower level of the englacial transport zone. Deposition of debris from the basal transport zone is usually subglacial. Material in the lower level of the englacial zone normally is exposed and deposited subglacially, though supraglacial deposition can occur.

Sudgen and John (1976) have proposed a model of depositional landscapes from which the zone of deposition, either active or stagnant, and therefore the place of deposition with respect to the ice sheet periphery can be inferred. Using the model, the lack of ice disintegration features in combination with the localized occurrence of drumlins and single crested eskers, indicate deposition of glacial debris at west Dismal Lakes occurred beneath the active zone of the ice sheet, a significant distance (>100 km) away from the ice sheet front.

The two subglacial deposition processes are lodgement and melt-out. Lodgement always occurs beneath active ice whereas melt-out usually takes place beneath stagnant ice. However, melt-out till can be deposited from stagnant ice blocks lodged beneath active ice (Boulton, 1970b; Haldorsen, 1982).

The process of melt-out beneath active ice generally follows a specific sequence of events (Boulton, 1970b; Haldorsen, 1982). As glacier flow increases over bedrock protuberances, debris-rich, less plastic ice proximal to the glacier sole is overridden by higher, plastically deformed, debris-poor ice. The debris-rich ice therefore becomes stagnant in relation to the overlying active ice. This stagnant ice then melts by a combination of the following basal heat sources: pressure melting, geothermal energy and friction produced by circulating meltwater. Thus in areas of irregular bedrock topography, stagnant ice blocks beneath active ice result in deposition of subglacial melt-out till.

This situation is possible for the deposition of the west Dismal Lakes till. The irregular bedrock topography and warm basal ice conditions which are believed to have existed during erosion and deposition of debris, provide the conditions at west Dismal lakes required for deposition of subglacial melt-out till.

A subglacial melt-out origin for the west Dismal Lakes boulders and associated till is also supported by valley topography. The boulder field is located where the west Dismal Lakes valley begins to widen significantly (Figure 29). The boulder field is at the crest of a continuous rise from Dismal Lakes. West of the boulder field the land gently slopes downward to the west. As the ice moved through the valley, extending and diverging flow commenced in the vicinity of the boulder field in response to a new convex profile and widening valley. In such an environment basal debris-rich ice is unable to respond to the changing flow dynamics and stagnates, forming subglacial ice blocks. The northwest limit of boulders in the field occurs as a sharp boundary between 22N, 16E and 17N, 11E (Figure 12), this limit may represent the maximum distance a debris-rich ice block(s) that contained the uraniferous sandstone boulders could diverge as it entered a widened valley, before it stagnated subglacially.

In summary, the west Dismal Lakes till may have been deposited from debris in subglacially stagnated ice blocks, with overlying debris poor active ice. If so, when the ice melted, the result would be that the surface till in the west Dismal Lakes area is a subglacial melt-out till.

B. POST GLACIAL PROCESSES

A knowledge of the surficial processes active in the west Dismal Lakes valley during the post glacial period helps the interpretation of boulder and geochemical data, and contributes the final segment in the reconstruction of the area's geologic history. At west Dismal Lakes a number of processes which modify the surficial sediments have been active during the post glacial period. Some processes operated over a short time span, such as those associated with proglacial meltwater, while others including drainage, slope and frost action processes have been and continue to be active since the withdrawal of ice. The boulder field and till geochemistry sampling sites have been modified to some degree by one or a combination of post glacial processes.

Immediately following the withdrawal of ice, the Dismal Lakes valley was flooded by Glacial Lake Coppermine. At west Dismal Lakes the maximum water level, at which the lake remained for a significant period of time, was approximately 320 m asl. The maximum elevation of beach ridges is at this elevation. St-Onge (1980) and St-Onge *et al*. (1981)

concluded that the maximum extent of Glacial Lake Coppermine was at the west end of Orphan Lake, indicating the maximum lake level was at approximately 350 m asl. The network of poorly formed runoff channels at elevations below 340 m asl in the west Dismal Lakes valley indicate that land up to this level was briefly flooded and then quickly drained. In areas below 340 m asl, the till plain was slightly reworked by lake and wave action processes. The uraniferous boulder field was not flooded by the lake as all boulders are on ground above 350 m asl. The northeast corner of the till geochemistry sampling grid consists of reworked till.

The main post glacial drainage processes at west Dismal Lakes are (1) fluvial erosion by, and alluvial deposition along and at the mouths of, intermittent streams and (2) slopewash. French (1976) believes slopewash can be a significant process of erosion and transport, even on very low angle slopes, in periglacial areas. Slopewash probably has moved an unknown amount of fine grained till material down slope at west Dismal Lakes. However, little if any modification to the uraniferous boulder field or till geochemistry samples is believed to have resulted from slopewash or processes along streams.

Gelifluction is widespread in the west Dismal Lakes area on slopes greater that 3 °. The rate of gelifluction has not been measured in the study area, however French (1976) measured the average annual movement on 2 to 4 ° slopes on Banks Island at 1.56 cm. None of the main boulder field area has slopes greater that 3 °. However, up to 20 scattered uraniferous sandstone boulders south of 10N and east of 25E occur on slopes greater than 3 °. These boulders have been moved a maximum, but probably much less than, 150 m downslope by gelifluction.

Frost action processes have been occurring within the active layer at west Dismal Lakes since the withdrawal of glacial ice. The products of frost action in the area of the boulder field and till geochemistry sampling grid, include block fields, mudboils, and uplifted and tilted boulders. However, none of the uraniferous sandstone boulders are located in, nor were till geochemistry samples taken from, block fields.

Frost heaving is the predominantly upward movement of water to the freezing plane and its subsequent expansion on freezing. It is primarily confined to the upper half of the active zone (French, 1976). Mudboils, a product of frost heaving, occur throughout the west Dismal Lakes area. Because till moves upward in mudboils, the sampling of

mudboils retrieves less weathered material from a deeper source with a minimum of digging.

The upfreezing of objects, a result of frost heaving, is common in sediments containing coarse particles in association with an appreciable fines content. West Dismal Lakes till has approximately 53 % fines in the matrix and abundant clasts, and therefore has the required conditions for the upfreezing of objects . The accumulation of boulders on the west Dismal Lakes till surface is, in part, a function of the upfreezing process. The boulders have moved upwards a maximum of 20 cm because the upfreezing process has little effect below this depth (French, 1976).

The tilting of objects is caused by differential frost heave at the top and bottom of objects, which results in their rotation. The effects of tilting on the uraniferous sandstone boulder distribution are believed to be minimal.

In summary, the distribution and orientation of the west Dismal Lakes uraniferous sandstone boulders probably have undergone slight modification by post glacial processes. Apart from the main boulder concentration, a few boulders that occur on slopes greater than 3 ° may have experienced some down slope movement by gelifluction. Some or all the boulders have been lifted a maximum of 20 cm to the till surface. All till geochemistry samples have undergone postglacial alteration from slopewash and solutional activity, but the amount of alteration is believed to be small. More alteration has been experienced by the till geochemistry samples in the northeast corner of the grid which were exposed to lake and wave action processes of Glacial Lake Coppermine.

C. A MODEL FOR THE EROSION, TRANSPORT AND DEPOSITION OF WEST DISMAL LAKES URANIFEROUS SANDSTONE BOULDERS

The distribution of west Dismal Lakes boulders agrees with the portion of Bayrock's (1980) modified dispersion curve outlined on Figure 17. A model of the processes leading to this non-ideal dispersion pattern can be used to speculate on the bedrock source of the boulders. Of greatest interest is the reason for the segment missing from the ideal dispersion curve. This segment extends from the bedrock source of the boulders to the main concentration of boulders.

Perhaps the missing segment results when the source area has been completely eroded away. This is a possibility at west Dismal Lakes, since the bedrock source of the boulders has yet to be found. However, there exists the possibility that only a small portion of the uraniferous sandstone has been eroded, and therefore a uranium deposit remains to be discovered. Following, therefore, is an alternative explanation of the missing segment and a discussion of the glacial history of the west Dismal Lakes boulders. This hypothesis assumes the boulders were quarried from a small area. The large size of the boulders and the concentration of boulders at the field centre cannot be explained by abrasion or by processes which acted over a large area. The uraniferous sandstone was fractured subglacially. Temporary changes in pressure and stress in subglacial sandstone protuberances, induced by the jerky stick-slip motion of debris-rich ice over the protuberance, led to sandstone fracturing at lee side positions (Boulton, 1974, 1978). The reconstruction of ice dynamics, which indicate that ice flow was modified by the irregular bedrock topography at west Dismal Lakes, supports this mechanism.

Plucking of the boulders from the rock / ice interface was by plastic ice flow into the lee side positions of bedrock protuberances (Boulton, 1974) and / or regelation in a region of warm basal freezing (Weertman, 1961; Boulton, 1972b). The irregular bedrock topography of west Dismal Lakes supports the first mechanism, and modeling of ice sheet conditions at the glacial maximum (Sugden, 1977) supports the second.

Erosion of the uraniferous sandstone likely occurred at the lee side of bedrock protuberances which are located in the middle of west Dismal Lakes valley and in a zone of converging or extending ice flow. Areas of high erosion potential were outlined earlier (Figure 29).

The lack of striae on the boulders, the angularity of the boulders and the dense concentration of boulders at the field centre indicate the boulders were moved upward away from the basal traction zone soon after plucking. Shear planes at the ice / rock interface, similar to that seen near glacier margins, is the best mechanism for moving the boulders into a higher transport zone (Nye, 1952; Moran, 1971; Clayton and Moran, 1974; Boulton, 1970a; Hambrey and Muller, 1978). A series of shear planes, similar to that illustrated by Moran (1971) is envisioned for the uraniferous boulders (Figure 30(a)). The ice could be sheared because the large debris load increased the ice's viscosity

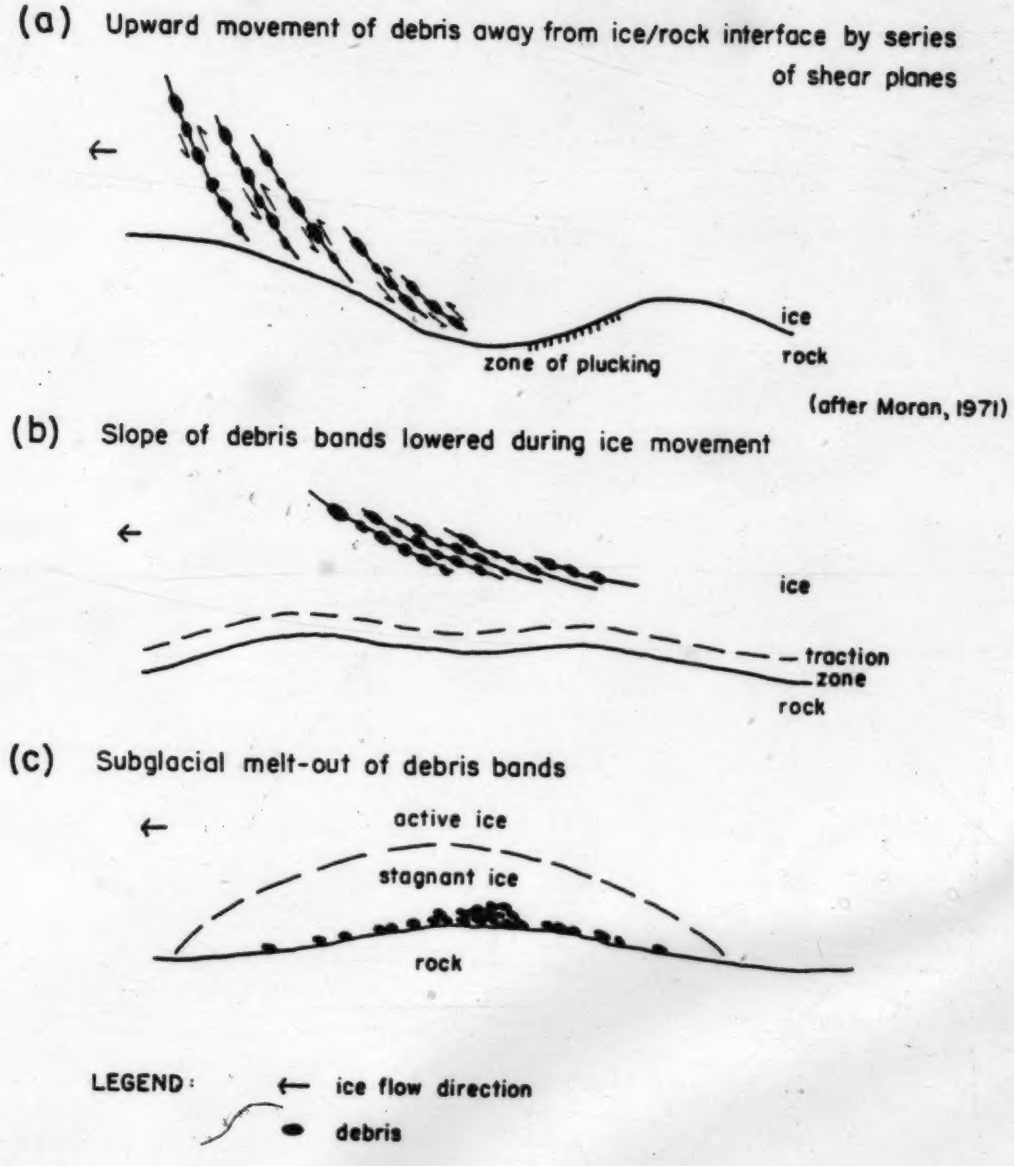

Figure 30. Model of boulder transport and deposition

(Sugden and John, 1976). The primary cause for the shear planes was bedrock protuberances, such as the topographically prominent diabase dike which crosses the west Dismal Lakes valley east of the boulder field. The formation of shear planes was also aided by the slightly concave valley profile and the nearby boundary between warm and cold based ice (Sugden, 1977). The result of this mechanism, was a series of essentially parallel debris-rich bands within the ice.

The shear planes, as envisioned, involved less than 5 % of the total thickness of the ice sheet. Shear planes of this type are not documented in the literature because (1) it is beneath glaciers, away from the margin and not available for viewing, and (2) it is small scale and therefore is difficult to detect with geophysical techniques. During ice movement, the slope of the debris bands was lowered. The debris bands became stacked, especially in the central area (Figure 30(b)).

Subglacial stagnation of debris-rich ice block(s), in response to a change to diverging flow as ice moves out of a confining valley and a change to a convex bedrock profile, may have resulted in subglacial melt-out at west Dismal Lakes. Subglacial melt-out would have caused material from the debris-rich bands, including the uraniferous boulders, to be lowered and would have resulted in material from the stacked bands to be concentrated in the central area (Figure 30(c)). Concentrations of debris decrease both opposite to, and in the direction of, glacier flow from this central area.

The source of west Dismal Lakes boulders is believed to be east of the fan apex; that is east of the easternmost uraniferous boulder. The gaps between the bedrock source and fan apex and the main boulder concentration are best explained by transport of the boulders above the ice sheet base (Minell, 1978).

V. CONCLUSIONS AND RECOMMENDATIONS

The purpose of this study was to reduce the exploration area for the bedrock source of the uraniferous sandstone boulders. The study was divided into three segments. The glacial geology segment involved the mapping of surficial sediments and the reconstruction of the glacial and post glacial geologic history with respect to the uraniferous sandstone boulders and west Dismal Lakes valley sediments. The boulder field segment assessed boulder distribution and angularity. The till geochemistry segment assessed anomalous areas for a number of elements, all in regards to locating the bedrock source. The conclusions for the three segments are summarized below. All results and interpretations are combined to propose the most likely bedrock source area for the uraniferous sandstone boulders. In addition, an evaluation of the boulder tracing and till geochemistry methods, and recommendations for future exploration work, are presented.

A. GLACIAL GEOLOGY

(a) Ice flow directions - Regional flow of the last ice in the Dismal Lakes area was westward. The regional ice flow direction, measured from striae at high elevations, is in agreement with published papers (St-Onge *et al.*, 1981 ; Craig, 1960). In the Dismal Lakes valley and in areas with moderate to high local relief, such as the west Dismal Lakes area, ice flow was modified by bedrock topography. Striae on large bedrock hills show that the last ice moved northwest along the Dismal Lakes valley. Just north of the granitic upland the ice was diverted west and then southwest. In the west Dismal Lakes valley, and at the boulder field, the direction of the last glacial advance was towards 260 °. The primary evidence for this orientation is striae measured from outcrops near the boulder field at a low elevation. Secondary evidence includes: the polished eastern ends of bedrock knobs, the crude crag and tail form of some bedrock knobs, till clast lithology, uranium and copper till geochemistry anomalous areas elongated east-west and located east of the boulder field, and the east-west elongation of the boulder field.

(b) Ice conditions during boulder erosion and deposition - It is believed that maximum erosion conditions were necessary for the excavation of the boulders, and that maximum erosion conditions occurred at or close to the glacial maximum. The first is based on the resistive nature of th highly silicified uraniferous sandstone in the west

Dismal Lakes boulder field. The second is based mainly on relevant literature (Robin, 1972; Sugden, 1978; Boulton, 1972b), but evidence is also provided by the lack of ice disintegration terrain in the west Dismal Lakes area. At the glacial maximum, the Dismal Lakes area was 400 km east of the ice front and covered by greater than 2,000 m of ice.

With greater than 2,000 m of ice in the area, it is believed two distinct flow layers existed. The upper layer, estimated at 1,500 m thick, flowed westward as a sheet. The lower layer, with a maximum thickness of 500 m, had flow modified by the local bedrock topography. The lower layer had zones of diverging, converging, compressive and extending flow. Flow in this layer was by internal deformation and/or basal sliding depending on the basal thermal regime. In addition, the lower layer may have contained occasional stagnant ice blocks which did not extend upwards the full thickness of the layer. These ice blocks stagnated in response to changing ice flow dynamics and the irregular bedrock topography.

The Laurentide ice sheet likely was warm based during the erosion of the uraniferous sandstone. The volume (greater than 10 m^3) of uraniferous sandstone excavated from a small area cannot be explained by the limited erosion capabilities of a cold based ice sheet. Ice sheet models described in the literature (Sugden, 1977, 1978; Boulton, 1972b, 1974) agree with the requirement of warm basal conditions for significant erosion. The latent heat of fusion from the freezing of interior derived meltwater has been suggested as the main basal heat source (Sugden, 1977).

(c) Erosion and plucking of the boulders - The occurrence of glacial striae and molded bedrock outcrops confirm that abrasion occurred at west Dismal Lakes. The fracturing of bedrock into boulder size blocks likely resulted from pressures and stresses created by the ice moving over an irregular bedrock surface. Plucking, or the incorporation of boulders into the ice sheet base, was likely caused by the plastic flow of ice into the lee side position of bedrock protuberances and/or by regelation in a region of warm basal freezing. Plucking of abrasion products was by regelation.

The probable area of maximum abrasion, fracturing and plucking of Unit 11 sandstone in the valley east of the uraniferous boulder fan, is postulated to exist 5 to 7 km east from the main boulder concentration, or 0.5 to 2.5 km east from the boulder fan's apex. In delimiting the area, major consideration was given to the zone of converging ice

flow as ice was funnelled into the valley. Within the area, abrasion dominated on stoss and lateral sides of bedrock protuberances, and fracturing and plucking occurred at the lee sides.

(d) Transport and deposition of the boulders - The glacial debris, including the boulders, was transported in the lower englacial or upper basal zones of the ice sheet. The glacial debris was moved away from the ice sheet base by a series of shear planes. This was possible below the ice sheet because the high debris content of the lowest ice layer shifted this ice closer to brittle behavior. Shear planes occurred in response to irregular bedrock topography, concave valley floor profile and the nearby transition between warm and cold basal conditions. The topographically prominent diabase dike which exists east of the boulder fan may have acted as a ramp for the boulders. Deposition of the glacial debris and boulders may have been by subglacial melt-out from an ice block(s) stagnated below the active ice sheet. The stagnation would have been caused by one or a combination of the following; the ice became overloaded with glacial debris, ice dynamics changed to diverging and extending ice flow as the ice expanded into a widened valley, and/or ice flow was blocked by irregular bedrock topography. Evidence for deposition of the till by subglacial melt-out is the probable transport of the boulders above the ice sheet base and landforms in the area indicative of active ice.

(e) Post glacial processes - The west Dismal Lakes uraniferous sandstone boulders have undergone slight modification by post glacial processes. Up to 20 boulders, which are all southeast of the main concentration and on slopes greater than 3 °, may have been moved down slope by gelifluction up to, but probably much less than, 150 m. Some or all boulders have been uplifted a maximum of 20 cm to the surface by frost heaving. All west Dismal Lakes till, and therefore, all geochemical sample sites, have undergone slopewash and solutional activity. The amount of alteration is not known with certainty, but is believed to be small. Till below 320 m asl was reworked and/or eroded by the waters of Glacial Lake Coppermine. Till at less than 10 geochemical sample sites was altered by this process.

B. BOULDER FIELD

(a) Shape - The outline of the boulder field is almost entirely due to glacial dispersion. The distribution of the boulders has a crude fan shape, centred on the easternmost boulder. An approximate northern fan boundary exists within the area prospected in detail. The southern fan boundary is speculative, since most of the area south of grid line 10N has not been prospected in detail. Prospecting data indicates two possible fan axes. In the area prospected in detail, the main boulder concentration is elongated east-west along grid line 11N. This line also bisects relatively sharp northern and southern fan boundaries found by detailed prospecting along grid line 20E. The second possible axis is the line bisecting the arc subtended by the fan's apex. The first axis deviates about 8 ° from the direction of last glacial flow through the area, the second deviates by only 1 °. The fan shape indicates the last ice flowed approximately west and that dispersion of uraniferous sandstone was from a point source. The sharp decline in boulders at right angles away from the axes and the 43 ° angle of the fan, indicate the fan is a result of only one glacial advance. The distribution of boulders can be fitted to Bayrock's modified dispersion curve (personal communication January 19, 1983).

(b) Boulder angularity and transport distance - The angularity of the boulders is a result of glacial processes. Angularity caused by post glacial processes can be distinguished and is minor. The angular nature of the boulders is a result of the quartzose sandstone's resistance to abrasion in combination with boulder transport above the ice sheet base. Transport above the ice sheet base is confirmed by the lack of increasing boulder roundness away from the source.

The high density of boulders at the field center combined with the thin drift thickness indicate the boulders travelled a short distance. Bayrock's formula (1980) indicates a minimum 2.5 km transport distance. A comparison with Shilts (1973b) indicates a maximum 9 km transport distance from the main boulder concentration to the bedrock source. Bayrock's modified dispersion curve indicates a 5 km transport distance between the same end points (personal communication January 19, 1983). Comparison with the Uke Lake boulder train places this transport distance in the realm of possibility. With the first boulder in the field (and the fan's apex) 4.7 km up ice from the main boulder concentration, boulder distribution and angularity indicate about a 1 km gap between the

bedrock source and the first boulders.

C. TILL GEOCHEMISTRY

(a) Uranium - Uranium till geochemistry values aid in the determination of the last ice flow direction at west Dismal Lakes. Elevated uranium values in till occur along a line that extends east from the main boulder concentration and is parallel to the last ice flow direction. The largest uranium in till anomalous area occurs 6.2 km east of the main boulder concentration; in general values decrease westward from that point. The location of the largest uranium anomalous area makes is likely that the bedrock source is nearby. There is, however, no obvious correlation of uranium values in till with the main boulder concentration that exists at west Dismal Lakes.

(b) Other elements - There is no statistical correlation of uranium with any other elements analyzed. A comparison of the contoured plots of till geochemistry values indicates there is no correlation of uranium with chromium, nickel, molybdenum, cobalt, iron and manganese. The correlation matrix indicates all analyzed elements, except uranium and copper, are at background concentration. Copper values in till crudely illustrate the last ice flow direction, but have no correlation with the main boulder concentration. This indicates a uranium-copper link may exist. Therefore, both uranium and copper in till appear to be related to the bedrock source of the boulders.

(c) PEC samples - PEC geochemical values do not provide any significant results or a dispersion model which can be compared with west Dismal Lakes geochemical results. PEC geochemical sampling did not fulfill the intended purpose of finding elements in the drift which were related to the PEC deposit.

D. BOULDER SOURCE AREA

The main relevant data pertinent to interpreting the source area of the uraniferous boulders are summarized below, and are illustrated on Figure 31.

(1) The bedrock source is in Unit 11 sandstone.

(2) The uraniferous bedrock source may be associated with large scale structural features such as faults.

(3) The last ice flow, which eroded, transported and deposited the boulders, was towards

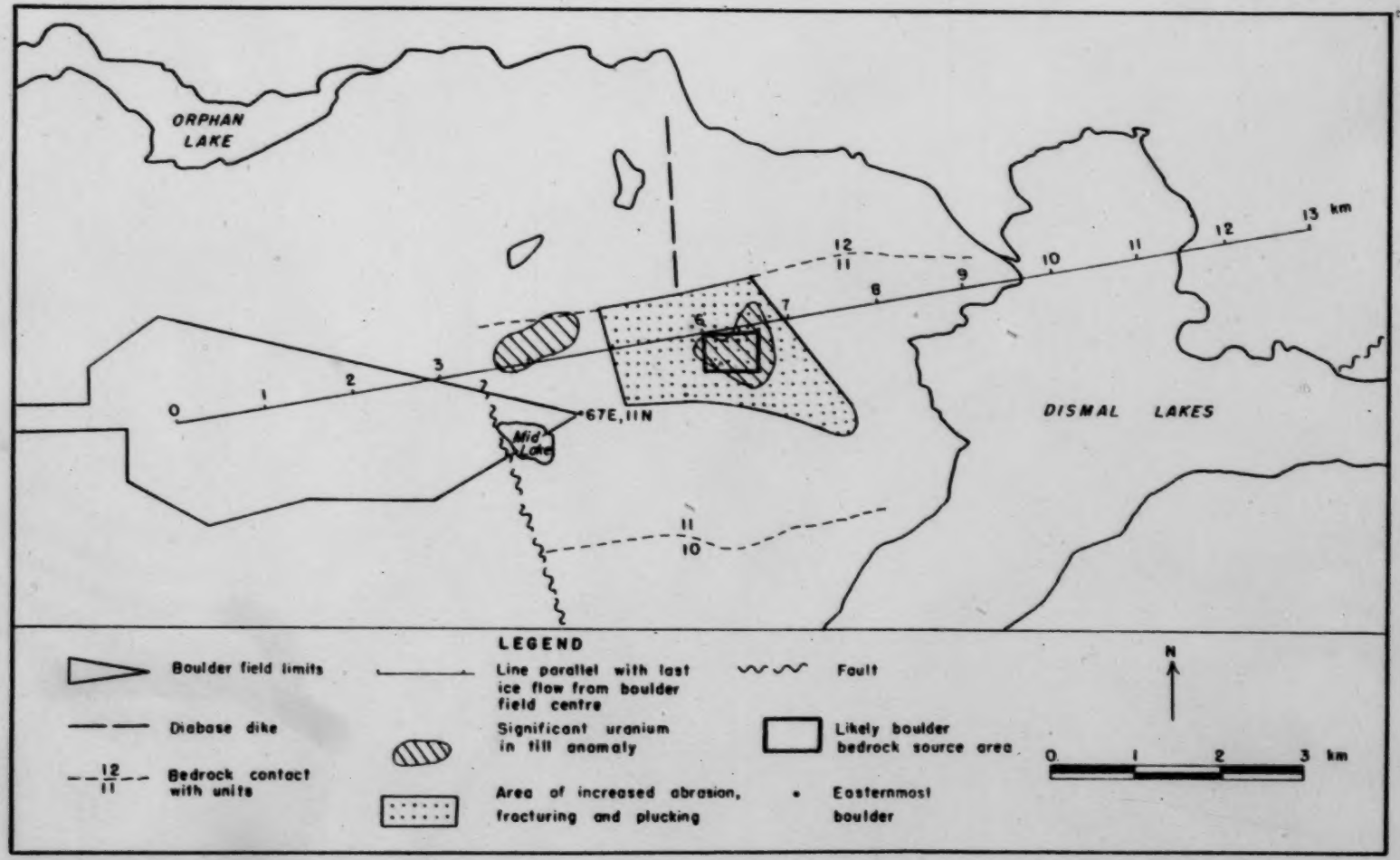

Figure 31. Boulder source area

260 °.

(4) The probable area of maximum abrasion, fracture and plucking in the valley east of the boulder field is 5 to 7 km east from the main boulder concentration, or 0.5 to 2.5 km northeast of the boulder fan's apex.

(5) The boulders were transported above the ice sheet base. The diabase dike 6 km east of the main concentration of boulders may have acted as a ramp to move boulders above the ice sheet base.

(6) The boulder field has a crude fan shape with an apex at 67E, 11N. The easternmost boulder is located at 67E, 11N. Possible fan axes are lines 268 ° and 259 ° azimuth.

(7) The transport distance of the boulders, from the main boulder concentration to the bedrock source, is between 2.5 and 9 km. The most likely transport distance is approximately mid way between these extremes.

(8) The largest uranium anomalous areas from till samples are 6.2 km northeast of the main boulder concentration along a line 260 ° azimuth.

The likely bedrock source of the boulders is shown on Figure 31. It is underlain by Unit 11, is just east of the mapped dike, and lies on a line parallel with the last ice direction and almost parallel to the boulder fan axes through the center of the main boulder concentration. The proposed source is in the probable area of maximum erosion and plucking, and in the zone of converging ice flow. The likely source is east of the easternmost boulder; the gap between them can be explained by transport above the ice sheet base. Being 6 to 6.6 km east of the main boulder concentration, the proposed source agrees with all transport distance indicators and almost exactly coincides with the largest uranium anomalous area from the till samples.

E. METHODS EVALUATION

(a) Boulder field analysis - From this study, it is concluded that the boulder field shape can indicate the last ice flow direction, provide an estimate of the distance of glacial debris transport and may indicate whether more than one glacial advance has influenced the distribution. Since the boulder volume plot provided similar results to the boulder distribution plot, it need not be recorded in future studies at west Dismal Lakes in the search for the source of the radioactive boulder train. Boulder angularity measurements

may provide worthwhile data if the glacial debris being traced was transported at the ice sheet base. However, if it is known that the glacial debris was transported above the ice sheet base, boulder angularity need not be measured. Boulder distribution data for an area that is prospected at consistent grid spacing, are easier to interpret. Thus, consistent prospecting grid spacing should be strived for, when possible, in future studies.

(b) Till geochemistry - From the results of this study, the following recommendations are made for future till sampling studies. Sample mudboils when possible since there are no geochemical differences between mudboil and undisturbed till samples, and mudboils are easier to dig, provide a less weathered sample and have less organic matter which may comtaminate samples. Do not compare samples from areas with greater than 0.3 m of drift with those of areas with less than 0.3 m of drift. The weathering differences between these sample types make combined results difficult to interpret. It is best to analyze the -2 μm fraction, since it gives the largest values, provides the best contrast between background and anomalous areas and is better at outlining glacial dispersion patterns. When analyzing for uranium, use DNC as a first choice over fluorometry. DNC results have better precision, due to the larger sample analyzed, and larger values. For future till geochemistry samples at west Dismal Lakes, the following elements should be analyzed for; uranium, copper, and manganese. Uranium and copper are likely associated with the source. Manganese values can be used as a check for severe weathering, and for quenching, if fluorometry uranium analysis is used.

F. RECOMMENDATIONS FOR FUTURE WORK

Diamond drilling will be required to locate the uranium source in bedrock, as it is probably drift covered, and to test the bedrock to the base of Unit II. However, further till sampling in the vicinity of the proposed source may better define geochemically anomalous areas of till and therefore reduce the amount of diamond drilling. Surface sampling of mudboils (till), utilizing a more detailed grid than used in this study, may refine the size and shape of the uranium in till anomalous area in two dimensions. To further trace the anomalous zone down to bedrock, it is important to know the local drift thickness. A small hand-held percussion drill would be a quick and portable method to survey the drift thickness. If the drift thickness is less than 2 m and the surface area of the anomalous

zone is small, diamond drilling probably would be the next phase of exploration. However, if the drift exceeds 2 m in thickness and/or the surface area of the anomalous zone is broad, and if a continuous sampling overburden drill is more cost effective than diamond drilling, then, a three dimensional till sampling program may be successful in tracing the anomalous zone to bedrock. An overburden drilling program can be an important exploration step in areas of thick drift. Geochemically anomalous zones in till frequently slope upwards in the direction of glacial advance, in areas of thick drift the top and bottom of the anomalous till zone can be offset a significant distance. If overburden drilling is undertaken, holes should extend a metre into bedrock. Deeper penetration into Precambrian bedrock is very slow and hard on equipment. For deep penetration into bedrock and for follow-up work, diamond drilling would be used.

VI. REFERENCES

Abercrombie, H.J., and Trigg, C.M. 1980. Geological research 1979 - 1980, YUK mineral claims, Mountain Lake, Mackenzie mining district, Northwest Territories. Unpublished report prepared by Trigg, Woollett Consulting Ltd. for Esso Minerals Canada.

Ahuja, S.P. 1974. Exploration YUK mineral claims, Mackenzie District, Northwest Territories. Unpublished report prepared by Trigg, Woollett & Associates Ltd. for Imperial Oil Limited.

Ahuja, S.P. 1978. Hornby Bay Basin Exploration, Mackenzie District, Northwest Territories. Unpublished report prepared by Trigg, Woollett Consulting Ltd. for Esso Minerals Canada.

Allan, R.J., and Hornbrook, E.H.W. 1971. Exploration geochemistry evaluation study in a region of continuous permafrost, Northwest Territories, Canada. *In* Geochemical Exporation, proceedings 3rd International Geochemical Exploration Symposium. Canadian Institute of Mining and Metallurgy, Special Volume 11, pp. 53-66.

American Society Testing and Materials. 1964. Standard method for grain size analysis of soils. *In* Procedures for testing soils. American Society Testing and Materials, Philidephia, pp. 95-106.

Baragar, W.R.A., and Donaldson, J.A. 1973. Coppermine and Dismal Lakes map areas 86 O and 86 N. Geological Survey of Canada, Paper 71-39, 20p.

Bayrock, L.A. 1980. Erratics, boulder trains and glacial dispersion. *From* Glacial geology in service of mineral exploration, a workshop. University of Toronto, Toronto, 10p.

Bjorklund, A. 1976a. The use of till in geochemical uranium exploration. *In* Exploration of uranium ore deposits. International Atomic Energy Agency, pp. 297-309.

Bjorklund, A. 1976b. Pauktajanvaara: Uranium in till above mineralization. *In* Conceptual models in exploration geochemistry. *Edited by* L.K. Kauranne. Journal Geochemical Exploration, 5(3), pp. 287-289.

Boulanger, A., Evans, D.J.R., and Raby, B.F. 1975. Uranium analysis by neutron activation delayed neutron counting. Atomic Energy of Canada Limited, commerical products division publication.

Boulton, G.S. 1970a. On the origin and transport of englacial debris in Svalbard glaciers. Journal of Glaciology, 9(56), pp. 213-229.

Boulton, G.S. 1970b. On the deposition of subglacial and melt-out tills at the margin of certain Svalbard glaciers. Journal of Glaciology, **9**(56), pp. 231-245.

Boulton, G.S. 1972a. Modern arctic glaciers as depositional models for former ice sheets. Journal Geological Society of London, **128**, pp. 361-393.

Boulton, G.S. 1972b. The role of thermal regime in glacial sedimentation. *In* Polar geomorphology. *Edited by* R.J. Price and D.E. Sugden. Institute of British Geographers, Special Publication 4, pp. 1-19.

Boulton, G.S. 1974. Processes and patterns of glacial erosion. *In* Glacial geomorphology. *Edited by* D.R. Coates. Publications in geomorphology, State University of New York, Binghamton, pp. 41-87.

Boulton, G.S. 1975. Processes and patterns of subglacial sedimentation: a theoretical approach. *In* Ice ages: ancient and modern. Geological Journal, Special Issue 6, pp. 7-42.

Boulton, G.S. 1978. Boulder shapes and grain size distributions of debris as indicators of transport paths through a glacier and till genesis. Sedimentology, **25**, pp. 773-799.

Boulton, G.S. 1979. Processes of glacier erosion on different substrata. Journal of Glaciology, **23**(89), pp. 15-37.

Boulton, G.S., Dent, D.L., and Morris, E.M. 1974. Subglacial shearing and crushing, and the role of water pressures in tills from south-east Iceland. Geografiska Annaler, **56(A)**, pp. 134-145.

Boyle, R.W. 1974. Elemental associations in mineral deposits and indicator elements of interest in geochemical prospecting. Geological Survey of Canada, Paper 74-45, pp. 18-19.

Cameron, E.M. 1977. Geochemical dispersion in mineralized soils of a permafrost environment. Journal of Geochemical Exploration, **7**(3), pp. 301-326.

Carol, H. 1947. The formation of roche moutonnees. Journal of Glaciology, 1(2), pp. 57-59.

Chamberlain, T.C. 1888. The rock scorings of the great ice invasions. United States Geological Survey, 7th Annual Report, pp. 155-248.

Clayton, L., and Moran, S.R. 1974. A glacier process-form model. *In* Glacial geology. *Edited by* D.R. Coates. Publications in geomorphology, State University of New York, Binghamton, pp. 89-119.

Craig, B.G. 1960. Surficial geology of north-central District of Mackenzie, Northwest Territories. Geological Survey of Canada, Paper 60-18, 8p. and map 24-1960.

Craig, B.G., and Fyles, J.G. 1960. Pleistocene geology of arctic Canada. Geological Survey of Canada, Paper 60-10, 21p.

Cubitt, J.M., and Henley, S. 1978. Editor's comments on papers 2 through 13. *In* Statistical analysis in geology. *Edited by* J.M. Cubitt and S. Henley. Dowden, Hutchinson and Ross, Inc., Stroudsburg, Pennsylvania, pp. 11-16.

Davis, J.C. 1973. Statistics and data analysis in geology. John Wiley and Sons Incorporated, New York, 550p.

DiLabio, R.N.W. 1979. Drift prospecting in uranium and base-metal sites, District of Keewatin, Northwest Territories, Canada. *In* Prospecting in areas of glaciated terrain. The Institute of Mining and Metallurgy, London, pp. 91-100.

DiLabio, R.N.W., and Shilts, W.W. 1979. Composition and dispersal of debris by modern glaciers, Bylot Island, Canada. *In* Moraines and varves: origin, genesis, classification. *Edited by* A.A. Balkema. Rotterdam, pp. 145-155.

Douglas, J. 1913. The copper bearing traps of the Coppermine River. Transactions of Canadian Mining Institute, 16, pp. 83-101.

Drake, L.D. 1972. Mechanisms of clast attrition in basal till. Geological Society of America, Bulletin 83, pp. 2159-2165.

Dreimanis, A. 1958. Tracing ore boulders as a prospecting method in Canada. Canadian Mining and Metallurgy and Geological Association of Canada transactions, X, pp. 49-56.

Dreimanis, A. 1982. Commission on genesis and lithology of Quaternary deposits. INQUA, work group 1, Genetic classification of tills and criteria for their differentiation, Progess Report on Activities 1977 -1982.

Duke, M.J.M. *et al*. 1982. Sensitivity, accuracy, precision and detection limits of the new University of Alberta Slowpoke Facility delayed neutron counting system. University of Alberta Slowpoke Facility, Annual Report, pp. R9-R10.

Dyke, A.S., Dredge, L.A., and Vincent, J.S. 1982. Configuration and dynamics of the Laurentide ice sheet during the Late Wisconsin maximum. Geographie Physique et Quaternaire, XXXVI, pp. 5-14.

Earle, S. 1980. Tills, oxidised and unoxidised with particular reference to uranium. *From* Glacial geology in service of mineral exploration, a workshop. University of Toronto, Toronto.

Elementary Statistics using MIDAS. 1976. Statistical research laboratory, The University of Michigan, Ann Arbor, 300p.

Embleton, C., and King, C.A.M. 1975. Glacial geomorphology. 2nd edition, Edward Arnold Publishers Limited, London, 573p.

Eyles, N. 1979. Facies of supraglacial sedimentation on Icelandic and Alpine temperate glaciers. Canadian Journal of Earth Science, **16**(7), pp. 1341-1361.

Fraser, J.A. *et al*. 1960. North - central District of Mackenzie, Nortwest Territories. Geological Survey of Canada, Map 18-1960.

French, H.M. 1976. The periglacial environment. Longman Group Limited, London, 309p.

Geddes, R.S. 1982. The Vixen Lake indicator train, northern Saskatchewan. *In* Prospecting in areas of glaciated terrain 1982. Canadian Institute of Mining and Metallurgy, Montreal, pp. 264-283.

Geldsetzer, H. 1974. A lithological and stratigraphic study of Hornby Bay Group and Dismal Lakes Group. Unpublished report prepared by Trigg, Woollett & Associates Ltd. for Imperial Oil Limited.

Glen, J.W. 1955. The creep of polycrystalline ice. Proceedings of Royal Society, London, Series A 228, pp. 519-538.

Gow, A.J., Epstein, S., and Sheehy, W. 1979. On the origin of stratified debris in ice cores from the bottom of the Antarctic ice sheet. Journal of Glaciology, **23**(89), pp. 185-192.

Grant, A.H. 1980. WD1, WD2, WD3 mineral claims exploration, Mackenzie mining district, Northwest Territories. Unpublished report prepared by Trigg, Woollett Consulting Ltd. for Esso Minerals Canada.

Grant, A.H., and Woollett, G.N. 1979. Hornby Basin exploration, Mackenzie mining district, Northwest Territories. Unpublished report prepared by Trigg, Woollett Consulting Ltd. for Esso Minerals Canada.

Grimaldi, F.S. *et al*. 1954. Summary of methods of analyses for the determination of uranium and thorium. United States Geological Survey, Bulletin 1006, pp. 1-9.

Haldorsen, S. 1982. The genesis of till from Astadelen, southeastern Norway. Norsk Geologisk Tidsskrift, **62**, pp. 17-38.

Haldorsen, S., and Shaw, J. 1982. The problem of recognizing melt-out till. Boreas, **11**, pp. 261-277.

Hallet, B. 1979. A theoretical model of glacial abrasion. Journal of Glaciology, **23**(89), pp. 39-50.

Hambrey, M.J., and Muller, F. 1978. Structures and ice deformation in the White Glacier, Axel Heiberg Island, Northwest Territories, Canada. Journal of Glaciology, **20**(82), pp. 41-66.

Hornbrook, E.H.W., and Allan, R.J. 1970. Geochemical exploration feasibility study within

the zone of continuous permafrost, Coppermine River region, Northwest Territories. Geological Survey of Canada, Paper 70-36, 35p.

Hughes, T. 1973. Glacial permafrost and Pleistocene ice ages. *In* Permafrost, North American contribution to second international conference, International Conference on Permafrost, Yakutsk, U.S.S.R.. National Academy of Sciences , Washington, pp. 213-222.

Hyvarinem, L., Kauranne, K., and Yletyinen, V. 1973. Modern boulder tracing in prospecting. *In* Prospecting in areas of glaciated terrain 1973. *Edited by* M.J. Jones, The Institute of Mining and Metallurgy, London, pp: 87-95.

Kamb, W.B., and LaChapelle, E. 1964. Direct observations on the mechanism of glacier sliding over bedrock. Journal of Glaciology, 5(38), pp. 159-172.

Kindle, E.D. 1972. Classification and description of copper deposits, Coppermine River area, District of Mackenzie. Geological Survey of Canada, Bulletin 214, pp. 1-4.

King, A., Wittstock, J., and Slack, D. 1979. Geological, ground and airborne geophysical, and lake sediment and water geochemical report on the SAN and MAL claims. Unpublished report by Hudbay Uranium Company, a division of Hudsons Bay Oil and Gas Company Limited, on file at the regional geologists office, Indian and Northerns Affairs, Yellowknife, Northwest Territories.

Klassen, R.A., and Shilts, W.W. 1977a. Uranium exploration using till, District of Keewatin. Geological Survey of Canada, Paper 77-1A, pp. 471-477.

Klassen, R.A., and Shilts, W.W. 1977b. Glacial dispersal of uranium in the District of Keewatin, Canada. *In* Prospecting in areas of glaciated terrain 1977. The Institute of Mining and Metallurgy, London, pp. 80-88.

Kolthoff, I.M., Elving, P.J., and Sandell, E.B. 1962. Treatise on analytical chemistry. Part II, section A, **9** , Interscience Publishing, New York, pp. 106-107.

Kruger, J. 1979. Structures and textures in till indicating subglacial deposition. Boreas, **8**, pp. 323-340.

Krumbein, W.C., and Graybill, F.A. 1965. An introduction to statisical methods in geology. McGraw-Hill Incorporated, New York, 475p.

Lawson, D.E. 1979. Sedimentalogical analysis of the western terminus region of the Matanuska Glacier, Alaska. United States army cold regions research and engineering laboratory, Report 79-9, 112p.

Lawson, D.E. 1981a. Sedimentalogical characteristics and classification of depositional processes and deposits in the glacial environment. United States army cold regions research and engineering laboratory, Report 81-27, 16p.

Lawson, D.E. 1981b. Distinquishing characteristics of diamictons at the margin of the Matanuska Glacier, Alaska. Annals of Glaciology, **2**, pp. 78-84.

Levinson, A.A. 1974. Introduction to exploration geochemistry. Applied Publishing Limited, Wilmette, Illinois, 614p.

Mark, D.M. 1973. Analysis of axial orientation data, including till fabrics. Geological Society of America, Bulletin, **84**, pp. 1369-1374.

Miller, J.K. 1979. Geochemical dispersion over massive sulphides within the continuous permafrost zone, Bathurst Norsemines, Canada. *In* Prospecting in areas of glaciated terrain 1979. The Institute of Mining and Metallurgy, London, pp. 101-109.

Minell, H. 1978. Glaciological interpretation of boulder trains for the purpose of prospecting in till. Sveriges Geologiska Undersokning, **C743**, 51p.

Moran, S.R. 1971. Glaciotectonic structures in drift. *In* Till / a symposium. *Edited by* R.P. Goldthwait. Ohio State University Press, pp. 127-146.

Morton, R.D., and Miller, R.G. Uranium geology. Manuscript in preparation, University of Alberta, Edmonton.

Nye, J.F. 1952. The mechanics of glacier flow. Journal of Glaciology, **2**, pp. 82-93.

Paterson, W.S.B. 1972. Laurentide ice sheet: estimated volumes during Late Wisconsin. Review Geophysics and Space Physics, **10**(4), pp. 885-917.

Paterson, W.S.B. 1981. The physics of glaciers. 2nd edition, Pergamon Press, Oxford, 380p.

Pawliuk, D.J., and Trigg, C.M. 1981. Hornby Basin exploration, Mackenzie mining district, Northwest Territories. Unpublished report prepared by Trigg, Woollett Consulting Ltd. for Esso Minerals Canada.

Powers, M.C. 1953. A new roundness scale for sedimentary particles. Journal of Sedimentary Petrology, **23**, pp. 117-119.

Prest, V.K. 1969. Retreat of Wisconsin and Recent ice in North America, speculative ice-marginal positions during recession of last ice-sheet complex. Geological Survey of Canada, Map 1257A.

Prest, V.K. In press. The Late Wisconsinan Glacier Complex. *In* International Geological Correlation Program regional report, Glaciations in the northern hemisphere. Geological Survey of Canada publication.

Prest, V.K., Grant, D.R., and Rampton, V.N. 1968. Glacial map of Canada. Geological Survey of Canada, Map 1253A.

Price, G.R., Ferrette, R.J., and Schwartz, S. 1953. Fluorophotometric determination of uranium. Analytical Chemistry, **25**, pp. 322-331.

Ridler, R.H., and Shilts, W.W. 1973. Exploration for Archean polymetallic sulphide deposits in permafrost terrains: an integrated geological / geochemical technique, Kaminak Lake area, District of Keewatin. Geological Survey of Canada, Paper 73-34, 33p.

Robin, G de Q. 1972. Polar ice sheets: a review. Polar Record, **16**(100), pp. 5-22.

Robin, G de Q., and Millar, D.H. 1982. Flow of ice sheets in the vicinity of subglacial peaks. Annals of Glaciology, **3**, pp. 290-294.

Rose, A.W., Hawkes, H.E., and Webb, J.S. 1979. Geochemistry in mineral exploration. 2nd edition, Academic Press, London, 657p.

Rothlisberger, H. 1968. Erosive processes which are likely to accentuate or reduce the bottom relief of valley glaciers. International Association of Scientific Hydrology, Publication 79, pp. 89-97.

Rothlisberger, H., and Iken, A. 1981. Plucking as an effect of water-pressure variations at the glacier bed. Annals of Glaciology, **2**, pp. 57-62.

Salat, H., and Arnaud, M. 1970. Report on the radiometric survey over the PEC claim group, Dismal Lakes area, Northwest Territories. Unpublished report by Aquitaine Company of Canada Ltd., on file at the regional geologists office, Indian and Northern Affairs, Yellowknife, Northwest Territories.

Sampson, R.J. 1975. Surface II graphics system. Series on spatial analysis, 1, Kansas Geological Survey, Lawrence, Kansas, 240p.

Shaw, J. 1977. Tills deposited in arid polar environments. Canadian Journal of Earth Science, **14**(6), pp. 1239-1245.

Shaw, J. 1979. Genesis of the Sveg tills and Rogen moraines of central Sweden: a model of basal meltout. Boreas, **8**, pp. 409-429.

Shaw, J. 1982. Melt-out till in Edmonton area, Alberta, Canada. Canadian Journal of Earth Science, **19**, pp. 1548-1569.

Shilts, W.W. 1972. Drift prospecting, geochemistry of eskers and till in permanently frozen terrain, District of Keewatin, Northwest Territories. Geological Survey of Canada, Paper 72-45, 34p.

Shilts, W.W. 1973a. Till indicator train formed by glacial transport of nickel and other ultrabasic components: A model for drift prospecting. Geological Survey of Canada, Paper 73-1A, pp. 213-218.

Shilts, W.W. 1973b. Glacial dispersal of rocks, minerals, and trace elements in Wisconsin till, southeastern Quebec, Canada. Geological Society of America, Memoir 136, pp. 189-219.

Shilts, W.W. 1974. Physical and chemical properties of unconsolidated sediments in permanently frozen terrain, District of Keewatin, Northwest Territories. Geological Survey of Canada, Paper 74-1A, pp. 229-235.

Shilts, W.W. 1975. Principles of geochemical exploration for sulphide deposits using shallow samples of glacial drift. Canadian Institute of Mining and Metallurgy, Bulletin, May 1975, pp. 73-80.

Shilts, W.W. 1976. Glacial till and mineral exploration. *In* Glacial till. Royal Society of Canada, Special Publication 12, pp. 205-224.

Shilts, W.W. 1977. Geochemistry of till in perennially frozen terrain of the Canadian Shield - application to prospecting. Boreas, **5**, pp. 203-212.

Shilts, W.W. 1978. Nature and genesis of mudboils, central Keewatin, Canada. Canadian Journal of Earth Science, **15**, pp. 1053-1068.

Shilts, W.W., and Cunningham, C.M. 1977. Anomalous uranium concentrations in till north of Baker Lake, District of Keewatin, Northwest Territories. Geological Survey of Canada, Paper 77-1B, pp. 291-292.

Smith, D.I. 1972. The solution of limestones in an arctic environment. *In* Polar geomorphology. Institute of British Geographers, Special Publication 4, pp. 187-200.

St-Onge, D.A. 1980. Glacial Lake Coppermine, north central District of Mackenzie, Northwest Territories. Canadian Journal of Earth Science, **17**, pp. 1310-1315.

St-Onge, D.A. 1983. Deglaciation pattern, Coppermine River region, Northwest Territories. Working manuscript, Department of Geography, University of Ottawa, Ottawa.

St-Onge, D.A. *et al*. 1981. Aspects of the deglaciation of the Coppermine River region, District of Mackenzie, Northwest Territories. Geological Survey of Canada, Paper 81-1A, pp. 327-331.

Stuckless, J.S. *et al*. 1977. A comparison of some analytical techniques for determining uranium, thorium and potassium in granitic rocks. Journal Research United States Geological Survey, **5**(1), pp. 83-91.

Sugden, D.E. 1977. Reconstruction of the morphology, dynamics and thermal characteristics of the Laurentide ice sheet at its maximum. Arctic and Alpine Research, **9**(1), pp. 21-47.

Sugden, D.E. 1978. Glacial erosion by the Laurentide ice sheet. Journal of Glaciology,

20(83), pp. 367-391.

Sugden, D.E., and John, B.S. 1976. Glaciers and landscape, A geomorphological approach. Edward Arnold Publishers Limited, London, 376p.

Thorez, J. 1976. Practical identification of clay minerals, a handbook for teachers and students in clay mineralogy. Editions G. Lelotte, B4820 Dison, Belgique, 90p.

Vagners, U.J. 1977. Quaternary geology of YUK claims and prospecting permit 316, Mackenzie mining district, Northwest Territories. Unpublished Imperial Oil Limited report.

Vagners, U.J. 1979. Geology of western Dismal Lakes, including Quaternary. Unpublished Esso Minerals Canada report.

Vanderveer, D.G., and Sparkes, B.G. 1982. Regional Quaternary mapping an aid to mineral exploration in west-central Newfoundland. *In* Prospecting in areas of glaciated terrain 1982. Canadian Institute of Mining and Metallurgy, Montreal, pp. 284-299.

Washburn, A.L. 1973. Periglacial processes and environments. Edward Arnold Publishers Limited, London, 320p.

Weertman, J. 1957. On the sliding of glaciers. Journal of Glaciology, **3**, pp. 33-42.

Weertman, J. 1958. Transport of boulders by glaciers and ice sheets. Bulletin of the International Association of Scientific Hydrology, **10**, p. 44.

Weertman, J. 1961. Mechanism for the formation of inner moraines near the edge of cold ice caps and ice sheets. Journal of Glaciology, **3**(30), pp. 965-978.

Weertman, J. 1965. The theory of glacier sliding. Journal of Glaciology, **5**, pp. 287-303.

Whillans, I.M. 1978. Erosion by continental ice sheets. Journal of Geology, **86**, pp. 516-524.

VII. APPENDICES

A. APPENDIX A

Procedure used for clay separations by the sedimentology and mineral tracing laboratory, Geological Survey of Canada.

This procedure, designed by P.J. Higgins and W.W. Shilts, utilizes bulk samples to yield approximately 40 clay size separations per day. Samples are defloculated in a dispersant, stirred in a milk shake sizes.

Equipment

- Centrifuge (International, model UV, 4 place head with 1000 ml capacity)
- Milk shake mixer - modified by removing steel baffles and blades. Nalgene blades used.
- Stainless steel mixer buckets (without baffles)
- Sodium metaphosphate (5 g/l)
- Nalgene cups, 100 ml capacity
- Stainless steel, long handled spatula
- Drying oven

Procedure

The samples were washed three times, approximately 200 ml each time, with metaphosphate solution. The amount of sample required varied with the percentage of fines, but usually 300-400 g was sufficient. After each washing, the suspension settled for 5 minutes and then the suspension was decanted into a 1000 ml centrifuge bucket.

After 4 samples were mixed, opposing centrifuge bottles were balanced to within 1 g and run for 3 minutes at 750 RPM. This left -2 μm grains (estimated spherical diameter) still in suspension while the silt was brought down. The supernatant (-2 μm) was decanted into a second series of bottles and was run at 2800 RPM for 14 minutes. Although some fines remained in suspension after this run, further centrifuging did not appreciably alter the amount of clay brought down.

The remaining fines in suspension were discarded. A spatula was used to scrape the clay from the bottom of the centrifuge bottles into nalgene cups. Distilled water was added to facilitate scraping. The clays were then dried overnight in an oven at 80 ° C and ground with an agate pestle the following day.

B. APPENDIX B

Analytical procedure followed by Bondar-Clegg & Company Ltd.

The analytical techniques followed in the uranium fluorometric analyses were as follows (personal communication, Bondar-Clegg & Company Ltd., 1983). The sample (0.1 g) was digested in concentrated HNO_3 acid for 2 hours. The digestion was performed in a hot water bath. After cooling, the sample was diluted to 10 ml with metal free water. After the solids had settled, an appropriate volume of sample extract was transfered to a Pt-dish. The sample was fused with NaF over a propane-air flame. After cooling, the fluorescence of the fused disc was measured by a Jarrell Ash Reflectance type fluorometer and compared against standards prepared by running solutions of known uranium concentration in the same manner.

The AAS procedure followed by Bondar-Clegg & Company Ltd. (personal communication, 1983) used 0.5 g of sample. The sample was digested for 2 hours in a hot water bath with a Lefort aqua regia acid mixture (3 HNO_3: 1 HCl). The sample and leach solution was diluted to a final volume of 10 ml with metal free water containing 1250 µg/ml Al. A Varian Techtron Model AA 875 atomic absorption spectrophotometer was used. The unit possesses a digital display with deuteruim background correction. Corrections were applied for the measurement of Pb, Co, and Ni.

C. APPENDIX C

DNC procedure

The DNC technique assumes that fission is the only nuclear reaction which produces nuclides emitting delayed neutrons, and that the number of delayed neutrons emitted following irradiation is a linear function of the amount of fissile material present in the sample. The only naturally occurring fissile nuclides are U^{235}, U^{233}, and Th^{232}. However, as only U^{235} is fissioned by thermal neutrons, delayed neutron counting is specific for the determination of U^{235}, or uranium assuming the normal isotopic abundance of 0.72 % U^{235} in natural uranium.

The DNC process involved: (1) the accurate measure of each sample, as close to 5.000 g as possible was used, (2) the irradiation of each sample for 20 seconds at a flux of 1×10^{12} n / cm^2.s, (3) the transfer of samples to a counting facility which consists of six BF_3 detector tubes embedded in paraffin, and (4) 10 seconds after irradiation the delayed neutrons from the sample were counted for 20 seconds. By the comparison of the delayed neutron count to that obtained from a standard (Canadian radioactive reference ore BL-1), the uranium content of the sample was determined.

The SLOWPOKE reactor contained a significantly fast neutron flux which can cause fisson of Th^{232}, producing similar delayed neuton products to U^{235} (Boulanger, Evans and Raby, 1975). The Th content of the till samples was unknown. Since a large Th content would cause erroneously high DNC uranium values, Instrument Neutron Activation Analysis (INAA) was performed on four -2 μm fraction samples to determine U and Th values.

D. APPENDIX D

X-ray diffraction procedure

The following procedure was used in the preparation of X-ray diffraction discs. The -2 μm fraction was saturated with a 3 % solution of bleach and then heated at 60 °C for two days to remove organic material. The samples were then washed with distilled water and centrifuged five times to remove any remaining bleach. Each sample was split into two, one half was saturated with a 2 molar solution of $CaCl_2.2H_2O$, the other was saturated with a 2 molar solution of KCl. Again the samples were washed with distilled water and centrifuged five times, after which the samples were tested with a 1 % solution of silver nitrate to ensure a clean supernatant. The samples were then freeze-dried. Oriented sample discs were produced so the basal peaks could be measured.

The samples were analyzed with CoK_α radiation at 2 ° 2θ/ minute with 1 ° slits for the range of 2 ° to 40 °. The calcium saturated discs were analyzed glycolated and at 54 % humidity. The potassium saturated discs were analyzed at 0 and 54 % humidity, and at 300 and 550 °C. In order to differentiate chlorite and kaolinite peaks, two additional analyses were performed. The calcium saturated discs were analyzed at 1 / 4 ° 2θ/ minute for the range 27 ° to 32 °. Also, a backpacked random oriented sample of either calcium or potassium saturated material for each sample was analyzed at 1 ° 2θ/ minute for the range 66 ° to 76 °.

E. APPENDIX E

Till pebble lithology data

PEBBLE LITHOLOGY PERCENTAGES

		sample number	1	2	3	4	8	10	9	11	5	7	6
quartzite	white		7	5	2	-	2	6	3	8	3	5	-
	white with mafics		-	-	-	2	-	-	-	-	-	2	-
	grey		9	3	8	3	3	10	3	19	3	3	1
	green		-	4	-	5	6	2	2	5	1	2	2
	black		4	9	11	6	3	4	1	8	9	1	2
	pink		1	1	5	1	4	5	4	-	1	1	-
	red		4	-	-	3	1	-	2	-	7	5	4
	purple		-	-	-	-	-	1	-	-	-	-	-
	mafics with white		-	1	5	-	1	-	-	-	-	-	-
	mafics		-	-	-	1	-	-	-	-	1	-	-
	red conglomerate		-	-	-	-	-	5	-	3	-	-	-
	green & white		-	-	-	-	-	-	2	-	-	-	-
	light chert		-	-	1	-	-	-	-	-	2	-	-
	dark chert		-	1	-	-	-	-	-	-	-	-	-
	white		33	21	22	13	27	26	33	15	7	3	-
	pink		4	14	11	9	14	6	6	9	7	7	-
	red		3	2	5	9	4	3	3	1	1	1	-
	dark		2	2	3	2	2	1	3	-	1	3	-
sandstone	conglomerate		-	1	-	-	-	-	3	-	-	-	-
	white with mafics		-	2	-	1	-	-	-	-	-	-	-
	red with mafics		-	-	1	-	-	-	-	-	-	-	-
	grey		-	-	-	-	-	1	1	-	-	1	-
shale/ siltstone	black		1	6	8	11	6	1	3	23	1	3	1
	red		-	3	-	1	4	8	4	1	5	3	1
	light		-	-	-	1	-	-	-	-	-	-	-
	massive dolomite		16	7	1	10	7	10	9	-	30	31	58
	conglomerate dolomite		2	1	1	4	1	4	2	-	10	20	20
	coarse grained granite		4	2	5	9	3	1	2	1	1	3	3
	fine grained granite		1	5	5	5	8	2	9	4	4	3	2
	igneous		5	7	5	-	2	2	4	3	3	3	2
	metamorphic		4	2	-	3	2	-	1	-	-	-	2
	vien quartz		-	1	1	-	-	2	-	-	1	-	-
	yellow cherty		-	-	-	1	-	-	-	-	3	-	2

BEDROCK LITHOLOGIES

UNIT	DESCRIPTION
A	Granitic rocks
7	Porphyritic rhyolite, quartz feldspar porphyry
8	Reddish sandstone
9	Dolomite, stromatolites, basal shaly dolomite
10	Red siltstone, shale, sandstone
11	Quartzose sandstone
12	Black shale, sandstone, siltstone
13	Dolomite, mudstone, sandstone, evaporite casts
14	Dolomite
15	Dolomite
16	Dolomite

SAMPLE SITE LOCATIONS

1	Central boulder field, 2250E 1000N
2	Central boulder field, 2000E 1000N
3	Central boulder field, 1750E 1000N
4	Central boulder field, 2000E 1000N
8	Central boulder field, 2000E 1100N
10	South of boulder field, 2000E 600S
9	1.5 km southeast of boulder field, on a slope
11	130 m north of Mid Lake
5	250 m east of Uke Lake (PEC)
7	375 m east of Uke Lake (PEC)
6	500 m east of Uke Lake (PEC)

Bedrock units in the direction opposite to glacial flow from sample sites

site number	LINE 10° AZIMUTH				IN A 30° ARC CENTRED ON LINE 10° AZIMUTH		
	1 km	5 km	10 km	20 km	1 km	5 km	10 km
1	?	11	11	11 12 13	?	11 12	A 8 10 11 12 13
2	?	11	11	11 12 13	?	11 12	A 8 10 11 12 13
3	?	11	11	11 12 13	?	11 12	A 8 10 11 12 13
4	?	11	11	11 12 13	?	11 12	A 8 10 11 12 13
8	?	11	11	11 12 13	?	11 12	A 8 10 11 12 13
10	?	11	11	8 11 12	?	8 9 10 11	A 8 9 10 11 12
9	?	11	8 11	8 11 12	11	8 9 10 11	A 8 9 10 11 12 13
11	?	11	11 13	11 12 13	?	11 12	8 11 12 13 14
5	9	8 9 11 12 13	7 8 9 11 12 13 14 15	7 8 9 11 12 13 14 15	9	A 8 9 10 11 12 13	A 8 9 10 11 12 13 14 15 16
7	9	8 9 11 12 13	7 8 9 11 12 13 14 15	7 8 9 11 12 13 14 15	9	A 8 9 10 11 12 13	A 8 9 10 11 12 13 14 15 16
6	9	8 9 11 12 13	7 8 9 11 12 13 14 15	7 8 9 11 12 13 14 15	9	A 8 9 10 11 12 13	A 8 9 10 11 12 13 14 15 16

? - area drift covered, bedrock beneath unknown

F. APPENDIX F

West Dismal Lakes boulder data

boulder number	grid E	grid N	boulder volume (in 1000 cm^3)	boulder radioactivity (in 1000 cps)	boulder angularity (cm)
1	204	1092	252	2	-
2	246	1137	5	2	-
3	522	1157	1	15	-
4	539	1152	6	3	-
5	552	1148	27	4	-
6	552	1159	65	1	-
7	560	1155	2	4	-
8	620	1101	50	1	-
9	611	1028	1	2	-
10	662	1062	3	7	-
11	820	1106	1	6	-
12	1107	997	3	1	-
13	1133	1092	1	1	-
14	1104	1164	3	1	-
15	1071	1165	2	3	-
16	1135	1670	3	3	6
17	1165	1511	12	1	-
18	1187	1087	8	1	-
19	1193	1024	1	2	-
20	1175	1022	1	2	-
21	1191	1015	2	5	-
22	1211	1003	3	3	-
23	1220	1134	-	2	-
24	1220	1347	2	1	-
25	1247	1513	112	1	-
26	1280	1727	16	15	-
27	1268	1705	12	6	9
28	1299	1481	2	1	-
29	1264	1238	36	5	-
30	1271	1112	13	14	7
31	1258	1066	5	5	-
32	1262	1044	22	3	-
33	1262	1020	91	10	-
34	1272	1016	19	3	-
35	1257	1012	100	7	-
36	1292	1006	4	2	-
37	1284	999	18	4	-
38	1395	1811	25	15	7
39	1391	1476	29	6	-
40	1351	1468	4	2	-
41	1395	1225	9	3	-

42	1384	1216	14	1	-
43	1400	998	1	2	-
44	1411	1018	144	1	-
45	1428	1027	1	2	-
46	1426	1038	5	6	-
47	1411	1042	6	8	-
48	1426	1496	5	5	-
49	1412	1897	6	2	-
50	1497	1942	77	13	-
51	1450	1806	6	2	-
52	1477	1744	9	14	4
53	1487	1442	12	2	-
54	1498	1378	6	8	-
55	1485	1323	5	1	-
56	1498	1112	72	3	-
57	1499	1101	24	2	-
58	1471	1124	27	9	-
59	1485	1101	54	2	-
60	1492	1092	15	7	-
61	1481	1080	26	15	-
62	1454	1035	1	7	-
63	1466	1018	2	1	-
64	1458	1005	23	1	-
65	1546	993	11	1	-
66	1548	1062	31	3	-
67	1520	1060	5	6	-
68	1526	1064	5	2	-
69	1520	1074	66	6	-
70	1516	1087	11	3	-
71	1503	1107	1	1	-
72	1544	1115	12	6	-
73	1547	1142	45	15	-
74	1528	1183	2	6	-
75	1521	1300	54	4	-
76	1520	1322	-	1	-
77	1579	1688	14	3	7
78	1583	1243	6	1	-
79	1590	1153	29	3	-
80	1574	1079	4	6	-
81	1562	1073	1	4	-
82	1576	1067	6	4	-
83	1564	995	20	6	-
84	1571	995	4	3	-
85	1599	1006	1	3	-
86	1620	999	8	15	-
87	1636	997	54	15	-
88	1650	1016	28	4	-
89	1607	1101	1	-	-
90	1640	1125	9	-	-

91	1646	1999	1	1	-
92	1630	2028	24	-	-
93	1665	2185	76	6	8
94	1690	2114	2	-	-
95	1675	2012	14	-	-
96	1680	1955	11	4	-
97	1669	1702	29	2	8
98	1675	1146	10	-	-
99	1677	1132	1	1	-
100	1680	1122	13	-	-
101	1682	1102	15	-	-
102	1674	1104	3	-	-
103	1668	1098	27	10	-
104	1675	1097	24	-	-
105	1681	1097	17	-	-
106	1660	1018	10	-	-
107	1692	996	12	4	-
108	1702	995	1	3	-
109	1704	1002	16	-	-
110	1765	2227	-	14	-
111	1798	2176	5	6	-
112	1756	2015	3	-	-
113	1761	1913	9	2	-
114	1753	1855	5	2	-
115	1765	1025	6	3	-
116	1793	1011	12	6	-
117	1775	997	9	6	-
118	1819	997	26	4	-
119	1828	1067	4	7	3
120	1817	1080	8	4	-
121	1837	1095	210	2	5
122	1834	1104	28	3	-
123	1821	1127	12	8	-
124	1811	1399	1	3	-
125	1835	1796	18	2	-
126	1813	2061	1	10	-
127	1875	1895	18	4	-
128	1857	1608	12	5	4
129	1899	1311	6	2	-
130	1899	1273	10	7	-
131	1877	1015	2	2	4
132	1862	999	9	13	-
133	1884	997	2	2	4
134	1891	996	4	1	-
135	1902	1005	2	1	-
136	1917	996	18	9	-
137	1946	996	10	1	-
138	1938	1031	10	4	-
139	1915	1027	4	6	-
140	1922	1080	53	9	-
141	1910	1092	1	2	-

142	1925	1114	19	2	-
143	1907	1130	7	7	7
144	1951	1129	21	2	6
145	1949	1323	1	4	-
146	1934	1597	18	15	-
147	1950	1651	20	10	6
148	1918	1823	23	1	4
149	1992	1377	8	5	-
150	1983	1375	7	2	5
151	1964	1374	29	6	-
152	2001	1321	48	3	-
153	1999	1201	16	7	4
154	1994	1206	1	1	-
155	1995	1192	3	2	6
156	1989	1187	224	3	-
157	2003	1150	3	3	5
158	1999	1132	33	1	-
159	1982	1084	2	1	-
160	1998	1054	9	2	5
161	1999	1049	9	6	4
162	1993	1019	15	3	5
163	1951	1003	6	2	-
164	1954	995	20	2	-
165	1970	999	5	2	-
166	2025	1020	1	5	5
167	2052	1017	2	1	-
168	2011	1062	2	1	6
169	2037	1088	3	1	4
170	2034	1097	4	1	-
171	2026	1098	2	2	-
172	2017	1119	3	1	-
173	2035	1129	11	3	-
174	2015	1132	15	4	-
175	2021	1149	19	1	5
176	2013	1162	5	3	4
177	2007	1199	4	3	-
178	2013	1270	7	1	-
179	2014	1333	3	3	-
180	2042	1351	1	3	3
181	2019	1352	8	2	5
182	2001	1451	3	3	5
183	2021	1499	20	3	-
184	2009	1598	20	1	7
185	2025	1619	10	2	-
186	2039	1717	2	1	5
187	2039	1728	1	5	-
188	2023	1920	11	5	-
189	2014	1931	15	3	5
190	2024	1938	6	12	-
191	2018	1948	8	2	6
192	2024	1960	2	1	6

193	2016	1957	20	4	-
194	2014	1964	12	3	-
195	2085	1799	2	8	3
196	2084	1700	7	9	-
197	2060	1568	58	1	4
198	2084	1232	2	4	4
199	2058	1089	2	2	-
200	2099	1052	29	1	3
201	2064	1013	4	5	-
202	2077	99	3	9	5
203	2081	996	42	2	7
204	2089	997	11	1	-
205	2103	995	7	2	6
206	2177	1007	6	4	-
207	2118	1017	6	8	-
208	2111	1028	10	10	6
209	2117	1075	5	1	-
210	2146	1153	2	1	-
211	2144	1192	80	2	-
212	2132	1219	37	3	-
213	2116	1215	2	8	-
214	2100	1253	17	1	-
215	2103	1276	1	1	-
216	2150	1249	13	6	-
217	2150	1268	4	1	6
218	2143	1279	2	1	-
219	2115	1298	24	2	-
220	2128	1327	165	5	-
221	2132	1376	52	1	5
222	2131	1409	1	1	-
223	2135	1457	7	1	-
224	2152	1496	5	3	4
225	2132	1544	12	1	8
226	2126	1573	1	2	-
227	2150	1750	2	5	2
228	2118	1777	2	1	-
229	2138	1787	4	2	-
230	2107	1896	3	1	4
231	2188	1674	10	5	-
232	2195	1591	13	2	4
233	2157	1566	1	14	-
234	2160	1434	13	7	4
235	2204	1424	3	2	5
236	2155	1328	36	1	7
237	2200	1193	2	2	-
238	2172	1179	88	4	-
239	2191	1176	15	1	-
240	2163	1166	3	1	-
241	2211	1188	5	11	5
242	2230	1545	8	2	-
243	2251	1560	126	10	-

244	2285	1050	31	1	6
245	2292	1098	1	1	-
246	2258	1237	25	2	6
247	2276	1378	4	1	-
248	2274	1605	9	2	-
249	2316	1638	17	2	5
250	2334	1563	21	2	-
251	2348	1376	98	2	9
252	2325	1294	23	1	-
253	2343	1193	16	2	-
254	2312	1056	1	2	-
255	2371	1206	6	6	5
256	2378	1244	54	4	-
257	2366	1313	17	4	6
258	2386	1318	2	2	-
259	2370	1358	30	7	-
260	2359	1397	7	3	7
261	2363	1573	13	2	5
262	2388	1583	6	3	-
263	2365	1755	2	2	-
264	2426	1261	66	2	-
265	2412	1203	6	4	-
266	2466	1411	18	1	-
267	2494	1499	31	8	-
268	2529	1716	3	4	-
269	2531	1498	28	1	-
270	2507	1473	16	9	-
271	2510	1377	-	1	-
272	2548	1353	74	2	-
273	2555	1101	4	10	-
274	2653	1234	8	3	-
275	2657	1504	1	1	-
276	2727	1851	2	1	3
277	2750	1444	1	1	2
278	2718	1385	2	2	3
279	2842	1429	1	10	-
280	3209	1511	2	2	-
281	3176	1170	7	3	-
282	3188	1106	25	1	-
283	3691	1089	5	4	3
284	4199	1155	60	2	-
285	4310	1382	3	3	3
286	4363	1164	8	3	-
287	4392	1035	8	7	5
288	4469	1256	61	2	-
289	4677	1010	14	5	6

- data not available

G. APPENDIX G

West Dismal Lakes geochemical results

site number	grid E	grid N	U (-2 μm) (PPM)	U (-60 μm) (PPM)	U (-250 μm) (PPM)	Cu (PPM)	Pb (PPM)	Zn (PPM)	Co (PPM)	Ni (PPM)	Cr (PPM)	Mo (PPM)	Mn (PPM)	Fe (%)	U (DNC) (PPM)
1	1493	983	2.1	-	-	161	34	124	12	38	49	2	430	4.1	-
2	1505	1268	3.0	2.5	1.3	216	34	134	16	34	75	x	490	5.5	-
3	1517	1514	1.0	-	-	173	19	97	14	34	42	4	520	3.8	2.84
4	1513	1775	1.0	0.8	1.8	138	18	88	16	36	42	x	735	4.3	2.87
5	1522	2030	1.1	-	-	125	28	136	18	44	68	2	600	6.0	3.12
6	1531	2303	1.7	0.8	1.3	108	15	80	14	32	66	2	345	3.8	3.72
7	1304	2326	0.9	-	-	122	15	85	18	32	62	2	650	4.4	2.96
8	1276	2020	1.4	-	-	137	20	88	14	36	71	2	440	5.0	3.38
9	1270	1771	0.7	-	-	160	34	118	16	36	72	x	650	4.8	2.92
10	1265	1528	1.1	-	-	158	16	89	16	42	49	2	540	4.1	2.83
11	1269	1292	1.4	-	-	131	12	84	16	38	40	1	640	3.8	2.91
12	1266	994	1.7	-	-	168	20	108	16	38	48	x	460	3.9	3.86
13	966	785	1.1	0.5	0.8	125	23	128	16	40	62	x	510	4.8	2.99
14	966	496	1.4	-	-	165	15	92	16	40	44	2	730	4.5	2.59
15	964	254	0.9	0.9	0.5	149	21	110	18	40	56	2	700	4.8	2.91
16	1489	245	1.4	0.8	0.5	149	18	98	14	38	50	3	460	4.3	2.87
17	1501	522	1.1	-	-	149	13	90	14	40	47	2	500	4.5	2.87
18	1482	771	1.2	0.8	0.4	132	16	85	16	42	46	2	590	3.9	2.86
19	2025	1002	1.6	-	-	190	30	143	18	42	60	2	540	5.1	-
20	2025	753	1.4	0.4	0.3	155	24	120	20	44	46	x	780	4.5	4.05
21	2032	510	1.6	-	-	80	22	112	16	34	50	1	625	4.7	3.89
22	2023	224	1.2	0.3	0.5	176	25	134	18	42	70	3	520	5.6	3.25
23	2313	1269	1.5	-	-	112	26	128	16	38	67	2	725	4.2	4.34
24	2316	1512	1.4	-	-	202	44	165	22	48	56	x	880	5.2	3.45
25	2315	1767	1.6	-	-	88	19	112	14	40	44	x	620	4.1	3.22
26	2290	2025	1.0	-	-	117	18	85	16	32	50	x	440	4.6	3.71

27	2296	2293	1.7	-	-	102	13	70	16	38	40	x	390	3.8	4.41
28	2526	2294	1.4	0.4	0.4	142	14	72	16	32	46	x	350	4.6	3.27
29	2539	2048	2.3	-	-	88	14	72	14	34	48	x	320	4.6	4.22
30	2536	1746	1.1	0.5	0.5	125	15	68	18	32	38	x	615	3.8	3.29
31	2533	1479	1.6	-	-	168	29	120	18	46	64	x	620	5.4	3.98
32	2541	1264	1.7	0.4	0.5	104	22	108	16	36	49	x	725	5.0	3.86
33	2543	975	1.4	-	-	86	16	100	10	32	49	x	335	4.5	3.40
34	2526	736	1.1	0.8	0.4	142	14	96	18	36	46	2	720	4.9	2.73
35	2542	487	0.7	-	-	72	12	92	16	36	48	1	410	4.2	3.01
36	2524	241	0.9	0.6	0.5	92	13	96	12	40	48	x	380	4.1	3.01
37	3019	221	0.9	0.2	0.3	80	15	88	12	32	46	2	315	4.0	3.33
38	3046	472	1.0	-	-	104	16	92	14	38	42	2	590	4.0	3.26
39	3029	719	1.0	0.3	0.3	137	17	88	16	42	46	1	640	4.3	3.70
40	3042	989	1.1	-	-	158	18	108	16	42	44	1	600	4.2	3.48
41	3038	1265	0.7	0.4	0.5	131	11	72	16	34	40	1	460	4.0	3.67
42	3062	1520	1.5	-	-	114	20	96	16	38	61	2	495	5.9	4.21
43	3059	1769	1.1	0.5	0.7	160	11	80	16	28	44	1	430	4.4	3.51
44	3073	2008	3.5	-	-	143	15	85	16	40	58	x	420	4.6	5.19
45	3559	1746	0.7	0.4	0.5	158	15	106	20	40	48	1	830	4.5	2.68
46	3566	1490	0.7	-	-	150	14	72	18	34	43	1	410	3.7	-
47	3557	1236	0.7	0.5	0.5	161	15	107	20	42	48	x	830	5.0	2.83
48	3558	984	0.6	-	-	143	15	90	18	42	50	2	800	4.7	-
49	3850	719	0.4	-	-	96	14	85	16	34	49	x	390	4.2	-
50	3842	477	1.5	-	-	89	19	96	16	36	52	x	415	4.5	-
51	3857	209	1.0	-	-	76	14	135	14	30	46	x	460	3.8	-
52	4389	200	0.7	-	-	165	18	100	18	46	54	2	705	4.8	-
53	4398	471	1.6	-	-	132	20	110	14	32	55	2	270	4.2	-
54	4378	714	1.1	-	-	196	21	112	16	34	50	x	700	4.6	-
55	4366	984	1.6	-	-	182	14	108	12	32	42	x	430	3.5	-
56	4387	1233	1.1	-	-	146	12	88	16	32	42	1	500	4.4	-
57	4386	1479	1.1	-	-	168	14	100	18	34	49	1	700	4.9	-
58	4369	1716	1.1	-	-	228	15	100	18	36	52	x	550	4.7	-
59	5120	1736	1.0	-	-	212	15	85	14	34	46	1	520	4.3	4.71

60	5136	1232	0.9	-	-	134	13	88	12	26	48	x	395	4.4	4.28
61	5133	720	1.4	-	-	148	14	108	18	44	52	x	570	4.6	2.96
62	5132	182	1.5	-	-	110	16	89	12	36	46	1	350	3.6	3.83
63	6173	177	0.9	-	-	204	13	113	16	34	49	x	530	4.1	-
64	6312	661	1.2	-	-	202	14	84	18	36	43	x	390	4.1	3.92
65	6175	1194	1.8	-	-	146	12	72	14	32	42	x	375	3.4	5.23
66	6182	1720	4.3	-	-	140	18	72	18	30	37	x	680	3.7	-
67	913	1815S	1.0	-	-	106	23	100	16	40	47	x	920	4.6	-
68	1457	1820S	0.7	-	-	112	13	112	14	38	45	x	520	4.4	-
69	2001	1819S	0.7	-	-	104	15	114	20	46	54	2	880	4.3	-
70	2538	1845S	1.0	-	-	142	13	106	16	38	54	2	680	4.3	-
71	2984	1850S	1.0	-	-	94	16	114	19	37	40	2	990	4.5	-
72	3562	1843S	1.0	-	-	74	16	116	14	35	47	1	675	4.8	-
73	4072	1844S	1.5	-	-	90	20	136	16	46	74	3	640	5.6	-
74	4646	1859S	0.7	-	-	128	15	116	18	37	51	1	880	4.5	-
75	5138	1856S	1.8	-	-	102	13	120	14	34	52	1	440	4.2	-
76	5670	1845S	1.1	-	-	136	12	124	12	39	56	x	600	4.6	-
77	6150	1848S	1.0	-	-	116	23	89	16	34	52	x	1385	4.4	-
78	6693	1877S	1.0	-	-	146	21	125	15	40	58	1	700	5.2	-
79	7212	1869S	3.5	-	-	96	18	116	14	32	58	2	580	4.7	4.92
80	7196	1420S	0.6	-	-	162	18	120	18	39	58	x	730	4.7	-
81	7199	347S	0.9	-	-	108	17	100	16	33	46	x	470	3.9	-
82	3541	2286	0.6	0.4	0.4	154	18	100	20	36	45	1	980	4.3	3.29
83	4121	2249	1.1	-	-	136	20	96	22	48	57	2	560	5.4	-
84	4656	2257	1.1	-	-	188	188	100	16	32	46	x	610	4.2	-
85	5129	2260	0.9	-	-	156	10	88	18	30	39	3	550	3.2	5.13
86	5676	2231	0.9	-	-	148	14	60	13	24	32	x	245	3.0	5.60
87	6192	2242	1.0	-	-	220	18	150	18	36	46	x	860	4.3	4.12
88	9342	2210	0.7	-	-	178	23	142	15	34	62	x	1230	5.4	3.44
89	9306	1846	0.6	-	-	176	16	102	16	35	34	x	870	4.4	-
90	9317	1421	0.6	-	-	200	14	80	14	33	49	x	295	3.6	5.96
91	9301	1007	0.6	-	-	150	10	83	12	24	38	x	240	2.5	-
92	9279	706	0.7	-	-	152	13	80	12	27	36	x	410	3.5	-
93	1795	1003	1.4	-	-	104	17	124	13	36	58	x	560	4.5	-

94	1794	1265	0.4	-	-	160	10	88	15	32	53	x	440	4.4	3.20
95	1799	1520	0.7	-	-	136	20	148	17	40	70	x	440	4.8	3.29
96	1779	1766	1.1	-	-	100	17	130	16	41	71	2	460	5.8	3.76
97	1794	2039	1.5	-	-	110	21	185	24	50	74	x	490	5.5	3.61
98	1799	2304	1.4	-	-	84	13	120	15	34	59	x	430	5.5	3.96
99	993	2300	1.8	0.5	0.8	70	13	108	14	33	58	2	395	4.8	4.37
100	984	2030	0.6	-	-	120	14	250	16	40	46	x	910	4.5	2.89
101	965	1754	0.9	0.4	0.6	104	14	110	16	36	51	x	710	4.5	2.86
102	960	1508	0.6	-	-	134	21	175	21	56	87	x	500	6.7	3.02
103	966	984	0.6	-	-	140	14	92	18	42	50	x	765	4.2	2.80
104	1229	748	3.0	-	-	140	20	160	19	44	88	x	390	5.3	5.12
105	1227	498	0.6	-	-	158	13	96	18	44	52	x	855	4.2	2.90
106	1218	243	0.9	-	-	140	23	112	15	40	68	2	500	4.6	3.20
107	1762	228	1.1	-	-	104	19	96	13	38	60	1	450	4.5	2.74
108	1765	492	1.1	-	-	120	21	140	13	43	70	1	460	5.3	3.12
109	1771	757	1.1	-	-	148	20	110	14	43	76	x	500	5.1	3.18
110	2287	994	1.6	-	-	108	18	110	14	46	48	x	715	4.3	3.68
111	2266	740	1.1	-	-	114	23	120	14	52	58	x	760	4.8	3.74
112	2273	487	0.8	-	-	126	14	100	16	42	49	x	720	4.4	3.04
113	2276	235	1.1	-	-	134	14	95	16	44	48	x	680	4.1	2.98
114	2007	1259	1.4	0.8	0.4	158	16	116	14	46	62	x	520	4.5	4.05
115	2015	1496	0.9	-	-	148	29	140	14	44	62	x	580	4.6	3.11
116	2015	1770	3.8	1.2	1.0	122	20	124	18	50	70	x	520	5.4	6.64
117	2015	2028	0.9	-	-	142	23	150	18	47	58	x	650	5.1	3.23
118	2028	2320	2.3	0.9	0.9	128	12	76	14	38	51	2	370	4.1	4.35
119	2805	2288	0.6	-	-	140	15	88	16	40	46	1	590	4.3	3.72
120	2802	2020	1.4	-	-	116	12	95	13	40	60	x	430	4.8	3.94
121	2805	1761	0.9	-	-	136	10	72	15	34	57	1	400	3.5	4.01
122	2804	1524	1.4	-	-	128	11	104	15	39	46	1	680	4.2	3.59
123	2797	1257	1.1	-	-	110	12	100	12	42	44	1	480	4.0	3.36
124	2782	999	0.9	-	-	114	18	112	16	45	47	1	660	4.3	3.41
125	2792	749	1.1	-	-	102	12	104	12	42	43	1	720	4.3	3.39
126	2774	485	1.0	-	-	128	14	108	16	42	42	x	700	4.2	3.41

127	2783	208	0.9	-	-	88	14	103	12	39	44	1	460	4.3	3.30
128	3293	191	0.9	-	-	116	12	98	14	40	44	x	460	4.2	-
129	3294	471	1.1	-	-	130	12	90	12	40	44	x	400	3.8	3.85
130	3296	711	1.5	-	-	152	14	100	14	45	48	1	465	4.1	3.99
131	3308	984	1.1	-	-	120	11	94	14	38	51	2	510	3.9	3.28
132	3317	1245	1.1	-	-	142	17	100	15	44	47	x	580	3.8	3.45
133	3307	1495	0.9	-	-	132	10	85	16	41	44	1	525	3.8	3.28
134	3316	1741	0.6	-	-	146	13	100	16	43	44	2	575	4.2	2.67
135	3315	1993	0.9	-	-	124	12	72	14	33	38	1	450	3.7	-
136	3073	2291	0.6	0.4	0.5	116	12	80	15	33	39	2	700	4.4	3.30
137	3844	1723	0.9	-	-	167	18	74	16	34	40	2	420	3.7	-
138	3839	1489	0.4	-	-	152	16	88	18	44	41	2	745	4.5	-
139	3849	1242	0.9	-	-	208	17	90	18	38	40	1	640	4.2	-
140	3821	970	0.6	-	-	161	15	82	18	38	47	x	355	3.8	-
141	3542	721	1.1	0.5	0.8	80	22	130	20	54	72	1	370	7.0	3.43
142	3539	459	1.2	-	-	84	14	88	12	34	48	x	265	3.8	-
143	3550	222	0.6	0.5	0.5	161	16	103	20	44	51	x	500	5.1	2.80
144	4084	204	0.9	0.5	0.3	140	19	92	18	56	50	x	510	5.1	3.28
145	4099	458	1.0	-	-	102	19	77	12	40	46	x	515	4.1	-
146	4089	702	3.9	0.2	0.3	155	22	105	16	42	62	1	660	5.6	-
147	4102	978	2.2	-	-	118	22	76	16	42	47	1	500	4.6	5.31
148	4073	1219	0.9	0.5	0.5	164	17	92	22	46	45	x	940	4.6	2.84
149	4094	1474	1.1	-	-	155	16	76	16	38	44	x	400	4.2	-
150	4088	1730	0.6	0.5	0.8	164	20	90	18	58	49	x	760	4.9	3.22
151	4629	1730	1.4	0.5	0.6	145	18	83	16	42	55	x	350	4.9	4.71
152	4617	1453	0.9	-	-	220	22	90	20	52	52	x	730	4.9	-
153	4615	1225	1.4	0.4	0.6	158	18	89	18	54	54	x	700	5.2	3.04
154	4627	954	1.5	-	-	94	19	109	16	40	66	x	330	7.3	-
155	4609	681	0.9	0.8	0.8	148	20	104	18	60	50	1	830	4.5	3.41
156	4610	459	1.4	-	-	137	19	112	14	46	80	2	460	6.5	-
157	4610	192	2.2	0.8	0.9	58	15	92	12	34	43	x	290	3.9	4.35
158	5652	679	0.9	-	-	134	19	95	16	42	55	x	440	4.6	3.01
159	5654	1190	0.4	-	-	152	16	84	18	42	47	x	500	4.5	4.64

160	5663	1719	0.4	-	-	164	14	60	16	38	31	x	390	2.7	5.59
161	939	815S	0.4	-	-	98	22	95	14	50	52	x	560	4.9	-
162	1459	811S	0.6	-	-	140	27	108	16	42	56	x	610	5.4	-
163	2012	821S	0.9	-	-	100	19	96	14	42	52	x	270	6.6	-
164	2522	845S	1.1	-	-	116	16	85	14	36	38	x	370	4.4	-
165	3021	852S	1.1	-	-	106	18	108	14	38	50	x	430	4.7	-
166	3556	865S	1.0	-	-	116	16	92	14	44	44	x	440	4.4	-
167	4088	858S	1.0	-	-	125	18	86	14	44	38	3	590	4.1	-
168	4641	877S	0.9	-	-	94	14	78	16	50	46	2	395	4.6	-
169	5140	863S	1.1	-	-	100	24	94	16	36	39	x	1230	3.6	-
170	5669	891S	0.9	-	-	89	25	94	16	50	56	x	560	5.1	-
171	5655	380S	0.6	-	-	134	15	120	18	55	72	1	840	6.2	-
172	6167	360S	1.0	-	-	76	19	72	12	29	42	x	700	3.8	-
173	6161	886S	1.0	-	-	166	12	94	14	34	42	x	740	4.3	-
174	6672	894S	1.1	-	-	66	17	106	14	39	60	x	630	5.6	-
175	7186	890S	0.9	-	-	100	11	83	10	26	33	1	625	3.5	-
176	8219	375S	1.4	-	-	130	27	88	20	37	78	x	1460	5.7	-
177	8189	897S	0.4	-	-	112	16	152	18	50	80	1	520	6.0	3.23
178	7225	154	1.1	-	-	150	20	160	18	54	95	x	620	7.0	-
179	7231	526	0.3	-	-	128	12	86	14	37	42	x	480	4.2	-
180	7230	954	0.6	-	-	176	13	90	17	41	45	x	580	4.4	3.61
181	7232	1357	1.5	-	-	148	9	63	11	31	38	x	200	2.9	5.96
182	7233	1825	0.6	-	-	154	19	100	14	39	55	2	530	4.4	-
183	7239	2185	0.9	-	-	220	20	92	15	34	44	x	430	4.0	4.71
184	8292	2198	1.1	-	-	230	17	120	12	38	50	x	280	3.8	5.16
185	8272	1820	5.6	-	-	154	13	38	13	24	32	x	240	2.5	-
186	8266	1371	0.7	-	-	160	13	120	22	70	67	x	885	5.2	2.57
187	8258	953	0.3	-	-	178	11	84	12	38	46	x	310	3.6	4.39
188	8252	495	0.8	-	-	99	7	64	10	27	28	1	190	2.5	-
189	8255	144	0.9	-	-	94	22	108	11	34	48	2	495	3.9	-
190	7850	2450	1.8	-	-	143	29	60	-	-	49	-	890	-	-
191	6900	2750	1.6	-	-	94	13	49	-	-	34	-	340	-	-
192	6500	2750	1.3	-	-	160	19	78	-	-	42	-	530	-	-
193	6500	2050	2.9	-	-	88	19	116	-	-	77	-	620	-	-

194	6500	1450	0.5	-	-	205	14	80	-	-	41	-	490	-	-
195	6500	750	0.8	-	-	150	12	77	-	-	45	-	440	-	-
196	7500	1000	1.3	-	-	62	6	28	-	-	34	-	125	-	-
197	7500	1600	2.2	-	-	117	10	60	-	-	46	-	350	-	-
198	7500	2200	1.1	-	-	123	10	51	-	-	34	-	360	-	-
199	7500	2750	3.5	-	-	96	18	88	-	-	66	-	380	-	-
200	8000	2750	1.6	-	-	112	19	89	-	-	64	-	740	-	-
201	8000	2150	1.0	-	-	136	16	59	-	-	35	-	460	-	-
202	7750	1900	1.3	-	-	84	18	68	-	-	65	-	900	-	-
203	8000	1700	1.3	-	-	86	15	48	-	-	36	-	320	-	-
204	8250	1900	1.0	-	-	108	15	76	-	-	48	-	470	-	-
205	8650	1900	3.7	-	-	146	14	64	-	-	34	-	250	-	-

x - below detection limit

- - not analyzed

H. APPENDIX H

West Dismal Lakes - Contoured Cr, Mn, Ni, Co, Mo, Fe results

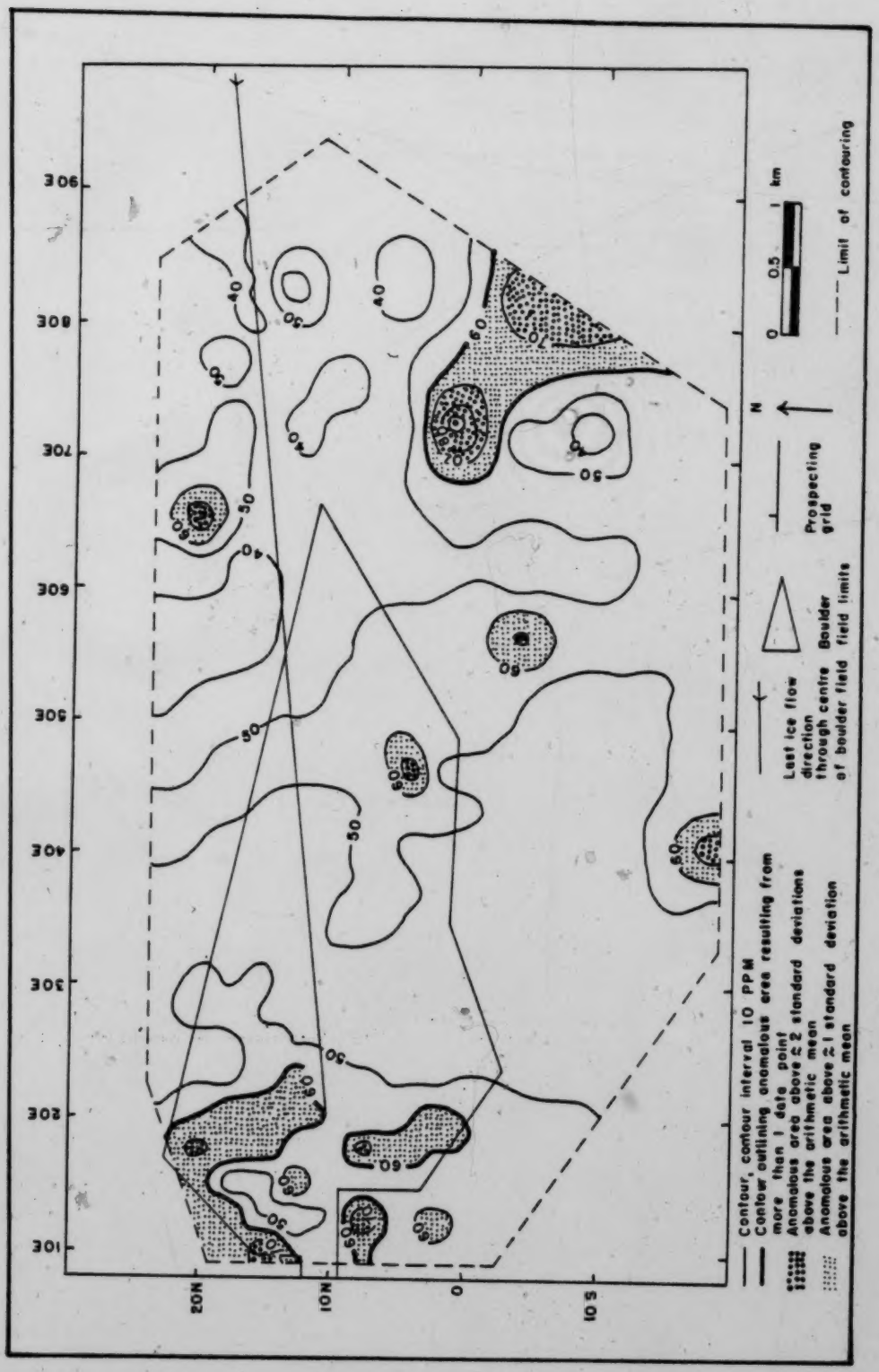
306
308
307
309
305
304
303
302
301
20N
10N
0
10S
Contour, contour interval 10 PPM
Contour outlining anomalous area resulting from more than 1 data point
Anomalous area above ≥2 standard deviations above the arithmetic mean
Anomalous area above ≥1 standard deviation above the arithmetic mean
Last ice flow direction through centre of boulder field
Boulder field limits
Prospecting grid
N
0
0.5
1 km
Limit of contouring

Chromium

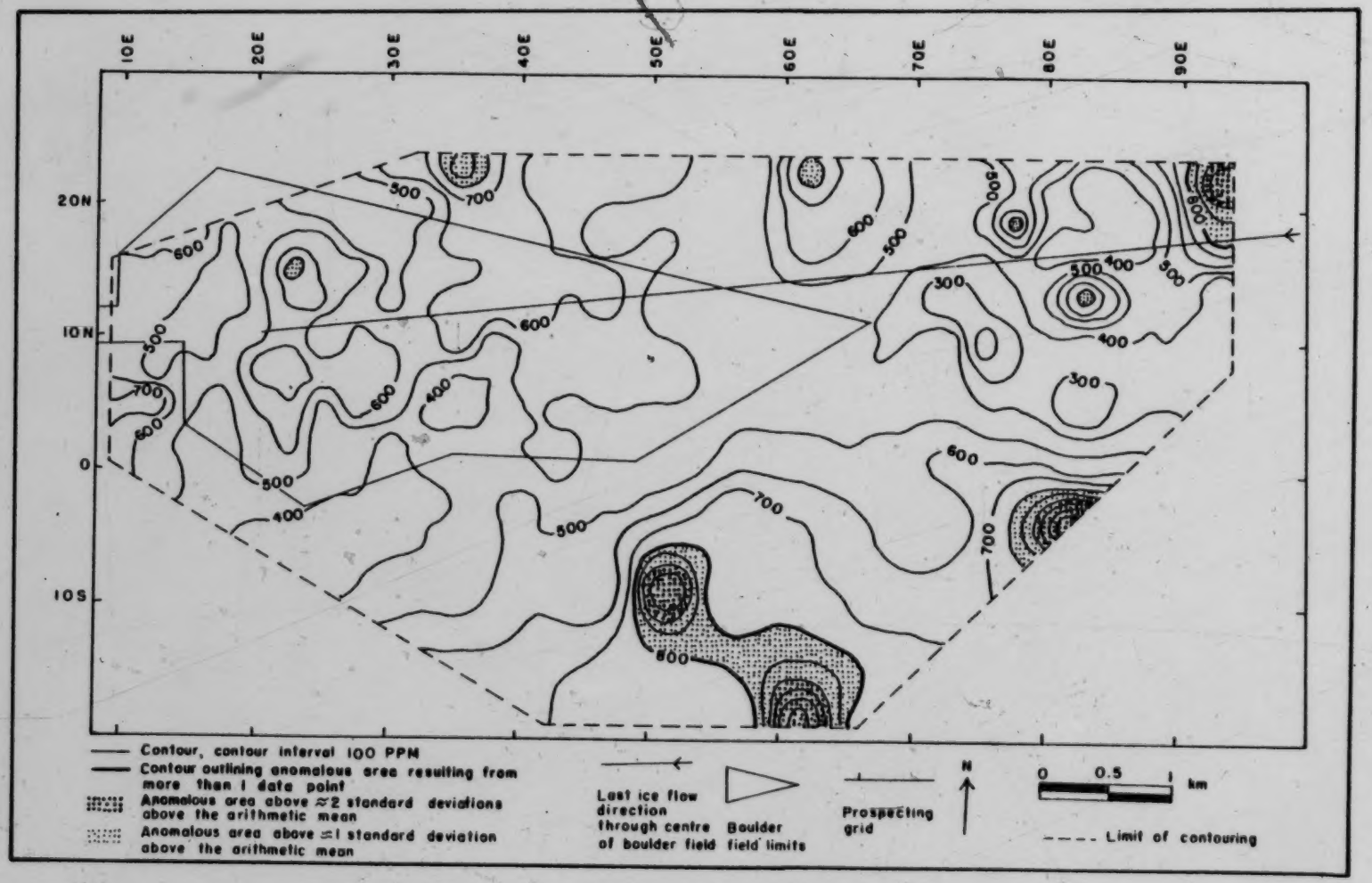
10E
20E
30E
40E
50E
60E
70E
80E
90E
20N
10N
0
10S
Contour, contour interval 100 PPM
Contour outlining anomalous area resulting from more than 1 data point
Anomalous area above ≥2 standard deviations above the arithmetic mean
Anomalous area above ≥1 standard deviation above the arithmetic mean
Last ice flow direction through centre of boulder field
Boulder field limits
Prospecting grid
N
0 0.5 1 km
Limit of contouring

Manganese

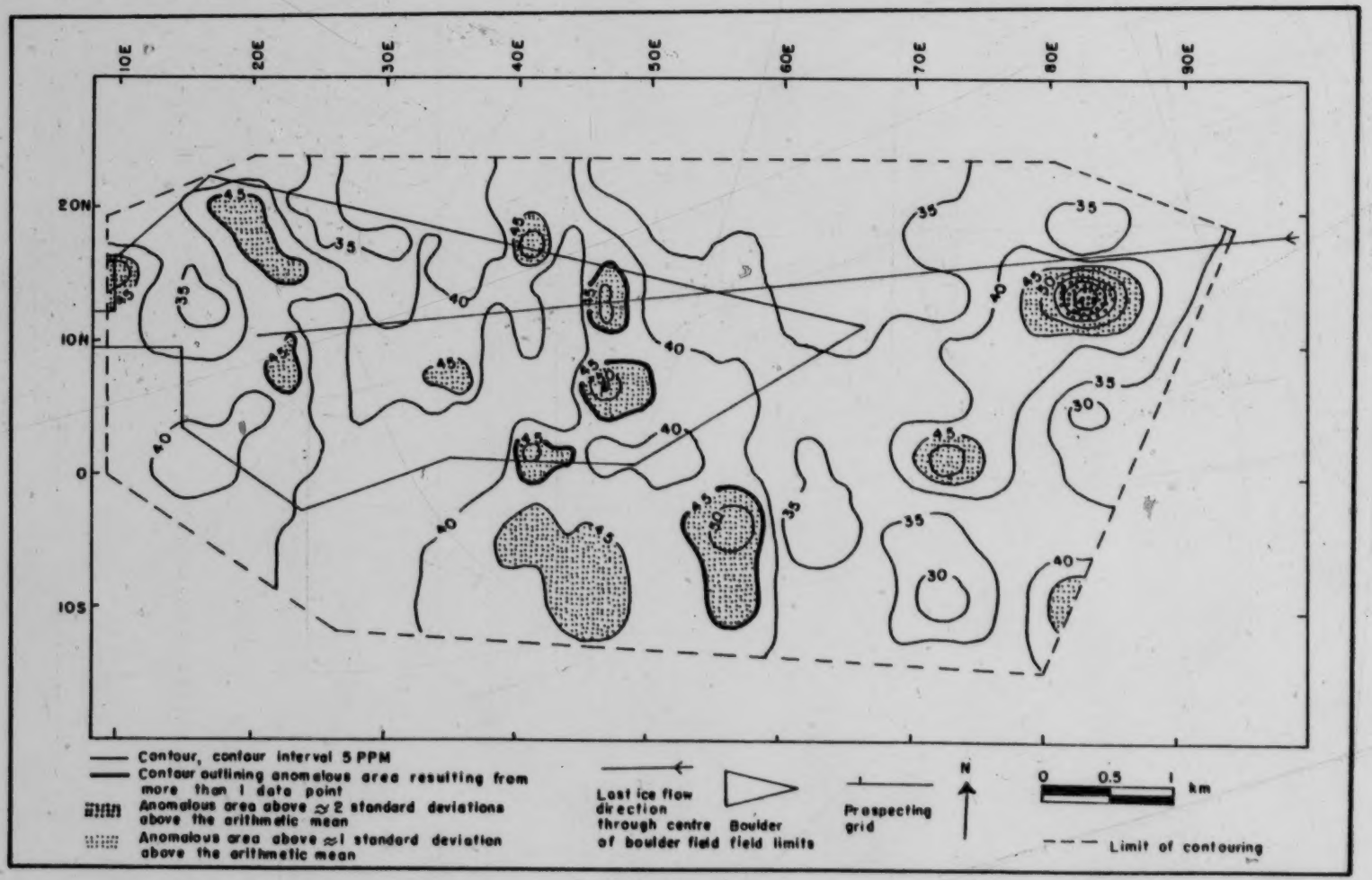
10E
20E
30E
40E
50E
60E
70E
80E
90E
20N
10N
0
10S
Contour, contour interval 5 PPM
Contour outlining anomalous area resulting from more than 1 data point
Anomalous area above ≈2 standard deviations above the arithmetic mean
Anomalous area above ≈1 standard deviation above the arithmetic mean
Last ice flow direction through centre of boulder field
Boulder field limits
Prospecting grid
N
0 0.5 1 km
Limit of contouring

Nickel

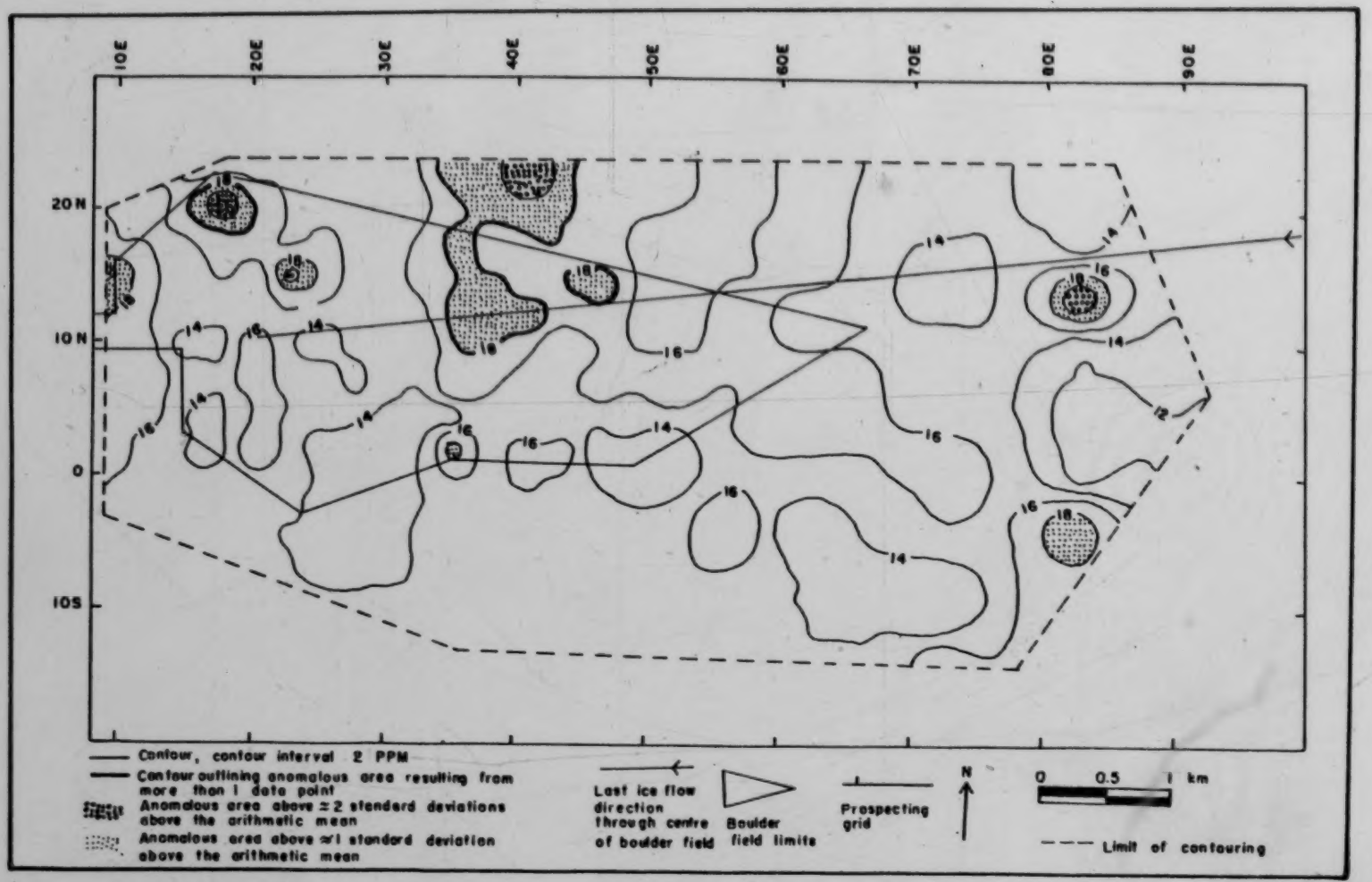
10E
20E
30E
40E
50E
60E
70E
80E
90E
20N
10N
0
10S
Contour, contour interval 2 PPM
Contour outlining anomalous area resulting from more than 1 data point
Anomalous area above ≥2 standard deviations above the arithmetic mean
Anomalous area above ≥1 standard deviation above the arithmetic mean
Last ice flow direction through centre of boulder field
Boulder field limits
Prospecting grid
N
0 0.5 1 km
Limit of contouring

Cobalt

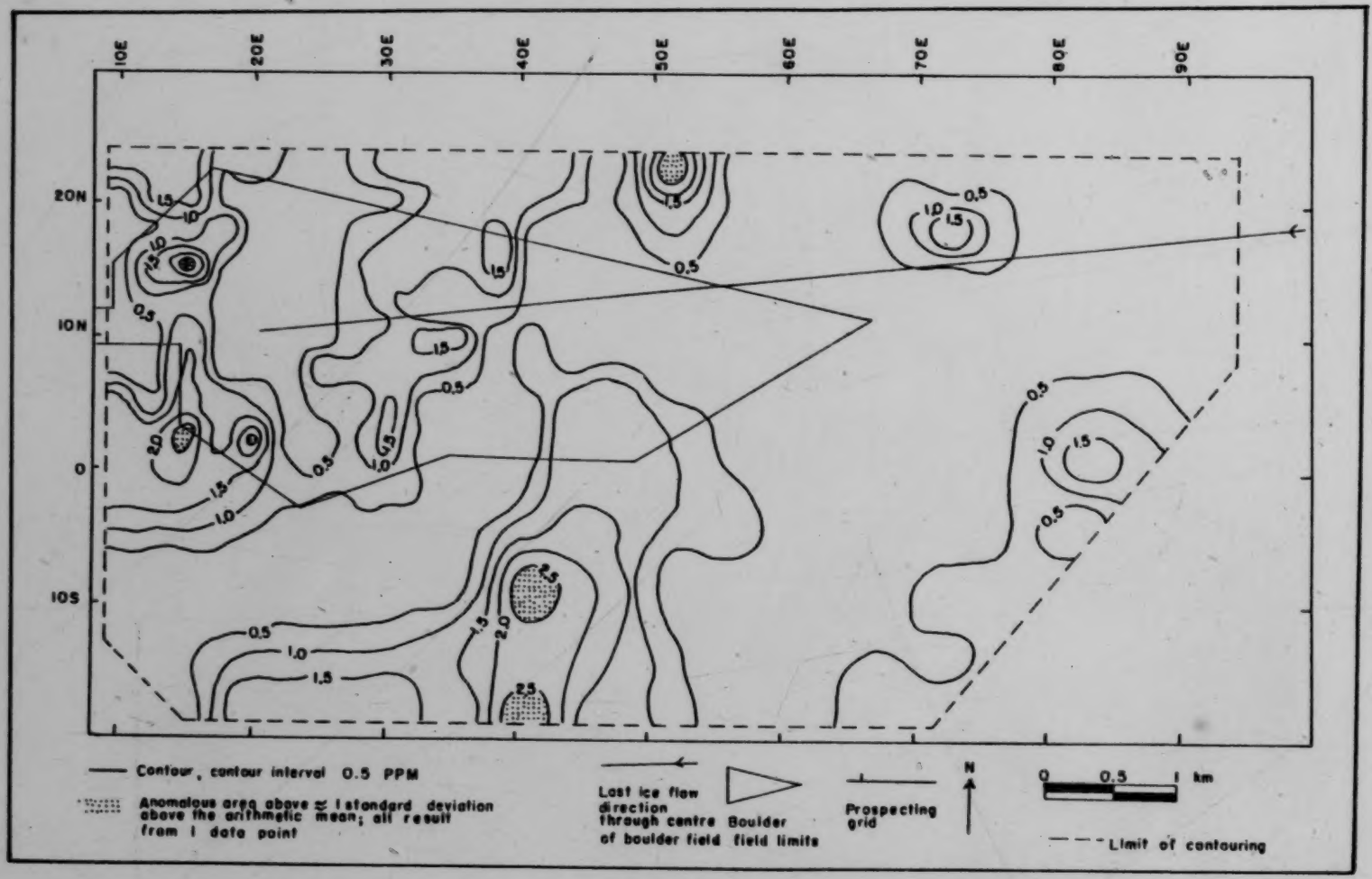
10E
20E
30E
40E
50E
60E
70E
80E
90E
20N
10N
0
10S
Contour, contour interval 0.5 PPM
Anomalous area above ≥ 1 standard deviation above the arithmetic mean; all result from 1 data point
Last ice flow direction through centre of boulder field
Boulder field limits
Prospecting grid
N
0 0.5 1 km
Limit of contouring

Molybdenum

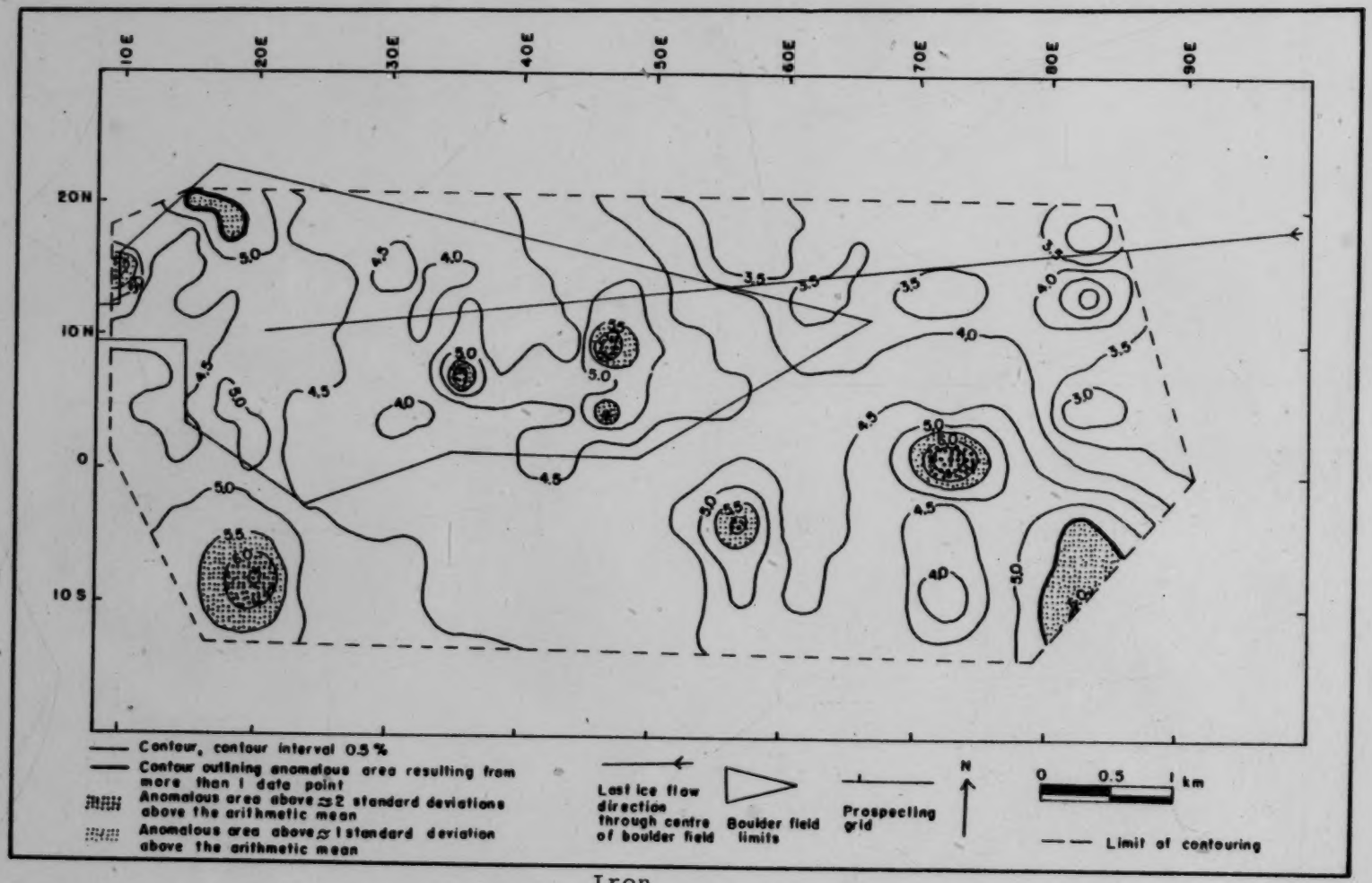
10E
20E
30E
40E
50E
60E
70E
80E
90E
20N
10N
0
10S
Contour, contour interval 0.5 %
Contour outlining anomalous area resulting from more than 1 data point
Anomalous area above ≥ 2 standard deviations above the arithmetic mean
Anomalous area above ≥ 1 standard deviation above the arithmetic mean
Last ice flow direction through centre of boulder field
Boulder field limits
Prospecting grid
N
0 0.5 1 km
Limit of contouring

Iron

I. APPENDIX I

X-ray diffraction results

site number	minerals	% total clay			quartz peak height (d = 4.2)	U (fluorometry) (PPM)	U (DNC) (PPM)	Fe (PPM)	Mn (PPM)
		illite	kaolinite	chlorite					
43	Q M A C I K	81	4	15	18.3	1.1	3.51	4.4	430
44	Q M A C I K	79	5	16	21.1	3.5	5.19	4.6	420
66	Q M A C I	88	0	12	11.2	4.3	-	3.7	680
87	Q M A C I K S	80	4	16	16.8	1.0	4.12	3.0	245
104	Q M A C I K	68	12	20	20.5	3.0	5.12	5.3	390
105	Q M A C I (K)	77	6	17	21.4	0.6	2.90	4.2	855
115	Q M A C I K	73	6	21	19.5	0.9	3.11	4.6	580
116	Q M A C I K	72	9	19	20.0	3.8	6.64	5.4	520
146	Q M A C I K	82	7	11	22.1	3.9	-	5.6	660
147	Q M A C I K	85	5	10	24.5	2.2	5.31	4.6	500
148	Q M A C I K	82	6	12	17.7	0.9	2.84	4.6	940
184	Q M A C I K	90	3	7	13.3	1.1	5.16	3.8	280

Q - quartz M - microcline A - albite C - chlorite I - illite K - kaolinite S - smectite
- not analyzed

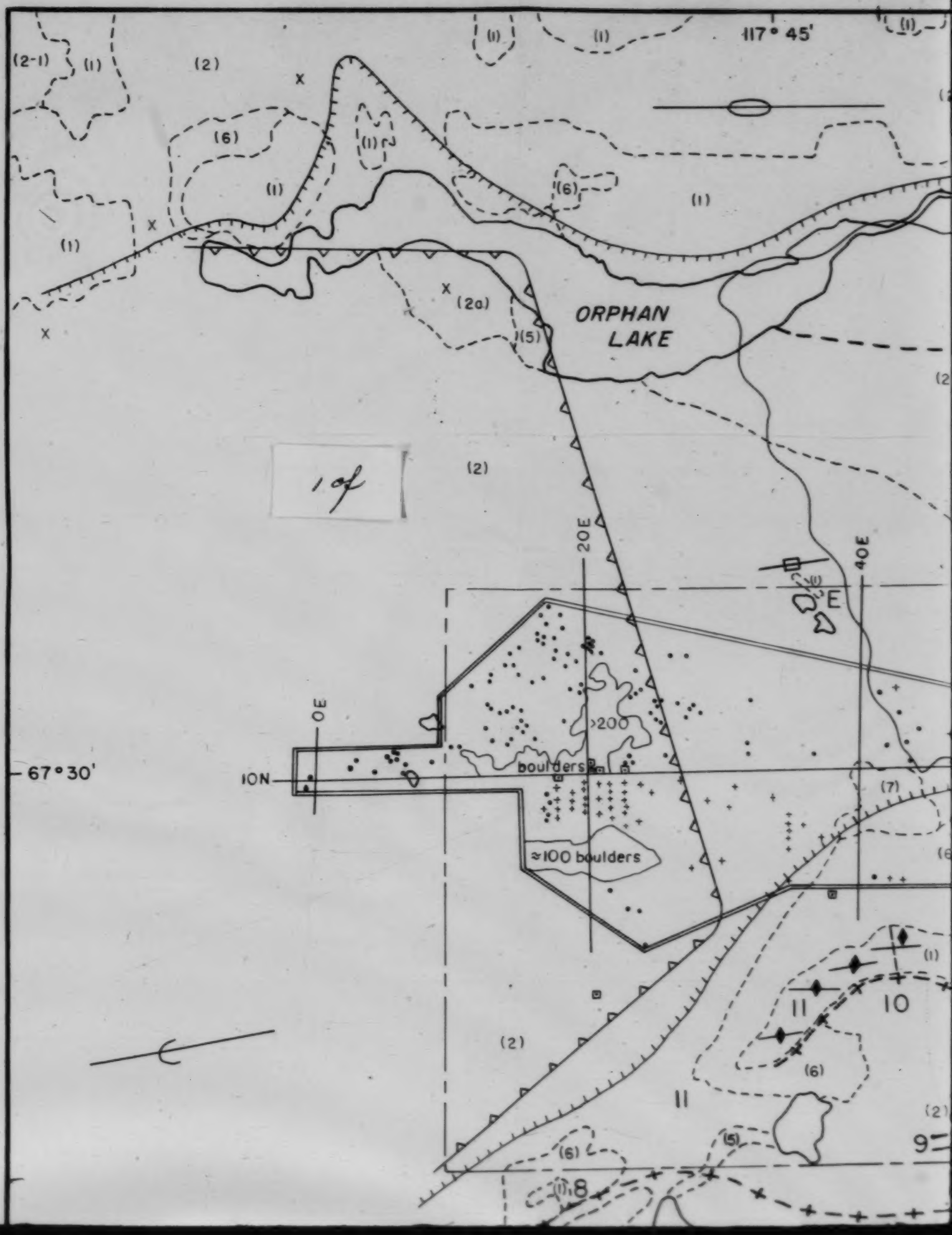
117° 45'
67° 30'
ORPHAN LAKE
(2-1)
(1)
(2)
(6)
(2a)
(5)
20E
40E
0E
10N
>200
boulders
≈100 boulders
(7)
11
10
9
8
1 of

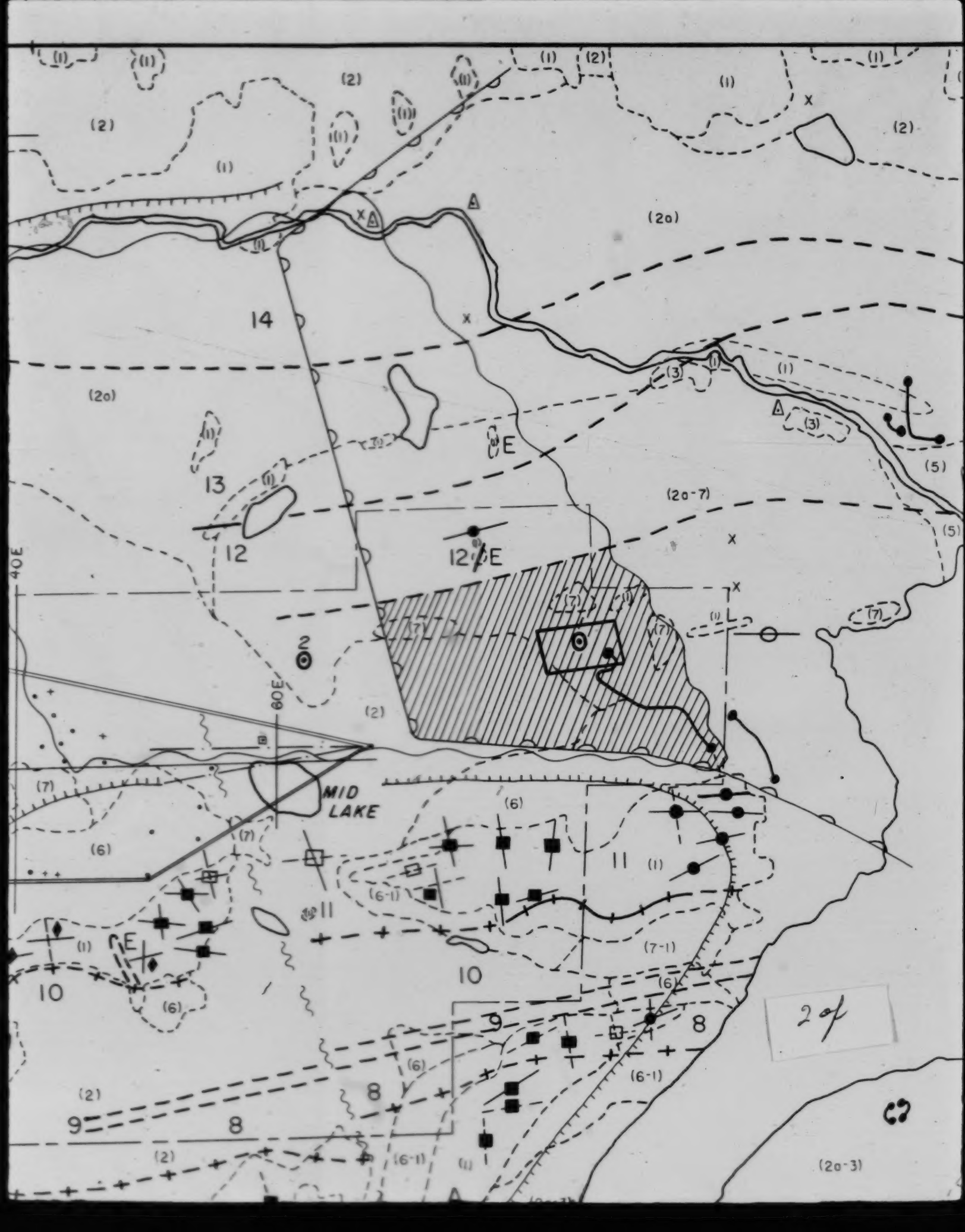
MID LAKE
40E
60E
14
13
12
11
10
9
8
2
E
(20)
(20-7)
(20-3)
(7)
(6)
(6-1)
(7-1)
(5)
(3)
(2)
(1)
2 of

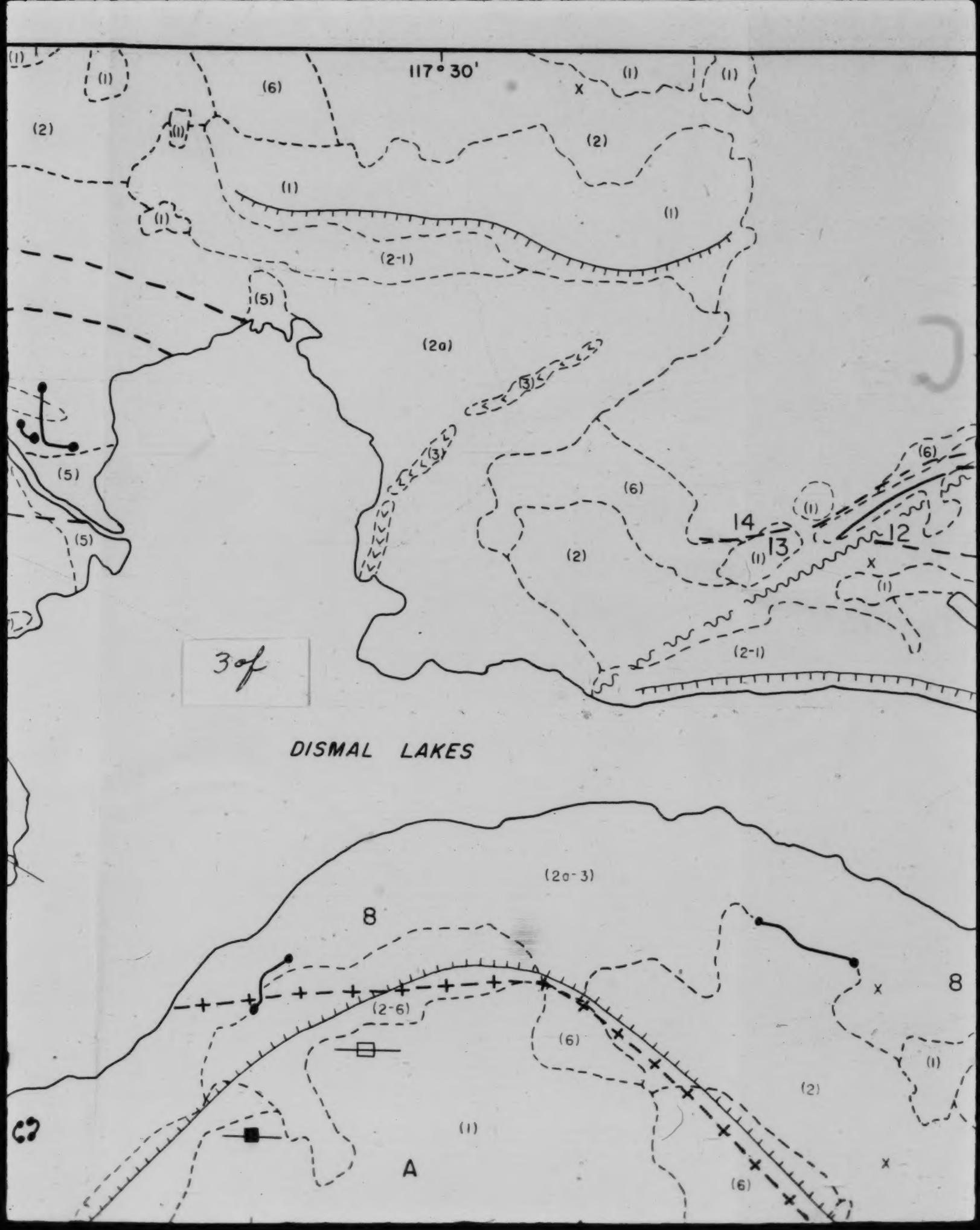
117° 30'
(1)
(6)
(2)
(2-1)
(5)
(2a)
(3)
(6)
14
13
12
3 of
DISMAL LAKES
(2a-3)
8
(2-6)
A

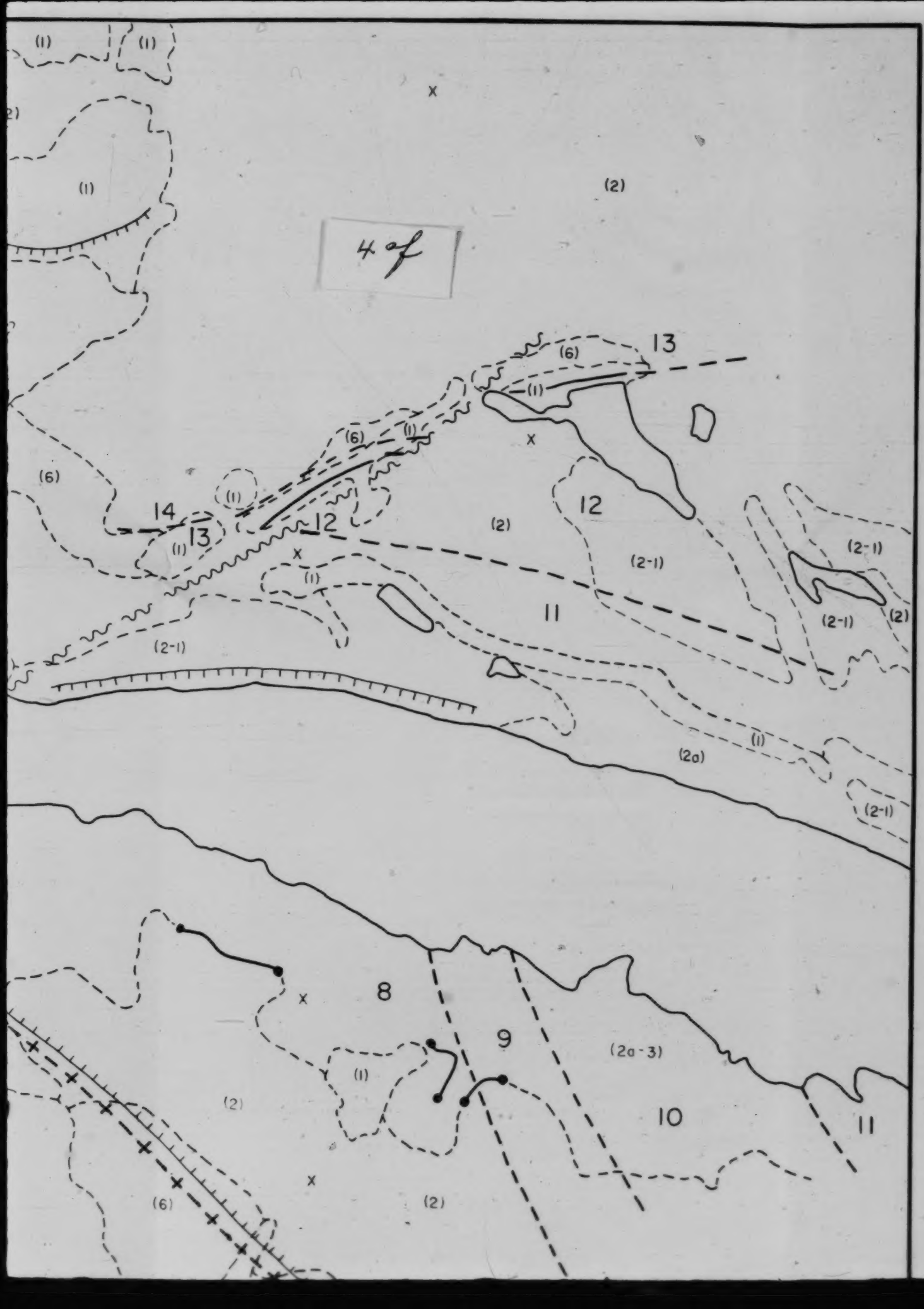
4 of
(1)
(1)
(1)
(2)
(6)
13
(1)
(6)
(1)
(6)
14
13
12
(1)
(2)
12
(2-1)
(2-1)
(1)
11
(2-1)
(2-1)
(2)
(2-1)
(1)
(2a)
(2-1)
8
9
(2a-3)
(1)
(2)
10
11
(6)
(2)

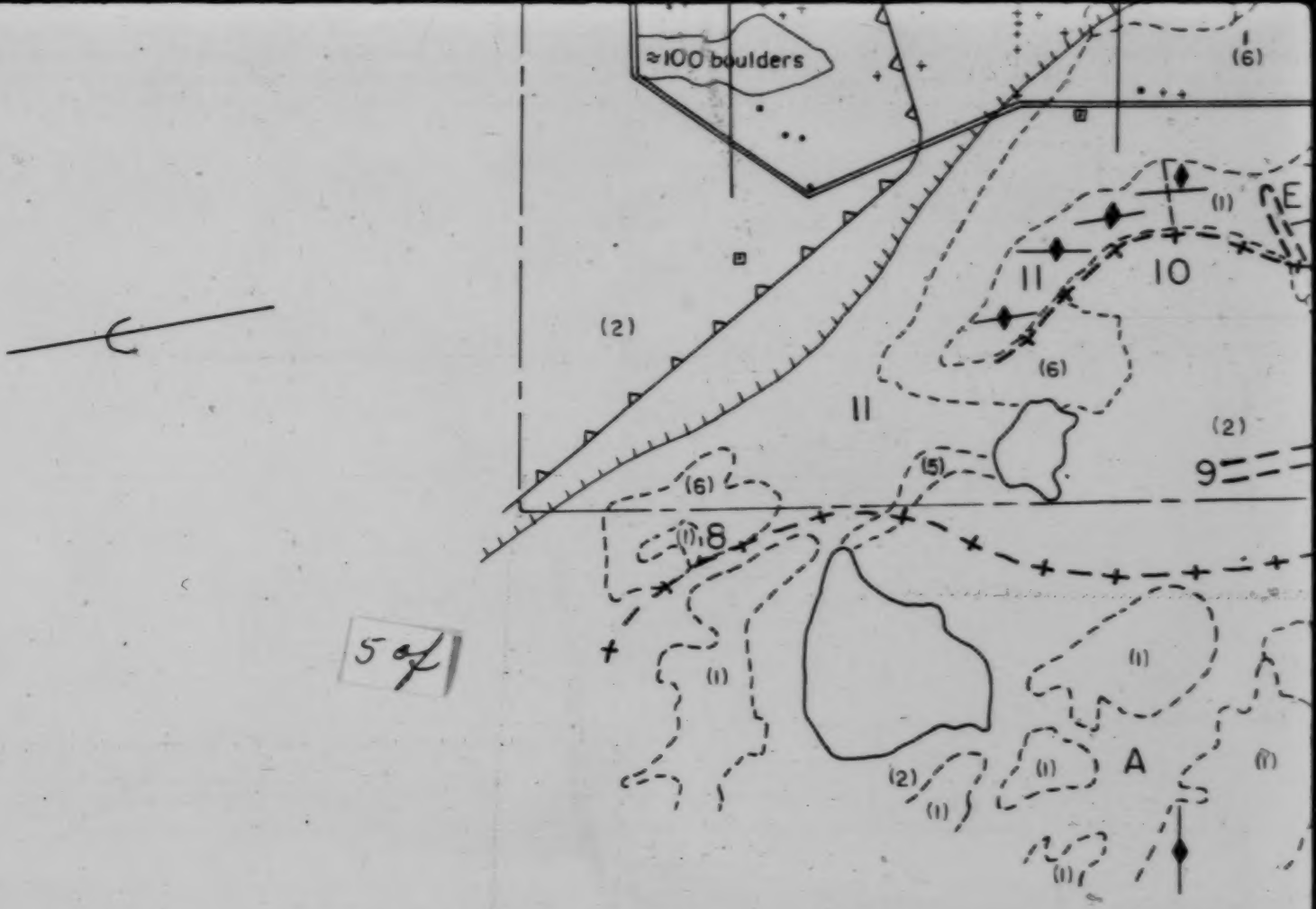

5 of 7

WEST DISMAL LAKES

COMPILATION MAP

N

SYMBOLS

- Cliffs and regionally significant slopes shading on downhill side
- Valley bottom parallel to ice flow
- Zone of extending and diverging ice flow
- Zone of converging and compressive ice flow
- Zone of increased abrasion, fracturing and plucking
- Likely boulder bedrock source area

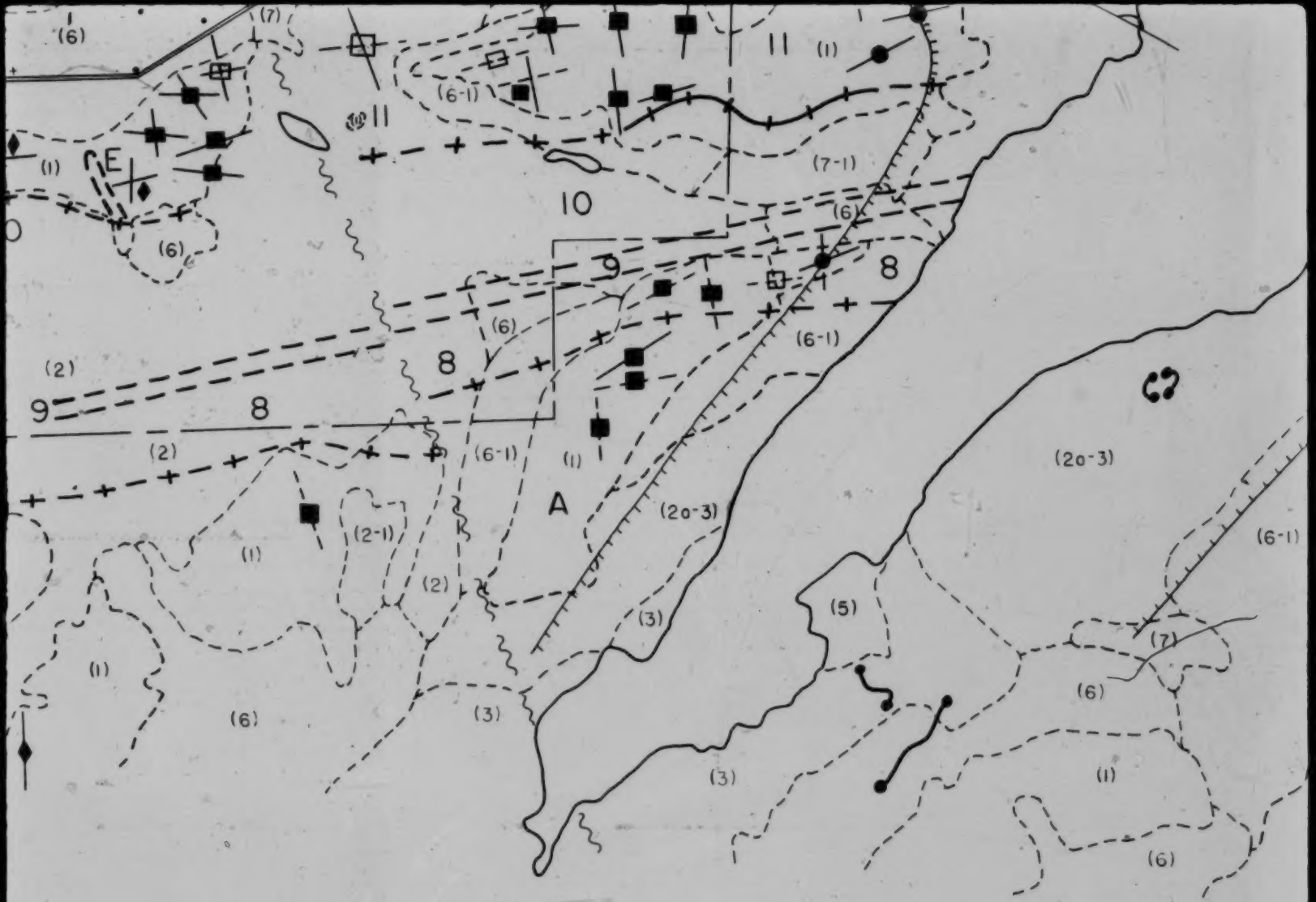

SYMBOLS

6 of

slopes

flow

ing ice flow

pressive

racturing

area

- Boulder, location and other data
- Boulder, location only
- Possible boulder fan axes
- Extreme boulder field limits
- Boundary of till-mudboil geochemistry sample area
- Uranium by fluorometry, significant anomalous sample, ranked in order of importance
- Last ice flow direction in west Dismal Lakes valley
- Till fabric site

BEDROCK GEOLOGY LEGEND

PROTEROZOIC

NEOHELIKIAN

- E — Diabase dike

DISMAL LAKES GROUP

- 14 — Dolomite
- 13 — Dolomite, sholy dolomite
- 12 — Shale, sandstone, siltstone
- 11 — Quartzose sandstone

PALEOHELIKIAN

HORNBY BAY GROUP

- 10 — Red siltstone, shale, sandstone
- 9 — Dolomite
- 8 — Reddish sandstone

APHEBIAN

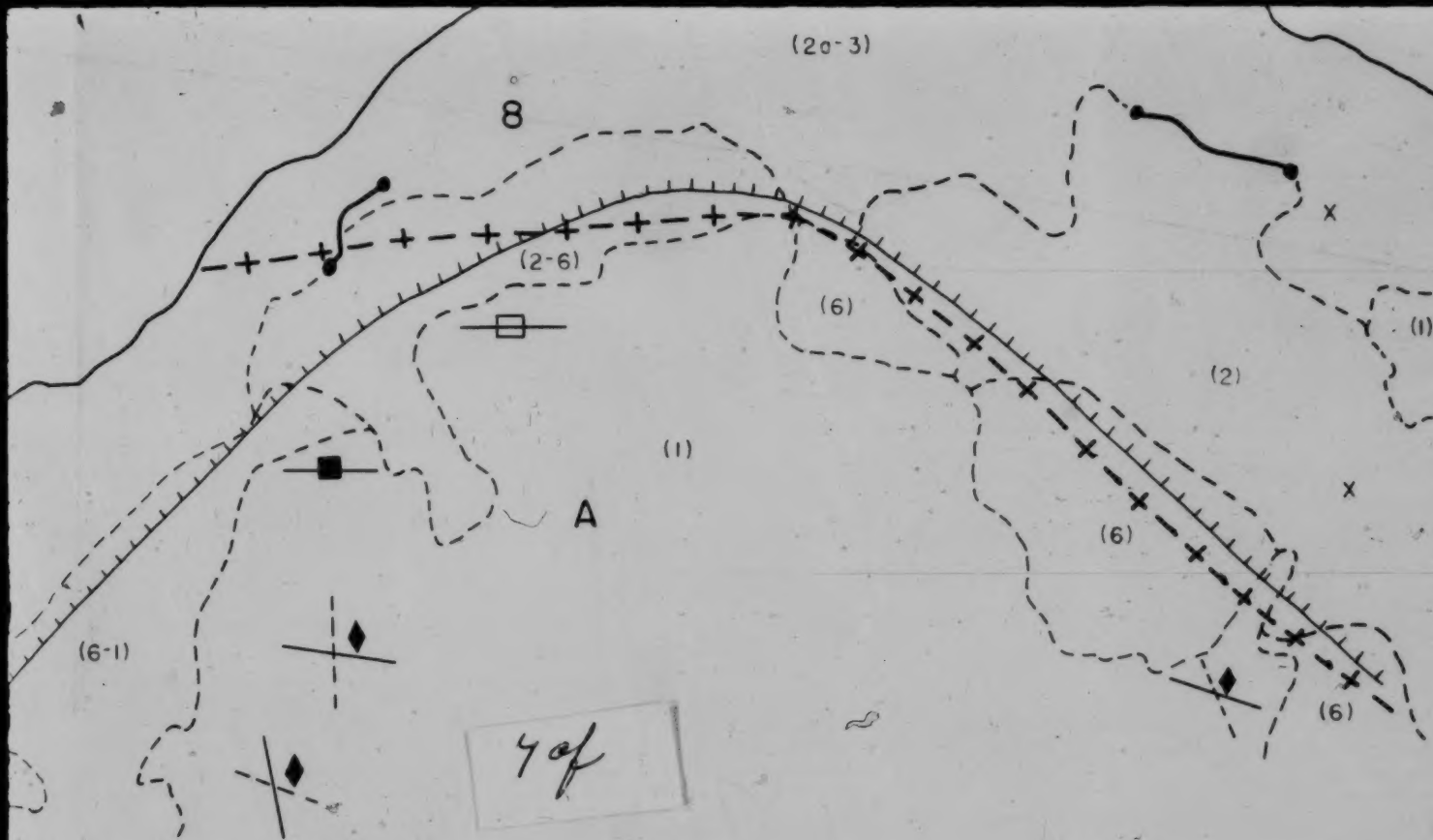

GEOLOGY SYMBOLS

- Bedrock geological contact (defined, approximate)
- Bedrock unconformity (defined, approximate)
- Fault
- Glacial striae (dominant, less dominant)
- 250 - 300 m elevation
- 301 - 350 m
- 351 - 400 m
- 401 - 450 m
- + 450 m
- Fluting
- Surficial geological contact (interpreted)
- Small bedrock outcrop
- Beach ridge, bluff or scarp

SURFICIAL

HOLOCENE

(7) Bloc

(6) Are

(5) Allu

PLEISTOCENE

(4) Glo

(3) Ice

(2) Till

(2

PRECAMBRIAN

(1) Bed

0

END

UP

nite

tone

sandstone

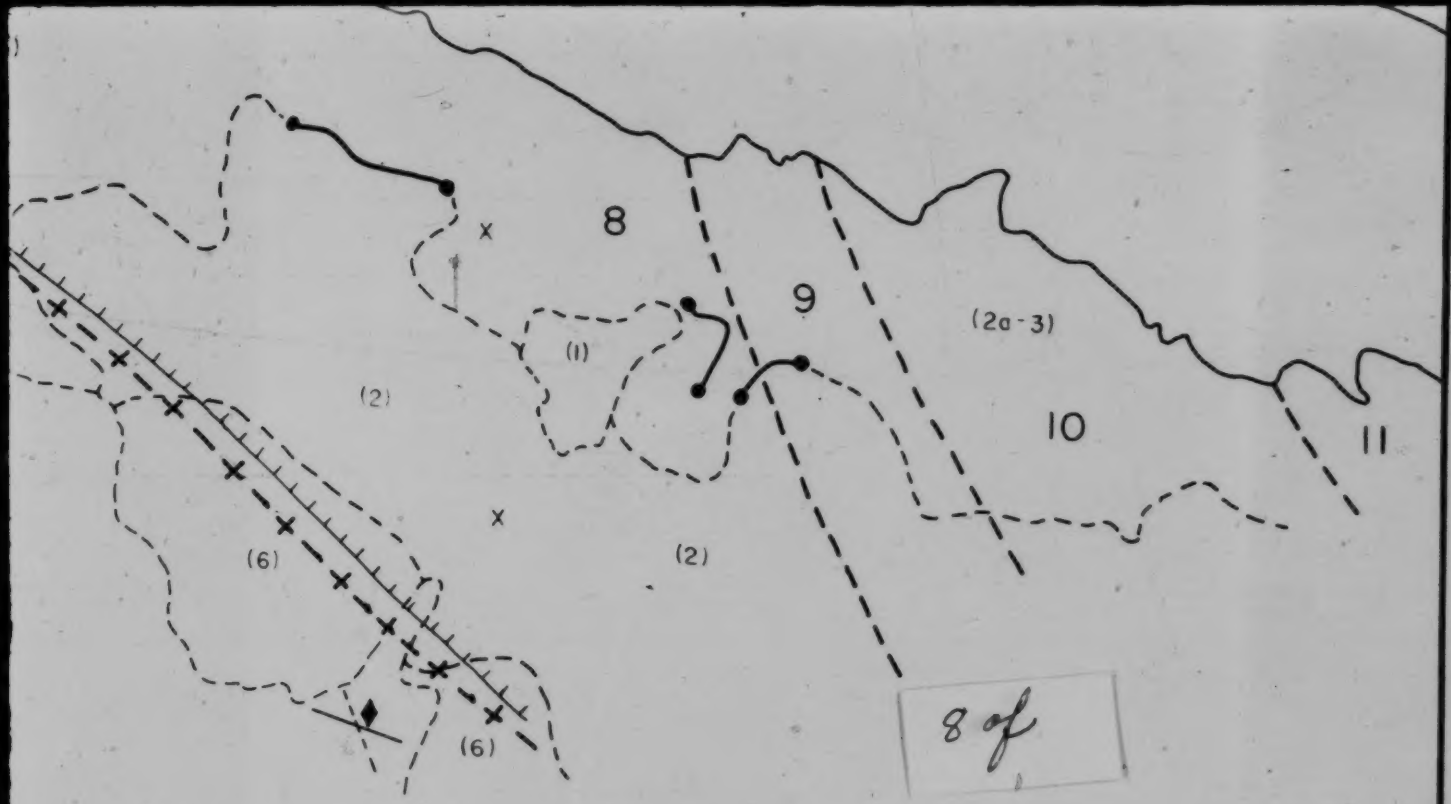

8 of

SURFICIAL GEOLOGY LEGEND

HOLOCENE

(7) Block field

(6) Area affected by mass wasting ; mostly till

(5) Alluvium and deltaic deposits ; silt, sand, gravel

PLEISTOCENE

(4) Glaciofluvial outwash ; gravel, sand

(3) Ice-contact stratified drift, gravel, sand, some till

(2) Till, clayey sand to sand

(2a) reworked and/or eroded

PRECAMBRIAN

(1) Bedrock

BOLS

gical contact
proximate)

nformity

pproximate)

(dominant,
t)

levation

gical contact

outcrop

bluff or scarp

0 300 1000 2000 m

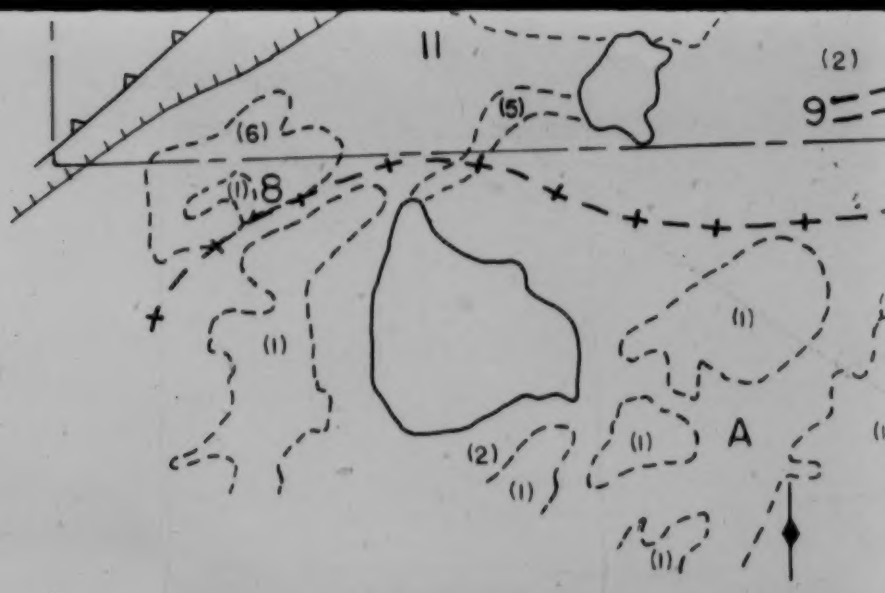

WEST DISMAL LAKES

COMPILATION MAP

N
W E
S

9 of

SYMB

- Cliffs and regionally significant slopes shading on downhill side
- Valley bottom parallel to ice flow
- Zone of extending and diverging ice
- Zone of converging and compressive ice flow
- Zone of increased abrasion, fracturing and plucking
- Likely boulder bedrock source area

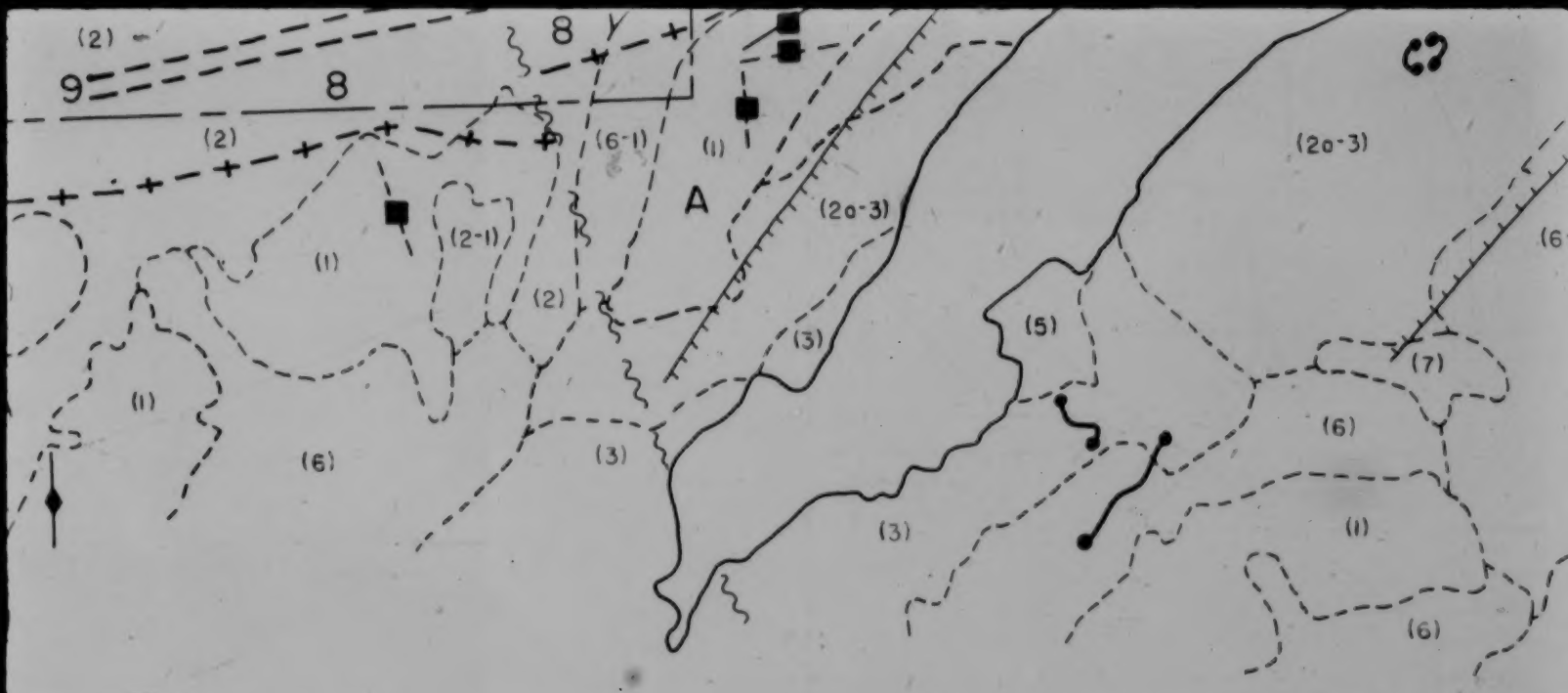

SYMBOLS

nt slopes

ce flow

rging ice flow

mpressive

, fracturing

e area

10 of

- Boulder, location and other data
- Boulder, location only
- Possible boulder fan axes
- Extreme boulder field limits
- Boundary of till-mudboil geochemistry sample area
- Uranium by fluorometry, significant anomalous sample, ranked in order of importance
- Last ice flow direction in west Dismal Lakes valley
- Till fabric site
- Natural exposure of surficial sediments

BEDROCK GEOLOGY LEGEND

PROTEROZOIC

NEOHELIKIAN

- E — Diabase dike

DISMAL LAKES GROUP

- 14 — Dolomite
- 13 — Dolomite, shaly dolomite
- 12 — Shale, sandstone, siltstone
- 11 — Quartzose sandstone

PALEOHELIKIAN

HORNBY BAY GROUP

- 10 — Red siltstone, shale, sandsto
- 9 — Dolomite
- 8 — Reddish sandstone

APHEBIAN

- A — Granite and related rocks

(after Grant, 1980)

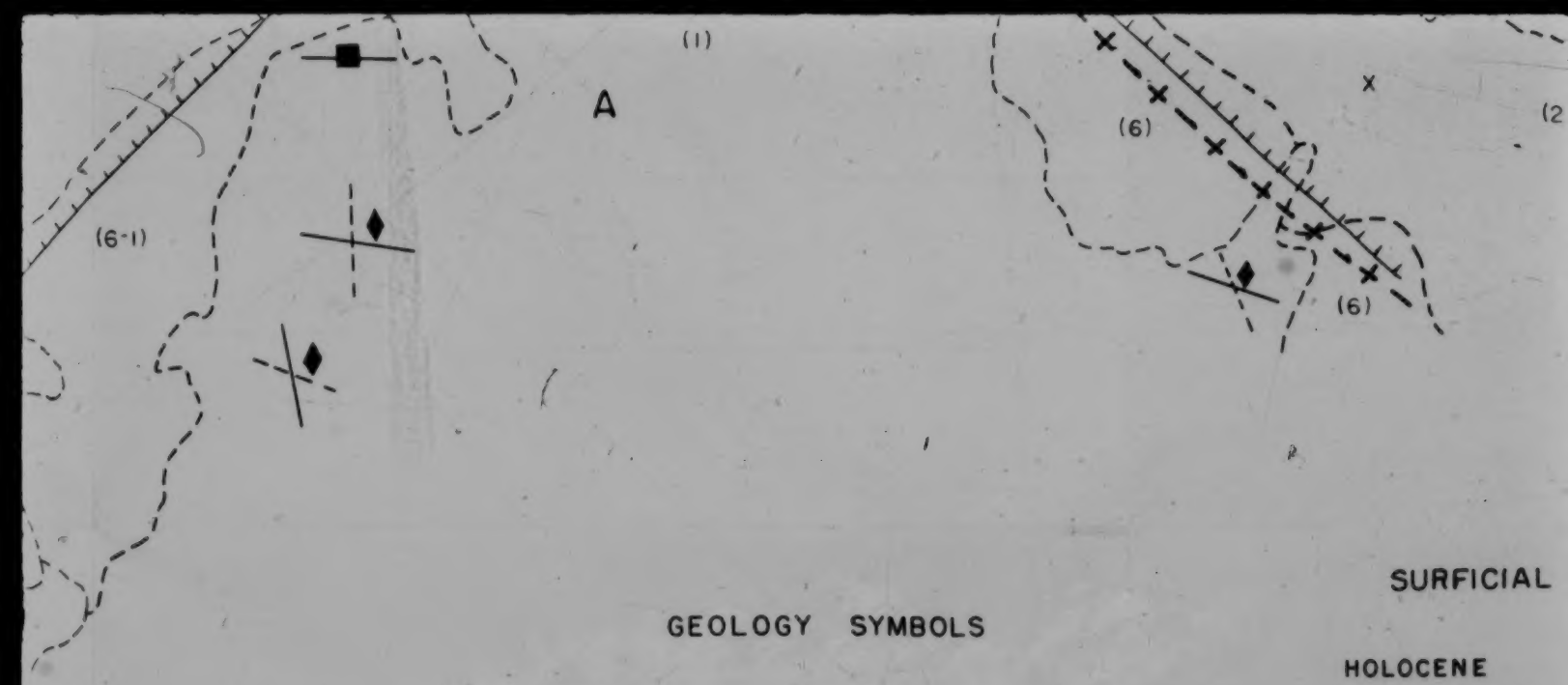

GEOLOGY SYMBOLS

- Bedrock geological contact (defined, approximate)
- Bedrock unconformity (defined, approximate)
- Fault
- Glacial striae (dominant, less dominant)
- 250 - 300 m elevation
- 301 - 350 m
- 351 - 400 m
- 401 - 450 m
- + 450 m
- Fluting
- Surficial geological contact (interpreted)
- Small bedrock outcrop
- Beach ridge, bluff or scarp
- Esker

SURFICIAL

HOLOCENE

(7) Block

(6) Area

(5) Alluv

PLEISTOCENE

(4) Glaci

(3) Ice-

(2) Till,

(2a)

PRECAMBRIAN

(1) Bedr

0

END

UP

mite

tone

P

sandstone

d rocks

)

11 of

SURFICIAL GEOLOGY LEGEND

HOLOCENE

(7) Block field

(6) Area affected by mass wasting; mostly till

(5) Alluvium and deltaic deposits; silt, sand, gravel

PLEISTOCENE

(4) Glaciofluvial outwash; gravel, sand

(3) Ice-contact stratified drift, gravel, sand, some till

(2) Till, clayey sand to sand

(2a) reworked and/or eroded

PRECAMBRIAN

(1) Bedrock

0 500 1000 2000 m

12 of 12